



January 2015

Preventing Or Mitigating The Irreversible RO Membrane Fouling Caused By Dissolved Organic Matter And Colloidal Materials During Surface Water Treatment

Raphael Ade Afonja

Follow this and additional works at: <https://commons.und.edu/theses>

Recommended Citation

Afonja, Raphael Ade, "Preventing Or Mitigating The Irreversible RO Membrane Fouling Caused By Dissolved Organic Matter And Colloidal Materials During Surface Water Treatment" (2015). *Theses and Dissertations*. 1857.
<https://commons.und.edu/theses/1857>

This Dissertation is brought to you for free and open access by the Theses, Dissertations, and Senior Projects at UND Scholarly Commons. It has been accepted for inclusion in Theses and Dissertations by an authorized administrator of UND Scholarly Commons. For more information, please contact zeinebyousif@library.und.edu.

PREVENTING OR MITIGATING THE IRREVERSIBLE RO MEMBRANE FOULING
CAUSED BY DISSOLVED ORGANIC MATTER AND COLLOIDAL MATERIALS
DURING SURFACE WATER TREATMENT

by

Raphael A. Afonja

Bachelor of Science, College of Staten Island, City University of New York, 2008

Master of Science, College of Staten Island, City University of New York, 2013

A Dissertation

Submitted to the Graduate Faculty

of the

University of North Dakota

in partial fulfillment of the requirements

for the degree of

Doctor of Philosophy

Grand Forks, North Dakota

December

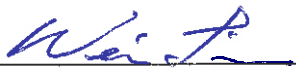
2015

Copyright 2015 Raphael Afonja

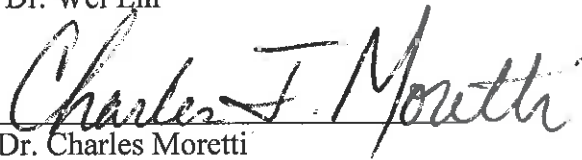
This dissertation, submitted by Raphael A. Afonja in partial fulfillment of the requirements for the Degree of Doctor of Philosophy from the University of North Dakota, has been read by the Faculty Advisory Committee under whom the work has been done and is hereby approved.



Dr. Harvey Gullicks



Dr. Wei Lin



Dr. Charles Moretti

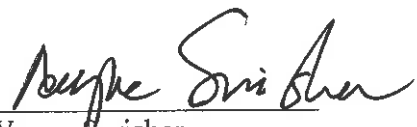


Dr. Howe Lim



Dr. Frank Bowman

This dissertation is being submitted by the appointed advisory committee as having met all of the requirements of the School of Graduate Studies at the University of North Dakota and is hereby approved



Wayne Swisher
Dean of the School of Graduate Studies



Date

PERMISSION

Title Preventing or Mitigating the Irreversible RO Membrane Fouling Caused
 by Dissolved Organic Matter and Colloidal Materials During Surface
 Water Treatment

Department Civil Engineering

Degree Doctor of Philosophy

In presenting this dissertation in partial fulfillment of the requirements for a graduate degree from the University of North Dakota, I agree that the library of this University shall make it freely available for inspection. I further agree that permission for extensive copying for scholarly purposes may be granted by the professor who supervised my dissertation work or, in his absence, by the chairperson of the department or the dean of the Graduate School. It is understood that any copying or publication or other use of this dissertation or part thereof for financial gain shall not be allowed without any written permission. It is also understood that due recognition shall be given to me and to the University of North Dakota in any scholarly use which may be made of any material in my dissertation.

Raphael Afonja
12/09/2015

TABLE OF CONTENTS

PERMISSION.....	iv
LIST OF FIGURES	viii
LIST OF TABLES.....	xvii
ACKNOWLEDGEMENTS.....	xx
ABSTRACT.....	xxiii
CHAPTER	
I. INTRODUCTION.....	1
II. FOULING PHENOMENA	16
2.1. Fundamentals of separation using reverse osmosis membranes	16
2.2. Background.....	24
2.2.1. Concentration polarization.....	27
2.2.2. Effects of inorganic scaling on RO performance	29
2.2.3. Effects of organic fouling on RO performance	34
2.2.4. Effects of silica complexes on RO performance	37
2.2.5. Effects of suspended solids on RO performance.....	40
2.2.6. Effects of water recovery on RO performance..	41
III. PREVENTION TECHNIQUES FOR THE FOULING OF REVERSE OSMOSIS MEMBRANES.....	43
3.1. Introduction.....	43
3.2. Coagulation–Flocculation–Sedimentation.....	45
3.3. Effect of the UF Stage on RO performance.....	54
3.4. Effects of antiscalants on RO performance	57
3.5. Effects of membrane cleaning on RO performance	57

IV.	MATERIALS AND METHODS	62
	4.1. Introduction.....	62
	4.2. Raw water source	66
	4.3. Schedule.....	68
	4.4. Laboratory techniques.....	69
	4.5. Pilot plant units and operation	72
V.	PRETREATMENT TRAIN OPTIMIZATION PROCESS.....	86
	5.1. Abstract.....	86
	5.2. Introduction.....	88
	5.3. Impact of raw water quality on pretreatment	89
	5.4. Optimization of coagulant or pH	97
	5.5. Methodology	100
	5.6. Results and discussion	107
	5.7. Conclusion	123
VI.	GFWTP REVERSE OSMOSIS PILOT PLANT PROCESS	126
	6.1. Abstract.....	126
	6.2. Introduction.....	128
	6.3. Source water chemical analysis	132
	6.4. RO operating parameters	136
	6.5. System or element recovery.....	137
	6.6. Concentration factor.....	138
	6.7. RO data normalization	138
	6.8. Reverse osmosis.....	142
	6.9. Results and discussion	149
VII.	RO MEMBRANE FOULING MITIGATION.....	177
	7.1. Abstract.....	177
	7.2. Introduction.....	179
	7.3. Results and Discussion	179
	7.4. Conclusion	185
	REFERENCE.....	187
	APPENDIX I	196
	Appendix II.....	199
	A. Design Criteria	199

B.	Operational Considerations	203
C.	Advantages and Disadvantages	204
D.	Design Criteria	205
E.	Operational Considerations	207
F.	Advantages and Disadvantages.....	208
G.	Design Criteria	208
H.	Operational Considerations.....	210
I.	Advantages and Disadvantages	211

LIST OF FIGURES

Figure		page
1.1.	Removal of TOC by coagulation–flocculation–sedimentation (PT) and ultrafiltration (UF) during a pilot study conducted at the GFWTP.	4
1.2.	Schematic of energy versus distance in the DLVO interaction profiles ⁸⁸	6
1.3.	Graph of UF TOC removal and the SDI test result during the 1 st GFWTP pilot study.....	9
2.1.1.	Schematic of diffusion in the case of reverse osmosis: (a) diffusion, (b) osmosis, and (c) reverse osmosis ⁸⁹	18
2.1.2.	Construction of a spiral-wound membrane element ⁸⁹	20
2.1.3.	Schematic of separation through a reverse osmosis membrane ⁸⁹	21
2.1.4.	Illustration of a compact fouling layer formed in the presence of Ca ²⁺ ⁸⁸	26
2.2.1.1.	Schematic of concentration polarization ⁸⁹	28

2.2.2.1.	Langelier Saturation Index Nomograph ⁹¹	32
2.2.3.1.	Schematic of the effect of solution chemistry on the configuration of NOM macromolecules in solution and on the membrane surface and the resulting effect on membrane permeate flux ⁸⁸	37
3.2.1.	Typical flow diagram for a water treatment process employing coagulation (chemical mixing) with conventional treatment, direct filtration, or contact filtration ⁸⁹	47
3.2.2.	Variation in particle charge with respect to pH ⁸⁹	48

3.2.3.	Structure of the electric double layer. Notably, the potential measured at the shear plane is known as the zeta potential ⁸⁹	49
3.2.4.	Solubility diagram for (a) Al(III) and (b) Fe(III) at 25 °C. Only mononuclear species have been plotted ⁸⁹	51
3.3.1.	UF membrane system operation	55
3.3.2.	Structure of an asymmetric UF membrane ⁸⁹	56
3.5.1.	Conceptual sketch of the swollen membrane matrix in different ionic environments ⁸⁶	60
3.5.2.	Illustration of the change in the organic fouling layer structure by EDTA ⁸⁸	61
4.1.1.	Schematic of the entire pilot plant at the GFWTP.....	63
4.1.2.	Schematics and flow diagram of the RO pilot plant.....	66
4.2.1.	Source waters (Red River & Red Lake River) in the GFWTP pilot study.	67
4.2.2.	GFWTP conventional plant and pilot study plant water treatment processes.....	68

4.5.1.1.	Pretreatment unit: MRI pretreatment, Raw water, acid and PACl feed point, and static mixer.....	73
4.5.1.2.	Mixer for coagulation.	73
4.5.1.3.	Top view of the MRI pretreatment unit.	74
4.5.1.4.	The UF feed tank and rear view of the pretreatment unit.	75
4.5.1.5.	Pretreatment unit influent and effluent turbidity graph.	76
4.5.2.1.	Jar test apparatus ⁸⁹	78
4.5.3.1.	Front view of the ultrafiltration unit from Evoqua.	79
4.5.3.2.	Rear view of the ultrafiltration unit from Evoqua.	80
4.5.4.1.	RO pilot system PW-4XM-14A-116 front view.....	81
4.5.4.2.	Figure 4.5.4.2. RO pilot system PW-4XM-14A-116 side view.....	82
4.5.4.3.	RO pilot system PW-4XM-14A-116 side view.	83
4.5.4.4.	RO pilot system PW-4XM-14A-116 rear view.	84

5.3.1.	Changes in SiO_2 concentration measured in mg/L during the pretreatment process.....	90
5.3.2.	Changes in SO_4^{2-} concentration measured in mg/L during the pretreatment process.....	91
5.3.3.	Changes in Cl^- concentration measured in mg/L during the pretreatment process.....	92
5.3.4.	Changes in conductivity measured in microsiemens during the pretreatment process.	93
5.3.5.	Changes in TDS during the pretreatment process (measured in mg/L).....	94
5.3.6.	Changes in TSS concentration measured in mg/L during the pretreatment process.....	95
5.3.7.	Changes in total alkalinity measured in mg/L during the pretreatment process.....	96
5.3.8.	Observed changes in total hardness measured as CaCO_3 in mg/L during the pretreatment process.	97
5.5.1.1.	Turbidity removal as a function of PACl dose.	102

5.5.1.2.	NOM removal as a function of PACl dose.	103
5.6.1.1.	Raw water turbidity during the pilot study.	108
5.6.1.2.	Raw water TOC during the pilot study.	108
5.6.1.3.	Percent removal of turbidity using PACl during pretreatment process as a result of acid adjustment and coagulant dose.	109
5.6.1.4.	Percent removal of turbidity using FeCl ₃ during pretreatment process as a result of acid adjustment and coagulant dose.	110
5.6.1.5.	Neural network diagram used in predicting effluent turbidity during the pretreatment process.	111
5.6.1.6.	Model fit for effluent turbidity.....	112
5.6.1.7.	Graph of effluent turbidity and the graph of the predicted effluent turbidity of the model fit over time.....	113
5.6.1.8.	Relationship between system parameters and effluent turbidity.	114
5.6.2.1.	Graph of influent and effluent TOC.....	115
5.6.2.2.	Percent removal of DOM using PACl during pretreatment process as a result of acid adjustment and coagulant dose.	116

5.6.2.3.	Percent removal of DOM using FeCl ₃ during pretreatment process as a result of acid adjustment and coagulant dose.	117
5.6.2.4.	Percent removal of turbidity using PACl during ultrafiltration process as a result of acid adjustment and coagulant dose.	118
5.6.2.5.	Percent removal of turbidity FeCl ₃ during ultrafiltration process as a result of acid adjustment and coagulant dose.	119
5.6.2.6.	Neural network diagram used in predicting effluent turbidity.....	120
5.6.2.7.	Model fit for effluent TOC.	121
5.6.2.8.	Graph of effluent turbidity and the graph of the predicted effluent turbidity of the model fit over.....	122
5.6.2.9.	Relationship between system parameters and effluent TOC.	123
6.2.1.	Effluent turbidity because of coagulation, flocculation, and sedimentation processes.	129
6.2.2.	Effluent TOC because of coagulation, flocculation, and sedimentation processes.	130

6.2.3.	Effluent TOC content after the ultrafiltration process.	131
6.9.1.1.1.	RO A normalized permeability observation by date.....	151
6.9.1.1.2.	Temperature observed by date.	151
6.9.1.1.1.1.	Permeability model predictions by date. Blue points represent the measured permeability rate data by date.....	153
6.9.1.1.1.2.	Behavior of permeability and their relation with temperature, feed flow, system recovery, NDP, and flux.	156
6.9.1.2.1.	RO B normalized permeability observation by date.....	157
6.9.1.2.2.	Permeability model predictions by date.....	158
6.9.1.3.1.	Change in permeability rates by date in RO C.	159
6.9.1.3.2.	Permeability model predictions by date.....	160
6.9.1.4.1.	Change in permeability rates by date in RO D.	161
6.9.1.4.2.	Permeability model predictions by date.....	162

6.9.1.5.1.	Change in percentage of salt passage concentrations by date in RO system D.....	163
6.9.1.5.1.1.	Percent of salt passage model predictions by date.....	165
6.9.1.6.1.	Change in the percent of salt passage concentrations by date in RO C...	168
6.9.1.6.2.	System salt passage model predictions by date.	169
6.9.1.7.1.	RO B normalized system salt passage observation by date.....	170
6.9.1.7.2.	System salt passage model predictions by date.	171
6.9.1.8.1.	Change in the normalized system salt passage concentration by date in RO A.....	172
7.3.1.	Unit A RO membrane recovery cleans.....	181
7.3.2.	Unit B RO membrane recovery cleans.	182
7.3.3.	Unit C RO membrane recovery cleans.	183
7.3.4.	Unit D RO membrane recovery cleans.....	185

LIST OF TABLES

Table		Page
1-1.	Water treatment processes removal credit ⁸⁹	2
1-2.	2013 GFWTP RO Membrane Pilot Operations and Results	8
3-1.	Chemical cleaning agents recommended by different manufacturers ⁸⁶	59
4-1.	GFWTP Water Quality Overview (December 2012–September 2013).....	65
4-2.	Routine Onsite and Laboratory Sampling Plan and Frequency	70
4-3:	RO system main component identification	85
4-4:	RO system main component identification	86
5-1.	Physiochemical water quality parameters in the pilot plant treatment train (8/13/2014).....	91
5-2:	Pilot Pretreatment Unit Testing Matrix using PACl salt	121

5-3:	Testing Matrix for the Pilot Pretreatment Unit (FeCl ₃).....	122
5-4:	Training and validation data of statistical analysis of effluent turbidity.....	128
5-5:	Training and validation data of statistical analysis of effluent TOC.....	138
6-1.	Chemical analysis work sheet for the GFWTP blend rivers	137
6-2.	Chemical analysis work sheet for RO feed water.....	138
6-3.	Summary of Finished Water Quality from the pilot study reverse osmosis process.....	145

6-4.	RO unit A parameter estimates.....	156
6-5.	RO A data effect tests	157
6-6.	RO D parameter estimates	168
6-7.	RO D effect tests.....	168
API-1.	GFWTP pilot study procedures of testing and the parameters that were tested.	197
API-2.	Daily data analysis recording sheet.....	199
API-3.	Daily data instrument recording sheet.....	200

ACKNOWLEDGEMENTS

I would like to thank the almighty God for bestowing his blessings on me and for guiding me through my dissertation. I would also like to express my gratitude to my advisor Dr. Harvey Gullicks for his support, guidance, and encouragement during the course of my dissertation. No words can express the gratitude I feel for the opportunity he has given me for completing my PhD under his supervision and guidance. I would also like to extend my gratitude to the committee members, Dr. Wei Lin, Dr. Charles Moretti, Dr. Frank Bowman, and Dr. Howe Lim, for the support and valuable input they provided throughout my dissertation.

Furthermore, I would also like to acknowledge the City of Grand Forks for making this project a success through financial and technical support during my research. I would like to thank Mr. John Goetz, Mr. Andrew Jobs, and everyone at the Grand Forks Water Treatment Plant who contributed to the success of this research, as well as for accommodating me at unearthly hours to collect data.

Furthermore, I would like to thank the AE2S team, Mr. Wayne Gerszewski, Mr. Adam Zach, Mr. Matt Erickson, Mr. Qigang Chang, and Mr. Seth DeMontigny for their support, contribution, and technical expertise during this pilot study.

Lastly, I would like to thank the University of North Dakota and the Civil Engineering department for giving me the opportunity to complete my dissertation, as well as staff from the School of Graduate Studies, UND, for always

accommodating me on several occasions, be it to obtain documents or to get forms signed.

Dedicated to my father, Dr. Joseph Adedibu Afonja, MD, my mother Titilola Onipede,
my children, and United States Armed Forces.

ABSTRACT

Reverse osmosis (RO) is increasingly being used for water treatment because of its small ecological footprint and improved membrane technology. However, a major challenge to the application of this technology in water treatment is the irreversible fouling observed in RO membranes. Fouling, mainly caused by dissolved organic matter (DOM) and colloidal materials (CM) in water, can increase the energy and maintenance costs and decrease the permeation flux and membrane life. Different pretreatments, such as coagulation, flocculation, sedimentation, and membrane-filtration, need to be applied upstream of the RO system to remove potential RO foulants. Membrane remediation by chemical cleaning also needs to be conducted to restore the membrane water flux. The purpose of the models constructed for the treatment trains in this pilot study is to investigate and identify system-specific performance parameters. The following paragraphs will discuss the findings from the investigations conducted during the Grand Forks Water Treatment Plant pilot study.

The pilot study on pretreatment indicated that DOM and turbidity could be effectively removed using ferric chloride (FeCl_3) or polyaluminum chloride (PACl) as coagulants if the pH and chemical coagulant dose were optimized. Under the optimized pretreatment conditions, the irreversible fouling of RO membranes could be reduced or mitigated. This research showed that pretreatment, including coagulation, flocculation, sedimentation, and ultrafiltration, lead to the removal of 42.2% and 59.44% of DOM on

using PACl and FeCl₃ as coagulants, respectively, indicating improvement over the average baseline removal of 30% under non-optimized conditions. In addition, the removal of more than 90% turbidity (with PACl, at temperatures >20 °C; with FeCl₃, at temperatures <4 °C) was achieved. PACl and FeCl₃ exhibited very good removal efficiency for DOM and turbidity at doses of 40 and 50 mg/L, respectively, at pH 6.5.

In this study, a new testable neural platform prediction model was constructed for the removal of turbidity and total organic carbon (TOC) in the pilot pretreatment study at the Grand Forks Water Treatment Plant. The model accurately predicted the quantitative dependence of the effluent TOC on coagulant dose, acid dose, temperature, influent-TOC, conductivity, and total dissolved solids (TDS). Similarly, it predicted the quantitative dependence of effluent turbidity on flow rate, coagulant dose, acid dose, temperature, influent-TOC, conductivity, TDS, and total suspended solids. These analyses investigate and identify system-specific performance parameters in the pretreatment unit that are responsible for turbidity and TOC removal.

A new testable mathematical model of normalized permeability and normalized system salt passage was developed to predict the quantity and quality of the product water during the pilot study on RO systems A and D. The model constructed from RO system A data accurately predicts the quantitative dependence of normalized permeability on temperature, feed flow, system recovery, net driving pressure, and system water flux. The model constructed from RO system D data accurately predicts the quantitative dependence of normalized system salt passage on temperature, feed flow, post-recycle feed conductivity, system recovery, permeate TDS, manufacturer's rated membrane salt passage, and system water flux. This analysis explains the manner in which fouling is

caused by both physical and chemical interactions between the membrane and fouling agents.

The strong interdependence of these fundamental operating conditions and the correlation between permeability and system salt passage were confirmed when the models were tested on data collected from RO systems A, B, C, and D. Although reasonable agreement between the results was obtained when the model was tested on these four RO systems, the models slightly overestimated the permeability values and underestimated the system salt passage values for RO system B. This discrepancy may be attributed to fouling, concentration polarization, the morphology and structure of the RO membrane. Additionally, system recovery (RO B ran at 75%, RO systems A and D ran at 82%) and the increase in membrane water flux for RO systems A and D from 11 gallons/ft²/day (gfd) to 12 gfd may also be important.

An effective cleaning sequence that restores 100% of membrane performance has been demonstrated for the RO membranes. The effects of fouling on RO permeability and salt rejection were studied by comparing the permeabilities of clean and fouled membranes, and by relating the values to the cleaning sequence used for recovery. The reported results indicate that the recovery of RO membrane performance depends on the physicochemical properties of the membrane foulant, the cleaners, and the sequence in which the cleaners are used. Caustic cleaning, followed by acid cleaning, was very effective, leading to a permeability recovery of more than 100%. On the contrary, acid cleaning followed by caustic cleaning only caused partial restoration of the membrane's ion retention ability. The use of either acid cleaning or caustic cleaning resulted in partial water flux recovery, while a combination of the two led to complete water flux recovery.

CHAPTER I

INTRODUCTION

According to the U.S. Geological Survey, the seas and oceans contain 96.5% of the Earth's water, while only 3.5% of the water is found in glaciers, below ground, in rivers, lakes, and polar ice caps. Approximately 68.7% of this 3.5% fresh water is found in glaciers and ice caps, 30.1% is present as ground water, while the remaining is brackish water existing as surface or other fresh water⁷⁷. Because of the limited amount of available fresh water, large populations of the world lack access to potable water. As fresh groundwater supplies are easier to treat, they are often targeted first. Increased population and water demand have led scientists, engineers, and community leaders to consider using surface waters of variable quality, fresh water from ice caps, anthropogenically contaminated groundwater, and reclaimed water as alternative raw water sources. Treating these surface waters is very challenging, however, because of the increasing complexity of surface water chemistry related to the geology of a specific geographical area.

Natural surface waters contain fine colloidal particles, natural organic matter (i.e., particulate and dissolved organic constituents), and inorganic (e.g., clay, silts, and mineral oxides) particles. Removing these species will improve water clarity and color, making the water potable. It will also reduce the possibility of the presence of infectious

agents in drinking water and the possibility of the adsorption of toxic compounds onto the surface of the species.

Producing pure water fit for human consumption from surface waters has proven difficult, and it is recognized that new, improved technologies are required to overcome the difficulties. Most scientists, engineers, and even localities worldwide favor the combination of techniques like sedimentation (after chemical conditioning by coagulation and flocculation) and reverse osmosis (RO) ⁸⁹. Membrane filtration is a developing technology currently being researched for the treatment of water and wastewater for producing potable and reclaimed water. Ultrafiltration (UF) and RO technology (ROT) are used for achieving various water treatment goals, including the removal of salts, pesticides, protozoans such as Giardia and Cryptosporidium, and bacteria (Table 1.1). ROT is favored because of the high quality of its product water as well as its low capital and operating costs¹.

Table 1-1: Water treatment processes removal credit ⁸⁹.

Treatment Process	Water Quality Issues								
	Turbidity	TOC	Sulfates	Hardness	Taste & Odor	Emerging Contaminants	<i>Cryptosporidium</i>	<i>Virus</i>	<i>Giardia</i>
Pretreatment	✓✓	✓✓							
Ultra Filtration	✓✓✓	✓					✓✓✓	✓	✓✓✓
Reverse Osmosis	✓	✓✓✓	✓✓✓	✓✓✓	✓✓✓	✓✓✓			
Disinfection							✓	✓✓✓	✓

Under certain extreme conditions, RO technology suffers from high operational and maintenance costs related to feed water chemistry, temperature, the physicochemical nature of membrane, and the interaction of feed water with the membrane ⁵. Because of these abovementioned drawbacks, RO membranes suffer from exhibited operational problems, such as high operating pressure, frequent cleaning requirement, and low membrane life. RO membranes are also highly susceptible to fouling and scaling caused by colloidal materials (CM) and the organic matter collected during the RO process, resulting in high maintenance costs. These fouling issues necessitate the installation of coagulation, flocculation, sedimentation, and ultrafiltration (UF) membranes upstream of the RO system. These pretreatment technologies have proven to be very reliable for RO membranes (Fig 1.1) ². Although continuous research has shown that UF and other conventional preventive measures have been effective for protecting RO membranes, CM and dissolved organic matter (DOM) remain concerning because of their effects on RO treatment and product water quality. DOM is a major precursor of disinfection by-products (DBPs) and pretreatment coagulant doses need to be increased to reduce DOM, and thereby DBP, in finished water.

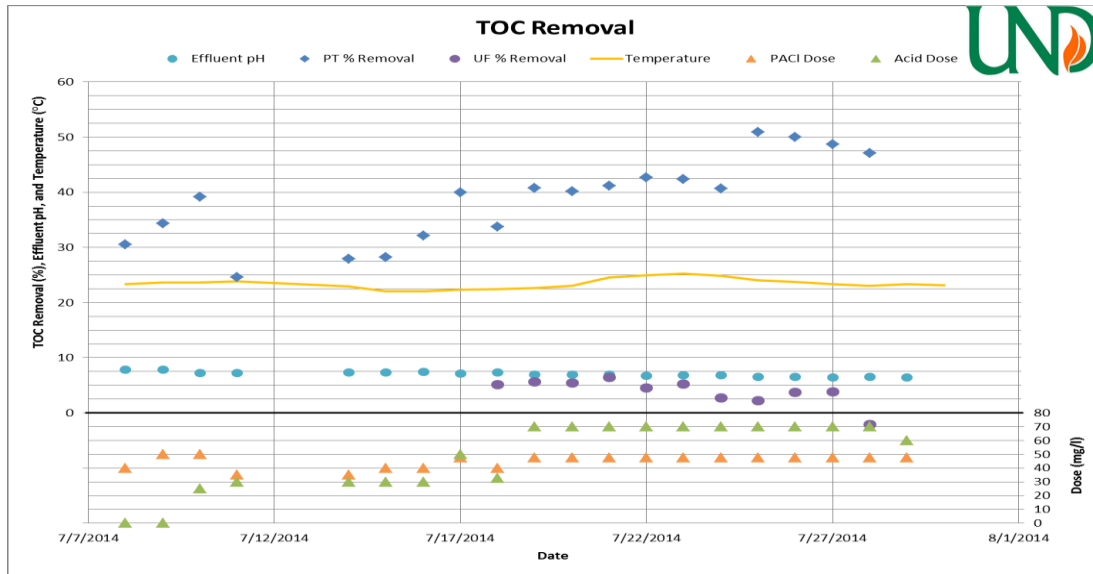


Figure 1.1. Removal of TOC by coagulation–flocculation–sedimentation (PT) and ultrafiltration (UF) during a pilot study conducted at the GFWTP.

The primary contributors to membrane fouling and scaling are DOM like humic substances; CMs like unreactive silica, carbonates, and sulfate compounds; oxidized soluble metals like Ca^{2+} , Mg^{2+} , Sr^{2+} , Ba^{2+} , Fe^{2+} , and Mn^{2+} ; and biological matter ³. RO membranes are thus expected to have a short life and experience loss of performance, such as decreased flux, increased pressure drop, and poor permeate quality when exposed to phenomena such as fouling and concentration polarization (CP) ⁴. Evidence has indicated that RO membranes exposed to feed water containing high total organic carbon (TOC), unreactive silica complexes, sulfate salts, carbonates, and DOM (especially humic substances) are easily fouled ⁷.

DOM and CM can easily diffuse through UF membranes and accumulate on RO membranes ¹³. These substances rapidly precipitate on the membrane surface and/or feed channel, which eventually results in RO membrane fouling and reduced water flow during the treatment of surface water and wastewater. If this phenomenon is common,

there are implications on studies aimed at understanding the fouling mechanisms and effect on RO membrane performance of DOM and CM.

For understanding the fouling phenomenon, it is imperative to recognize the forces of interaction existing between membrane surfaces and the particles they come in contact with. The fundamental principle behind the interactions between particles and surfaces in an aqueous environment is the Derjaguin–Landau–Verwey–Overbeek (DLVO) theory of colloid stability⁸⁸. This theory results from the summation of the van der Waals and electrostatic double-layer forces. Figure 1.2 shows the DLVO theory interaction profiles with the summation of the van der Waals and electrostatic double-layer forces. From these interaction profiles, it can be inferred that van der Waals forces, in contrast to the electrostatic double-layer forces, are not influenced by pH or electrolyte concentration. Membrane fouling can thus be mitigated by reducing the interactions between the particles and membrane through pH adjustment and/or chemical addition.

Besides membrane fouling attributed to complexes formed by CM and DOM as well as CP, the operating conditions can also play an important role in the mechanisms contributing to irreversible fouling. High system and element recoveries can create a favorable condition for fouling due to the high recycling of RO concentrates, which increases the concentration factor at the membrane surface. Studies have indicated that a high system recovery, ranging between 82% and 90%, is aggressive, thereby creating favorable conditions for fouling⁴. On the other hand, a lower system recovery creates a higher cross-flow velocity, which can be utilized to prevent fouling⁸⁸.

The first GFWTP pilot membrane operation analysis suggested that RO membrane fouling was most likely due to a heterogeneous mixture containing 92% DOM and 7.1% CM (such as unreactive silica) in combination with low biofouling. A 20% loss in permeability occurred during the 6 month pilot study, including a 30% loss in the tail element. The foulants observed on the RO membrane were described as “dark brown gelatinous,” which is typical for silica and natural organic matter (NOM), and mainly consisting of humic substances^{7, 8}. Table 1-2 shows the operating conditions and results of the 2013 GFWTP RO membrane pilot study.

Table 1-2: 2013 GFWTP RO membrane pilot operations and results

RO Operating Conditions and Performance					
Feed Water					
Average SDI		~2.8			
Average pH		~7.0			
Cleaning Conditions					
Type of Cleaning			Cleaning Frequency		
Recovery Cleaning*			30–45 days		
* low pH (Avista P303)		* high pH (Avista P312)			
RO Operating Phases					
Start Date		Phase	Flux	Condition	% Recovery
GE	Toray		(gfd)		
3/4/2013	3/6/2013	I	12	Cold Water	85
4/23/2013	5/1/2013	II	11	Spring Runoff	82
5/30/2013	5/30/2013	III	13	Warm Water	82
8/25/2013	8/21/2013	Mimicked Initial Operating Conditions			
RO Performance					
	Objective	Results	Comments		
Inorganic Rejection	>98%	>98%			
Organic Rejection	>98%	75–95%	Although the objective was not achieved, it was determined to not be problematic as no trace organic or DBP issues were observed.		
Fouling/Cleaning Loss of Permeability/ Irreversible Fouling	<10%	20–30%	Based on the pilot and autopsy results, irreversible fouling observed was higher than expected. ~20% loss in total system permeability ~30% loss in tail element permeability		
Cleaning Frequency	90 days	30–45 days	Cleaning was triggered by a 15–20% loss in permeability.		
Seasonal Variations	Observe Trends	Winter: 30–45 day cleaning; little to no irreversible fouling Spring: >45 day run times (No clean needed); no irreversible fouling Summer: ~30 day run times; irreversible fouling observed			

In addition, the resulting UF in–out graph constructed from the extracted data sets from the first pilot study confirmed that marginal amounts of TOC were removed at the UF stage (Fig. 1.3). The UF filtrate had a high TOC concentration, indicating that the TOC in the UF feed water was largely soluble. In addition, molecular weight was found to affect solubility, suggesting that larger molecules tend to be less soluble than smaller molecules having similar characteristics. The presence of TOC in the source water has been used for the determination of organic matter as a potential RO membrane foulant

that must be controlled^{14, 15}. Organic carbon typically originates from plant substances that have decomposed in water.

Red River & Red Lake water treatment by UF/RO

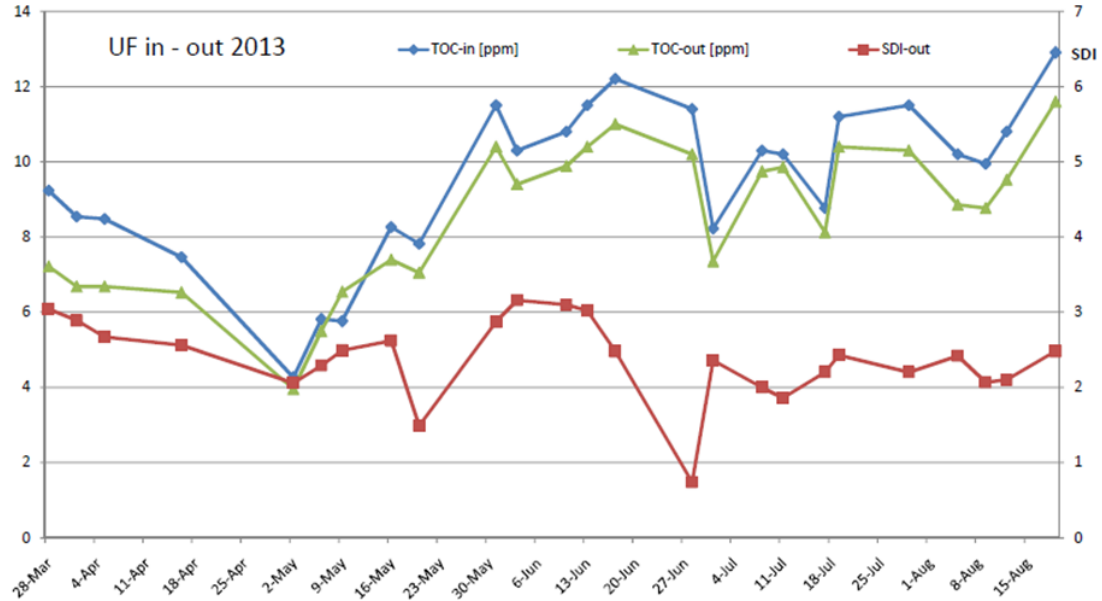


Figure 1.3. Graph of UF TOC removal and the SDI test result during the 1st GFWTP pilot study

During the 1st GFWTP pilot study, the measured silt density index (SDI) for the UF effluent ranged between 1.9 and 3.2, with a relatively high average of 2.4, which is consistent with RO membrane fouling by NOM (Fig. 1.3)^{11, 12}. The fouling propensity of the RO feed water is mainly expressed using the SDI test, which measures the fouling rate of a 0.45 μm filter at a pressure of 30 psi⁹¹. Kremen and Tranner have shown that SDI is a function of the flow resistance, caused by its molecular weight fraction, of a foulant (R_t in psi)⁶⁰. They have stated that the total flow resistance results from the combination of membrane resistance and the resistance resulting from accumulation of a foulant on the membrane over time (R_F). Hence, an exponential relationship exists

between increasing CP (caused by large-size compounds) and increasing SDI, which indicates a decline in flux.

Each geographical area has its own unique geology that affects the chemistry of the surface water flowing above it. In addition, seasonal changes such as rain events both increase and decrease the acid and metal concentrations and their loadings from wastes sites and unmined mineralized areas into receiving streams. The composition of the discharge from anthropogenic activities is another major contributor to surface water variations in drainage basins. These natural and anthropogenic factors affect the overall chemistry of surface waters and impart some unique characteristics that determine the treatment sequence needed for different surface waters. Source water variations are the major reason for conducting pilot studies during the design of a water treatment plant.

This dissertation will evaluate the optimized coagulant dose, pH control, and membrane pretreatment methods that will reduce CM and any corresponding DOM upstream and downstream of the RO stage and optimized cleaning strategies. These optimized conditions will mitigate and prevent irreversible RO fouling caused by CM and DOM, while extending the service life of RO membranes and reducing operational costs and cleaning frequency²³. In addition to the SDI test, the Langelier Saturation Index (LSI) test is also employed for determining the scaling potential of RO feed water and evaluating the pretreatment performance and fouling propensity in the RO membrane during the GFWTP design process⁸⁹.

Currently, there is interest in processes that can effectively control foulants accumulating on membrane surfaces. In particular, there is interest in developing a method for minimizing the transport of soluble TOC and CM in feed water while

preventing the precipitation of metal ions in the RO feed concentrate. In addition to bench scale tests for optimizing the additives, understanding the chemical and physical properties of the RO feed water and the impact of feed water recovery on the fouling propensity of DOM and CM can help prevent membrane fouling. As they relate to an RO membrane element, evaluating these processes will help understand the irreversible fouling activities on the membrane surface and provide insight into the techniques required for mitigating fouling regardless of feed water conditions and seasonal changes.

The objectives of this dissertation are to investigate the methods and operational conditions required for mitigating and preventing irreversible RO membrane fouling while increasing the water recovery and decreasing RO concentrate disposal. Important considerations for the design of RO membrane water treatment plants include appropriate pretreatment methods, operational conditions, and membrane filters for removing and controlling foulants in source water. The main experimental parameters in this research are source water, coagulant and acid type, pH, coagulant and acid dose, turbidity, total organic carbon (TOC), dissolved organic carbon (DOC), transmembrane pressure, permeability, flux, antiscalant dose, net driving pressure (NDP), and RO membrane feed pressure. This dissertation will focus on the following research ideas in terms of preventing or mitigating irreversible fouling:

1. The fouling tendencies of RO membranes of the Red River (RR) and Red Lake River (RLR) depend on feed water chemistry and foulant characteristics (size, structure, charge characteristics) ⁷⁵. The monitoring, profiling, and analysis of the surface waters parameters will allow for their classification as physical, chemical, and biological conditions as well as for differentiation

between natural and anthropogenic parameters. The SDI and LSI of the blend water from these two rivers can be used to predict the fouling potential of CM and DOM in RO feed water. Although SDI values have not always been indicative of RO fouling and an improved predictive methodology is needed, SDI data were collected while researching new methods for predicting the fouling potential. LSI was also examined for obtaining a better correlation between the fouling tendencies and RO operating conditions, such as flux decline and CP, during the design of RO systems^{37, 89}. Through these indexes, this proposed study can identify scale-forming constituents that can be either removed or controlled during the pretreatment and/or the UF stage.

In this research, water samples were collected from different sampling points along the pilot study water treatment train. In these samples, the concentrations of DOM, SiO₂, and ions such as SO₄²⁻, Cl⁻, Na⁺, Ca²⁺, Mg²⁺, Al³⁺, Fe²⁺, Mn²⁺, NO₃⁻, HCO₃⁻, and total PO₄³⁻ were determined. In addition, field sampling and testing were conducted for parameters such as temperature, pH, acidity, total dissolved solids (TDS), electrical conductivity (EC), and alkalinity. These analyses were used to identify the causes of the mineral instability of major ions, which resulted in irreversible fouling tendencies in the first pilot study.

2. Pretreatment methods include coagulation, flocculation, sedimentation, and the ultrafiltration membrane process. Pretreatment also has environmental significance with respect to disinfecting public waters to kill harmful organisms. However, in the presence of high turbidity, especially those from

suspended solids in polluted water and wastewater, pathogens and harmful organisms are encased in turbid particles, thereby protecting them from disinfectants. During pretreatment, high turbidity and TOC removal is required to ensure effective disinfection, thus controlling residual disinfectant and DBP formation, and preventing bacteria growth in distribution systems. This study will evaluate the effect of coagulation pretreatment on turbidity and TOC removal, membrane performance, and the impact of pH in enhancing coagulant performance. It will also help optimize the coagulant dose and pH during pretreatment for achieving a turbidity of less than 2 NTU while removing more than 40% of TOC ^{16, 22, 24, 25, and 26}.

3. According to Seungkwan and Elimelech, the concentrations of CM and DOM on the membrane surface increase with increasing permeate flux, and element and system recovery rates ¹⁷. If the RO system continues to simultaneously operate at a high feed pressure and recovery rate, membrane fouling may rapidly advance from reversible to irreversible in order to attain a high permeate flux. When operating RO systems at a high recovery rate, there is potential for flux decline, while at a high feed pressure there is potential for increase in ion passage even without high flux ³⁹. The recovery rate is an important factor that affects the possibility of scale formation, increase in osmotic pressure, decrease in permeate flux, and deterioration of permeate water quality. This research will explore the possibility of a relationship between membrane performance and the specific operating conditions of the RO system. A range of element operating conditions is recommended for

minimizing the possibility of fouling and increasing membrane life span. This study will also demonstrate the limiting conditions that must be imposed on the RO system for maximizing the recovery (system and element) rates and average permeate flux, and minimizing concentrate flow rate, flux decline rate, and salt passage rate.

4. During desalination using an RO system, an operating condition that needs to be considered is the NDP, which can trigger routine system shutdown. Wei et al. (2010) have stated that when NDP increases by 15%, membrane flushing as well as recovery and maintenance cleaning are required. Literature reviews have indicated that flushing RO systems with permeate water, recovery, and maintenance cleaning help in the removal of foulants from membrane surfaces ^{4, 26, 32, 36, 37, 47, 54, 70, and 88}. This stems from the concept that the increase in flux results in a stronger drag force toward the membrane, while the increase in the CP leads to stronger bonds between particles as well as between particles and the membrane. This study will determine methods for optimizing membrane flushing. It will also compare and optimize different antiscalants, cleaning methods, and cleaning frequencies that can be employed when the system is idle, with the aim of restoring RO system performance to its initial operating baseline ³⁵. After selecting the most effective chemical(s) ^{23, and 37}, it is necessary to develop an appropriate cleaning method and use an optimized reagent concentration.

Chapter 2 provides a literature review on the fouling phenomena of RO membranes, such as CP and the fouling mechanism. It also describes the

chemistry of interaction between different chemical species such as DOM and divalent ions, which result in scaling and fouling. Chapter 3 discusses different preventive techniques such as coagulation, flocculation, sedimentation, and UF membrane filters for mitigating the RO fouling observed in the first pilot study. Chapter 4 discusses the materials and methods used for the GFWTP pilot study. Chapter 5 summarizes the water quality analytical parameters of the blended river water from RR and RLR and focuses on the optimization of PACl performance during coagulation–flocculation–sedimentation. This includes identification of system-specific performance parameters that relate to the pretreatment unit. In Chapter 6, system-specific performance parameters that relate to the behavioral responses of permeability and salt rejection during RO system membrane operation are investigated and identified. Additionally, the operating conditions that affect RO membrane performance during surface water treatment are identified. Chapter 7 discusses the recovery and maintenance cleaning of RO membranes. Through recovery cleaning investigations and analyses, an appropriate cleaning method is recommended for restoring RO membrane performance to its initial operating baseline. The key results and objectives are highlighted in a summary at the beginning of each chapter.

CHAPTER II

FOULING PHENOMENA

2.1. Fundamentals of separation using reverse osmosis membranes

The performance of the reverse osmosis (RO) process, which includes the contaminant removal efficiency and the rate of separation when one material is transferred from one phase to another, e.g., liquid to solid by adsorption, is often governed by the mass transfer rate⁸⁹. Mass transfer through a semipermeable membrane during osmosis only occurs in response to a driving force caused by a concentration gradient. Because of this concentration gradient, the flux of the particle from a higher-concentration region to a lower-concentration region is directly proportional to the driving force, which is described by the following equation:

$$J = k(\Delta C) \quad [2.1.1]$$

Here, J = mass flux of the solute, $\text{g/m}^2 \cdot \text{s}$

k = mass transfer coefficient, m/s

ΔC = concentration gradient of the solute, mg/L

The diffusion of molecules from a high-concentration region to a low-concentration region is dependent on the kinetic energy of molecules in the solution, assuming that no external force is responsible for the motion of the fluid. Hence, the

concept of molecular diffusion is critical to understanding the mass transfer in a system. The two key concepts of mass transfer are Brownian motion and Fick's first law of diffusion.

Brownian motion describes the random, albeit constant, motion of fluid particles or molecules because of their internal energy, which implies that they are constantly bombarded by other particles and molecules from the same fluid ⁸⁹. As a result of these collisions, unequal forces develop between particles and molecules in fluids, leading to their movement in random directions. This random movement induces the flow of matter in the bulk solution from higher-concentration regions to lower-concentration region.

Fick's first law describes diffusion in the presence of fluid flow with respect to the centroid of the diffusing mass of solutes. This law states that a fluid in motion undergoes mass transfer because of diffusion. This principle can be used for describing flux as follows:

$$J = \frac{QC}{A} \quad [2.1.2]$$

Here, J = mass flux of matter due to advection, $\text{mg}/\text{m}^2 \cdot \text{s}$

A = cross-sectional area perpendicular to the flow direction, m^2

Q = flow rate of a fluid perpendicular to A , m^3/s

C = concentration of a solute, mg/L

Osmosis is a natural process that occurs when a liquid, such as water, passes across a semipermeable membrane because of osmotic pressure from a dilute to a concentrated solution. However, the osmotic pressure of a solution increases with concentration. For reversing this process, pressure greater than the osmotic pressure must

be applied on the concentrated solution side for the liquid to pass from the concentrated side to the dilute side (see Figure 2.1.1 below). This process is called “reverse osmosis.”

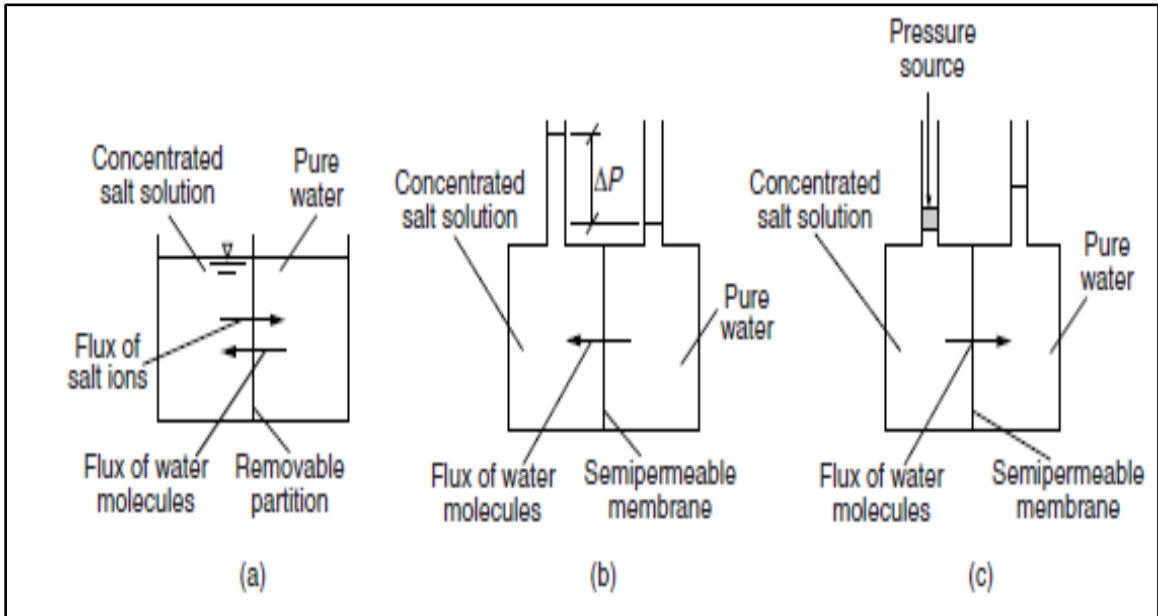


Figure 2.1.1. Schematic of diffusion in the case of reverse osmosis: (a) diffusion, (b) osmosis, and (c) reverse osmosis ⁸⁹.

RO is a water treatment process that utilizes membrane (semipermeable material) technology for separating dissolved solutes from water. This technology aims to remove extremely small contaminants (as small as 0.0001 μm), silicates, synthetic organic chemicals, hardness, disinfection-by-product (DBP) precursors like natural organic matter (NOM), and dissolved monovalent and divalent ions (such as Ca^{2+} , Mg^{2+} , Cl^- , and Na^+) from solutions. Membrane separation leaves behind a concentrate, and allows the solvent to permeate through the membrane layer. During filtration, mass transfer between the influent and permeate sides and the separation efficiency of RO depend on influent solute concentration, positive hydrostatic pressure, and the water flux rate (membrane diffusion) ⁷⁸.

The smallest component of an RO system is called a membrane element. RO membrane elements are fabricated in either spiral-wound or hollow fine-fiber configuration. Figure 2.1.2 shows the assembly of a spiral-wound membrane element. The outer wrap and membrane flat sheets are joined together, with the grooved permeate collection side of the outer wrap facing the membrane, and sealed on three sides to form an envelope.

A spacer is added in contact with the membrane flat sheet, which creates a flow path for feed solution and permeate flow perpendicular to the membrane. The permeate passing through the membrane enters the grooved permeate collection zone of the envelope. The flow in the spacer creates turbulence in the feed water and concentrate stream, and prevents membrane material compression ². The outer wrap and membrane are rolled around a perforated permeate collection tube, along with the feed channel spacer. The permeate follows a spiral flow path along the grooved outer wrap to the perforated permeate collection tube. The feed channel spacer of the element is exposed to feed water at one end and allows the concentrate to exit from the other end of the element.

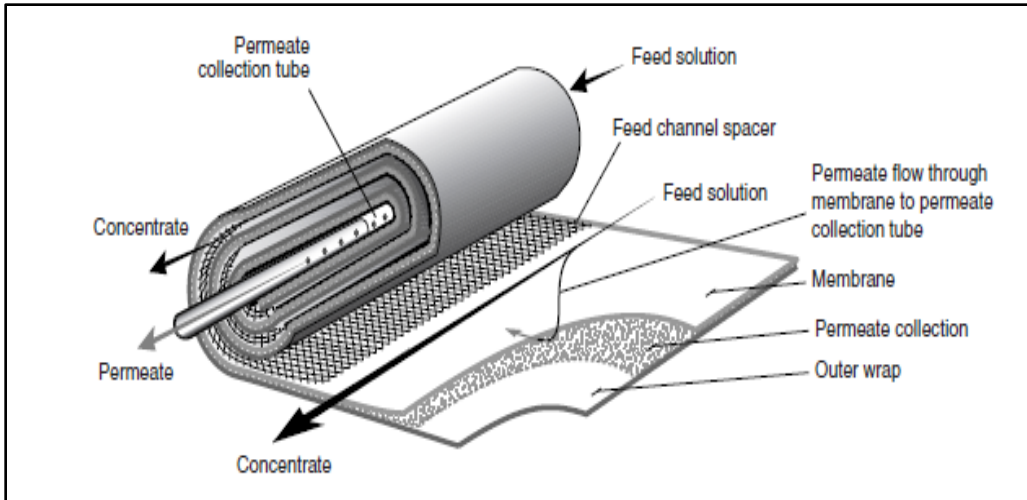


Figure 2.1.2. Construction of a spiral-wound membrane element ⁸⁹.

Figure 2.1.3 shows the schematic of RO process operation. The RO membrane technology can be operated in two ways: (1) maintaining a constant permeate flux (flow rate to membrane area, L/m^2h) by changing the net driving pressure (NDP) or (2) maintaining a constant NDP by allowing permeate flux to vary. Most RO systems are designed to operate in the latter way ⁶⁹.

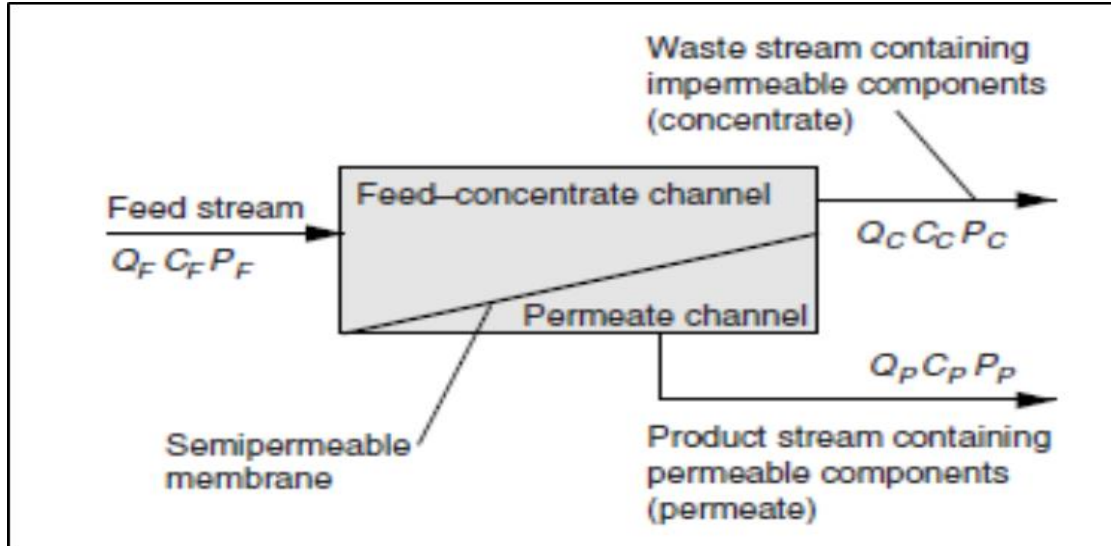


Figure 2.1.3. Schematic of separation through a reverse osmosis membrane ⁸⁹.

As the permeate flows through the spiral-wound membrane elements, the applied pressure decreases, while osmotic pressure (π) increases along the length of the feed-concentrate channel. NDP accounts for changes in feed and permeate pressures, feed channel head loss, and osmotic pressure ⁸⁹.

$$\text{NDP} = \Delta P - \Delta\pi \quad [2.1.3]$$

$$\Delta\pi = \text{pressure concentrate side} - \text{pressure permeate side}$$

ΔP is the difference in transmembrane pressure (TMP), and $\Delta\pi$ is the difference in the osmotic pressure of the influent. A very good approximation of π is 10 psi for every 1000 mg TDS/L. However, osmotic pressure is dependent on the operating temperature (T) and ion concentration of the solution (C). The relationship between π , T, and C is as follows ⁸⁹:

$$\pi = CRT \quad [2.1.4]$$

$$L = \frac{DSV}{RTl} \quad [2.1.5]$$

Here, R is the ideal gas constant, L is a function of water diffusivity (D), S is the water solubility (S), V is the partial molar volume of water, T is the operating temperature (T), and l is the membrane thickness ⁵⁶:

The driving pressure that permits water diffusion through the semipermeable membrane is described in terms of the concentration gradient or the Gibbs free energy (G). Diffusion is said to occur under thermodynamic equilibrium if $G = 0$; however, in an RO process, pressure and concentration are unequal ⁸⁹. During this RO process, feed water flows perpendicularly across the membrane surface, allowing some portion of the pressurized water to pass through the membrane into the permeate collection tube, leaving behind the concentrated fluid that exits the element.

The mass transfer across an RO membrane can be described by the following formula:

$$N_A = L \times NDP \quad [2.1.6]$$

Here, N_A (gfd) is the water flux that passes through the membrane, and L is the permeability coefficient.

RO membranes are composed of different materials including polymers that are layered in a web-like structure through which water and other particles must exit to reach the permeate side through various pore-sized passages (approximately 0.1nm).

Depending on the molecular weight cut-off of the membrane, particles are physically retained on the membrane surface ³⁷. These membrane properties make RO membranes a very important tool for producing potable water from the ocean or brackish water.

The production of potable water is accomplished by the reduction of salts, which almost eliminates inorganic constituents, and the removal of NOM. The removal of NOM from the surface water is critical for the producing potable water because NOM controls the formation of DBPs, such as trihalomethanes and haloacetic acids, in the presence of free chlorine. However, the permeation of water through an RO membrane occurs in three stages: adsorption of water onto the membrane, diffusion in the membrane, and desorption from the membrane surface ³⁷.

The basic mechanism responsible for the separation of solutes from water molecules during RO operation is rooted in the solubility–diffusivity model (affected by polarity, charge, and size), along with electrostatic repulsion at and near the membrane surface. The RO membrane structure consists of ionized functional groups, such as carboxylates, which makes these membranes negatively charged during operation. RO membranes consequently have the ability to reject both negatively and positively charged ions to maintain electroneutrality in the feed and permeate water ⁸⁹. In addition, the presence of polar functional groups in the RO membrane structure increases the solubility of polar compounds like water over nonpolar compounds. Because of this mechanism, a high water flux is achieved through the membrane.

The rejection capability of the GFWTP RO system membrane was evaluated in terms of the percent salt rejection values. Salt rejection is expressed as follows:

$$\text{Rej} = 1 - \frac{C_P}{C_F} \quad [2.1.7]$$

Here, Rej = rejection, dimensionless (expressed as a fraction)

C_P = concentration in the permeate, mg/L or mol/L

C_F = concentration in the feed water, mg/L or mol/L

2.2. Background

RO membranes can become susceptible to fouling and scaling by various mechanisms. Although RO membrane performance decreases with time, the water flux through RO membranes is often limited by temperature, pressure, feed water velocity, and the very low hydraulic permeability of dissolved colloidal materials (CMs) precipitating on the RO membrane surface. According to Howe et al., the primary sources of fouling are particulate matter, biological matter, inorganic precipitates, and oxidized soluble metals ⁸⁹.

For evaluating the actual decline in the performance of RO systems caused by fouling, the permeability rate and system salt passage must be compared to the baseline condition in the membrane in its clean state. However, two opposing forces contribute to the rate at which water flows through a semipermeable membrane: (1) concentration gradient and (2) pressure gradient. The design of an RO plant presents equations that incorporate correction factors for both temperature and pressure during a procedure that normalizes membrane performance ⁷⁸. The unsteady conditions that occur over time, caused by changing the operating parameters (e.g., temperature, feed TDS, permeate flow, and recovery) and fouling, require the normalization of RO data such that it can be compared to the baseline. This will help determine whether changes in membrane performance are caused by fouling, changes in the operating conditions, or by membrane damage. The equations for standard membrane performance are as follows:

$$Q_{P,S} = Q_{P,M} (TCF) \frac{NDP_S}{NDP_M} \quad [2.2.1]$$

$$SP_S = SP_M \left(\frac{NDP_M}{NDP_S} \right) \left(\frac{C_{FC,S}}{C_{FC,M}} \right) \left(\frac{C_{F,M}}{C_{F,S}} \right) \quad [2.2.2]$$

where, Q_p = permeate flow rate, m^3/h

TCF = temperature correction factor, dimensionless

NDP = net driving pressure, psi

SP = salt passage, percentage

C_F = feed concentration, mg/L

C_{FC} = average feed-concentrate concentration, mg/L

Subscript S-system

Subscript M-membrane

Salt passage is defined as the ratio of permeate concentration to feed concentration:

$$SP = \frac{C_P}{C_F} = 1 - Re_j \quad [2.2.3]$$

As the temperature increases or decreases, fluid viscosity as well as membrane morphology and structure are affected. However, the relationship among flux, temperature, and material morphology varies with individual membranes, and the relationship is provided by the manufacturer. The following relationship is typically utilized for the calculation of TCF if it is not provided:

$$TCF = (1.03)^{T_s - T_m} \quad [2.2.4]$$

where T = temperature, °C; the standard temperature for RO operation is 25 °C.

During the RO process, the chemical constituents and dissolved materials are transported to the surface of the membrane by several mechanisms such as advection and sorption⁸⁹. Furthermore, because of the limited porous properties of RO membranes, particles accumulate on the RO membrane surface and form a cake layer. This cake layer in thickness and degree of compaction and increases the resistance across the membrane over time, resulting in low permeate flow and poor water quality⁶⁹ (Figure 2.1.4 below).

The aggregation of colloid particles (less than approximately 1 μm) on the surface of a membrane can be attributed to both van der Waals attractions and electrostatic interactions between the surface and particles ⁷². The sticking probability of this behavior is dependent on the chemistry, geometry, temperature, and hydraulic conditions (fouling mechanisms) of the surface water.

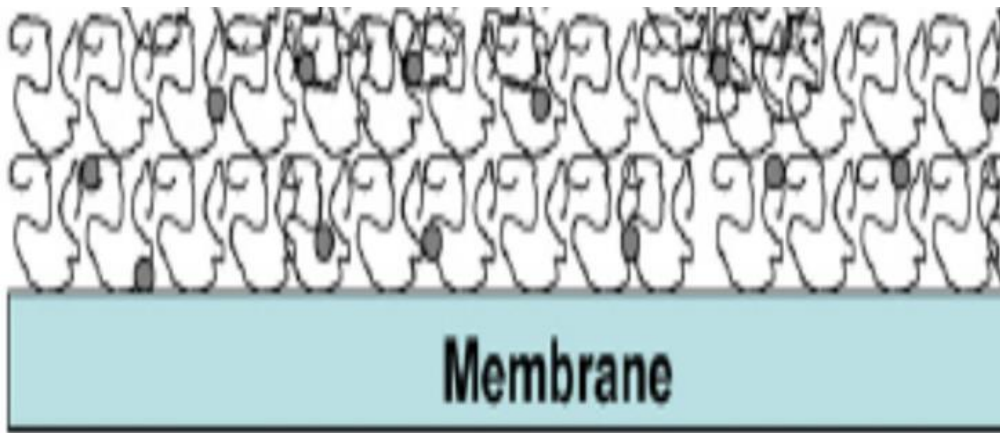


Figure 2.1.4. Illustration of a compact fouling layer formed in the presence of Ca^{2+} ⁸⁸.

The process of membrane scaling (microfouling) involves three major stages: electrostatic attraction between oppositely charged ions, leading to precipitation, continuous and ordered nucleation of the precipitated ions, and crystallization of nuclei formed during the second stage. According to Howe et al., the first two stages are reversible and can be restored to their original starting point using appropriate techniques like permeate flushing and chemical cleaning ⁸⁹. The third stage, crystallization, leads to irreversible membrane fouling if not controlled in its early stages ³⁷. Membrane fouling, as well as the characteristics of the foulants, can be determined by analyzing the

composition, water chemistry, temperature, mode of operation, initial permeate flux, and cross-flow velocity of the feed water⁷⁰.

2.2.1. Concentration polarization

During the first few hours of desalination, there is an increase in the ratio of the concentration of solutes on the surface of the membrane to that in the bulk solution; this process is called CP. Typically, CP occurs when salt ions accumulate on the surface to form a thin boundary layer^{44,51}. As the permeate is removed by adsorption through the surface of the membrane, CP (macrofouling) and osmotic pressure at the membrane surface increase while flux decreases because of the resistance of a gel-like layer⁷². CP can be viewed as the vehicle for the transportation of fouling, in the sense that immobile solids accumulate at the interface between the solution and membrane, which eventually accelerates fouling.

In RO systems, CP results in an increase in solute concentration at the membrane. In their study, Ng and Emlimelech suggested that CP contributes to the decrease in not only the permeate flux but also the rejection of trace organic compounds in RO membranes⁷⁴. They stated that the cake layer formed on the membrane surface creates hydraulic resistance and prevents diffusion back into the bulk solution, resulting in a reduced permeability rate and salt rejection. The increase in the concentration of colloids near the membrane surface affects the performance of the RO system in several ways:

1. Decrease in water flux caused by the increased pressure drop.
2. Decrease in separation efficiency caused by the increased solute flux and the decreased water flux through the membrane.

3. Increase in ion concentration in the bulk solution may allow the solutes to exceed their solubility limits, leading to precipitation and scaling.

Figure 2.2.1.1 shows the schematic of CP experienced by membrane elements during RO. As shown in the schematic, feed water flows parallel to the membrane surface on the left, while the permeate passes through the membrane on the right. As the feed solution flows toward the membrane surface, water passes through the membrane while increasing the concentration of the solutes rejected by the membrane, which begin to accumulate on the membrane surface and create a boundary layer. As the concentration of the solutes near the membrane surface increases, the solutes begin to diffuse back into the bulk solution. This takes place until equilibrium is reached between the amount of solutes on the membrane surface and the concentration of solutes in the feed water.

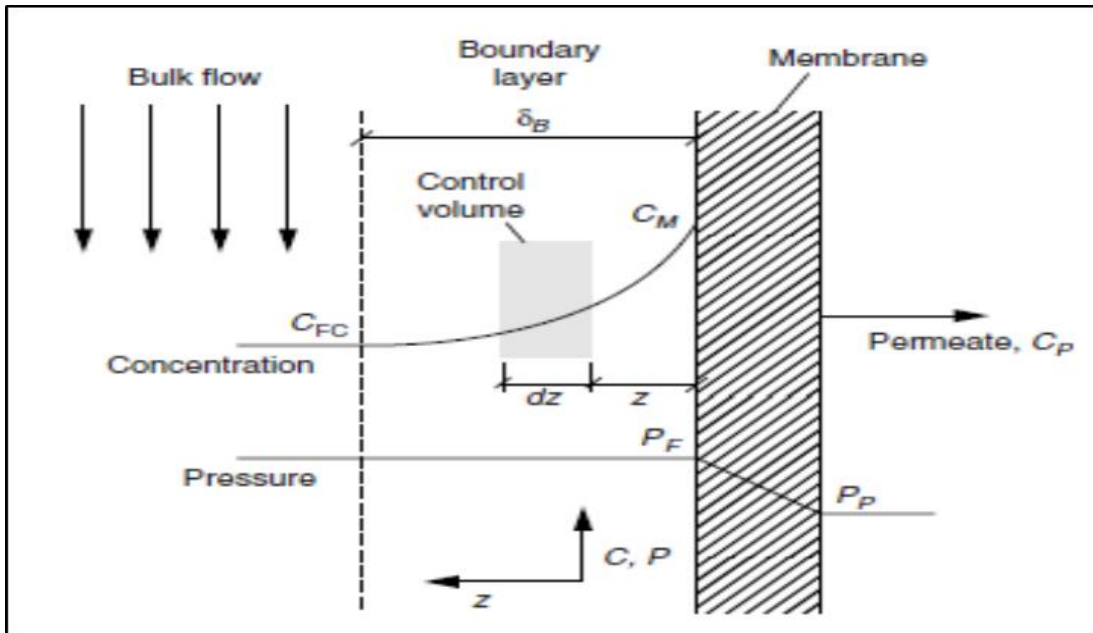


Figure 2.2.1.1. Schematic of concentration polarization ⁸⁹.

The salt flux toward the membrane surface because of the convective flow of water is described by this equation:

$$J_s = J_w C \quad [2.2.1.1]$$

Under continuous operation of an RO system, without mass accumulation in the steady state, solute flux toward the membrane is balanced by the diffusion of solute flux away from the membrane and by the passage of those solutes to the permeate side⁸⁹. This phenomenon can be described by the following expression:

$$[\text{accum}] = [\text{mass in}] - [\text{mass out}]$$

$$\frac{dM}{dt} = 0 = J_w C a - D_L \frac{dC}{dz} a - J_w C_p a \quad [2.2.1.2]$$

Here, M = mass of solute, g

t = time, s

D_L = diffusion coefficient of the solute in water, m^2/s

z = distance perpendicular to the membrane surface, m

a = surface area of the membrane, m^2

CP varies along the length of a membrane element and is expressed as the ratio of the concentration of solute on the membrane (C_M) to the concentration of solute in the feed-concentrate channel (C_{FC}) as follows:

$$\beta = \frac{C_M}{C_{FC}} \quad [2.2.1.3]$$

Here, β = concentration polarization factor, dimensionless⁸⁹.

2.2.2. Effects of inorganic scaling on RO performance

Scaling occurs when the concentration of salt in the RO feed water exceeds its solubility limit, leading to precipitates. Calcium (Ca^{2+}) and magnesium (Mg^{2+}) are the most common ions in natural waters, and their interaction with other species can lead to

adverse effects due to the potential fouling of an RO membrane during adsorption. The control of inorganic scaling on RO and other membrane filters is critical for maximizing the productivity of these membrane systems.

The scaling of membranes by compounds such as CaSO_4 , CaCO_3 , BaSO_4 , and SrSO_4 is attributed to the precipitation of these soluble salts. The risk of scaling also depends on the recovery rate of the element or system and the rejection or removal of the species by the membrane systems. If the amount of these salts in an RO concentrate increases, their solubility at ambient temperature (25 °C) and ionic strength increases, leading to scale formation. Solubility is an important property that affects the behavior of a chemical species. Highly soluble compounds exhibit a low tendency for adsorption when they come in contact with a membrane surface. The solubility of solids in a liquid typically increases with increase in temperature, while the opposite is true for the solubility of gases in liquid, because of the decrease in water vapor pressure at the gas-liquid interface ⁹². As a result, the decrease in permeability, increase in feed pressure for maintaining the productivity and recovery of water, and deterioration in water quality are observed. Energy will thus be expended, and cleaning might not be effective for the removal of scales after they are formed.

The ability to continuously monitor, predict, and control scaling is imperative for the design of a new water treatment plant. For example, for controlling CaCO_3 scaling, studies have demonstrated that the pH for the saturation of CaCO_3 (pH_s) should not exceed the pH of the concentrate stream (design recovery). The pH_s of CaCO_3 represents the pH of water if it were at equilibrium with solid CaCO_3 . pH_s can be estimated as follows ⁹¹:

$$pH_s = pCa + pAlk = K \quad [2.2.2.1]$$

Here, pH_s = the pH at which $CaCO_3$ saturation occurs

pCa = negative logarithm of the molar calcium ion concentration

$pAlk$ = negative logarithm of the molar bicarbonate ion concentration

HCO_3^- = molar bicarbonate ion concentration; at pH less than 9, it is approximately equal to alkalinity, in mg/L as $CaCO_3$, divided by 50,000

K = constant related to ionic strength (TDS) and temperature.

The scaling propensity of $CaCO_3$ during membrane filtration can be determined by calculating the Langelier Saturation Index (LSI) of the feed water and RO concentrate. Positive LSI values possibly indicate the scaling and corrosiveness of $CaCO_3$, while negative LSI values possibly indicate the presence of dissolved $CaCO_3$ ⁹¹. LSI can be estimated as follow:

$$LSI = pH_c - pH_s \quad [2.2.2.2]$$

Here, pH_c is the pH of the RO concentrate.

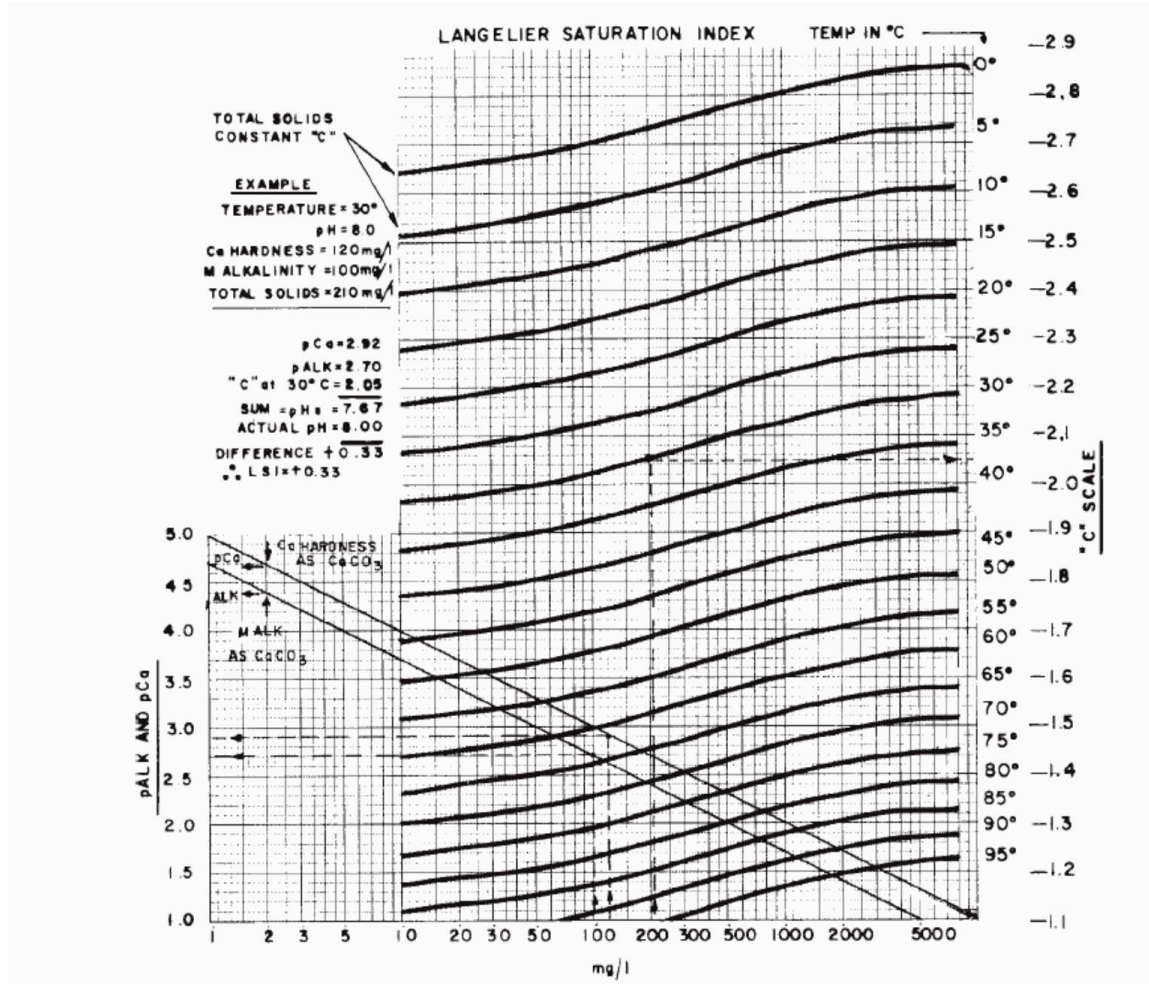
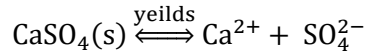


Figure 2.2.2.1. Langelier Saturation Index Nomograph⁹¹.

The scaling potential of sparingly soluble salts can be determined by comparing the salt solubility product (K_{sp}) at the temperature of interest to the ionic product (IP) of each salt in the source water, RO feed water, and RO concentrate. For example, if a slightly soluble compound such as $BaSO_4$ is added to water, equilibrium exists between the solid and ions in solution⁸⁹. The more soluble the compound, the more ions are generated in solution and the greater the solubility product. The precipitation reaction for a typical salt is as follows:



Hence, K_{sp} can be calculated as follows:

$$K_{\text{SP}} = \{\text{Ca}^{2+}\} \{\text{SO}_4^{2-}\} = \gamma_{\text{Ca}}[\text{Ca}^{2+}] \gamma_{\text{SO}_4} [\text{SO}_4^{2-}] \quad [2.2.2.3]$$

Here, K_{SP} = solubility product

$\{\text{Ca}^{2+}\}, \{\text{SO}_4^{2-}\}$ = activity of calcium and sulfate

$[\text{Ca}^{2+}], [\text{SO}_4^{2-}]$ = concentration of calcium and sulfate

$\gamma_{\text{Ca}}, \gamma_{\text{SO}_4}$ = activity coefficients of calcium and sulfate

The increase in calcium or a slight increase in sulfate because of the addition of sulfuric acid will increase the supersaturation of the solution while decreasing the solubility of the scale-forming compound.

The scaling potential of an ion can also be predicted by comparing the K_{sp} and IP (actual concentration present). If the IP of a compound is greater than its K_{sp} , the solution is said to be supersaturated, and there is a higher possibility that the compound will precipitate. Conversely, if the IP of the compound is less than its K_{sp} , the compound is said to be unsaturated, and there is a lower possibility that the compound will precipitate in the solution.

The presence of ions in RO feed waters tends to lower the ionic strength of dissolved organic matter (DOM), which increases their size during the reaction and decreases their solubility⁸³. Studies have reported that Ca^{2+} can easily bind with DOM (making the resulting compound insoluble) and form a bridge between the negatively charged molecules and the membrane surface. This interaction will also compress the electrical double layers (EDL) at the membrane surface, making it easier for the chemical

species to interact with the membrane⁸³. These characteristics constitute a favorable environment for fouling. Furthermore, the reduction in the ionic strength of foulants, such as DOM, in the RO feed water can also increase the fouling tendencies of the foulants. This is attributed to the fact that solubility is a function of ionic strength, which can increase the tendency of DOM to adsorb onto a membrane surface, as indicated by previous studies^{7, 13, 15, and 70}.

2.2.3. Effects of organic fouling on RO performance

NOM originates from the combination of different natural resources that embody biological matter of different origins. Biological matter can be classified into four types of compounds: carbohydrates, lipids, amino acids, and nucleic acids. Conversely, NOM can exist in two forms: DOM (approximately 80%), which is negatively charged, and particulate organic matter (approximately 10%), which in combination are referred to as TOC⁸³. DOM measured as dissolved organic carbon (DOC) is defined as the fraction of NOM that can pass through a filter having a pore size of 0.45 μm . The fouling of RO membranes by DOM is a critical concern for the membrane industry and is one of the industry's constraints for the application of RO systems during the treatment of water or wastewater. The characteristics of NOM, such as size (average molecular weight), functionality (carboxylic and phenolic groups), and structure (hydrophilic or hydrophobic content), affect biogeochemical processes. The characteristics of NOM are also important for water quality analysis and should be considered for the prediction of RO fouling⁷⁵.

According to Guo et al., 50% of DOC, a major fraction of NOM, consists of humic substances (HS)⁶⁹. It is imperative to understand the complex interactions between humic substances (a major foulant in membrane systems⁷¹) and RO membranes

for implementing preventive measures that will address organic matter pools in natural waters. Addressing this may mitigate the irreversible fouling tendencies observed in RO systems. HS can be classified into three types: humin (insoluble under any pH), humic acids (precipitates at $\text{pH} < 2$), and fulvic acids (soluble under all pH conditions)⁷¹. Studies have reported that fouling in RO membranes occurs at low pH and high ionic strength^{4, 7, 8, 9, 83, 89, and 90}. According to Shi et al., the reduction measured by the deprotonation of acidic functional groups in HS is attributed to low pH. This leads to reduced electrostatic repulsion and allows strong van der Waals forces between HS molecules, and these strong forces promote fouling tendencies⁷⁶.

Other studies have also stated that at low and very high pH, a humic solution tends to adsorb onto the membranes because of the reduction in repulsive forces between the membranes and humic substances^{11, 13, 26, and 78}. It was proposed that pH between 6 and 7 mitigates the possibility of fouling during RO. Conversely, under high ionic strength conditions, the hydrodynamic radius of HS is compressed, thereby allowing HS to diffuse through the pores of the membrane more easily. This adsorption onto pores results may result in the fouling of RO membranes⁷⁶.

Studies have indicated that pH significantly affects the behavior of NOM particles containing carboxylic acid groups, which lose their surface charge at low pH^{48, 51, 53, 58, and 64}. It is reported that at pH below 4 the molecular configuration of humic acid is modified, which significantly reduces the adsorption of humic acid during most effective water treatment. This is attributed to reduced inter-chain electrostatic repulsion and size as well as increased hydrophobicity, and allows for easier passage of these macromolecules through a membrane. The same reports have also indicated that high pH

promotes fouling at high calcium concentrations and calcite precipitates are easily formed, allowing for the adsorption of NOM particles on the membrane surface. It was thus concluded that the co-precipitation of complexes containing calcium and organics increases with increasing pH. Al-Amoudi and Lovitt have stated that, under high ionic strength conditions, the forces responsible for the structure of NOM are altered, resulting in the restructuring of NOM particles. The authors further state that the structure of NOM particles will linearly stretch at low concentrations, low ionic strength, and neutral pH ⁸⁶.

Figure 2.2.3.1 shows the impact of pH, ionic strength, and divalent cations on the promotion of membrane fouling by NOM. Among these three fouling conditions, the presence of divalent cations has major implications because they permit ionic bridging between NOM particles. The figure also shows that fouling by NOM occurs at a high permeation rate even under unfavorable fouling conditions such as low ionic strength, low levels of divalent cations, and high pH. It can be concluded that the rate of fouling depends on the relationship between permeation drag and EDL repulsion in feed water particles ^{67, 88, 94, 95, 97, and 98}.

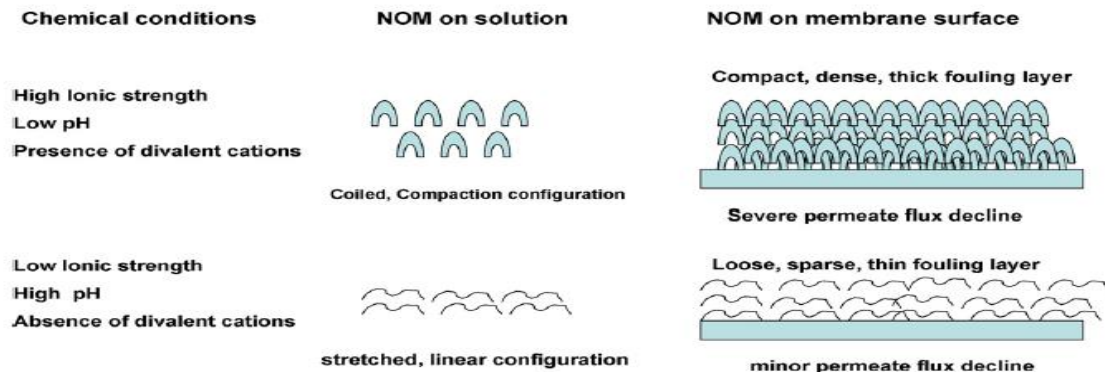


Figure 2.2.3.1. Schematic of the effect of solution chemistry on the configuration of NOM macromolecules in solution and on the membrane surface and the resulting effect on membrane permeate flux. Fouling by NOM, as described in the diagram, is applicable for permeation rates above the critical flux. The difference between the shown chemical conditions becomes less clear at very high permeate flux. At low permeate flux (below the critical flux), no significant fouling is observed for both conditions ⁸⁸.

2.2.4. Effects of silica complexes on RO performance

In certain areas of the world, including the western United States, silica is abundant in natural waters, with concentrations generally ranging between 20 and 60 ppm but reaching as high as 120 ppm. Silica has a significant impact on surface water chemistry ⁶⁵ and is one of the major foulants in the desalination of brackish water. Silica content between 30 and 120 mg/L limits the water recovery rate and poses a serious threat to RO systems when it is deposited on the membrane surface because of its difficult removal and control ^{65, 81}. Because of the insolubility of silica (hydrophobic) in water, whose concentration should not exceed 150 mg/L during water treatment, the recovery of an RO membrane is limited to below 75% ⁶⁵. Silica can be categorized into three forms: silicic acid (dissolved silica), which is the most soluble and reactive (e.g., silicates, $\text{Si}(\text{OH})_4$); colloidal silica (unreactive), which results from the polymerization of silicates; and particulate silica (e.g., clays, silts, and sands).

Issues such as precipitation and deposition of silica are commonly observed by most plant engineers and operators during RO system operation. Studies have shown that the concentration of total SiO_2 in feed waters cannot be used for predicting the scaling potential of an RO membrane^{65, and 85}. These studies indicate that the accumulation of unreactive SiO_2 on the membrane surface, with the help of mechanisms such as CP, can potentially increase RO operating parameters, such as temperature and ionic strength, in the presence of metal ions over time. This represents a significant research opportunity because of the potential for crystallization, which can become irreversible if not controlled in its early stages.

It is thus imperative to devise an effective strategy to limit the concentrations of unreactive silica (dissolved silica) and amorphous silicates within their solubility range, which will help control the concentration of SiO_2 in the RO membrane concentrate stream. The hydrolysis of silica–oxygen–silica bonds, which generates silicic acid and silicates in the aqueous phase, oxidation occurring during filtration, and CP, which can cause irreversible fouling, should be investigated. Preventive measures such as inhibition, which prevents the polymerization of soluble silica, and/or dispersion, which prevents silica particle agglomeration and in turn results in scale and fouling, should also be investigated⁷⁹.

Orthosilicic acid, which is the most prevalent form of silica, interacts with most metals to form metasilicic acids $(\text{H}_2\text{SiO}_3)_n$ at low n values. Although it is weak in nature, it dissociates at a pH of less than or equal to 6.5. Its presence in natural waters is attributed to the dissolution of siliceous rocks and minerals. According to Iler, silica particles tend to repel each other at pH 7; this repulsion decreases in the presence of salts,

which favor unreactive silica complex aggregation and gel formation ⁶³. Silicates of potassium and sodium are soluble, while those of iron, aluminum, and crystalline silica (typically observed in the bedrocks of the Red River basins) exhibit very low solubility and are unreactive.

Once the concentration of silica or silicate compounds increases in the bulk solution of the RO feed and scale begins forming on the membrane surface, they become less permeable, resulting in the increase in flux decline. The removal of scaling is difficult and expensive, and studies have indicated that the solubility of silica in the RO feed water is dependent on temperature and increases with pH ⁶⁴. For preventing membrane fouling by surface waters with high silica content, the effective control of silica depends on factors such as the polymerization and dispersion of silica species in water ⁶⁴. This research aims to inhibit polymerization, disperse precipitates of silica or silicate compounds, and increase the solubility of silica during CP in RO filtration.

Fouling by polymerized colloidal silica or silica gel, because of the polymerization of supersaturated silicic acid, in feed water occurs when its concentration is between 120 and 150 mg/L in the RO brine ⁶⁴. This reaction occurs more rapidly at higher temperatures (mostly during summer), but is significantly slower at lower temperatures (especially during winter). Studies have also indicated that the polymerization of silica at concentrations greater than 180 mg/L is not a function of temperature ^{65, and 85}. Multivalent metal ions such as Fe³⁺, Al³⁺, Ca²⁺, and Mg²⁺ (Al and Fe must not exceed 0.05 mg/L in feed water), which serve as catalysts in feed water, can absorb and complex with silica, which in turn will polymerize silica and can cause membrane scaling ⁹⁰.

It is thus imperative to monitor and control the concentration of these ions in the source water fed to the RO system for investigating the effects of silicate polymerization on the fouling of RO membranes. Recent studies have demonstrated that the reaction between $\text{Mg}(\text{OH})_2$ and silicate ions leads to the formation of magnesium silicate ($\text{MgO}:\text{XSiO}_2\cdot\text{H}_2\text{O}$) precipitates. These precipitates have been shown to be a major foulant because of their insolubility as well as temperature and pH ($\text{pH} > 9$) dependence^{65, and 85}. Therefore, the scaling potential of feed water is dependent on the pH and SiO_2 content in the concentrate.

2.2.5. Effects of suspended solids on RO performance

The presence of suspended solids in the feed water can decrease the overall performance of a membrane system. Moreover, the decreased loading rate of these solids can protect the membrane from fouling, thereby leading to a reduction in the required cleaning frequency. In the design of most water treatment plants, pretreatment for UF and RO is usually carried out to decrease the concentration of suspended solids and turbidity as well as the organics in the feed water to as low as 2 NTU and/or TOC removal of 40%. For water containing high turbidity and TOC, pretreatment such as coagulation–flocculation–sedimentation has been employed. This pretreatment improves the quality of feed water, leading to an increase in flux, and decreases the surface area of the membrane, which is required for producing quality water. Studies have shown that suspended solids, DOM, turbidity, and dissolved solids are the parameters of feed water mostly used for the prediction of fouling in membrane systems (UF/RO). Hence, indexes such as SDI and LSI are tools required for predicting the fouling potential of feed water

89, 90

2.2.6. Effects of water recovery on RO performance

In an RO system, water recovery can be defined as the ratio of permeate flow to the flow for a specific membrane. High water recovery leads to an increase in the concentration of ions on the membrane surface, while low water recovery leads to a decrease in the overall concentration of chemical species in the feed water. Recovery can be decreased by reducing the recycle feed flow.

Another method of increasing recovery is to increase operating pressure. A high operating pressure leads to the production of a high amount of permeate. If the feed flow is maintained close to its original level, then high recovery is achieved. High recovery can also be achieved by increasing the amount of concentrate that is recycled back into the feed flow by reducing the amount of concentrate that is discharged to waste. This reduction will then increase the volume of concentrate that is sent back to be filtered by the membrane. These operating conditions can provide a favorable environment for the fouling of RO membranes.

It is thus imperative to limit permeate recovery with the aim of mitigating precipitation. The allowable recovery in most RO systems is the highest possible recovery that can be attained before salts (called limiting salts) begin to precipitate⁸⁹. The allowable recovery that can be designed for any RO plant depends on the solubility limits of each salt in the concentrate stream that can be recycled for achieving high recovery. The highest concentration of solutes exists in the bulk solution of the tail element prior to water exiting the RO system. Therefore, the concentration of solutes in the concentrate stream is an indicator of the level of CP, and can be adjusted accordingly

⁸⁹.

The fouling tendency of RO feed water is assessed by an empirical test known as the silt density index (SDI). Although it has proven to not be a reliable predictor of the fouling propensity of water, it can provide a rough guideline for the acceptable quality of RO feed water. SDI is a timed filtration test conducted by applying a pressure of 30 psi to push water through a 0.45 μm membrane filter during three time intervals. The duration of the first interval is the time necessary to collect 500 mL of filtrate, after which the filtrate is allowed to run for another 15 min without measuring the volume (second interval). At the end of the second interval, 500 mL of filtrate is again collected for the third interval, and the time taken to collect the filtrate is recorded. SDI is then calculated from these time intervals ⁸⁹:

$$\text{SDI} = \frac{100(1 - t_1/t_F)}{t_T} \quad [2.2.6.1]$$

Here, SDI = silt density index, min^{-1}

t_1 = time required to collect the first 500 mL sample, min

t_F = time required to collect the final 500 mL sample, min

t_T = duration of the first two intervals (15 min)

The results from the SDI test may suggest the need to carry out pretreatment upstream of an RO system to minimize particulate fouling. An SDI of less than 5 is considered an acceptable threshold for an RO system feed water. An SDI of less than 5 indicates that the membrane will foul at a very slow rate. Coagulation–flocculation–sedimentation and pre-filtration through a 0.45 μm filter, which lower the colloidal concentration to an acceptable level, are considered necessary for the protection of the membrane elements.

CHAPTER III

PREVENTION TECHNIQUES FOR THE FOULING OF REVERSE OSMOSIS MEMBRANES

3.1. Introduction

During the first Grand Forks water treatment plant (GFWTP) pilot study, pretreatment operations were solely based on the production of consistent RO feed water. Therein, approximately 30% of total organic carbon (TOC) was removed during pretreatment and less than 3 NTU of turbidity was sent to the UF membrane filters. For achieving this goal, an average dose of 30 mg/L of polyaluminum chloride (PACl) was added to water at a flow rate of 55 gpm, a pH of 7, a floc time of 28.6 min, and a surface loading rate of 0.3 gpm/ft² during sedimentation. Because of these operational techniques, turbidity during the winter months averaged 1.80 NTU, while during the spring months, it averaged 3.85 NTU. Consequently, the TOC averaged 9.25 mg/L (28% removal) during the winter months and 6.25 mg/L (34% removal) during the spring months.

The primary objective of the different pretreatment stages is to lower the fouling propensity of surface water by removing suspended solids, reducing inorganic salts, reducing natural organic matter (NOM), reducing turbidity, and increasing the recovery rate in RO systems. This will extend the life span of the membrane and mitigate any fouling issues. The recovery of RO systems can range

between 35% and 90%, and is dependent on several factors, such as limitation of the recovery rate, osmotic pressure, fouling propensity, concentration polarization, and the solubility of dissolvable ions^{59, 39}. Scaling is caused by the presence of silica complexes and a high concentration of major ions such as Ca^{2+} , Mg^{2+} , Fe^{3+} , Al^{3+} , PO_4^{3-} , SO_4^{2-} , and CO_3^- in the feed water. Hence, when RO systems are not operated under appropriate conditions, colloidal fouling can occur. However, the different pretreatment stages upstream of an RO system can help prevent scaling in the presence of soluble salts⁷⁸. An effective method for removing silica and dissolved organic matter (DOM) from raw water is precipitation using PACl or ferric chloride (FeCl_3).

During filtration, as the water diffuses through the membrane, the concentration of the solute on the influent side continues to increase with time. Without a pretreatment stage, solubility decreases in the presence of inorganic salts, and insoluble metal silicates are formed under favorable alkaline environments, which precipitate to cause membrane fouling²⁰. The precipitation of these salts can be mitigated by reducing recovery rate, optimizing pH to induce a change in salt solubility, carrying out adsorption, applying antiscalants to prevent salt crystallization, or by a combination of these four techniques.

Another important process is the pretreatment filtration (UF) stage, which can help remove total suspended particles (such as particulate matter) and some DOM carried over from the sedimentation stage. In most cases, membrane filtration is necessary for surface waters. Although membrane filtration is important for preventing fouling, the application of disinfectants and biocides, such as chloramines, is also an important pretreatment step for preventing fouling caused by bacterial growth (bio fouling).

The prevention of irreversible colloidal fouling depends on operational conditions such as recovery rate, temperature, and hydrodynamic conditions⁷³. Pretreatment will minimize but not totally eliminate the potential for fouling. As is evident from the pretreated water chemistry of this pilot study pretreatment stage, DOM and fine colloidal particles such as silica, silicates, and clay still exist in the pretreatment effluent, which can contribute to RO fouling. Ng and Emlimelech have suggested that, rather than large particles, it is the small colloidal and dissolved particles that control the fouling tendencies observed in RO membranes⁷⁴.

3.2. Coagulation–Flocculation–Sedimentation

The process of coagulation–flocculation–sedimentation is primarily based on the principles of electrical charge, van der Waals forces, and gravity (Figure 3.2.1). In this process, it is imperative to understand the interactions between coagulants, chemicals, water, and various species in natural waters⁸³. The dissolved species may either be positive or negative, but the solution remains electrically neutral. When dissolved in water, most colloidal materials dispersed in water are negatively charged. Colloids with like charges tend to repel each other to remain dispersed in the feed water. The purpose of coagulation is to neutralize the charge and to allow colloids to come together during flocculation, so that van der Waals forces can overcome repulsion; the flocs consequently become larger, denser, and stronger.

The presence of suspended and colloidal (<1 µm) particles in water increases the turbidity and renders the treatment of water expensive and difficult. Removing them will increase the time required between cleanings and prolong membrane life. Although coagulants destabilize particles and must be removed during water treatment, they are

also effective agents for reducing the concentration of dissolved constituents (such as DOM).

Coagulation can simply be defined as a process in which flocc-forming chemicals are added and rapidly mixed with water or wastewater for the destabilization of colloidal particles, making them enmesh and clump together to form insoluble macro-flocs.

Flocculation is conversely the process of gently stirring the rapidly mixed combination of wastewater or water and coagulants for allowing the destabilized colloidal particles to aggregate, forming a rapidly settling macro-floc⁹³. Next, the aggregated flocs of colloids and NOM are removed by gravity sedimentation. In this process, hydrogen ions are released and react with the alkalinity in water. It may be beneficial to maintain pH in an optimal range to reduce the energy barrier between colloids with the aim of allowing the particles to come together and aggregate. Alkalinity may need to be increased to prevent pH depression. Acid addition may be needed to reduce the pH to an optimal value. As depicted in Figure 3.2.1 coagulation, flocculation and sedimentation are the three important pretreatment techniques applied during water treatment.

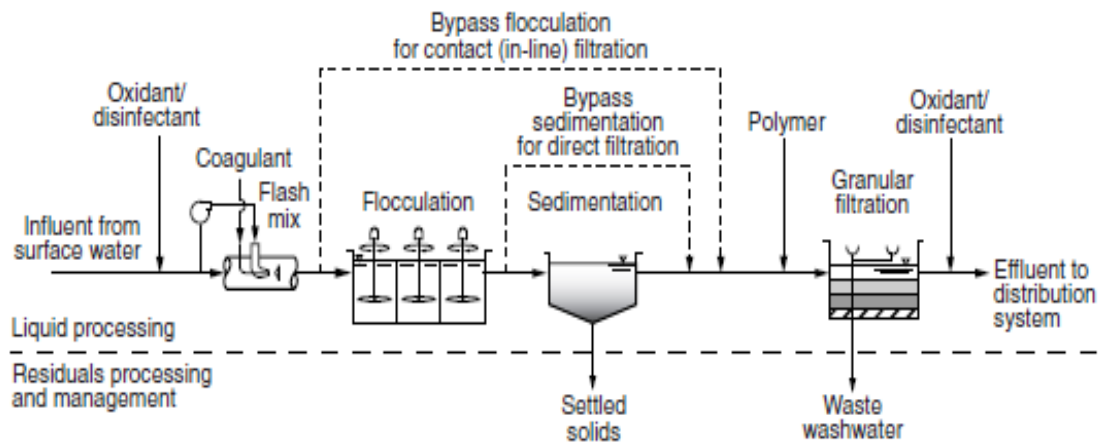


Figure 3.2.1. Typical flow diagram for a water treatment process employing coagulation (chemical mixing) with conventional treatment, direct filtration, or contact filtration ⁸⁹.

Coagulation can occur in four ways: electric double layer (EDL) compression caused by increased ionic strength in solution; adsorption and charge neutralization; adsorption and bridging when Al^{3+} neutralizes negatively charged particles by adsorbing them onto its surface; and sweep floc (enmeshment in precipitate), which occurs because of oversaturation of the solution containing coagulants ⁸³.

Particles in surface water are classified as hydrophobic or hydrophilic. Because of their low affinity for water molecules and because they are thermodynamically unstable, hydrophobic particles tend to aggregate and settle over time. Unlike their hydrophobic counterparts, hydrophilic particles such as clay, humic acids, silica, and hydrated metal oxides exhibit very high affinity for water molecules. Particles that are hydrophilic in nature exhibit surface charge (electrical property), which contributes to their instability in water, causing them to remain suspended without aggregation. The electrical properties of most particles manifested in four ways: (1) isomorphous replacement; (2) structural

imperfection; (3) preferential adsorption of specific ions; and (4) ionization of inorganic surface functional groups ⁸⁹.

In natural waters, the pH corresponding to a surface charge of zero is defined as the zero point of charge (ZPC). However, pH above the ZPC will have a negative (anionic) surface charge, while pH below the ZPC will have a positive (cationic) surface charge. For example, Figure 3.2.2 shows that the ZPC of silica is pH 2, while the ZPC of alumina is pH 9. Most particles in natural water have a resultant negative charge ⁸⁹.

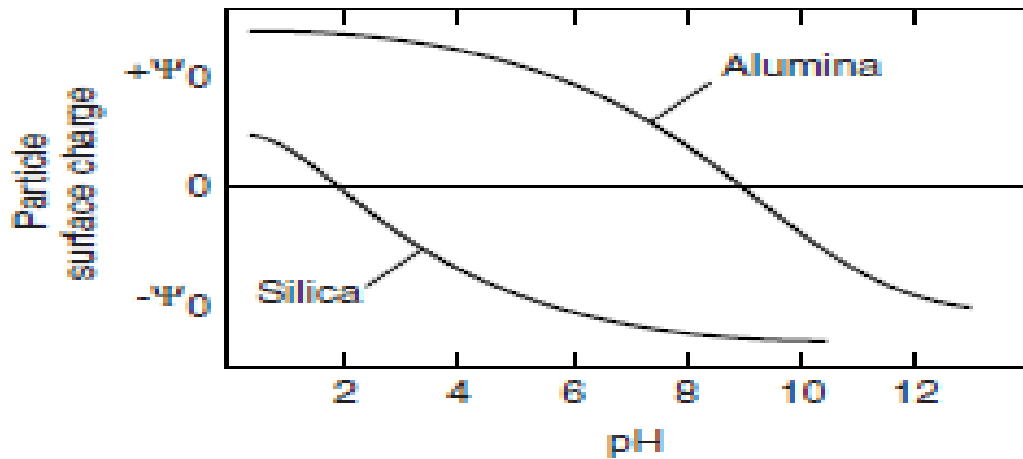


Figure 3.2.2. Variation in particle charge with respect to pH ⁸⁹.

With the above principle in mind, negatively charged particles in surface water are attached to positive ions to satisfy their electroneutrality. Figure 3.2.3 shows the interactions between negatively charged particles and cations, which form a fixed adsorption layer (0.5 nm in thickness, known as the Helmholtz layer) ⁸⁹. To the right of the Helmholtz layer are unstable but moving net negative charges and electric fields, which attract cations and repel anions (transported to the Helmholtz layer by diffusion). This process continues until surface charge and electric potential are eliminated, and

electroneutrality is satisfied. These layers are together known as the EDL (diffuse layer and the Helmholtz layer).

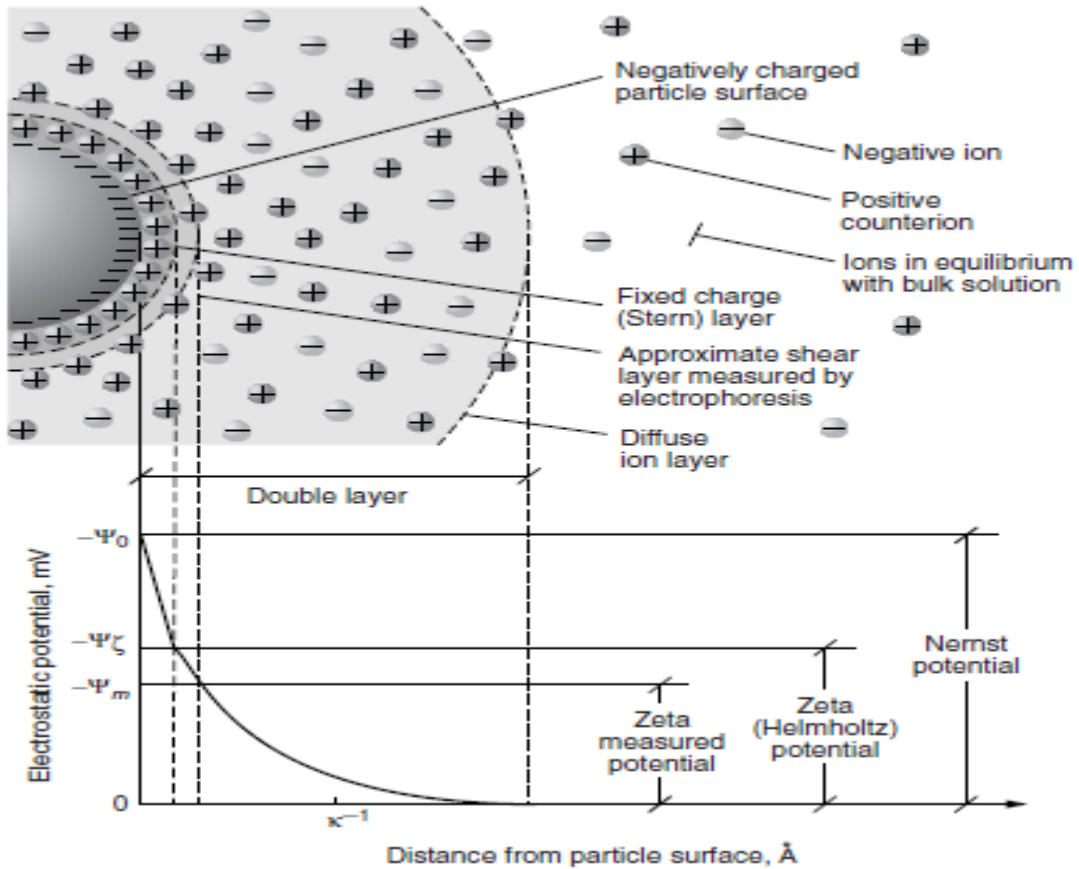


Figure 3.2.3. Structure of the electric double layer. Notably, the potential measured at the shear plane is known as the zeta potential. The shear plane typically occurs in the diffuse layer⁸⁹.

As mentioned in the introduction, the van der Waals force is responsible for the potential for destabilizing particles in natural waters. This force originates from magnetic and electronic resonance (attractive and repulsive) interactions between particles in water. However, most particles in natural waters exhibit a negative surface charge; therefore, the stability of particles in suspension is due to electrostatic repulsion. For

destabilizing particles and permitting the van der Waals force to bring the particles together by flocculation, the repulsive energy barrier between the interacting particles must be overcome. Reducing or entirely eliminating this energy barrier will give the particles the opportunity to aggregate ⁸⁹.

For overcoming this energy barrier for particle destabilization, the EDL must be compressed using coagulating chemicals. When coagulating chemicals that contain polymers, such as PACl, are introduced into natural waters during pretreatment, they destabilize particles by adsorbing and neutralizing oppositely charged particles. Three steps occur during coagulation: (1) hydrolysis and polymerization of metals ions, (2) adsorption of hydrolyzed products onto the surface of the particle, and (3) neutralization of charges ⁸⁹.

Studies have shown that, depending on the feed water chemistry, the concentration of coagulants during coagulation should not exceed 35 mg/L, and sometimes is less than 10 mg/L ^{62, 61, 46, 43, and 57}. It is also reported that the coagulant dose can have either a positive or a negative effect on the membrane. According to Howe & Clark, low residual coagulant doses significantly increase the fouling potential of a membrane ⁸³. Increased doses significantly decrease fouling, especially in the presence of humic substances. The selection of an appropriate coagulant chemical and its dose for pretreatment depend on economics (chemicals used as coagulants can be expensive) and the parameters of raw water such as alkalinity, pH, temperature, turbidity, and total organic carbon (TOC).

A recent study was conducted at the GFWTP to optimize the PACl coagulant dose. After applying a dose of approximately 35 mg/L PACl, the effluent water exhibited

appreciable removal of TOC and turbidity. As the concentration of PACl (a coagulant with a polymer, which adds density to slow-settling flocs) was increased from 35 mg/L to 90 mg/L, the TOC and turbidity significantly decreased, and Al residues (between 0.01 mg/L and 0.03 mg/L) were detected in the pretreatment stage effluent. For instance, Figure 3.2.4 shows that aluminum and iron form insoluble precipitates, and the particles become entrapped in amorphous precipitates when higher doses of coagulant chemicals are used ⁸⁹. Figure 3.2.4 shows the plot of log molar concentration of metal coagulant salts species versus pH. As can be observed from the figure, aluminum and ferric hydroxides precipitate within the shaded region. The shaded region also corresponds to the pH and dose ranges required for achieving sweep coagulation ⁸⁹.

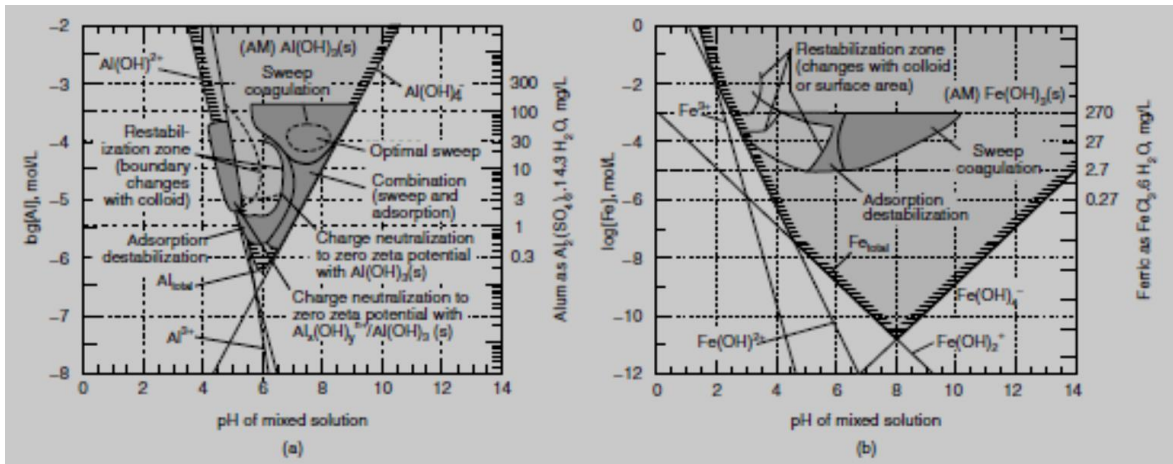
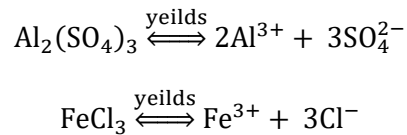


Figure 3.2.4. Solubility diagram for (a) Al(III) and (b) Fe(III) at 25 °C. Only mononuclear species have been plotted. The metal species are assumed to be in equilibrium with the amorphous precipitated solid phase ⁸⁹.

For preventing membrane fouling, it is important for the concentration of Al carryover in the RO feed water to be below 50 µg/L ⁸⁰. Aluminum in RO feed water is colloidal (rather than ionic) in nature and will react with ambient silica, DOM, and

components of antiscalants to form potential foulants in the RO concentrate ⁸⁰. When coagulant salts such as Al³⁺ and Fe³⁺ are added to water, they are dissociated and hydrated to form aquo-metal complexes. The dissociation of the metals is expressed as follows:

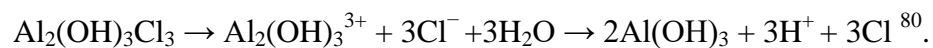


In the presence of Al³⁺ and at pH greater than or equal to 7, silicic acid (a prevalent form of silica) dissociates and forms the silicate anion, which precipitates to form aluminum silicate ⁸⁰. Also, as shown in other studies, in the presence of Al³⁺ at pH greater than or equal to 7, fulvic acids (a prevalent form of DOM) dissociate and form the fulvate anion, which precipitates to form aluminum fulvate ⁸³. The formation of these compounds on the membrane surface can lead to the scaling of silica and organic fouling of the RO membrane. Silicates can also precipitate (insoluble silicates) in the presence of divalent and trivalent cations such as Ca²⁺, Fe³⁺, and Mn²⁺. Furthermore, studies have also indicated that the simultaneous presence of Al³⁺ and Fe³⁺ with silicic acid increases the precipitation of this acid below its saturation concentration. Therefore, it is imperative to keep these materials as soluble as possible in RO feed and ensure that the Al³⁺ and Fe³⁺ concentrations are below 0.05 mg/L.

An important part of RO process operation optimization should include the frequent testing of Al³⁺ and Fe³⁺ to ensure that their levels are below 0.05 mg/L. The source of Al³⁺ could be raw water or from the addition of coagulant chemicals (such as PACl) during pretreatment. Although significant removal of TOC and turbidity is observed on increasing the coagulant dose, the presence of Al residues in pretreatment effluent (PT-

Eff) is due to the formation of Al complexes with sulfate, organic compounds, and silicates⁸³. As fouling due to metal silicates possibly occurs through chemical reactions and precipitation (scaling), the PACl dose should be lowered as this is economical in the long run. Also, coagulant performance should be optimized by lowering the pH of water by adding sulfuric acid, which is cheaper than PACl. Feed water acidification below pH 7 increases the solubility of the metal silicate with the aim of preventing or mitigating the membrane scaling tendency. Preventive acid cleaning and the use of antiscalant chemicals are also possible measures for preventing scaling by metal silicates.

The effectiveness of a coagulant also depends on the pH and alkalinity of the raw water source. When PACl is added to water, it typically hydrolyzes between pH 5.8 and 7.5 to form Al(OH)₃ flocs and hydrogen ions. The pH of the source water for the GFWTP is greater than 8 and contains significant alkalinity, and hence acidification is required for decreasing its pH. Acidification is a process in which hydrogen ions are released during hydrolysis, which then react with the alkalinity in water to reduce its pH. During the hydrolysis of PACl, three hydrogen ions are released:



Lowering the pH of the feed water increases the solubility of Al during coagulation⁸⁰. Acidification can prevent the association of silica or fulvic acid in the RO feed water with aluminum to form aluminum silicates or fulvates, respectively that can foul the membrane^{71, 78, 80, 82, 84, 87, and 89}. On the contrary, soluble Al³⁺ can precipitate or co-precipitate with negatively charged DOC, which can then be easily removed during pretreatment and using UF. For effective and complete coagulation, the concentration of

alkalinity must supersede the amount of alkalinity neutralized by the acid released from the coagulants.

According to a recent study, coagulation, flocculation, sedimentation followed by ultrafiltration has been an effective and successful pretreatment method for mitigating the fouling experienced during desalination using an RO membrane⁸⁸. This coagulant removes contaminants and forms a cake-like structure that is porous enough to not block the pores of the membrane and decrease the filtrate flux. The authors of these studies have concluded that coagulation does not necessarily prevent fouling; instead, it slows down the mechanisms that encourage irreversible fouling⁸³. In their critical review of RO desalination, Greenlee et al. stated that coagulants and antiscalants cannot be applied in the same line because they can easily react to form foulants³⁷. Instead, it was proposed that coagulants should be applied upstream of the pretreatment membrane, while antiscalants should be applied in line between the pretreatment membranes and the RO membranes.

3.3. Effect of the UF Stage on RO performance

Membrane filtration methods, such as ultrafiltration (UF), are membrane-based physicochemical processes used for removing microorganisms and other particles in natural waters. Unlike RO membranes, UF membranes, which are typically less than 1 mm in thickness, are composed of materials exhibiting high porosity, narrow pore distribution, or sharp molecular weight cut-off. They also exhibit good polymer flexibility, permanent hydrophilic characteristics, a wide range of pH stability, good chlorine tolerance, and high polymer mechanical strength and durability^{19, and 31}. UF membranes are fabricated in two geometric forms: hollow fibrous or tubular. As can be

observed in Figure 3.3.1, in the operation of a pressure-driven UF membrane, the filtration flow path can be inside-out or outside-in. Inside-out operation affords the flexibility of operating in cross-flow mode, which possibly permits a higher flux while filtering feed water having high turbidity. In contrast, outside-in operation can produce more filtrate when operating at the same flux rate. The blue and red arrows represent the filtrate and retentate, respectively (see Figure 3.3.1).

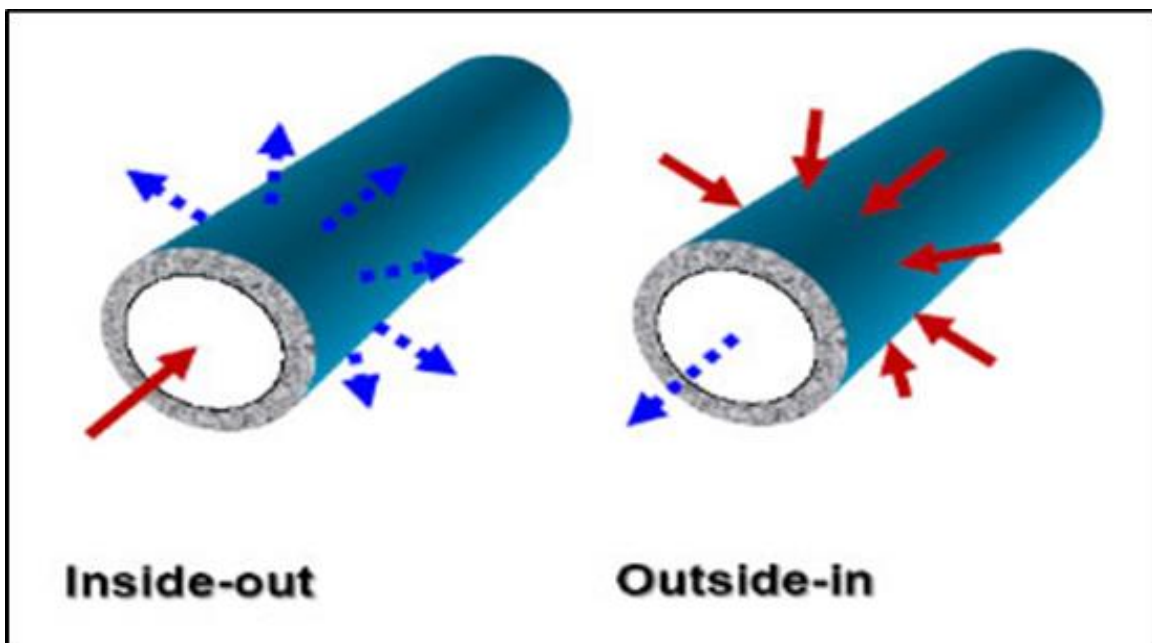


Figure 3.3.1. UF membrane system operation ¹⁰⁸.

Pressure-driven UF membranes exhibit a continuous forward-flow process for producing permeates, which takes between 15 and 60 min. For removing the foulants from the membrane surface, a backwash of 30 to 60 s is required every 15 to 60 min. Figure 3.3.2 shows the active and supporting layers of an asymmetric membrane, which appear similar to a thin skin with low porosity and very small voids. These membrane characteristics are responsible for significant resistance to flow, which can be minimized

by making the active layer as thin as possible. To prevent membrane clogging, membrane manufacturers add active layers on both sides of the membrane with a supporting layer in between the two active layers⁸⁹. Chemically enhanced backwash is employed for 1 to 15 min once or twice a day for removing foulants that cannot be removed by regular backwash. In addition, a maintenance wash using chlorine and acid is carried out for an hour once every 72 h for protecting the membrane from biofouling and colloidal fouling. The optimization and implementation of techniques are critical when trying to prevent fouling in membrane filters such as UF.

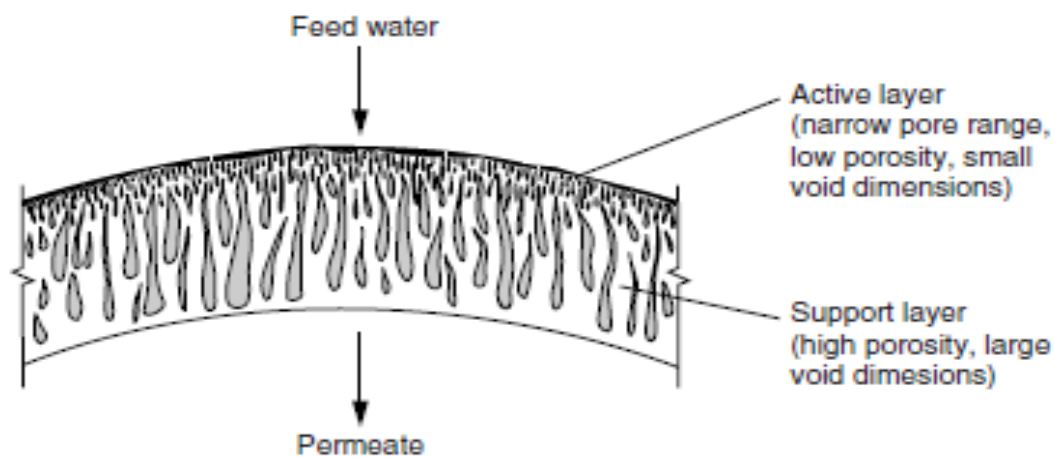


Figure 3.3.2. Structure of an asymmetric UF membrane⁸⁹.

Besides using conventional pretreatment that employs chemicals to nullify the threat posed by complex feed water, several pilot studies of membrane filters with small pore size have been carried out for pretreating RO feed water. These pilot studies have demonstrated the importance of installing UF modules for the removal of CM, DOM, and suspended solids, which will then reduce the fouling propensity of the feed water in an

RO system^{53, 54, 66, 50, 49, 45, 55, 58, 38, 41, and 67}. Studies have also shown that membrane pretreatment will lower the turbidity of feed water to less than 0.05 NTU and reduce the SDI to less than 2^{89, 55, 58, 49, and 41}. Reduction in turbidity and TOC by membrane pretreatment will reduce the frequency with which the RO membranes need to be replaced, thereby reducing the operating costs of the system.

3.4. Effects of antiscalants on RO performance

During pretreatment, antiscalant chemicals are used for reducing the nucleation, via adsorption onto the surface of the membrane and crystals, of precipitates, thereby preventing the formation and growth of crystals. This process allows ions to repel one another to prevent irreversible fouling. In cases with high ion concentrations, these antiscalants cannot totally prevent membrane scaling, and, if overused, the antiscalants themselves can become membrane foulants by promoting precipitation and bacterial growth^{37, 46, 52, 47, and 42}. For achieving appropriate floc formation and filter performance, it is thus imperative to optimize the doses of the chemical reagents used during pretreatment.

3.5. Effects of membrane cleaning on RO performance

Membrane remediation is usually conducted by chemical cleaning. Membrane cleaning is classified into chemical and physical methods. Physical methods involve the use of hydrodynamics under varying temperatures conditions, which will enhance the extraction of foulants from the membrane surface. On the other hand, chemical cleaning involves the use of chemical(s) to reverse the interactions between foulants and the membrane surface while favoring electrostatic repulsive forces between the solute–solute and solute–membrane surface⁷⁶.

Membrane cleaning requires the combined use of physical and chemical methods, such as turbulence, acidic agents, surfactants, metal chelating agents, alkalis, and oxidants such as sodium hypochlorite, chloramine, or potassium permanganate. Acids include acetic acid, hydrochloric acid, phosphoric acid, sodium hydrosulfate, and sulfamic acid, while alkalis used in membrane cleaning include sodium lauryl sulfate, sodium hydroxide, and sodium ethylenediaminetetraacetic acid (EDTA)^{37, and 59}. Table 3-1 shows the different chemical agents used for different foulants on different types of membranes. It also lists the doses of the chemical reagents recommended by various membrane manufacturers. The choice of chemical cleaning combination depends on the chemistry of the feed water and membrane type. Acid cleaning has been demonstrated to be effective for reducing scaling from compounds such as CaCO_3 , while caustic cleaning is said to be effective for removing organics⁹⁹.

Table 3-1. Chemical cleaning agents recommended by different manufacturers ⁸⁶.

Type of foulant	Type of membranes					
	DuPont B-10'	FilmTec FT-30	Fluid System	Nitro Denko	Toyobo	Toray
CaCO ₃	HCl at pH 4, citric acid (2%w) pH 4 (NH ₄ OH), Nutek-NT 600 (5%w), citric acid (2%w) + Na ₂ EDTA (2%w), pH 4 (NH ₄ OH)	HCl (0.2%w), phosphoric acid, H ₃ PO ₄ (0.5%w), citric acid (2%w), pH 4, sulfamic acid, NH ₂ SO ₂ H (0.2%w)	Citric acid (1%w), pH 2.5	Citric acid (2%w) pH 4 (NaOH)		Citric acid (1–2%), pH 2.5-4 (NH ₄ or NaOH), ultrasil 70 0.5% pH 2-2.5, peracetic acid 100–200 ppm
CaSO ₄ /BaSO ₄ SrSO ₄ /CaF ₂	Citric acid (2%w) pH 8 (NH ₄ OH), EDTA (1.5%w), pH 7–8 (NaOH/HCl), sodium hydrosulfite, Na ₂ S ₂ O ₄ (1%w)	HCl (0.2%w), phosphoric acid, H ₃ PO ₄ (0.5%w), Citric acid (2%w), pH 4, sulfamic acid, NH ₂ SO ₂ H (0.2%w)		Sodium tripolyphosphate, STP (2%w) + Na ₄ EDTA (0.85%w), pH 10 (H ₂ SO ₄)		
SiO ₂	NaOH, pH 11, Biz (0.5%w), pH 11 (NaOH)	NaOH (0.1%w) + Na ₂ EDTA (0.1%w), pH 12, max 30 °C	–	–	Citric acid (2%w) pH 4 (NH ₄ OH)	
Metal oxides	Citric acid (2%w) pH 4 (NH ₄ OH), sodium hydrosulfite, Na ₂ S ₂ O ₄ (1%w), citric acid (2%w) + EDTA (2%w) pH 4 (NH ₄ OH), v	Phosphoric acid, H ₃ PO ₄ (0.5%w), sodium hydrosulfite, Na ₂ S ₂ O ₄ (1%w), sulfamic acid, NH ₂ SO ₂ H (0.2%w)	Citric acid (1%w), pH 2.5	Citric acid (2%w) pH 4 (NaOH)	Citric acid (2%w) pH 4 (NH ₄ OH)	–
Inorganic colloids	HCl at pH 4, citric acid (2%w) pH 4 (NH ₄ OH), NaOH, pH 11, Biz (0.5%w), pH 11 (NaOH), Drewpene 738 (1%w), SHMP (1%w)	NaOH (0.1%w) + sodium dodecylsulfate Na-DSS (0.05%w), pH 12, max 30 °C	–	Sodium tripolyphosphate, STP (2%w) + Na ₄ EDTA (0.85%w), pH 10 (H ₂ SO ₄)	Citric acid (2%w) pH 4 (NH ₄ OH)	–
Biological matter	Formalin (0.25–2%w) followed by Biz (0.25%w)	NaOH (0.1%w) + Na ₂ EDTA (0.1%w), pH 12, max 30 °C, NaOH (0.1%w) + sodium dodecylsulfate Na-DSS (0.05%w), pH 12, max 30 °C, sodium tripolyphosphate, STP (1%w) + trisodium phosphate, TSP (1%w) + EDTA (1%w)	Sodium tripolyphosphate, STP (1%w) + trisodium phosphate, TSP (1%w) + EDTA (1%w) pH 10–11 (HCl)	Sodium Tripolyphosphate, STP (2%w) + Na ₄ EDTA (0.85%w), pH 10 (H ₂ SO ₄), Sodium Tripolyphosphate, STP (2%w) + sodium dodecyl benzene sulfonate (0.25%w), pH 10 (H ₂ SO ₄)	1–5 ppm chlorine, pH 6.5–7.5, Formalin (0.5–2%w)	Sodium lauryl sulfate 0.2% pH 10–11 by NaOH, ultrasil 10 0.7% pH 10–11
Organics	NaOH, pH 11, Biz (0.5%w), pH 11 (NaOH), SHMP (1%w)	NaOH (0.1%w) + Na ₂ EDTA (0.1%w), pH 12, max 30 °C, NaOH (0.1%w) + sodium dodecylsulfate Na-DSS (0.05%w), pH 12, max 30 °C, Sodium tripolyphosphate, STP (1%w) + trisodium phosphate, TSP (1%w) + EDTA (1%w)	Sodium tripolyphosphate, STP (1%w) + trisodium phosphate, TSP (1%w) + EDTA (1%w) pH 10–11 (HCl)	Sodium tripolyphosphate, STP (2%w) + Na ₄ EDTA (0.85%w), pH 10 (H ₂ SO ₄), sodium tripolyphosphate, STP (2%w) + sodium dodecyl benzene sulfonate (0.25%w), pH 10 (H ₂ SO ₄)	1–5 ppm chlorine, pH 6.5–7.5, formalin (0.5–2%w)	–

Flow rate velocity as high as possible, pressure as lowest as possible, temperature does not exceed manufacturer recommendation (<45 °C).

Chemical techniques have proven to be effective for removing foulants from membrane surfaces and restoring permeability while reducing the net driving pressure (NDP). It is a necessary to optimize the cleaning strategy for preventing fouling in a membrane. Li et al. demonstrated the effectiveness of using a high concentration of sodium hypochlorite (NaOCl) (2000–3000 mg/L) for recovering membrane permeability. The combination of NaOCl with other reagents, such as NaOH or HCl, afforded better improvement in recovery compared to the use of NaOCl alone ¹¹⁰. In this pilot study, NaOCl and H₂SO₄ were used for the maintenance and recovery cleaning of the membrane. Overall, most of the decline in the permeability rate can be recovered by chemical cleaning. Figure 3.5.1 shows the potential impact of ionic strength and pH on

the membrane structure because of changes in the EDL. The membrane exhibited more swelling and a smaller pore size at low ionic strength and high pH than at high ionic strength and low pH.

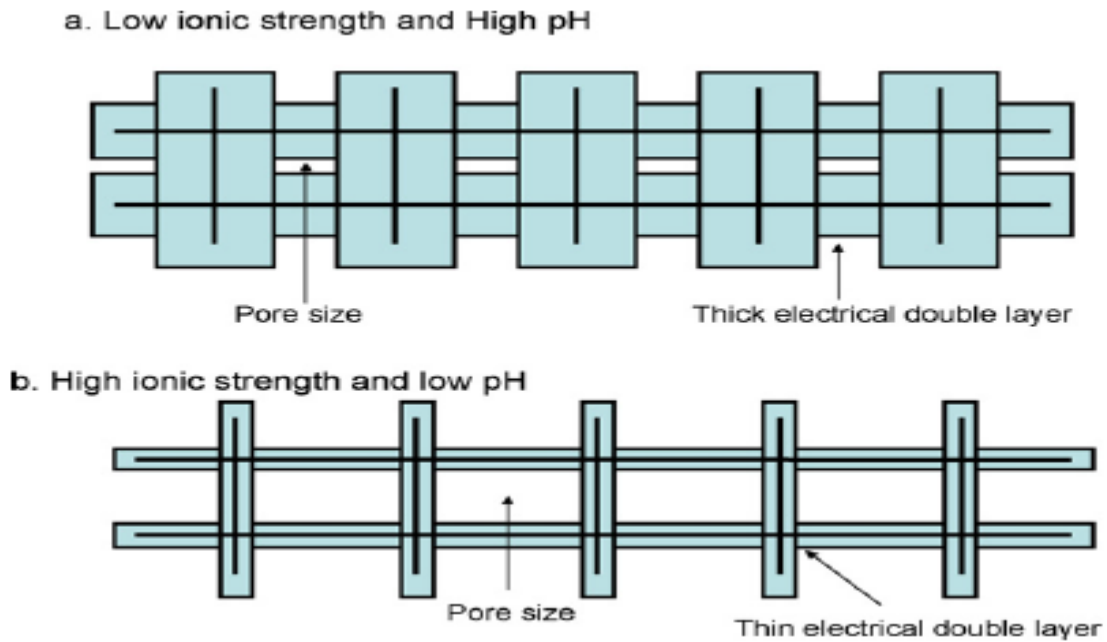


Figure 3.5.1. Conceptual sketch of the swollen membrane matrix in different ionic environments. (a) Thick EDL at high pH and low ionic strength and (b) thin EDL at high ionic strength and low pH⁸⁶.

The objective of the cleaning processes is to restore membrane performance when the expected permeate flux typically decreases by 10% or the NDP increases by approximately 15%. While frequent chemical cleaning of RO membranes removes foulants, it can also be detrimental to membrane integrity. The ideal cleaning processes should not only be effective at removing foulants, but should also be gentle to the membrane so as to maintain and restore its characteristics. Mechanical techniques such as the use of permeate water for flushing (reversing NDP) the membrane surface can help

loosen and dislodge any foulants. This is an important mechanism and can be used frequently instead of chemical cleaning when trying to prevent RO membrane fouling. Figures 3.5.2 shows the combined mechanism of chemical cleaning using EDTA and permeates flushing to dislodge the NOM foulant formed in the presence of Ca^{2+} , as proposed by Li and Elimelech. These authors have stated that, when EDTA is used for membrane cleaning, the EDTA molecules decrease the number of intermolecular bonds between Ca ions and NOM particles and form strong bonds with Ca ions by replacing the NOM particles. This improves the ease of flushing CaEDTA and NOM away from the membrane surface.

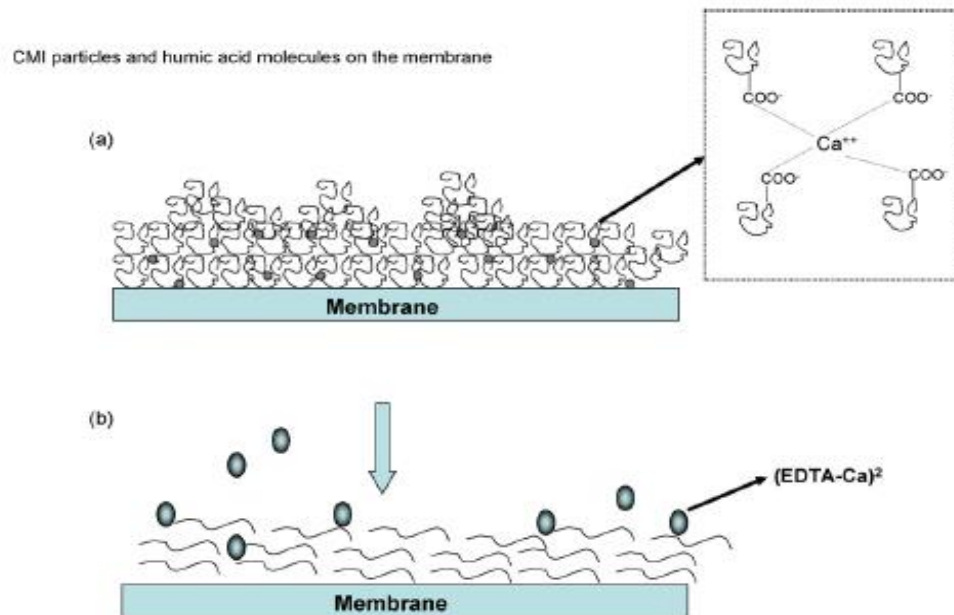


Figure 3.5.2. . Illustration of the change in the organic fouling layer structure by EDTA. (a) Compact fouling layer formed in the presence of Ca^{2+} . (b) Loose structure of the fouling layer after EDTA addition⁸⁸.

CHAPTER IV

MATERIALS AND METHODS

4.1. Introduction

The impetus for this dissertation has originated from the irreversible fouling tendencies observed by employing reverse osmosis technology (ROT) in the first pilot study conducted by the city of Grand Forks, North Dakota. The general objective of a pilot study is to obtain sufficient real-time data that can be used to evaluate the coagulant dose necessary for achieving effluent turbidity $< 3\text{NTU}$ and reducing total organic carbon (TOC) by 30%.. The pilot can also help evaluate RO system performance and recovery cleaning and demonstrate the technical feasibility of the interpretation of these analysis for the design of a full-scale water treatment plant (WTP). Figure 4.1.1 provides a schematic diagram of the pilot study plant, which was set up at the GFWTP and includes the pretreatment train, ultrafiltration (UF), and four parallel RO systems. The city of Grand Forks is planning to install a new hybrid WTP that will operational concurrently with their current conventional WTP. The GFWTP faces various challenges associated with several sources of surface water around the area. The raw water in Grand Forks is obtained by blending water from the Red River of the North (Red River, RR) and the Red Lake River (RLR). This allows Grand Forks to use any one supply when the other's quality is undesirable, or blend both

sources for improving treatability, decreasing chemical costs, and achieving a desired influent water quality.

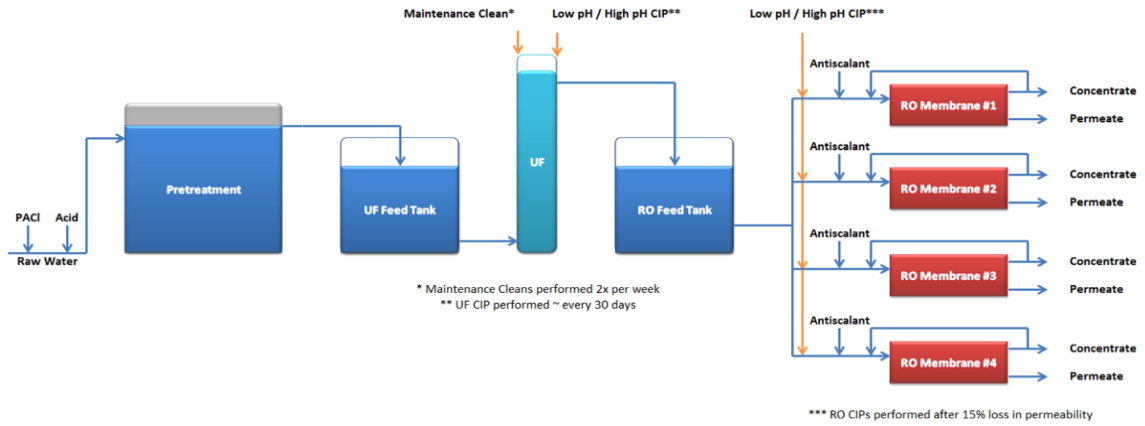


Figure 4.1.1. Schematic of the entire pilot plant at the GFWTP. RO membrane #1 is unit A, RO membrane #2 is unit B, RO membrane #3 is unit C, and RO membrane #4 is unit D.

Both RR and RLR river systems exhibit significant seasonal changes in water quality depending on climatic (precipitation and weather), agricultural, municipal, and industrial impacts. As a result, their water quality may change within short periods of time. Table 3 illustrates the significant fluctuations of selected parameters from both water sources. This table was created from the data collected during the first pilot study (December 2012 through August 2013).

Table 4-1. GFWTP water quality overview (December 2012–September 2013)

Source	Constituent	Average	Max	Min	95th Percentile	5th Percentile
Red River	Turbidity (NTU)	88	596	3	304.8	4.3
	Temperature (°C)	6.3	26.3	0.4	22.6	1.0
	Total Organic Carbon (mg/L)	11.3	14.4	8.8	13.6	9.4
	Total Hardness as CaCO ₃ (mg/l)	467	752	164	700.0	196.0
	Total Alkalinity as CaCO ₃ (mg/l)	266	510	105	387.0	141.8
	pH	8.0	8.5	7.6	8.31	7.73
	Conductivity	987	1735	315	1704.5	380.0
	Sulfate (ppm)	360	680	80	632.5	89.5
	Bromide (ppm)	0.162	0.333	0.022	0.3274	0.0283
Red Lake River	Turbidity (NTU)	31	284	3	129.7	4.0
	Temperature (°C)	6.3	26.3	0.4	22.6	1.0
	Total Organic Carbon (mg/L)	15.2	18.9	11.7	18.0	11.8
	Total Hardness as CaCO ₃ (mg/l)	267	360	116	327.9	136.0
	Total Alkalinity as CaCO ₃ (mg/l)	215	418	129	256.8	165.1
	pH	7.9	8.3	7.5	8.20	7.60
	Conductivity	441	616	205	536.8	236.4
	Sulfate (ppm)	55	80	30	80.0	50.0
	Bromide (ppm)	0.025	0.030	0.020	0.0296	0.0202

This research included field tests, bench scale tests, and pilot tests. The pretreatment and RO process in the pilot study consisted of three major trains: the MRI skid, the UF, and the RO skid (see Figures 4.1.1 and 4.1.2), which are operated in series throughout this study. The RO skid has four RO units that are operated separately to replicate different conditions, such as different recovery rates, cleaning agents, and cleaning techniques. A summary of the influent water quality data and data collected along the train is presented in the methods and results section. For the duration of this pilot study, the water source used was a blend of the RR of the North and the RLR, which is an operational constraint for replicating the current source water for the conventional WTP used by the City of Grand Forks.

The methods and sample collection techniques used for chemical analyses have been described in the Standard Methods for Examination of Water and Wastewater, 20th

Edition. Most water quality parameters were measured in terms of their relative concentration (mg/L). Data are shown in subsequent chapters. The effect of pH and antiscalant dose on the solubility of silica was investigated by a photometric method. The measurement of silica and DOM concentration in the RO concentrate, when frequently monitored, can be used for predicting the potential RO membrane fouling.

The variation in the concentrations of cations and anions, process sequence, pH, temperature, hydrodynamic conditions, chemical dosage, RO system performance, and chemical cleaning duration was interpreted and explored using the data analysis software JMP Pro. JMP (pronounced “jump”) is a statistical computer program that focuses on exploratory analytics (identifying major independent parameters). It enables users to investigate the relationship between input data and the response^{105, and 106}.

In the first part of the pilot study, the MRI pretreatment unit was operated for a two-month period for screening a range of coagulant doses and operating conditions (flocculating speed and settling time). Subsequently, the steady-state performance for coagulation, flocculation, and sedimentation was optimized and established. In the second part of the pilot test, the UF was installed, tested, and optimized using non-chemical and chemical clean-in-place (CIP) while ensuring that there was no potential foulant carryover from the filtrate to the RO system under steady-state pretreatment conditions. During the third part of the pilot test, the RO system was installed and tested.

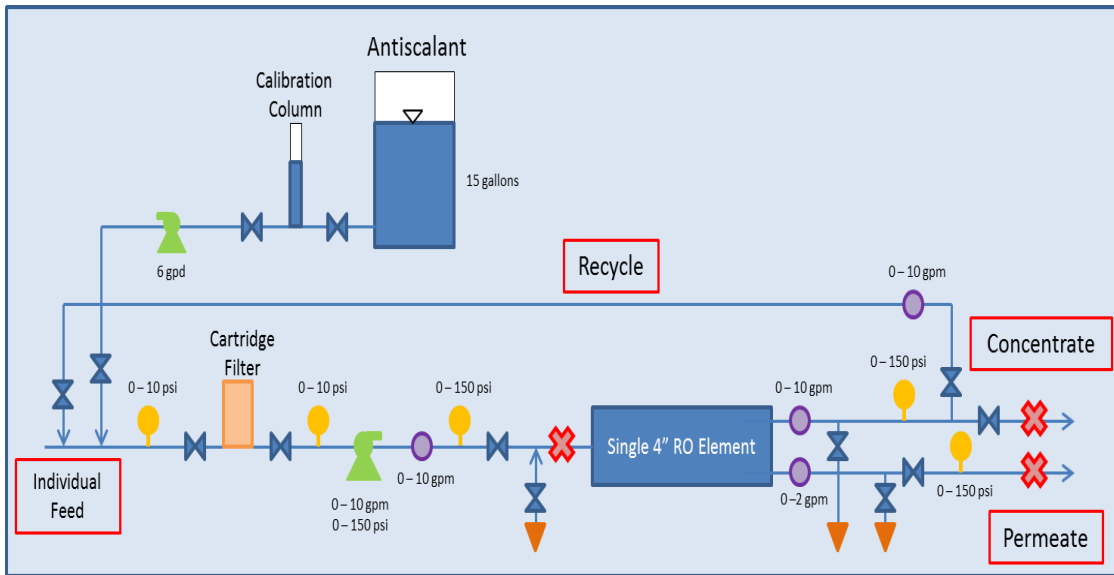


Figure 4.1.2. Schematics and flow diagram of the RO pilot plant.

4.2. Raw water source

For this pilot study, the source includes water from the RLR and RR of the North, currently blended at 90% and 10%, respectively (Figure 4.2.1). The combined use of these two rivers allows the GFWTP to bring in water that can be easily treated while improving water treatment operation, reducing treatment costs, lowering the use of chemicals, and reducing the cleaning frequency. The RR exhibits higher turbidity, higher hardness, higher sulfate content, and lower organics than the RLR. The blending of these two rivers depends on water quality changes (seasonally and/or daily) in response to climate changes and Devils Lake discharge events.

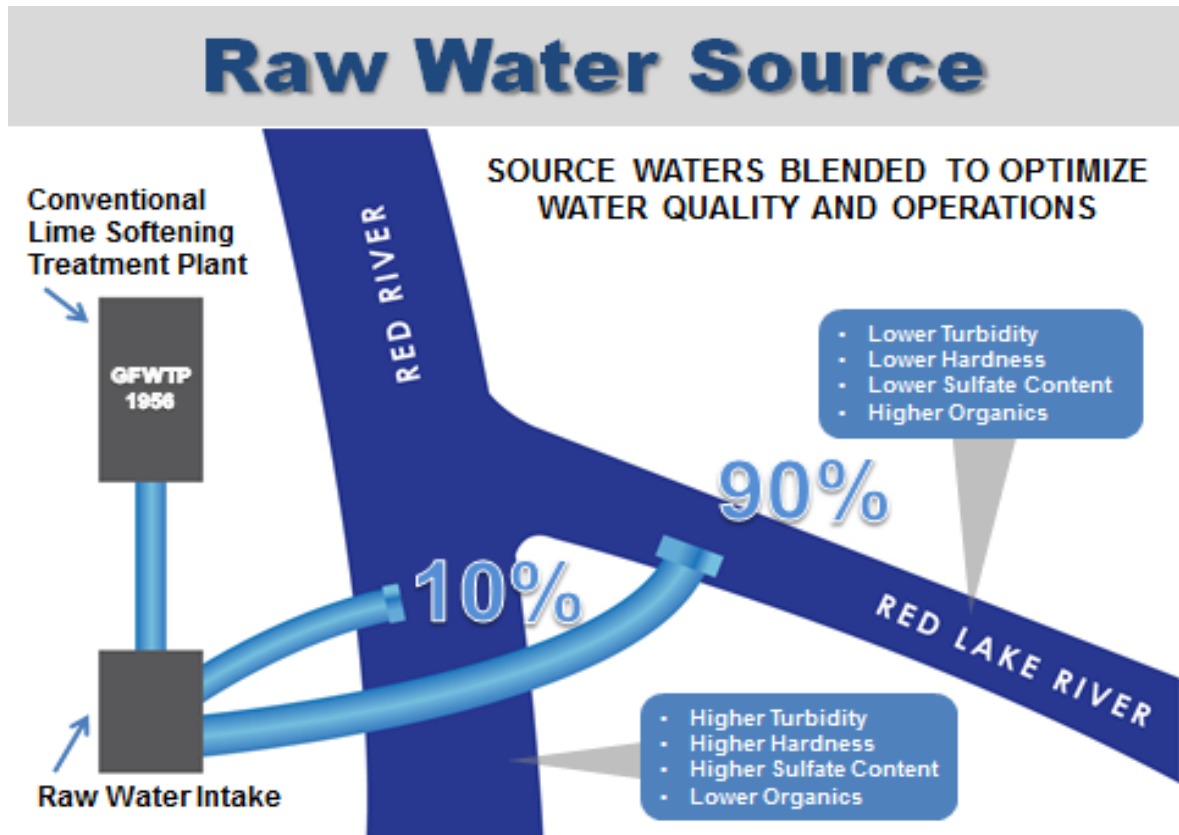


Figure 4.2.1. Source waters (Red River & Red Lake River) in the GFWTP pilot study.

It is imperative that source water quality is taken into account during the design of membranes, which will allow designers to anticipate future changes in water quality parameters. The pilot study was conducted to determine how to efficiently pretreat the source water before feeding it into the RO unit. The water source for this pilot study is tapped after blending the two rivers at the GFWTP. The raw water intake station for the pilot plant contains a suction pump and piping systems, which are used to transfer blended water into the pretreatment unit (Figure 4.2.2).

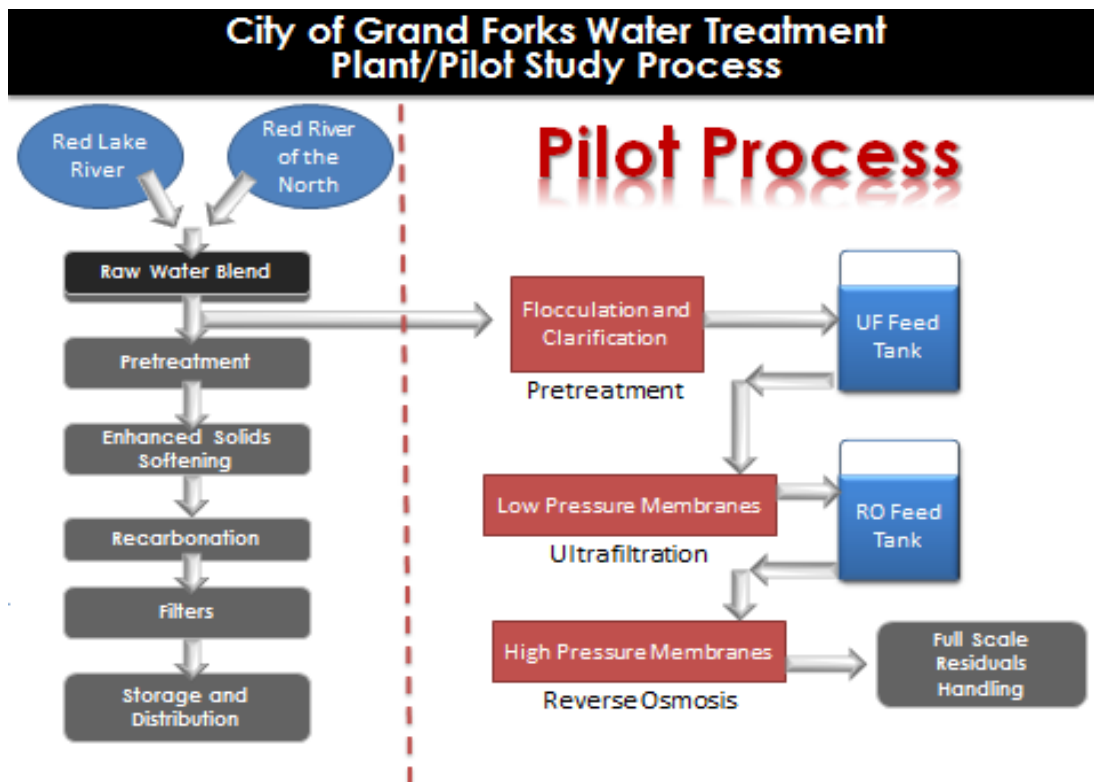


Figure 4.2.2. GFWTP conventional plant and pilot study plant water treatment processes.

4.3. Schedule

The pilot study was scheduled for a total duration of approximately 8 months. The pilot equipment and test protocol were procured in the first month, followed by approximately 2 months of pretreatment pilot operation and optimization. The following tables were developed for summarizing the pilot test and optimizing the schedules of the equipment used during the pilot study. Furthermore, the testing matrix tables for the RO system were constructed according to the predetermined draft protocol with flexibility for making necessary changes.

4.4. Laboratory techniques

4.4.1. Sampling and analysis

This section describes the sampling and analysis procedures used in this pilot study. Various water quality parameters were sampled and analyzed, and the frequencies of analysis are detailed in Table 4-2. Onsite, field, and external lab analyses were performed for these sampling events.

Table 4-2. Routine onsite and laboratory sampling plan and frequency

Test / Data Collected	Sample Location									
	Full Scale GFWTP			Pilot Study						
	Red Lake River	Red River	Raw Water (Blended)	Pretreatment Influent	Pretreatment Effluent	UF Influent	UF Filtrate	RO Influent	RO Permeate	RO Concentrate
Coagulant Dose				D						
Acid Dose				Bi-W						
Antiscalant Dose								D		
Temperature			D	D	D		D			
pH			D	D	D		D		D	
Turbidity			D		D					
TOC	Bi-W	Bi-W	D		D		D		D	
Conductivity							D		D	
SDI								2x		
HPC			W		W	W	W	W	W	
Aluminum					D		D			
Cation/Anion *	Bi-W	Bi-W					Bi-W		Bi-W	Bi-W
ORP **								Bi-W		
D = Daily										
2x = Twice a week										
W = Weekly										
Bi-W = Bi-Weekly										
* Samples sent for outside analysis by Fargo WTP Lab										
** Samples taken after UF Maintenance Cleans / CIPs										

With assistance from the GFWTP staff, several field and onsite analyses were performed for obtaining immediate water quality parameters for optimization and stability verification. This included pretreated effluent water (pH, temperature, Al, TOC, alkalinity, and total hardness measured as CaCO₃); UF module (transmembrane pressure (TMP), flux, permeability, pH, temperature, Al, TOC, silt density index (SDI), Langelier Saturation Index (LSI), conductivity, and dissolved organic carbon (DOC)); RO module (four membranes in parallel): RO influent (pH, temperature, Al, TOC, SDI, conductivity,

TOC, HPC, free Cl, antiscalant dose, and biocide); and permeate (pH, temperature, Al, DOC, SDI, TDS, total suspended solids, conductivity, heterotrophic plate count (HPC), and Cl residuals).

4.4.2. Specific analytical procedures

Table API, Appendix I summarizes the procedures utilized for analyses during this pilot study. Furthermore, the following subsections provide detailed standard methods and quality control procedures that were employed during this study.

4.4.2.1. Total organic carbon

For TOC analysis, a sample filtered through a 0.45 μm filter was used. Samples collected from the 0.4 μm UF membrane filter effluent were classified as DOC samples, and additional filtration was not performed. Samples collected during bench-top jar tests were filtered in a 100 mL filtration cell using 0.45 μm filters. The filter in the cell was soaked, rinsed with deionized water several times, and the deionized water rinse was disposed. The filter was then connected to a vacuum pump at a pressure of 2 psi. The filtrate was collected into pre-cleaned 40 mL TOC vials, discarded and refilled, and then preserved with phosphoric acid and stored in a fridge at 4 °C.

TOC was measured using a model TOC analyzer. The instrument automatically obtained three TOC measurements from each vial before averaging the data. The TOC analyzer was calibrated once a month, and an internal calibration curve was maintained. Calibration curves were compared with the previous calibration for checking the reliability of the data. The TOC data were reported in mg/L.

4.4.2.2. pH

The pH meter purchased by the GFWTP was calibrated daily using a 3-point calibration curve. The pH standards utilized were 4, 7, and 10. The auto-calibration mode available on the Thermo Scientific Orion VERSA STAR advance electrochemistry bench-top meter was used. Before and after a calibration point, the pH probe was thoroughly rinsed before the next calibration was conducted. pH data were recorded to the nearest 0.01 pH unit.

4.4.2.3. Conductivity

The conductivity meter purchased by the GFWTP was calibrated daily using 1-point calibration solution. The conductivity of the standard solution used was 1413 $\mu\text{S}/\text{cm}$. The auto-calibration mode available on the Thermo Scientific Orion VERSA STAR advance electrochemistry bench-top meter was used. The conductivity probe was thoroughly rinsed before and after calibration.

4.4.2.4. Turbidity

The turbidity meter was calibrated using Hach StablCal primary standards of 10 NTU, 20 NTU, 100 NTU, and 800 NTU. This meter was calibrated daily during the pilot study. Turbidity was recorded to the nearest 0.01 NTU when the turbidity was less than 10 NTU, or to the nearest 1 NTU when the turbidity was greater than 10 NTU.

4.4.2.5. External lab analysis

An external laboratory in Fargo analyzed the oxidation-reduction potential (ORP) and HPCs of cation and anion samples collected from the RO system and along the

treatment train to complement the on-site tests. A table in the results section presents a summary of the laboratory results for these samples.

4.5. Pilot plant units and operation

4.5.1. Pretreatment unit

The pilot plant pretreatment intake was located prior to the conventional GFWTP pretreatment stage. This study can thus evaluate every treatment train that will be recommended for the new GFWTP facility (Figures 4.5.1.1 to 4.5.1.4). Precipitation was achieved using a MRI coagulation–flocculation–sedimentation pilot unit with a nominal flow of 54.56 gallons per min (gpm), flocculation time of 26 min (optimized during the jar test), and a loading rate of 0.3 gpm/ft² for replicating the full-scale system (see Appendix II). Water entered the unit through a 2 in hose containing a static mixer, where the coagulant and sulfuric acid were added in a rapid mixing chamber. The mixing chamber was capable of achieving G-values (mixing energy) of up to 1000 per second with a detention time of 1 min. This mixing protocol was the same as that for the jar test. Sulfuric acid and poly aluminum chloride (PACl) were introduced through an injection point with the goal of precipitating ions like Ca²⁺, Mg²⁺, Sr²⁺, and Ba²⁺, silica, and TOC, before passing through a static mixer, wherein the initial mixing between raw water and the chemicals was carried out.



Figure 4.5.1.1. Pretreatment unit: MRI pretreatment, Raw water, acid and PACl feed point, and static mixer.



Figure 4.5.1.2. Mixer for coagulation.



Figure 4.5.1.3. Top view of the MRI pretreatment unit.

The coagulated water then exited into the MRI pretreatment unit's flocculation chamber. Flocculation was achieved by a three-stage process at varying speeds and at a detention time of 26 min, as stated above. The raw water pretreated with the coagulant from the flash mixer was fed into the flocculation–sedimentation pilot for assisting in the formation of flocs and settling of solids. The flocculation section included three stages so that mixing energy can be tapered and optimized in successive flocculation stages. The water exited the flocculation chambers through a hose into an inclined plate settler, where the water was baffled downward to the bottom of the plates. Subsequently, the water flowed up through the plates and exited the effluent trough at a predetermined angle and entered a pipe leading into the UF holding tank. Plate settlers were provided in the sedimentation unit to allow maximum surface hydraulic loading. Solids were removed from the sedimentation basin every 2 h using a manual valve and peristaltic pump

arrangement. During this optimization phase of the pretreatment unit, the removal efficiency of the potential membrane fouling agents (TOC, particulates) was monitored.



Figure 4.5.1.4. The UF feed tank and rear view of the pretreatment unit.

PACl and H_2SO_4 were continuously introduced into the flash mixer to maintain a uniform concentration during dosing. Based on the bench and pilot test results, the feed rates were set at 15 mL/min (PACl) and approximately 19.5 mL/min (H_2SO_4). The feed rate of the acid pump was continuously adjusted to maintain a target pH between 6.5 and 7. The target pH was based on bench-scale jar test results and literature reviews. The PACl dose was selected based on the optimal turbidity and DOM removal determined through a series of jar tests. This jar test evaluated different PACl doses ranging between 15 and 75 mg/L, and the removal of turbidity and DOM was compared against a control dose with no coagulant. High coagulant doses were effective for the removal of turbidity,

but were not feasible because of restrictive chemical costs. Doses between 47.5 and 35 mg/L were further investigated to ensure that they met the minimum requirements for the removal of turbidity and DOM, which might impact RO and UF performance and membrane fouling tendencies. MRI pretreatment effectiveness was demonstrated by the data snapshot in Figure 4.5.1.5.

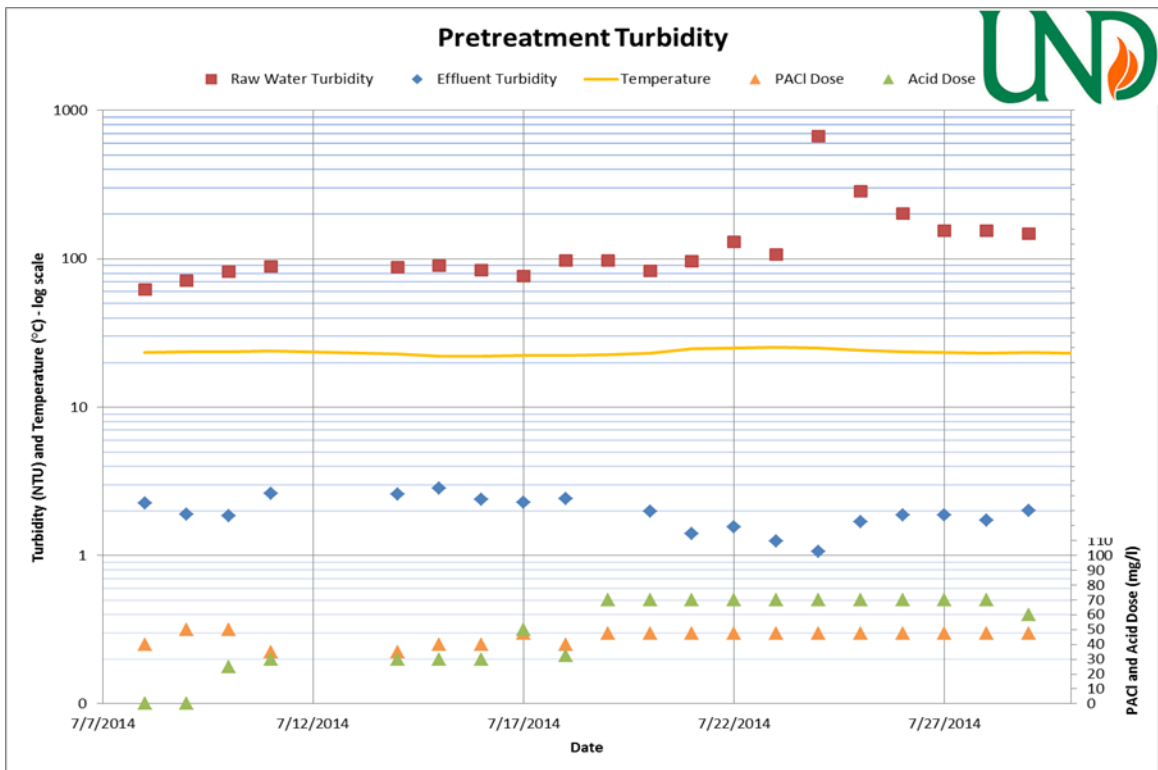


Figure 4.5.1.5. Pretreatment unit influent and effluent turbidity graph.

4.5.2. Bench-scale protocols

Surface waters tend to have a high turbidity and are susceptible to frequent changes in water quality. For such waters, it is imperative to adjust the coagulant dose for achieving optimal coagulation. Standard operating procedures need to be established for controlling coagulation. Jar tests (Figure 4.5.2.1) can be used to establish appropriate

control of coagulation. Through a jar test, different coagulant doses are tested to simulate different coagulation/flocculation/sedimentation conditions during pretreatment. Bench tests were performed at the GFWTP using blended water from the RR and RLR. These bench tests were periodically conducted in the months preceding the installation of the UF and RO units.

The first step of a jar test involved the addition of sulfuric acid, to lower the pH, and coagulants to raw water in beakers before rapid mixing for approximately 1 min at 300 revolutions per minute (rpm) to simulate the mixer used in the pilot study. The next step involved the slow, low-energy mixing of the water for a longer period of time to mimic the flocculation stage of the pilot study. Flocculation speeds of 40, 26, and 17 rpm were used for 9.5 min. The mixer was finally stopped and the flocs were allowed to settle for approximately 10 min to mimic the sedimentation stage in the pretreatment unit. The clarified supernatant was tested in terms of turbidity and other pertinent parameters to assess the effectiveness of various coagulants and doses.

4.5.2.1. Materials

- Volumetric flask (1000 mL)
- Analytical balance
- Coagulants
- A stirring machine with six paddles capable of speeds varying from 0 to 300 rpm
- Beakers (2 L)
- Pipettes (10 mL)
- Clock
- Sample tubes and turbidometer



Figure 4.5.2.1. Jar test apparatus. Notably, square containers are used to limit vortex flow formation, wherein particles rotate in the same position relative to each other ⁸⁹.

4.5.3. Ultrafiltration unit

Ultrafiltration was carried out following chemical treatment and sedimentation-precipitation conducted in the MRI pretreatment unit. A pilot-scale UF unit with a nominal flow of 6 gpm and a turbidity influent concentration of <2 NTU was used. In this study, two different UF membranes were used in two separate UF units (Evoqua and Koch (Figures 4.5.3.1 and 4.5.3.2)). The membranes had the same nominal size of 0.1 μm , but were made from different polymers. Filtration was carried out using these two UF membranes parallel throughout this pilot study. Both membranes were pressurized hollow fiber systems, and were operated in an inside-out flow pattern.

The Evoqua (see figure 4.5.3.1 and 4.5.3.2.) and Koch membranes were operated at the same flux using different manufacturer-recommended run cycles (filtration; air

turbulence; hydraulic backwashing). The UF membrane pretreatment units were operated prior to the arrival and installation of the RO units. This allowed the determination of the optimum flux rate, chemically enhanced clean-in-place (CIP) procedures, durations and frequencies, and filtrate backwash frequencies and durations. The data from this test period were used to establish the operating parameters for the full-scale WTP. In addition, the optimization period for the UF membrane system was limited to 1 h so that UF operation would not affect RO system operation. This unit ran for the duration of this pilot study.



Figure 4.5.3.1. Front view of the ultrafiltration unit from Evoqua.



Figure 4.5.3.2. Rear view of the ultrafiltration unit from Evoqua.

4.5.4. Reverse osmosis system

RO systems are typically designed and constructed as multiple skids that are placed in series. The final skid is typically fed with more concentrated water, which has a greater tendency of causing membrane fouling. The design of the RO pilot system was used to simulate the tail-end or the final stage of the proposed RO design of the full-scale GFWTP. The RO system unit was designed and supplied by Applied Membrane Inc. As shown in Figures 4.5.4.1 to 4.5.4.4 and Tables 4-3 and 4-4, the pilot units included membrane elements; pressure vessels; pumps; feed, permeate, and concentrate headers; system support frames; chemical feed systems; flow measurement and pressure measurement apparatus; controllers; CIP apparatus; and numerous valves. The RO pilot

system had only one stage, which was used to simulate the tail element of a multistage RO system. The four pilot skid membrane elements were parallel to each other, and the permeate from the RO membrane systems was blended in the final permeate tank.

The RO pilot unit was continuously fed with UF filtrate from the filtrate collection tank using an RO booster pump. An antiscalant was added prior to the RO booster pump for minimizing the precipitation of sparingly soluble salts like calcium carbonate on the membranes. Appendix III shows the primary design of the RO system.



Figure 4.5.4.1. RO pilot system PW-4XM-14A-116 front view.

Table 4-3. RO system main component identification

#	Item	Description
1.	Pump P10A	Booster Pump w/motor to System
	Temperature Gauges	Not in photo – post Pump P10A and pre-Pump P90A
2.	Booster Pump controller	Manual on/off switch for booster pump P10A
3.	pH Probe	pH measurement of feed water
4.	A57 Antiscalant System	Doses antiscalant; one for each system - A and B; 15 gal / 6 gpd
5.	Cartridge Filter Housing	Houses 5 micron sediment filter; one for each system – A,B,C,D
	CF psi PI 19 / PI20	Pressure gauges for inlet/outlet of cartridge filters – A,B,C,D
6.	High Pressure Pump P20	High pressure pump & motor; one for each system – A,B,C,D
7.	Low pressure switch	Off 8 psi low; on psi 20. One for each system – A,B,C,D
8.	IROC 250 Controller	Controls RO systems; one for each system – A,B,C,D
9.	System psi Gauge	System (Feed) pressure – one for each system - A,B,C,D
10.	Concentrate psi gauge	Concentrate pressure PSI40 – one for each system - A,B,C,D
11.	Feed Flow Meter FI20	One for each system – one for each system - A,B,C,D



Figure 4.5.4.2. RO pilot system PW-4XM-14A-116 side view.



Figure 4.5.4.3. RO pilot system PW-4XM-14A-116 side view.

Table 4-4. RO system main component identification

#	Item	Description
12.	Pressure vessel w/ mem	Pressure vessel w/ RO element; one for each system – A and B
13.	Flow meter panel	Concentrate, recycle and permeate flow meters for systems A and B
14.	Permeate Outlet	Permeate lines 1/2" tubing or 1" NPT – determined by 3 way valve
15.	Concentrate/Drain Line	1" NPT
16.	CIP / Flush Tank T90	30 gallon
17.	CIP Pump P90A	CIP Pump 1 HP
18.	CIP pump controller	On/Off CIP Controller;
19.	CIP tank level switch	LSL90 Low tank level switch protects Pump P90A
20.	CIP Flow meter FI90	Measured flow rate of CIP
21.	CIP Heater	Immersion heater – 110V
22.	CIP cartridge filter CF90	Big Blue cartridge filter housing w/ 5 micron sediment filter

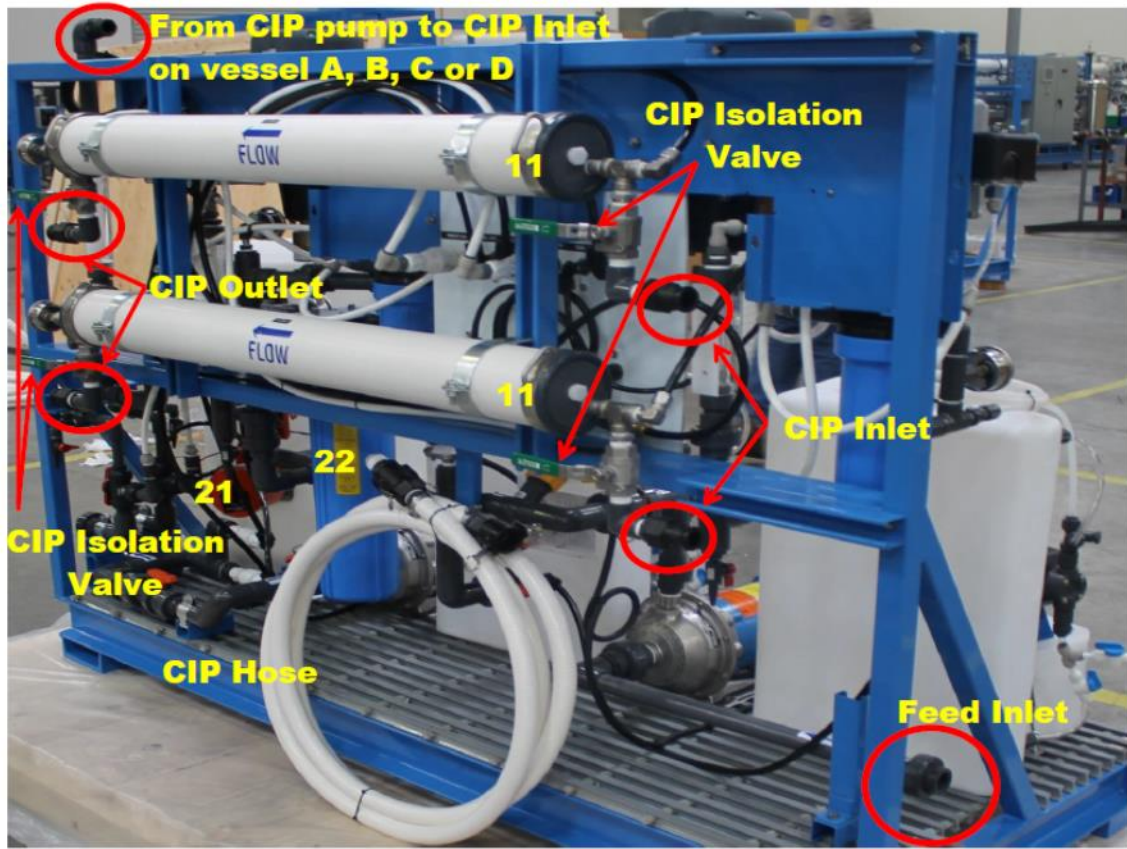


Figure 4.5.4.4. RO pilot system PW-4XM-14A-116 rear view.

4.5.5. Cleaning and chemical use

The GFWTP RO systems employed periodic permeate flush and CIP procedures during operation. Six types of chemicals were utilized during the study. In the CIP procedure for RO A and RO B, heated potable water (35 °C) was used to fill the membrane tank. While the tank was being filled, Avista 303 (typically 2% solution, acid cleaned, pH = 3.0) was added to remove all inorganics. The membranes were soaked for 60 min, the Avista 303 solution was drained, the membranes were rinsed with permeate water, and heated permeate water (35 °C) containing a 2% Avista P312 solution (caustic clean, pH = 11.5) for removing organics was applied to the membranes. The RO

membranes were then soaked, drained, rinsed with permeate, soaked again for 12 h, and returned to service.

In the CIP procedure for RO C, heated potable water (35 °C) was used to fill the membrane tank. While the tank was being filled, PWT Lavasol II (typically 2% solution, caustic cleaned, pH = 10.5) was added for removing organics. The membranes were soaked for 12 h, the solution was drained, the membranes were then rinsed with permeate water, and heated permeate water (35 °C) with a 2% PWT Lavasol I solution (acid clean, pH = 2.0) was used for removing all inorganics. The membranes were again soaked in permeate for 60 min before being returned to service.

In the CIP procedure for RO D, heated potable water (35 °C) was used to fill the membrane tank. While the tank was being filled, AWC C-236 (typically 2% solution, caustic clean, pH = 12.5) was added for removing organics. The membranes were soaked for 12 h, the solution was drained, the membranes were then rinsed with permeate water, and heated permeate water (35 °C) with a 2% AWC C-209 solution (acid clean, pH = 2.4) was used for removing all inorganics. The membranes were again soaked in the permeate for 60 min before being returned to service.

CHAPTER V

PRETREATMENT TRAIN OPTIMIZATION PROCESS

5.1. Abstract

A pilot study on pretreatment indicated that, by optimizing pH and coagulant dose, DOC and turbidity could be effectively removed using ferric chloride (FeCl_3) or polyaluminum chloride (PACl) as coagulants. The optimized pretreatment conditions possibly reduced, mitigated, or prevented the irreversible fouling experienced by most RO membranes during surface water treatment.

This study showed that an enhanced combined pretreatment process can remove 42.20% and 59.44% of DOM using PACl and FeCl_3 , respectively, which is an improvement over the average baseline removal of 30% without optimization. The optimized combined pretreatment process also achieved a turbidity removal of more than 90% (using PACl at temperatures greater than 20 °C) and 90% (using FeCl_3 at temperatures less than 4 °C). At pH 6.5 and a coagulant dose of 40 mg/L, PACl performed better for the removal of DOM. At the same pH and a coagulant dose of 50 mg/L, FeCl_3 also performed very well. In addition, both coagulants performed very well for the removal of turbidity under the same conditions.

In this study, a new testable neural network platform was constructed as a prediction model for turbidity and TOC removal in a pilot study for the pretreatment of

water at the Grand Forks Water Treatment Plant (GFWTP). The neural platform model accurately predicted the quantitative dependence of effluent TOC on coagulant dose, acid dose, temperature, influent TOC, conductivity, and TDS. The neural network platform also accurately predicted the quantitative dependence of turbidity on flow rate, coagulant dose, acid dose, temperature, influent TOC, conductivity, as well as TDS and total suspended solids (TSS).

5.2. Introduction

The results from the pilot tests will be presented in the following chapters in terms of both water quality and the hydraulic performance of the pilot processes. This chapter aims to summarize the analysis of the source water and to demonstrate the impact of the coagulants on the concentration of the chemical species measured. Additional results will be reported to document the impact of coagulants on DOM and other species, as well as the effect of pH in enhancing the coagulant for obtaining the maximum performance at an optimized dose during coagulation. This chapter will contain background information that can be used for predicting and evaluating the performance of the RO system.

The water quality parameters listed in Table 5-1 represent the water analysis conducted using the samples collected along the treatment train on August 13, 2014. For the Red River (RR), the annual average values of total alkalinity measured as CaCO_3 , total hardness measured as CaCO_3 , DOM, sulfate, and turbidity were 266 mg/L, 467 mg/L, 11.3 mg/L, 360 ppm, and 88 NTU, respectively. The corresponding values for the Red Lake River (RLR) were 215 mg/L, 267 mg/L, 15.2 mg/L, 55 ppm, and 31 NTU, respectively. The raw water pH was between 7.9 and 8.23. pH was controlled during coagulation by adding sulfuric acid to lower the acidity of the water to 6.5. In previous chapters, it has been stated that these two rivers are blended at 90% (RLR) and 10% (RR).

Table 5-1. Physiochemical water quality parameters in the pilot plant treatment train (8/13/2014). Blend: represents the combined rivers (RR and RLR). PT-Effluent: represents the pretreatment effluent. UF-Filtrate: represents the filtered water from the ultrafiltration module.

Water Parameters	Blend (mg/L) (90/10)	PT Effluent (mg/L)	UF Filtrate (mg/L)
Ca ²⁺	60.7	58.0	56.2
Mg ²⁺	23.3	21.6	20.9
Mn ²⁺	0.165	0.032	0.032
Fe ²⁺	2.36	0.053	<0.020
K ⁺	4.04	3.63	3.53
Na ⁺	10.14	10.40	9.99
Ba ²⁺	0.077	0.047	0.046
Sr ²⁺	0.142	0.136	0.131
HCO ₃	183.1	126	124
Cl ⁻	5.30	12.5	12.5
F ⁻	<0.02	<0.20	<0.20
SO ₄ ²⁻	53.7	97.2	97.0
NO ₃ ⁻ NO ₂ as N		<0.200	<0.200
Total P as PO ₄ ³⁻	0.46	<0.20	<0.20
SiO ₂	33.6	14.4	13.8
pH	7.9	6.9	6.8
Conductivity	470	406	323
TDS	234.4	366	348
TSS	98.08	4.4	<1.0
Total Alkalinity as CaCO ₃	183.1	126	124
Total Hardness as CaCO ₃	247.5	234	226
Turbidity	57.9	1.76	0.098
TOC	14.70	8.51	8.44

5.3. Impact of raw water quality on pretreatment

Figure 5.3.1 shows the results obtained via coagulation–flocculation–sedimentation and ultrafiltration (UF) pretreatment for the removal of total silica from the feed water. It was observed that the removal of total silica occurred during the

pretreatment stage, and no silica was removed through the UF membrane. It can be concluded that silica passing through the UF membrane has a smaller molecular weight cut-off (MWCO) than that of the membrane, which can be referred to as dissolved silica. One can thus assert that the adsorption of silica on PACl during coagulation–flocculation–sedimentation affects the equilibrium and thermodynamics of silica polymerization, facilitating precipitation and easy removal during pretreatment.

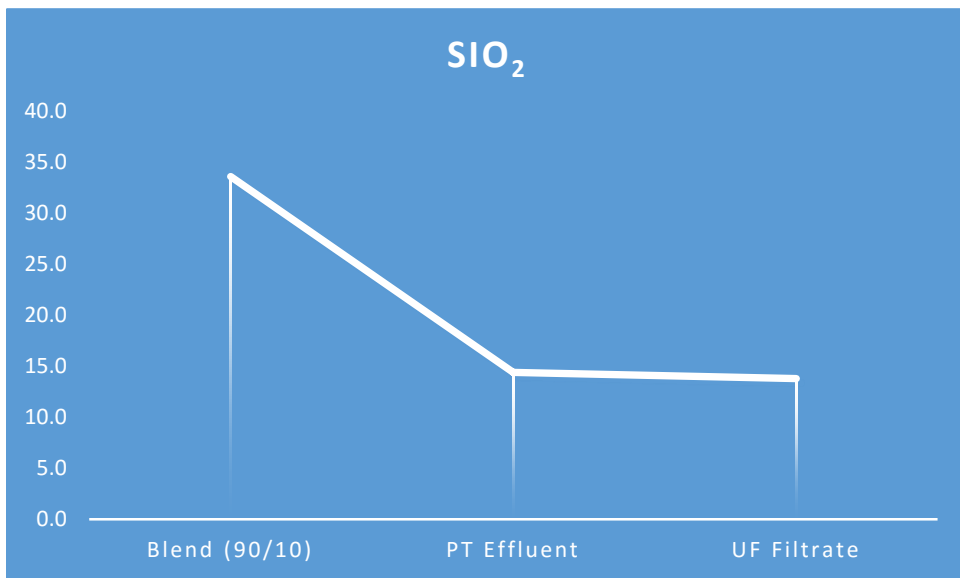


Figure 5.3.1. Changes in SIO₂ concentration measured in mg/L during the pretreatment process.

As shown in Figure 5.3.2, the sulfate ion increased during pretreatment and remained the same throughout the UF stage. This can be attributed to the addition of sulfuric acid (19.5 mL/min) to lower the pH of the feed water during coagulation–flocculation–sedimentation.

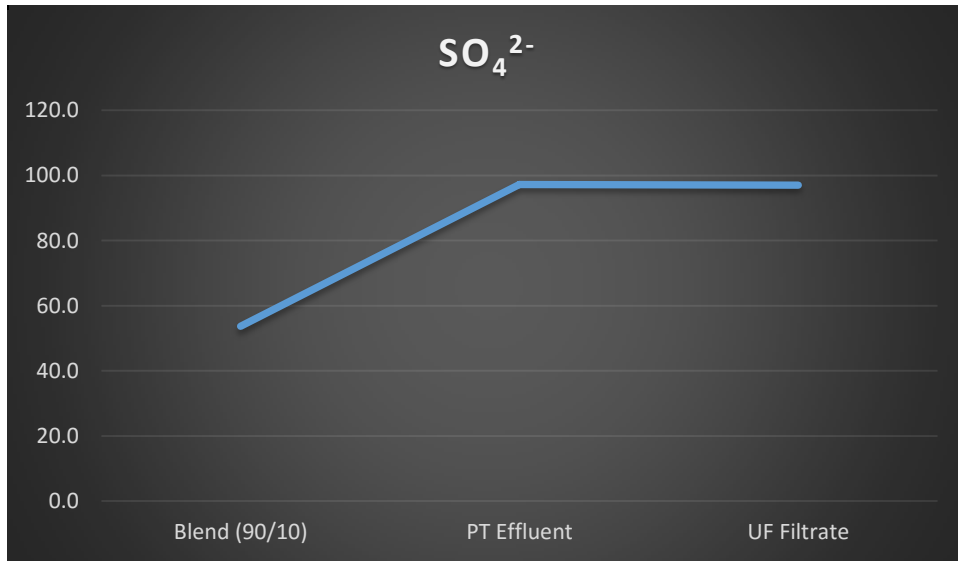


Figure 5.3.2. Changes in SO_4^{2-} concentration measured in mg/L during the pretreatment process.

As can be observed in Figure 5.3.3, the increase in chloride ions indicates that most of the added chloride ions originate from pretreatment. The increased chloride concentration can be ascribed to the PACl added as a coagulant during the pretreatment of feed water. Hence, the graph shows an increment during pretreatment, which stabilizes during UF. It can also be concluded that chloride ions are smaller than the MWCO of the membrane, and hence pass through without being removed during UF.

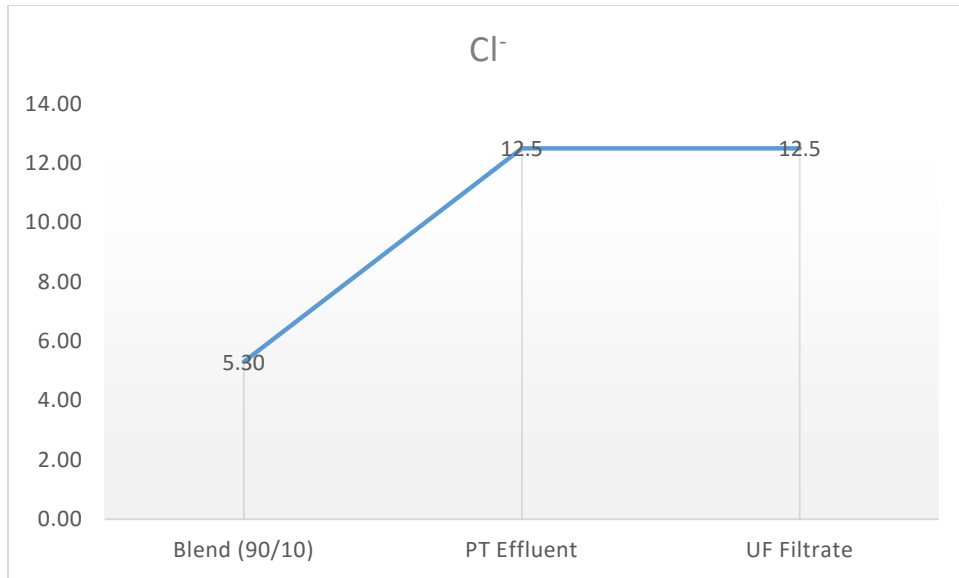


Figure 5.3.3. Changes in Cl⁻ concentration measured in mg/L during the pretreatment process.

Conductivity, based on the principles of electricity, measures the ability of water to conduct electricity, which can be transmitted in the presence of dissolved ions. The more that ions are removed from water, the less its electrical conductance becomes. It is concluded that the decrease in conductivity, as can be observed in Figure 5.3.4, can be attributed to the removal of ions during coagulation.

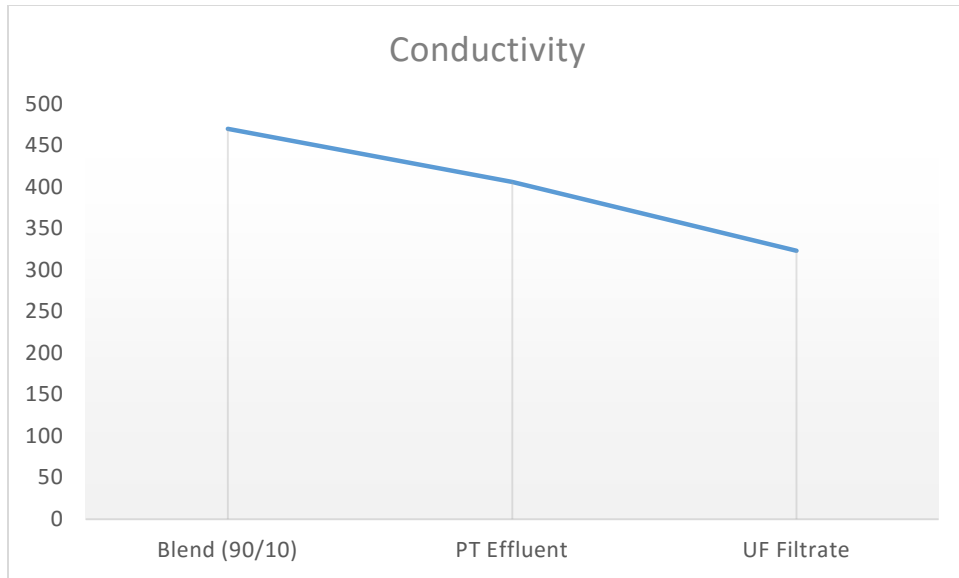


Figure 5.3.4. Changes in conductivity measured in microsiemens during the pretreatment process.

The increase in total dissolve solids (TDS) in the result below (see Figure 5.3.5) can be attributed to coagulation upon addition of chemicals. The rapid mixing of chemicals with water allows for the dissolution of chemical species for some time before precipitation occurs during flocculation. Some salts, however, remain dissolved throughout coagulation. Pretreatment can be effective for the removal of colloidal particles, while a low pH below 7 can also increase the solubility of chemical species that are too small to be removed by the pretreatment unit, but not small enough to be removed by UF. The graph indicates that TDS were added to the feed water at the pretreatment stage, while some TDS were removed by the UF membrane.

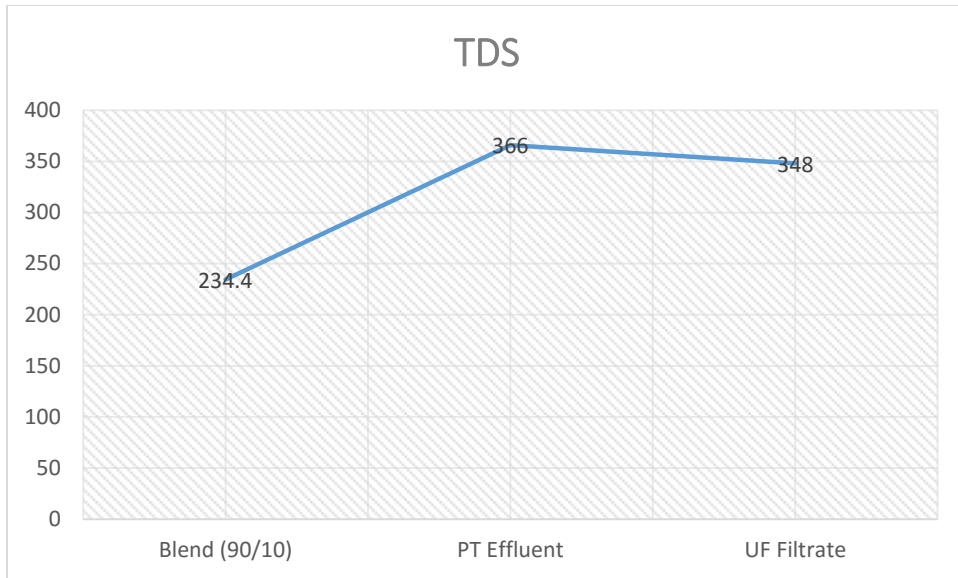


Figure 5.3.5. Changes in TDS during the pretreatment process (measured in mg/L).

Through appropriate coagulation, and with the aid of polymers, TSS can be easily removed when they floc and aggregate together to form highly dense solids that slowly settle down to the bottom of the pretreatment unit during sedimentation. The figure below shows the effectiveness of pretreatment for removing TSS and particulate matter from the feed water during sedimentation.

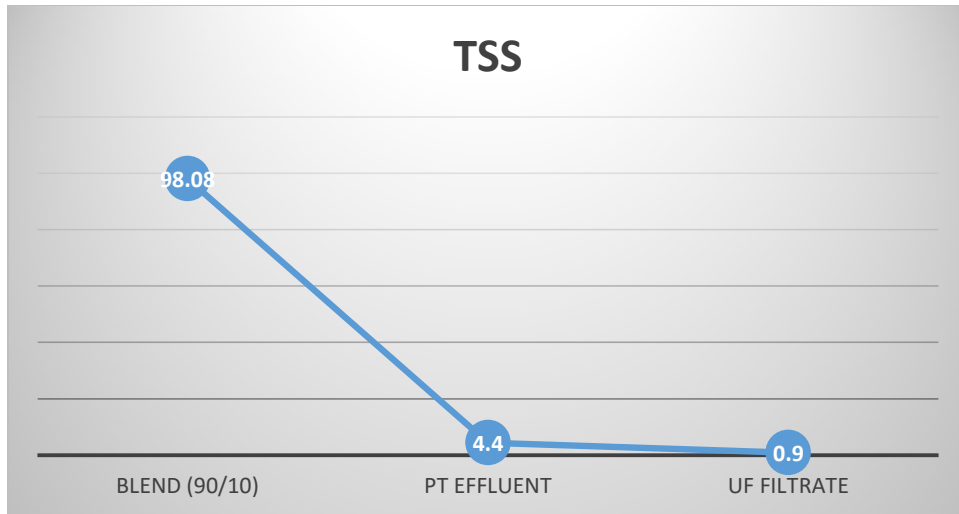


Figure 5.3.6. Changes in TSS concentration measured in mg/L during the pretreatment process.

Alkalinity primarily comprises bicarbonate, carbonate, and hydroxide ions, which function as the Earth's natural buffering system against sudden pH changes resulting from the addition of chemicals. Most of the feed water entering a water treatment plant requires some type of pH adjustment, which will aid in coagulation for achieving the optimal removal of impurities during initial water treatment. Coagulation using coagulants and acids is employed for making adjustments that impact alkalinity, which generally changes the pH of the water. The acids convert carbonates to bicarbonates, and bicarbonates are then converted to CO_2 , which causes the changes observed in the water pH level. During pretreatment, alkalinity is required for providing anions such as OH^- , which help in the formation of insoluble compounds that can be easily precipitated and removed. The dramatic decrease in alkalinity, as can be observed in Figure 5.3.7, is attributed to the chemical reaction that occurs during coagulation for achieving optimal impurity removal.

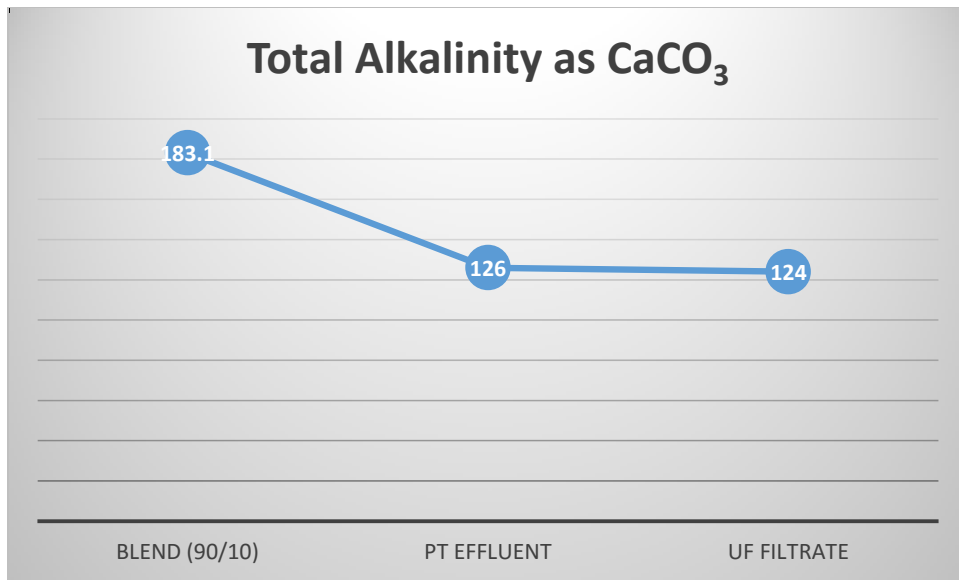


Figure 5.3.7. Changes in total alkalinity measured in mg/L during the pretreatment process.

Divalent ions such as Ca^{2+} and Mg^{2+} are the major components of hardness in surface water. Studies have indicated that the total hardness measured as CaCO_3 affects the kinetics of coagulation, which allows flocs, especially those of coagulants made from aluminum salts, to aggregate. Decrease in total hardness of the pretreatment effluent water shown in Figure 5.3.8 can be correlated to the coagulation performance of the Al species of PACl, which decreases the pH of the feed water. In their study, Wang et al. have demonstrated the effect of the increase in total hardness on the performance of coagulants in removing humic substances (HA) ⁸⁴.

The chemical bonds in inorganic salts such as PACl dissociate, thereby allowing their ions to participate in different chemical reactions with the species existing in natural water. For example, the chloride ions in PACl react with Ca^{2+} to form CaCl_2 , which then binds with HA to increase its molecular size and alter its properties (neutralizing their charge and increasing their growth rate). The precipitation of Al salts improves the

efficiency of the removal of HA through interaction with CaCl_2 by allowing CaCl_2 and HA to form large flocs during coagulation–flocculation. As shown in the results below, Cl^- and Ca^{2+} can react because of these chemical reactions and the continued dissociation of CaCO_3 and PACl during rapid mixing, and the total hardness of feed water during pretreatment starts to decrease ⁸⁴.

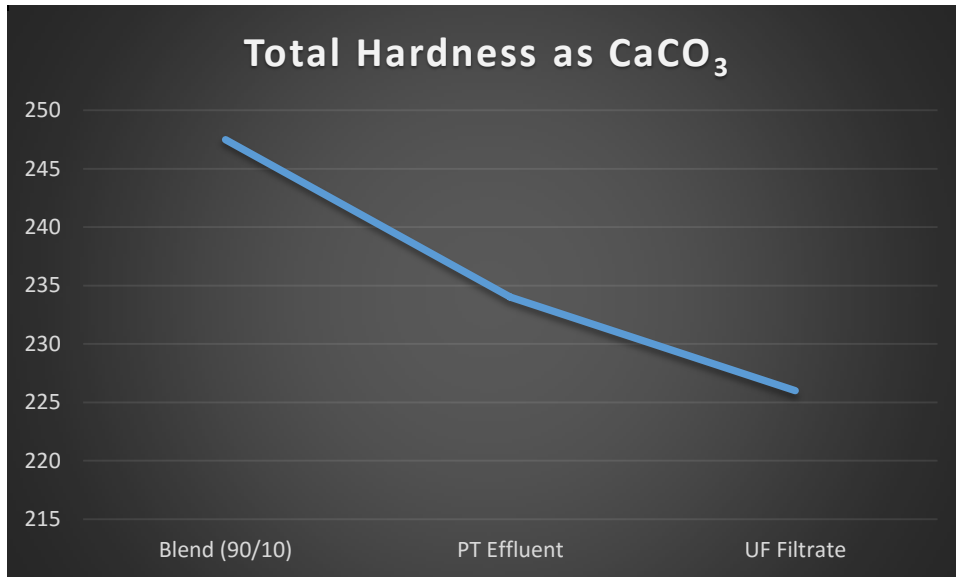


Figure 5.3.8. Observed changes in total hardness measured as CaCO_3 in mg/L during the pretreatment process.

5.4. Optimization of coagulant or pH

Without appropriate pretreatment before membrane operation, maintenance costs increase with frequent membrane cleaning, thereby increasing the downtime and reducing the performance efficiency of the membrane. In most cases, this is attributed to the precipitation of certain sparingly soluble salts and DOM that accumulate on the membrane surface and lead to membrane fouling. This may be minimized by adjusting the pH and optimizing the coagulant dose.

For accomplishing this task, the coagulation of DOM and turbidity using aluminum salt, without pH adjustment, is shown in Figures 5.5.1.1 and 5.5.1.2 below. The pretreatment unit of the pilot plant was run on a matrix of different coagulants, doses, and pH values to identify the combination of these parameters that will improve the removal of turbidity and DOM upstream of the RO membrane.

Studies have shown that variation in pH affects the surface charge of particles in the feed water. This allowed for the development of a testing matrix to obtain the optimized pH and coagulant dose for the removal of TOC and turbidity. Results from this testing matrix allow for the selection of the most effective coagulant through comparison of the two coagulant salts.

Studies have shown that the variation in pH affects the surface charge of particles in the feed water^{1, 3, and 9}. A testing matrix was thus utilized to obtain an optimized pH level and coagulant dose for the removal of TOC and turbidity. In addition, two coagulant salts were compared for the selection of the most effective coagulant.

Previously, a GFWTP pilot study indicated that the performance of RO membranes was related to the effectiveness of coagulation for the removal of DOM and turbidity. One of the goals of this research was to investigate the effect of enhanced coagulation in achieving optimal DOM removal from RO feed water. Although jar test results from this research have demonstrated that an increase in coagulant dose can be very effective for DOM removal, it can be expensive to continuously feed high levels of coagulant during pretreatment. The over-feeding of a coagulant salt during this pilot study resulted in the presence of excess dissolved metals in the RO. These metals may

eventually precipitate and crystallize on the membrane surface, thereby reducing performance.

In addition, this dissertation aims to examine and determine the combination of variables responsible for the removal of TOC and turbidity during coagulation–flocculation–sedimentation. For understanding any relationship, we need to investigate the possible underlying relationship among the pretreatment unit’s principle operating conditions, added chemicals, the chemistry of water fed into the system, and any physical phenomena that explain the observed variability. A statistical hypothesis is presented, and the significance of this hypothesis is investigated before interpreting the results in the context of the explanations given by previous literature.

First, we quantify the uncertainty in the data set using probability modeling and model the likelihood of different possible outcomes. This will help in understanding the behavior of fundamental parameters, by studying the relationships among them, and the role of these parameters in predicting the performance of the enhanced pretreatment methodology. The parameters include flow rate, flocculation time, loading rate, flocculation speed, coagulant and acid dose, temperature, influent turbidity, TOC, conductivity, TDS, and TSS. For investigating the linear or non-linear relationship among these parameters, we apply the neural network platform method. In this project, regardless of whether linear or non-linear relationships are observed among the operating parameters of coagulation–flocculation–sedimentation, the quality of the numerical approach is checked by applying a numerical model. The model can not only classify the data but also can be applied to data obtained from other pilot studies with known TOC and turbidity behaviors. Notably, the previous Grand Forks Water Treatment Plant

(GFWTP) pilot study on the relationships between pretreatment operating parameters of coagulation–flocculation–sedimentation concluded that there are cause–effect relationships between the operating parameters. The relationship between the other operating parameters needs to be revisited for considering the unexplained variations and anomalies.

This study will focus on the following research questions regarding the behavioral responses for the removal of TOC and turbidity during their interaction with coagulant chemicals, pH adjustment, and the pretreatment unit features during surface water treatment.

- Is there any relationship between the operating parameters in coagulation–flocculation–sedimentation? If yes, is it statistically significant?
- Can a mechanistic model be constructed from the interaction between the explanatory operating conditions and the response observed in the performance of coagulation during the removal of TOC and turbidity. If yes, are the model assumptions met?
- How should we collect data for future studies?

5.5. Methodology

The motivation for this research has originated from the analyses of physicochemical processes that control the removal of TOC and turbidity by the combination of pretreatments such as coagulation, flocculation, and sedimentation conducted during the pilot study at GFWTP. An experiment was conducted for investigating the effect of optimizing the chemical coagulant and pH for the removal of

turbidity and TOC. The observed variation in the removal rates of TOC and turbidity was further explored by using a neural software platform JMP Pro. JMP (pronounced “jump”) is a computer program for exploring analytics statistics, which enables users to investigate the relationship between the input data and the response^{105, and 106}.

5.5.1. Experimental method

As discussed earlier, jar testing and pilot testing were initially performed for evaluating the effect of a range of pH and coagulant doses on the removal of TOC and turbidity. Coagulation was performed by utilizing a series of five doses of PACl in five jars containing blended water, while the sixth jar, which has no PACl, serves as the experimental control. These doses were selected for investigating the ineffectiveness of coagulation in the absence of PACl by the optimal removal of turbidity in the presence of a coagulant. The initial doses were selected on the basis of literature reviews^{7, 8, 16, 22, and 26}.

PACl was added to 2 L jars in increments of 15 mg/L to a maximum dose of 75 mg/L at the same pH of 6.8. The doses required for ineffective coagulation and optimal turbidity were established on the basis of the percent removal of turbidity and NOM (as TOC) from the source water during the test. The turbidity of the settled water ranged between 3.16 and 75 NTU, and TOC ranged between 9.82 and 18.30 mg/L at the dose for the optimal removal of TOC and turbidity from the blended source water. A dose of 47.5 mg/L was selected as the optimal dose, based on its effectiveness for removing a little over 90% of turbidity and greater than 31% of TOC. Although it is not the most efficient dose as compared to higher doses such as 60 and 75 mg/L, which removed 94% turbidity

and 97% TOC, respectively, 47.5 mg/L is more feasible than the other higher doses because of the mild chemical impact on the environment and economic analysis.

Results obtained from the jar tests (Figures 5.5.1.1 and 5.5.1.2) conducted during the pilot study have demonstrated that the increase in the dose of PACl can be very effective for the removal of DOM; moreover, the continuous feeding of high levels of coagulants during pretreatments can incur high cost. In addition, the over-feeding of a coagulant salt will result in the transfer of excess dissolved metals to the RO, which will eventually precipitate and crystallize on the membrane surface, thereby affecting the membrane performance.

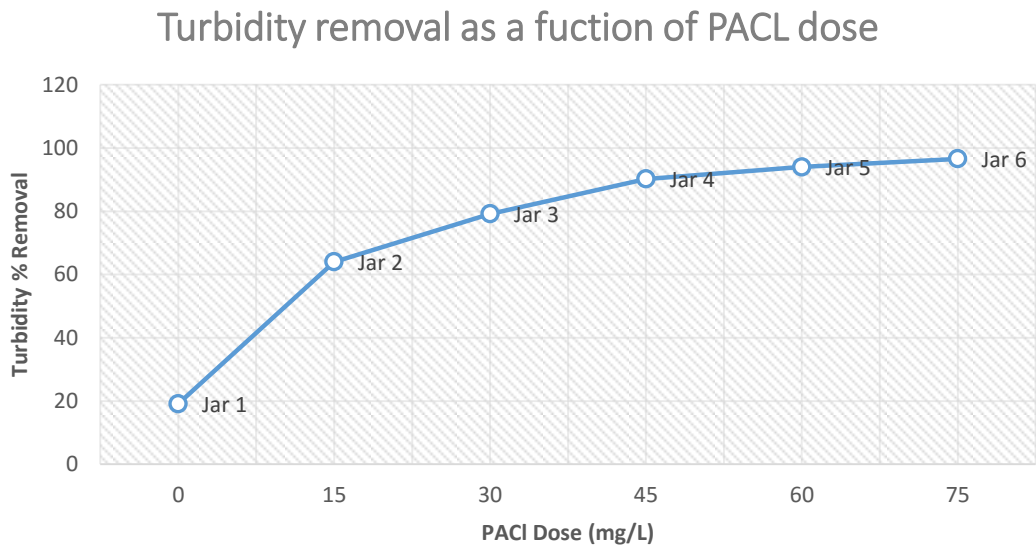


Figure 5.5.1.1. Turbidity removal as a function of PACl dose.

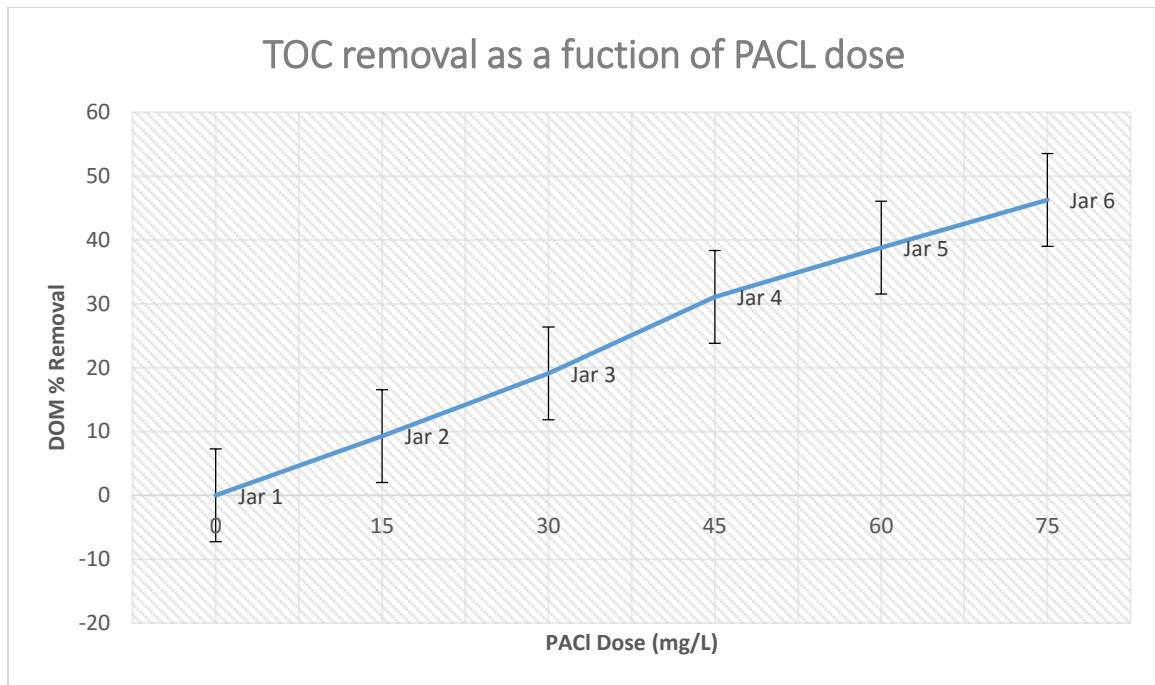


Figure 5.5.1.2. NOM removal as a function of PACl dose.

Tables 5-2 and 5-3 show the testing matrices for pH and coagulant doses selected for this pilot study, respectively. These matrices were based on the initial results obtained from jar tests and literature reviews. The individual elements observed in the matrix represent certain coagulant doses added to the influent water and specified pH levels established before they were entered into the pretreatment unit. The hydraulic residence time for each pretreatment unit experiment in the pretreatment unit was 6 h before any change was made to the system; periodic testing on the pretreatment effluent was performed with the aim of achieving desired pH. To obtain the effluent pH in the pretreatment unit for this investigation, appropriate amounts of sulfuric acid were added to the unit flow of the pretreatment influent. Coagulant doses were also adjusted for the influent flow of the pretreatment unit.

Table 5-2 shows the testing matrix for the pH and coagulant doses (PACl) selected for this study. PACl was used as a coagulant salt in the testing matrix of the first experimental process. On Day 1 (row 1 of the testing matrix), the turbidity of raw water was 98.6 NTU, pH was 8.2, temperature was 20.5°C, and DOM was 16.1 mg/L. On Day 2 (row 2 of the testing matrix), the turbidity of raw water was 88.5 NTU, pH was 8.3, temperature was 20.9°C, and DOM was 16.6 mg/L. On Day 3 (row 3 of the testing matrix), the turbidity of raw water was 78.1 NTU, temperature was 20.2°C, DOM was 16.3 mg/L, and pH was 8.3.

Table 5-2. Pilot pretreatment unit testing matrix using PACl salt.

PACl Dose (mg/L)	35	40	47.5
pH	6	6	6
	6.5	6.5	6.5
	7	7	7

Table 5-3 shows the testing matrices for pH and doses of coagulant (ferric chloride, FeCl₃) selected for this study. The addition of FeCl₃ to the pretreatment feed water resulted in the decrease of pH to near 7. On Day 1 (row 3 of the testing matrix), the turbidity of surface water in the pretreatment feed was 6.67 NTU, pH was 8.05, temperature was 3.4°C, and DOM was 14.7 mg/L. On Day 2 (row 4 of the testing matrix), the turbidity of pretreatment surface feed water was 6.42 NTU, pH was 7.93, temperature was 3.4°C, and DOM was 14.9 mg/L.

The data and samples collected on Day 3 coincide with elements J_{7, 50} and J_{7, 60} of the testing matrix. The turbidity of water in the pretreatment feed was 6.39 NTU, temperature was 2.8°C, DOM was 12.4 mg/L, and pH was 8.07. In addition, the data and samples collected on Day 4 coincided with elements J_{6.5, 50} and J_{6.5, 60} in the testing matrix shown in Figure 4. The turbidity of water in the pretreatment was 5.47 NTU, temperature was 3.2°C, DOM was 13.3 mg/L, and the base pH was 7.97.

Table 5-3. Testing matrix for the pilot pretreatment unit (FeCl₃).

FeCl Dose (mg/L)	35	40	50	60
pH	6.5	6.5	6.5	6.5
	7	7	7	7

5.5.2. Mathematical modeling

JMP was used to create neural network models by utilizing a neural platform, which is an automatic fit procedure. Neural platforms are statistical models that identify one or more response variables in a distributed data set. They also allow users to compare the predictive ability of a fully connected multilayer perceptron with one or two layers by using the combination of interaction effects among the independent variables. A model report created for every neural network provides summary about model fits, effect significance, and model parameters for the training and validation data sets^{105, and 106}. The

main approach is to specify the validation method, structure of the hidden layer, and a specific fitting option.

Because of the flexibility of neural networks models, they sometimes tend to overfit data. When overfitting occurs, the model predicts the data very well, but poorly predicts data from other systems. For preventing overfitting, the neural platform applies penalty on the data set (called the training set) of parameters, which will be used in creating the model. This will randomly hold back part of the data, which is called the validation set. The neural platform then uses the validation data set to assess the predictive ability of the model. This process is called validation. However, the holdback method randomly divides the data set into training and validation sets¹⁰⁷.

As previously mentioned, neural platforms can fit one- or two-layer neural networks. This hidden layer(s) contains nodes where activation functions such as TanH, Linear, and Gaussian are applied. In the present study, TanH was utilized. This process generates a model report for the neural network, which shows the measure of fit for the training and validation sets. Missing data points were replaced using the “impute missing data approach,” which can only be performed when the data table contains a missing value. The cluster hierarchical technique produces new data, which duplicate the original table and replace the missing data by the mean of the variable. This imputed data will be included in the model^{105, 107, and 106}.

The measure of fit obtains the value of R^2 (scaled to have a maximum value of 1) for the relationship between the independent operating parameters and the response of the output parameter. R^2 for the correlation relationship between the cause and the effect would be characterized as follows: less than or equal to 0.20 is very weak; greater than

0.20 and less than or equal to 0.40 is weak; greater than 0.40 and less than or equal to 0.60 is moderate; greater than 0.60 and less than or equal to 0.80 is strong; and greater than 0.80 is very strong. The R^2 value of 1 represents a perfect model, and the value of 0 implies that the obtained model is no better than the predicted model. The measure of fit report also gives the difference between the values of the original measurement and those predicted by the model. This is called the root mean square error (RMSE). In addition, the report gives the discrepancy between the observed data and the estimated model data, and is called the error sum of squares.

5.6. Results and discussion

5.6.1. Turbidity

Figure 5.6.1.1 shows the plot of turbidity of the influent from pretreatment versus date, and Figure 5.6.1.2 shows the plot of variation in the amount of turbidity measured in the effluent water coming out of the pretreatment unit versus date. Some of the spikes in the effluent turbidity plot are attributed to events of precipitation, which increased the turbidity of the influent. Other observed spikes can be attributed to events when the feeding of coagulant chemicals was stopped during coagulation.

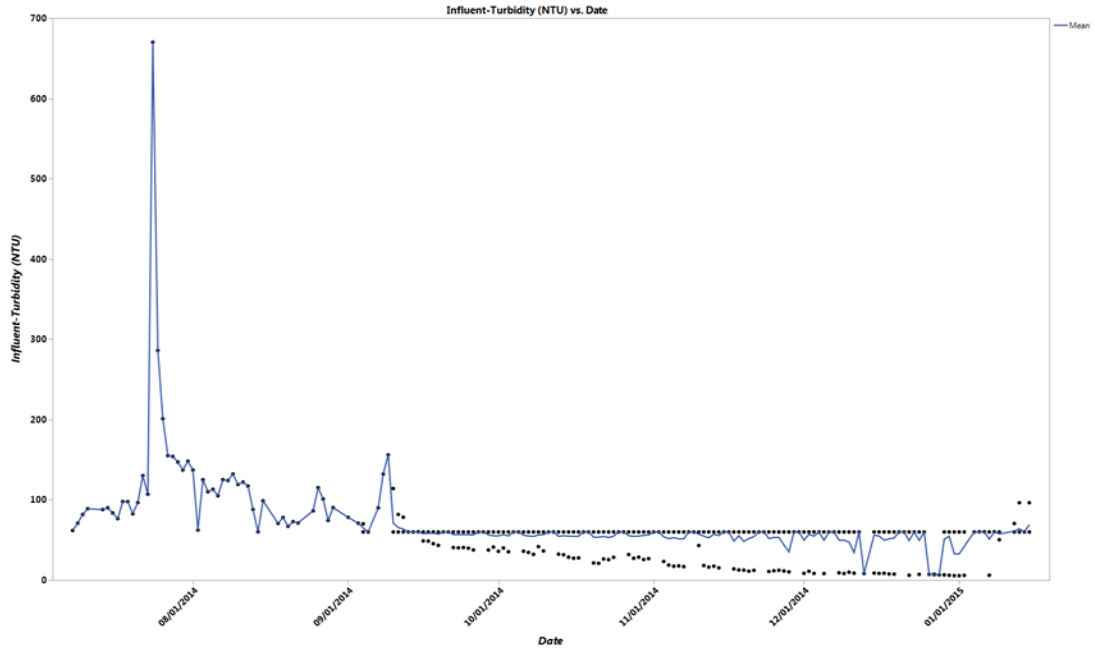


Figure 5.6.1.1. Raw water turbidity during the pilot study.

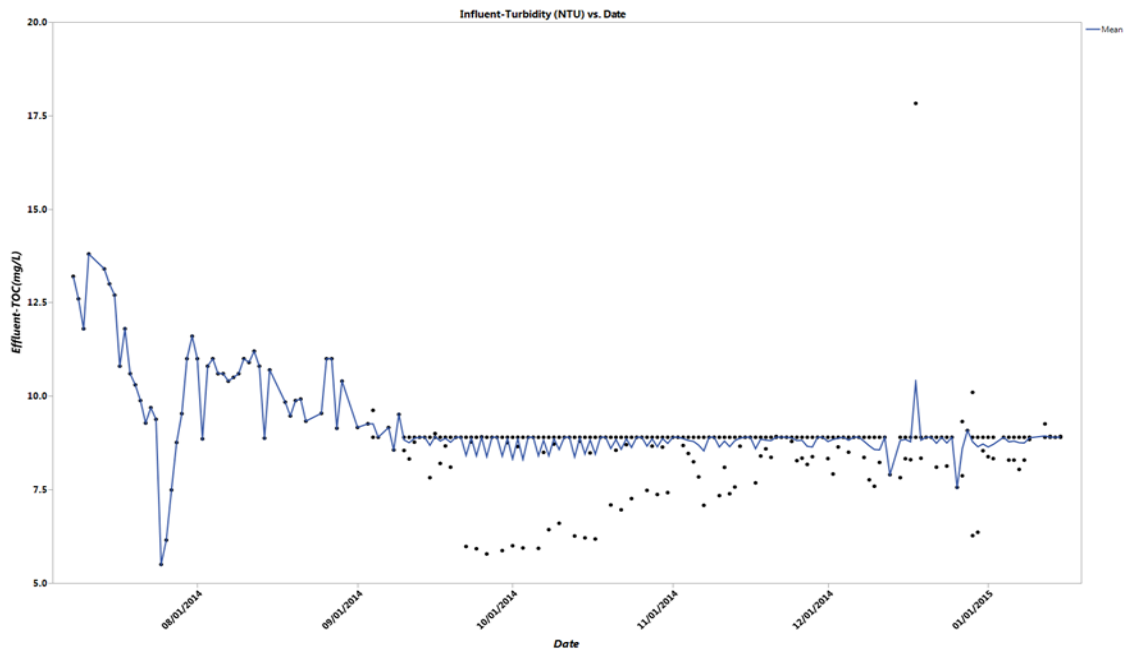


Figure 5.6.1.2. Raw water TOC during the pilot study.

Figure 5.6.1.3 shows the effect of pH and dose of coagulant on the turbidity removal performance of PACl coagulation and sedimentation. The increase in the

coagulant dose correlates to the increase in the removal of turbidity, which is in agreement with the jar test results. At a PACl dose of 47.5 mg/L and at pH of 6.5 and 6, the removal of turbidity increased more than that at PACl dose of 47.5 mg/L and pH 7. This trend of pH effects on coagulation can also be observed at the other doses (40 mg/L and 35 mg/L). Although an increase in the coagulant dose produces the desired reduction in turbidity, there is a concern for aluminum carryover. Therefore, pH adjustment and a lower PACl dose will optimize the pretreatment performance of the coagulant while minimizing the carryover into the RO process.

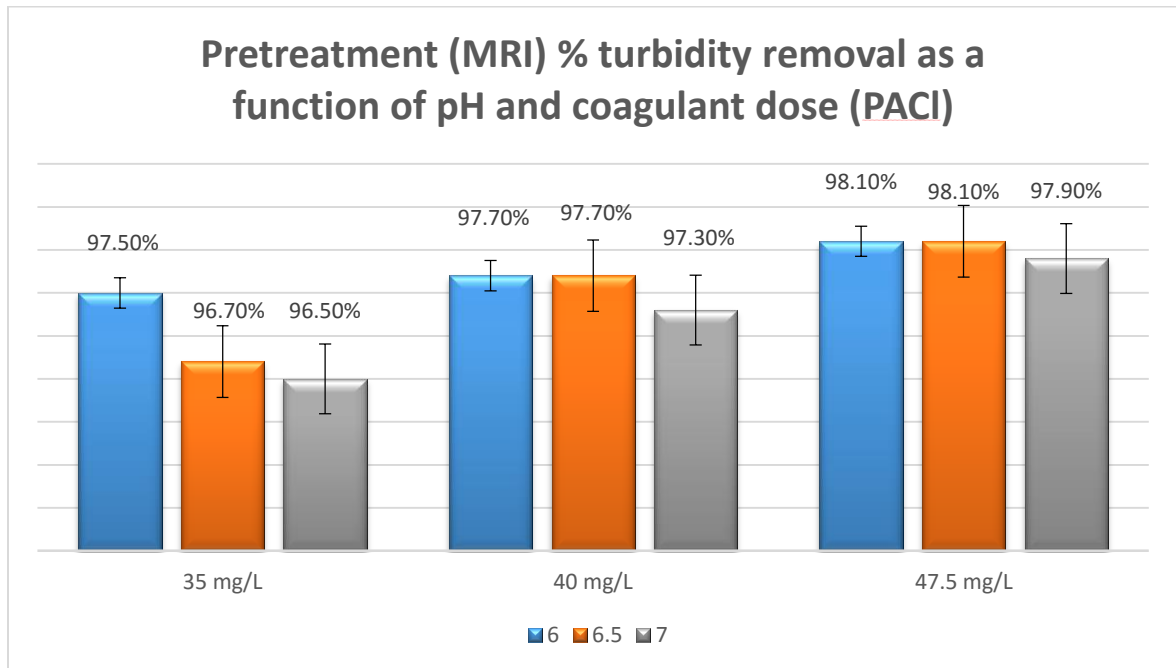


Figure 5.6.1.3. Percent removal of turbidity using PACl during pretreatment process as a result of acid adjustment and coagulant dose.

As shown in Figure 5.6.1.4, the impact of pH adjustment can be observed through the performance of FeCl_3 for the removal of turbidity. As shown in the figure, pH 6.5 in combination with any dose showed better removal of turbidity compared to the same dose at pH 7. The optimal combination was pH 6.5 and a coagulant dose of 50 mg/L.

Although an increase in the coagulant concentration during the jar test typically results in a higher reduction of turbidity, the possibility of carryover for dissolved ferric ion exists, which could foul the RO membrane. Hence, the reduction in pH and a lower FeCl_3 dose will control the iron(III) carryover while optimizing the performance of this coagulation process.

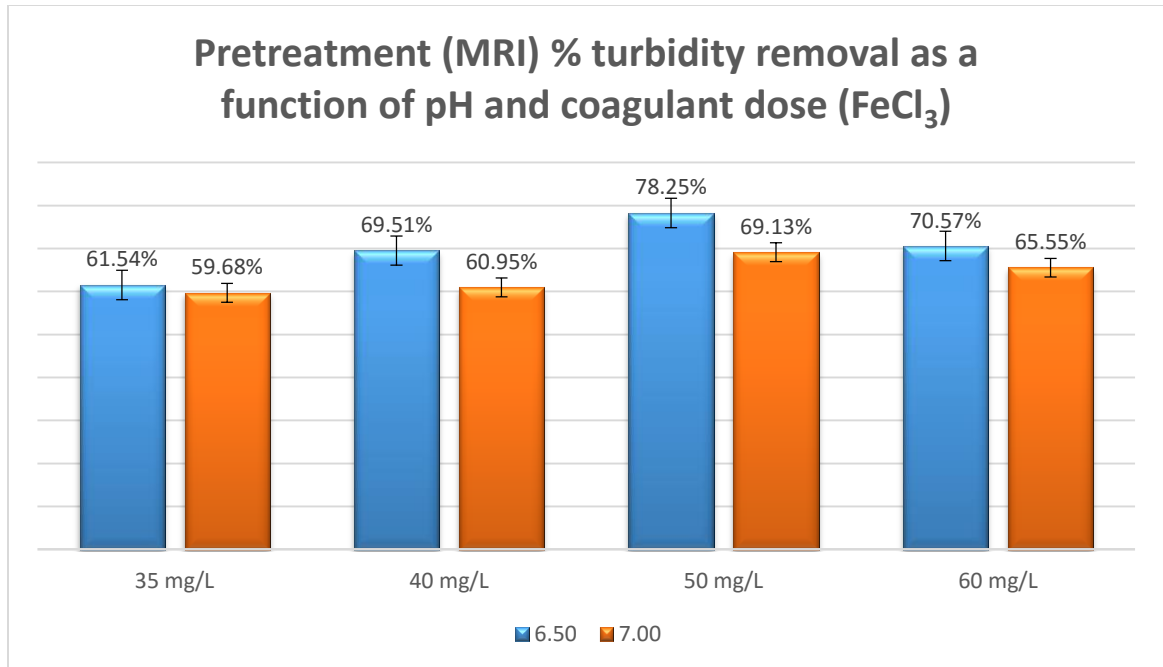


Figure 5.6.1.4. Percent removal of turbidity using FeCl_3 during pretreatment process as a result of acid adjustment and coagulant dose.

Figure 5.6.1.5 shows a one-layer neural network with eight X variables (flow rate, coagulant dose, acid dose, temperature, influent TOC, conductivity, TDS, and TSS), which were used to construct the response observed in the Y variable (effluent turbidity). The layer has three nodes (H_1 , H_2 , and H_3), which are a function of the eight X variables. The predicted Y variable is also a function of the three nodes in the layer. The function applied at the node on the hidden layer is called the activation function. This activation

function is the transformation of the linear combination of the X variables. However, the function applied at the response is the linear combination of the X variables (Appendix I).

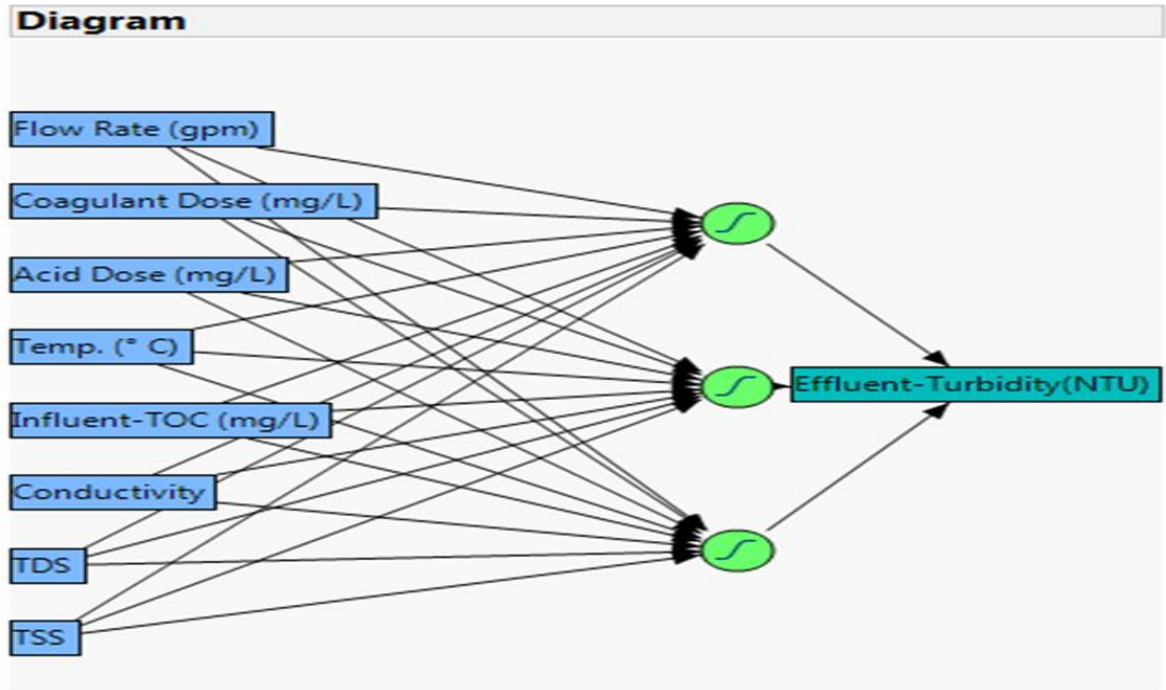


Figure 5.6.1.5. Neural network diagram used in predicting effluent turbidity during the pretreatment process.

Table 5-4 shows the results obtained from both training and validation sets. The results of the validation set represent the predictive power of the model for future observations. The R^2 statistic for the validation set is 92%, which implies that the model well predicts the data that were not used to train the model.

Table 5-4: Training and validation data of statistical analysis of effluent turbidity (SSE, sum of squares)

Effluent-Turbidity (NTU)- Training Result		Effluent-Turbidity (NTU)- Validation Result	
Measures	Value	Measures	Value
RSquare	0.980325	RSquare	0.9155849
RMSE	0.0477556	RMSE	0.1052079
Mean Abs Dev	0.0188706	Mean Abs Dev	0.0295129
-LogLikelihood	-780.5282	-LogLikelihood	-200.7237
SSE	1.0969689	SSE	2.6675572
Sum Freq	481	Sum Freq	241

Figure 5.6.1.6 shows the additional assessment of the model fit. The validation plot shows that the points were along the line, suggesting that the predicted values are similar to the actual measured values.

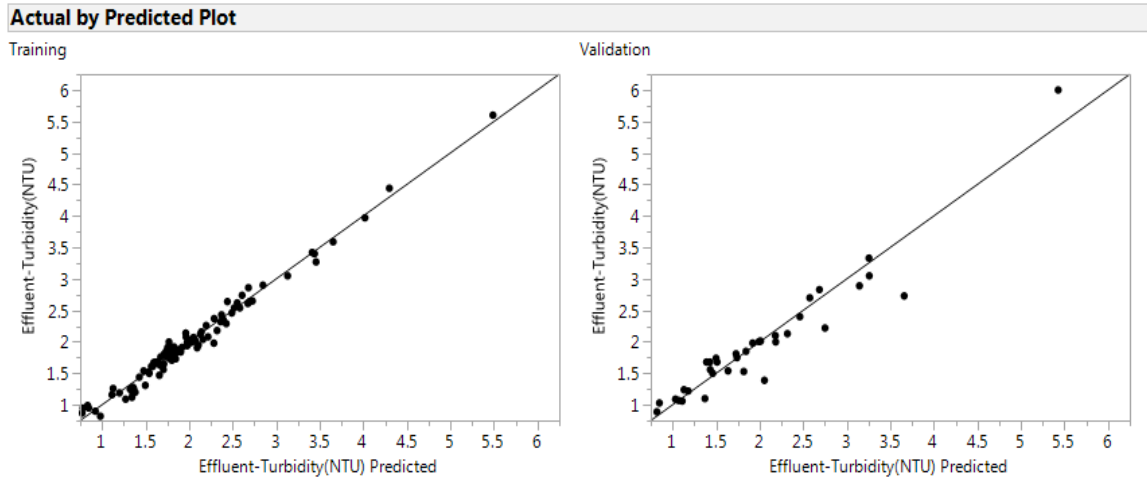


Figure 5.6.1.6. Model fit for effluent turbidity.

Figure 5.6.1.7 shows blue points, which represent the variation in effluent turbidity measured during the day, while the red points represent effluent turbidity rates predicted by utilizing the properties of the model affected by pretreatment to determine whether its measured turbidity is similar to that of the effluent water obtained after

treatment. Accordingly, we observed that the pattern of effluent turbidity rates created by the model approximately fitted with the behavioral pattern of the actual measurements of turbidity values observed for the pretreatment unit.

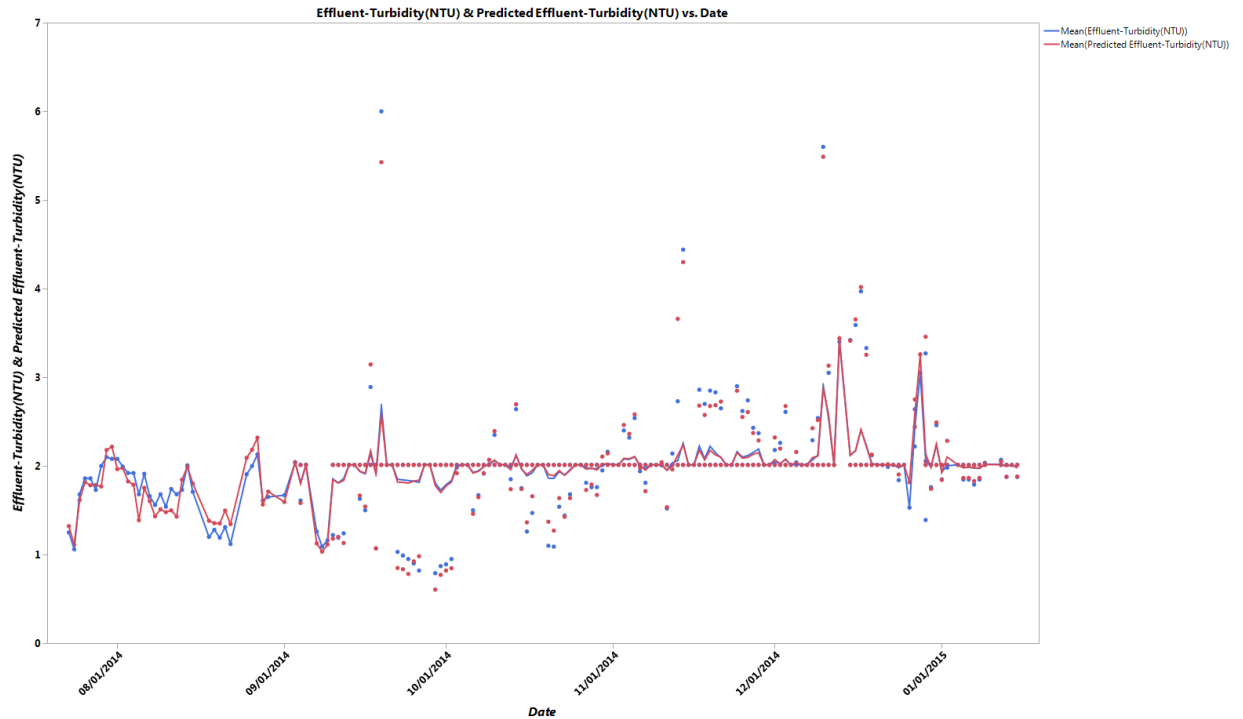


Figure 5.6.1.7. Graph of effluent turbidly and the graph of the predicted effluent turbidity of the model fit over time.

Figure 5.6.1.8 shows the interactions between the effluent turbidity rate and the most significant operating parameters such as temperature, flow rate, coagulant dose, acid dose, TDS, conductivity, influent TOC, and TSS used in creating the model employed in this study. The prediction profiler shows prediction traces for each independent parameter. The vertical dotted line for each parameter correlates with its current setting and can be changed at a time to examine its effect on the dependent variable. A positive (direct) relationship exists between the turbidity of the effluent and the temperature, flow rate, conductivity, and influent TOC. In contrast, the graph exhibited a negative (inverse)

relationship when permeability interacts with the coagulant dose, acid dose, TDS, and TSS.

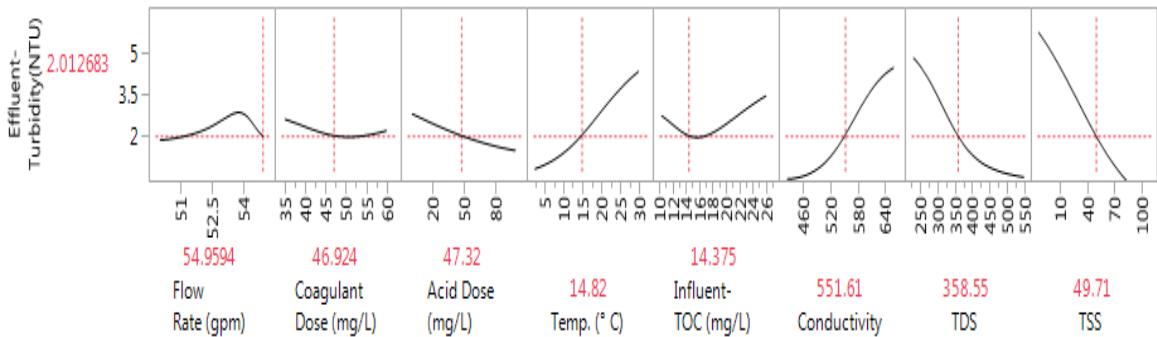


Figure 5.6.1.8. Relationship between system parameters and effluent turbidity.

5.6.2. Dissolved organic matter (DOM)

The blue line in Figure 5.6.2.1 represents the plot of the pretreatment influent TOC versus date. Also shown in the figure is a red line, which represents the variation in the amount of TOC measured in the effluent water coming out of the pretreatment unit. In this graph, some of the spikes in the effluent TOC were attributed to events of precipitation, which increased the influent TOC. Other observed spikes can be attributed to events that occurred when the feeding of coagulant chemicals was stopped during coagulation.

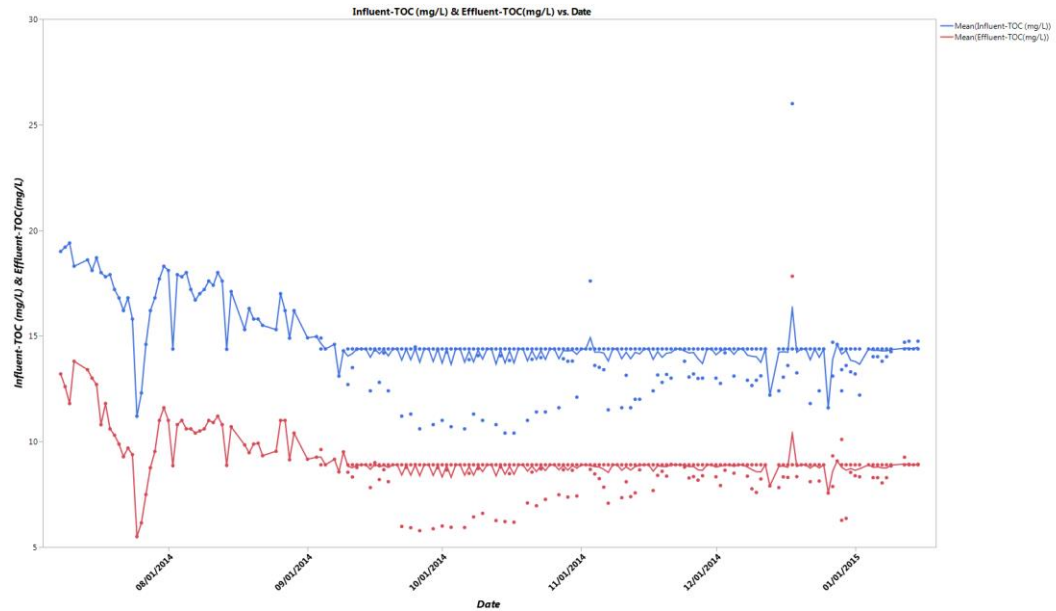


Figure 5.6.2.1. Graph of influent and effluent TOC.

Figure 5.6.2.2 shows the percentage of DOM removal with varying pH and dose of PACl during pretreatment (coagulation, flocculation, and sedimentation). A pH of 6.5 and a PACl dose of 40 mg/L in pretreatment represented economically optimal conditions, which reduce chemical costs of the treatment facility while precipitating the dissolved aluminum by hydrolysis. These conditions also helped achieve nearly the same DOM removal as a higher PACl dose of 47.5 mg/L and a higher pH of 7 or as a lower PACl dose of 35 mg/L and a lower pH of 6 does.

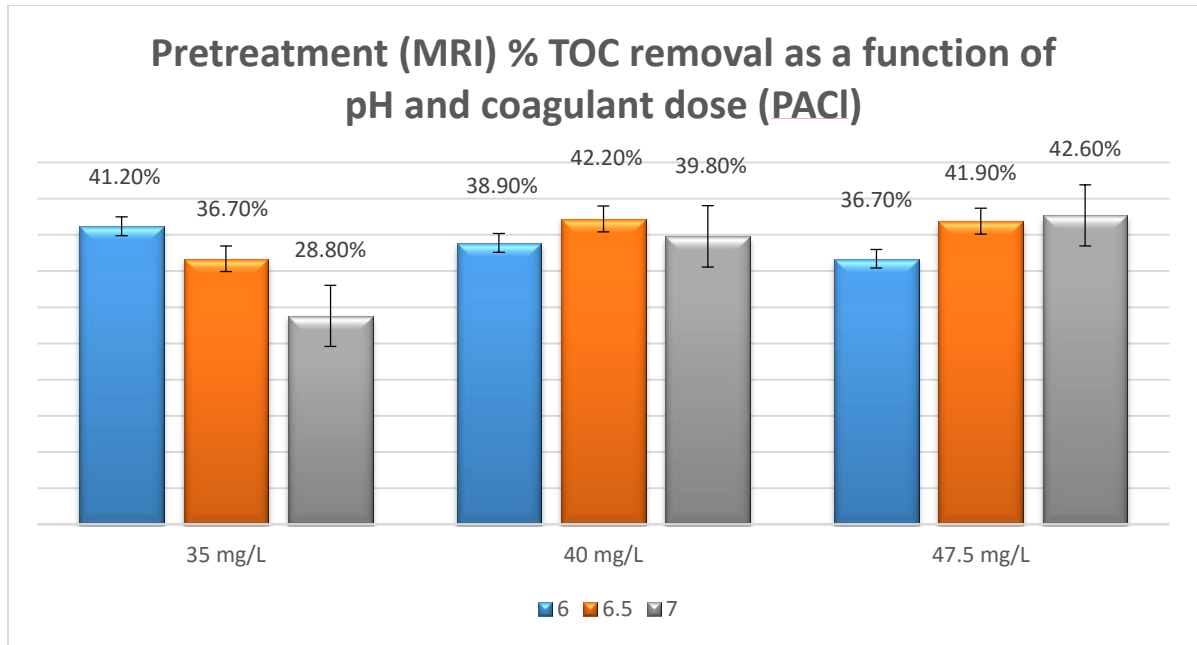


Figure 5.6.2.2. Percent removal of DOM using PACl during pretreatment process as a result of acid adjustment and coagulant dose.

Figure 5.6.2.3 shows the percentage of DOM removal with varying pH and FeCl_3 doses during coagulation and flocculation. The optimal pH and coagulant dose to enhance the performance of FeCl_3 are 6.5 and 50 mg/L, respectively. Therefore, reducing the coagulant dose to 50 mg/L (as opposed to 60 mg/L) at pH 6.5 will reduce the chemical costs while precipitating the dissolved iron(III) metal through hydrolysis and achieving the highest DOM removal.

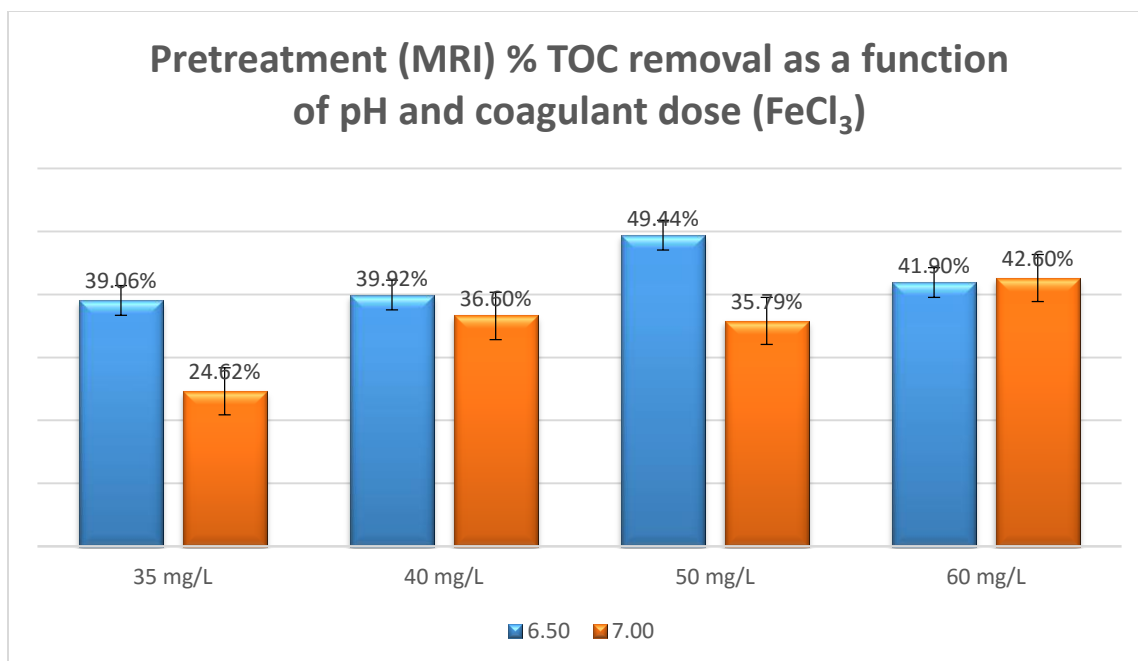


Figure 5.6.2.3. Percent removal of DOM using FeCl₃ during pretreatment process as a result of acid adjustment and coagulant dose.

Figure 5.6.2.4 shows the effect of pH on the performance of low-pressure UF membranes for DOM removal. The graph was constructed to investigate the impact of pretreatment optimization in improving the performance of UF. Because of UF membrane pore size, low-pressure UF membranes are relatively ineffective for the removal of DOM during the filtration of surface water. However, they are very effective for the removal of turbidity. Thus, it is imperative to investigate the optimum conditions that will increase the efficiency of UF in DOM removal.

In the filtration of pretreated effluent water with pH 7, the UF membrane removed approximately 5.3%–7.4% TOC (Figure 5.6.2.5). At pH 6, the removal efficiency of DOC from the membrane decreased to less than 5% of the UF influent TOC. These results indicate that the threshold of aggregation and the precipitation of DOM, as well as optimal removal of DOM, occurred at pH 6.5 and PACl dose of 40 mg/L, with a removal

efficiency of 8.7%. Hence, it can be concluded that pH 6.5–7 allowed for the aggregation of DOC and the formation of matter whose molecular size was greater than that of the nominal MWCO of the UF membrane used. Similar conditions for the optimal removal of DOM were observed in the pretreatment using PACl. These results suggest that UF alone, as compared to the combination of pretreatment comprising coagulation and sedimentation processes, is less effective for the removal of DOM.

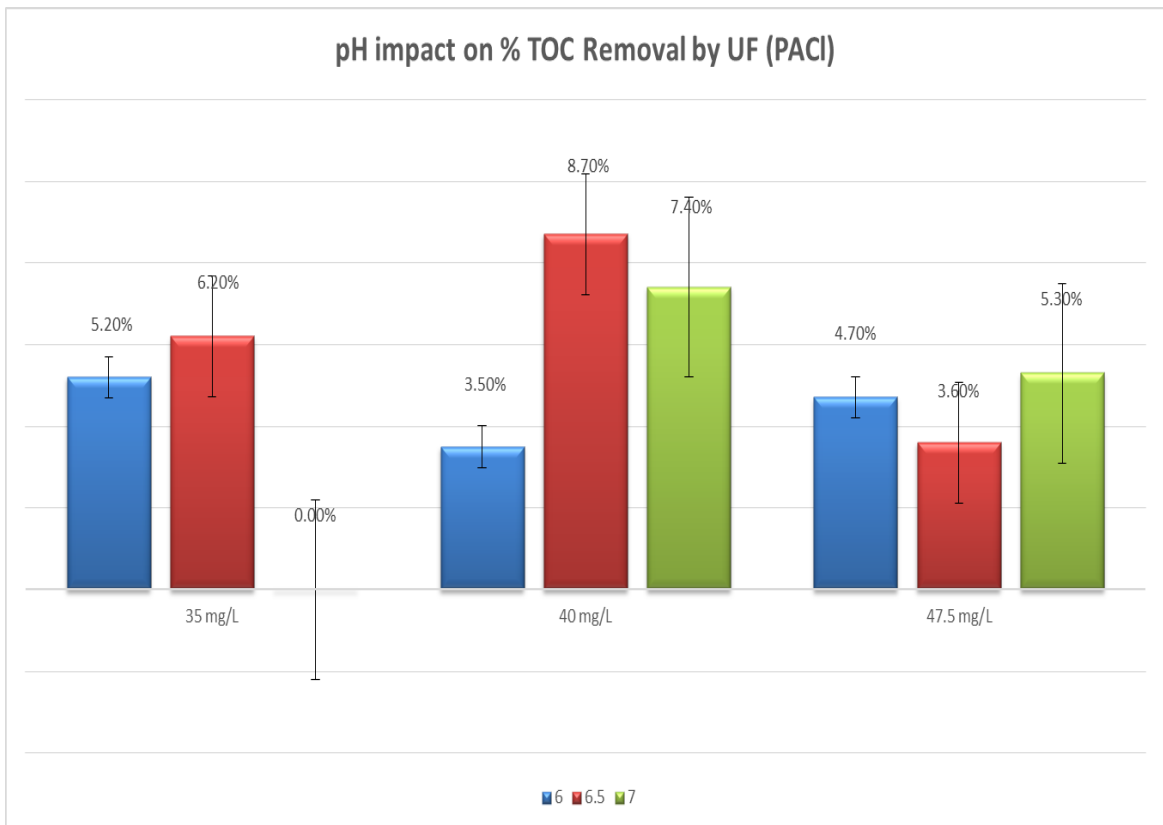


Figure 5.6.2.4. Percent removal of turbidity using PACl during ultrafiltration process process as a result of acid adjustment and coagulant dose.

Figure 5.6.2.5 shows the effect of pH and FeCl_3 dosage on the performance of the UF membrane for DOM removal. Low-pressure membranes (such as UF), owing to their pore size, are very effective for the removal of turbidity, but are less effective for the

removal of DOM. However, these data show that the efficiency of UF for the removal of DOM can be optimized. The optimal UF conditions are as follows: FeCl₃ doses, between 35 mg/L and 40 mg/L; pH, 6.5, and DOM removal efficiency, 30.8% of the UF influent DOM. Higher coagulant doses and lower pH levels lowered the effectiveness of UF for the removal of DOM, which is possibly attributed to better turbidity and DOM removal efficiency. In conclusion, pH levels below 7, but not less than 6.5, allow for the aggregation of DOM and formation of particles whose MWCO is larger than that of the nominal MWCO of the membrane. As compared to the combination of coagulation, sedimentation, and UF, UF alone is less effective for the removal of DOM.

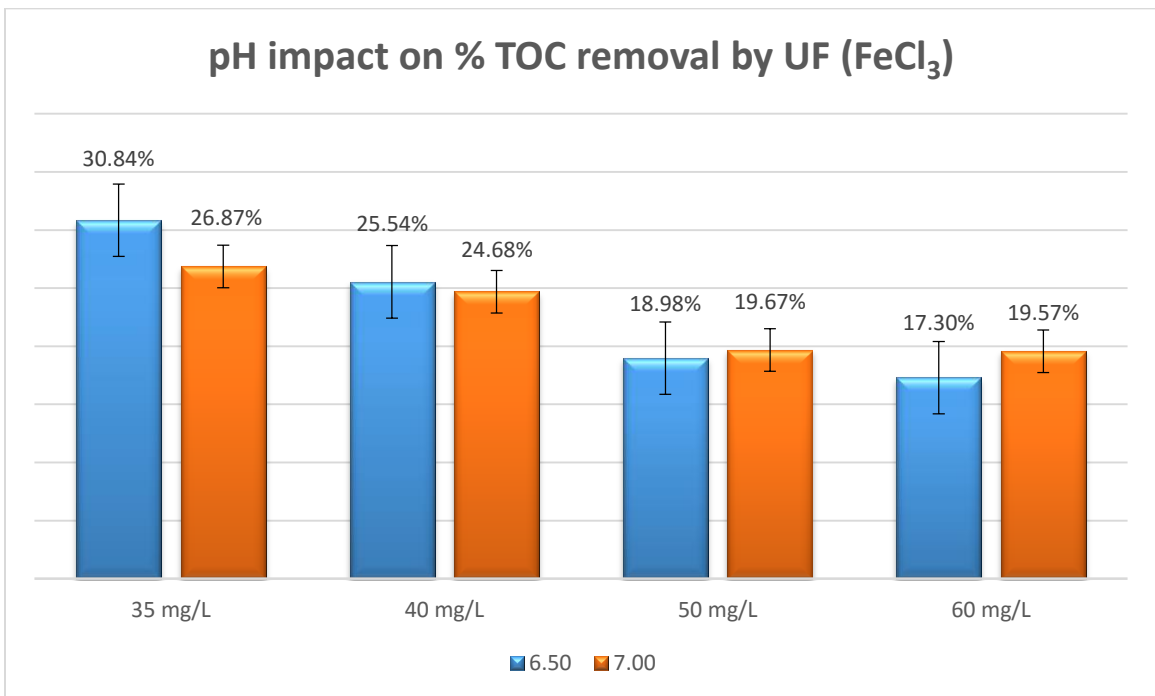


Figure 5.6.2.5. Percent removal of turbidity FeCl₃ during ultrafiltration process process as a result of to acid adjustment and coagulant dose.

Figure 5.6.2.6 shows a one-layer neural network with six X variables (temperature, coagulant dose, acid dose, TDS, conductivity, and influent TOC), which

were used to construct the response observed in the Y variable (effluent TOC). The layer has three nodes, which are a function of the six X variables. The predicted Y variable is also a function of the three nodes in the layer. The function applied at the node on the hidden layer is called the activation function. This activation function is the transformation of a linear combination of the X variables. However, the function applied at the response (effluent TOC) is a linear combination of the X variables (Appendix II).

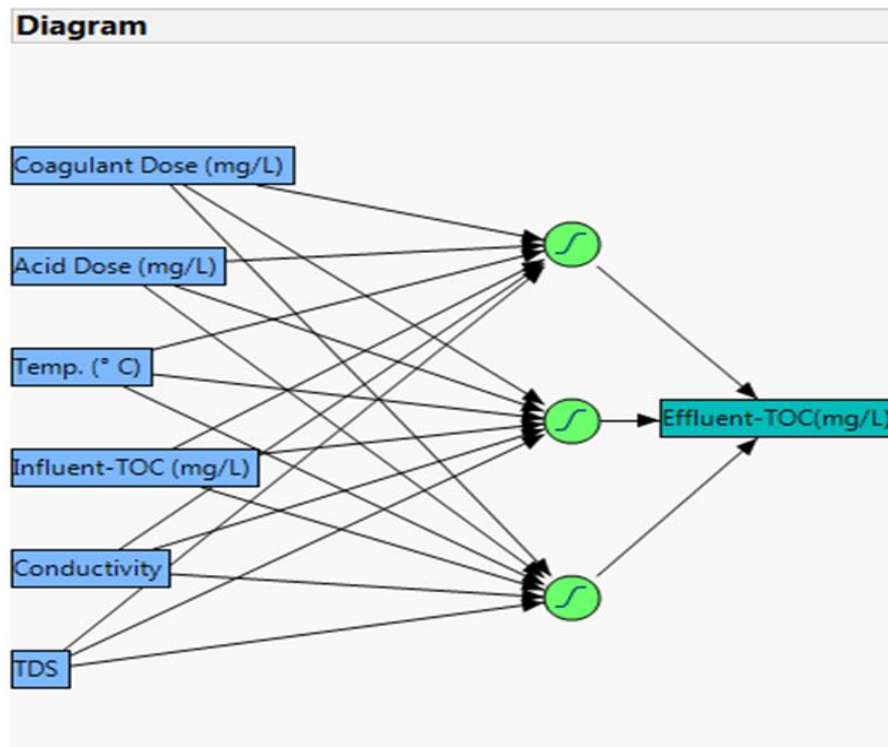


Figure 5.6.2.6. Neural network diagram used in predicting effluent turbidity.

Table 5-5 lists the results obtained from both training and validation sets. The results of the validation set represent the predictive power of the model on future observations. The R-Square statistic for the validation set was 96%, which indicates that the model well predicts the data not used to train the model.

Table 5-5: Training and validation data of statistical analysis of effluent TOC

Effluent-Turbidity (NTU)- Training Result		Effluent-Turbidity (NTU)- Validation Result	
Measures	Value	Measures	Value
RSquare	0.9639201	RSquare	0.8982615
RMSE	0.1357803	RMSE	0.1947403
Mean Abs Dev	0.0401759	Mean Abs Dev	0.0629653
-LogLikelihood	-277.9116	-LogLikelihood	-52.33314
SSE	8.8678511	SSE	9.1396305
Sum Freq	481	Sum Freq	241

Figure 5.6.2.7 shows the additional assessment of the model fit. The validation plot shows that all points were along the line, suggesting that the predicted values are similar to the actual values.

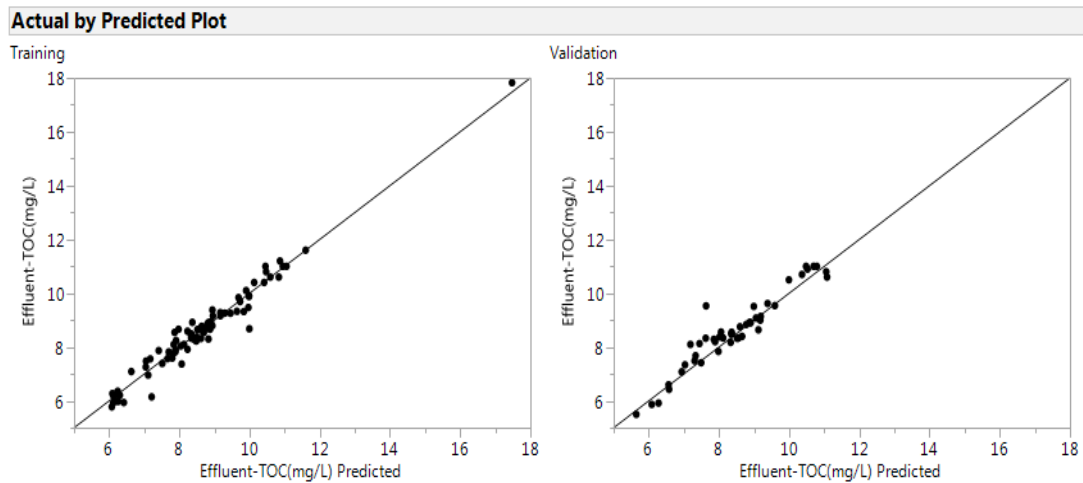


Figure 5.6.2.7. Model fit for effluent TOC.

As shown in Figure 5.6.2.8, blue points represent the concentration of the measured TOC in the effluent by day, and red points represent the effluent TOC concentration. Both these points represent concentrations predicted using the properties of the model affected by pretreatment to determine whether its measured TOC is similar

to that of the effluent water obtained after treatment. Accordingly, we observed that the pattern of the effluent TOC concentration created by the model slightly fitted with the behavioral pattern of the actual measurements of TOC concentration observed for the pretreatment reactor.

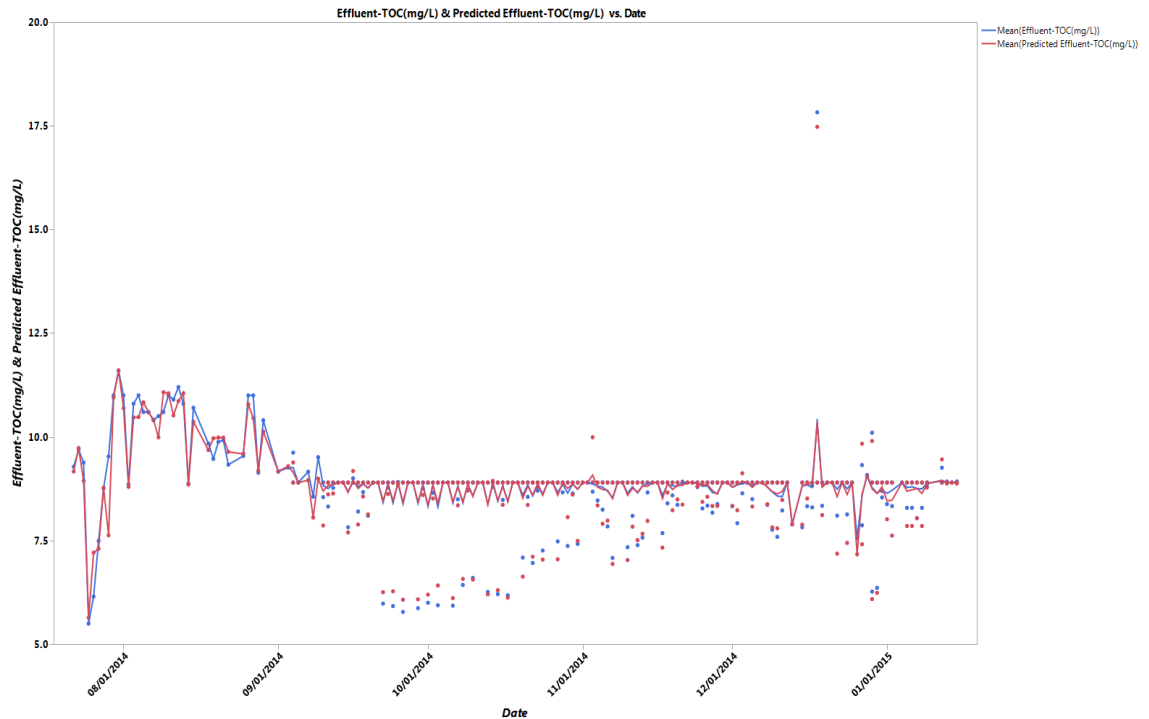


Figure 5.6.2.8. Graph of effluent turbidity and the graph of the predicted effluent turbidity of the model fit over.

Figure 5.6.2.9 shows the interactions between the effluent TOC rate and the most significant operating parameters (temperature, coagulant dose, acid dose, TDS, conductivity, and influent TOC) used in the creation of the model employed in this study. The prediction profiler shows prediction traces for each independent parameter. The vertical dotted line for each parameter correlated with its current setting and can be changed at a time to examine its effect on the dependent variable. A positive (direct) relationship existed between the effluent TOC and the temperature, acid dose, TDS, and

influent TOC. In contrast, the graph exhibited a negative (inverse) relationship when the effluent TOC interacts with the coagulant dose and conductivity.

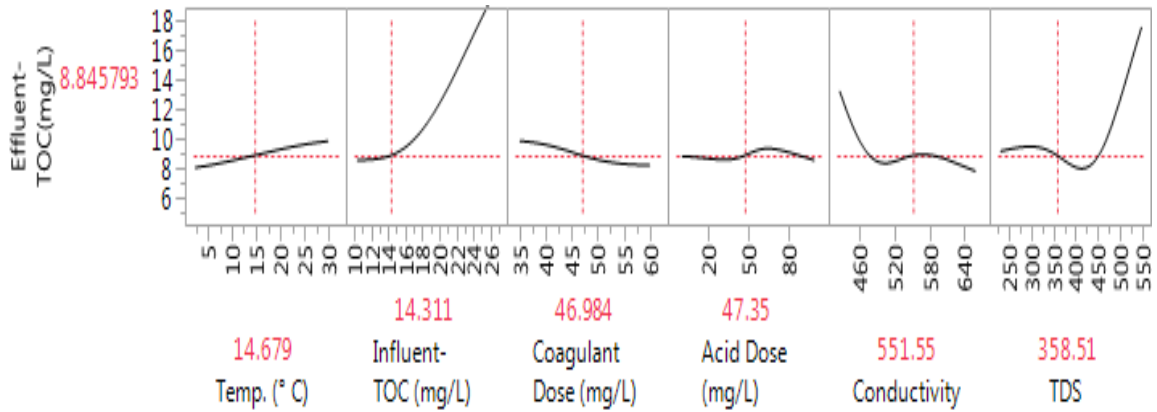


Figure 5.6.2.9. Relationship between system parameters and effluent TOC.

5.7. Conclusion

The analysis of coagulation, flocculation, and sedimentation pretreatment for blended surface waters at the GFWTP (Red Lake, 80–90% ; Red River, 10–20%) with pH adjustment revealed the optimal pH values and doses for both coagulants (PACl and FeCl₃) used in this study. Based on the result obtained, it can be concluded that the decrease in the surface water pH by adding sulfuric acid allowed for the reduction of the coagulant dose while maintaining the efficiency of turbidity and DOM removal.

At a pH of 6.5, coagulant concentration of 40 mg/L of PACl, and temperature of 20.9 °C, the combined pretreatment exhibited a significant increase in the removal of DOM (42.20%) and turbidity (99.70%). At a pH of 6.5, 50 mg/L of FeCl₃, and temperature of 2.8 °C, the combined pretreatment exhibited the most effective removal for DOM (59.44%) and turbidity (99.13%).

At a pH of 7, 40 mg/L of PACl, and a temperature of 20.2 °C, the combined pretreatment removal values for DOM and turbidity were 35% and 97.30%, respectively. At a pH of 7, 50 mg/L FeCl₃, and a temperature of 3.2 °C, the combined process using iron(III) salts exhibited the most effective removal for DOM (48.42%) and turbidity (97.13%).

A previous pilot study on pretreatment processes at the GFWTP has revealed some inconsistencies in the removal of TOC and turbidity found in the analyzed surface waters. Because of water chemistry and conductivity, pretreatment effluent TOC and turbidity decreased on increasing the coagulant chemical dose; it further decreased when the pH was less than 7 during the pretreatment. As predicted by the model used for this study, the impact of pH adjustment and coagulant chemicals and the interaction between chemical species in surface water played a significant role in the distribution of TOC and turbidity. The overall relationship and interaction between these aqueous species was statistically significant, and its strength was accurately characterized using data mining techniques. The estimated coefficient for all variables was also statistically significant, and the directions of the relationships were accurately characterized using these techniques. The methodology developed in the present study for this pretreatment can be approximately generalized.

In addition, this model building approach can be applied to other coagulation, flocculation, and sedimentation pretreatment processes regardless of the chemistry of the water being treated. Another consideration of this model is the representativeness of the variable construct using a neural network platform. The neural network platform is designed to find the predictors that are most effective in predicting the dependent

variables that lead to a model. The prediction model developed in this study employed independent variables that were measured on the same day as the dependent variable (TOC and turbidity).

Overall, this research has indicated that enhanced coagulation additives and pH in an upstream pretreatment unit operation will benefit downstream membrane treatment processes. However, a previous GFWTP pilot study research has demonstrated that when more DOM and turbidity are removed by coagulation, RO membrane fouling levels are reduced.

Future research will involve the characterization of hydrophobic and hydrophilic fractions of organic matter present in the surface water treated by the City of Grand Forks Water Treatment Plant. It would also be interesting to examine the effect of temperature on DOC removal and RO filtration in future investigations.

CHAPTER VI

GFWTP REVERSE OSMOSIS PILOT PLANT PROCESS

6.1. Abstract

In this study, a new testable prediction of the quantity and quality of product water was derived for reverse osmosis (RO) systems A (permeability) and D (system salt passage) to explain the system performance and separation efficiency in RO A, B, C, and D. The prediction was carried out using a mathematical model of normalized permeability and system salt passage. This analysis was conducted to provide understanding of conditions of the RO system, and can be used to troubleshoot potential problems before they become serious.

The model constructed from RO system A data accurately predicted the quantitative dependence of permeability on temperature, feed flow, system recovery, net driving pressure (NDP), and water flux. The system D data model accurately predicted the quantitative dependence of salt passage on temperature, feed flow, post-recycle feed conductivity, system recovery, permeate TDS, manufacturer's rated salt passage, and water flux. Strong interactions with the fundamental operating conditions of the RO systems and the interaction between permeability and system salt passage were confirmed when the model was tested in RO systems A, B, C, and D. Although reasonable agreement was obtained when the model was tested in these four RO systems,

it appears that the model-predicted permeabilities were slightly higher than the permeabilities recorded in RO system B. It also appears that the model-predicted salt passage were lower than the salt passage recorded in RO system B. These discrepancies may be attributed to the linear model constant related to the solubility of the chemical species in the feed water and the morphology and structure of the RO membrane used. Additionally, system recovery (75%, RO B, 82%, RO A and 82%, RO D) and changes in ROs A and D (predictive model) water flux from 11 gallons/ft²/day (gfd) to 12 gfd may also be important.

6.2. Introduction

ROT is a membrane technology that is used to demineralize solutions. The solution is pushed through a semipermeable membrane by applying enough pressure to overcome the counter pressure created by osmosis. Osmosis is a naturally occurring phenomenon that occurs when liquid from a dilute solution migrates through a semipermeable membrane into a concentrated solution, thereby creating osmotic pressure. A semipermeable membrane is a membrane with a definite pore size that prevents the passage of most atoms and molecules. As previously mentioned, osmosis tends to occur in the absence of energy and produces a pressure. However, the reverse of osmosis can occur when energy in the form of pressure is applied to overcome osmotic pressure, which allows the flow of a liquid from a concentrated solution through a semipermeable membrane into the dilute side. This process makes ROT an important technology for the removal of contaminants from water during treatment.

The performance of ROT significantly relies on the understanding of the composition of the water source and RO feed water. A complete and accurate analysis of the water source, RO feed water, and RO concentrate chemistry must be carried out during ROT design. These results can be used to recommend proper pretreatment method(s), which may be necessary upstream of the ROT, feasible RO recovery rates (system/element), cleaning methods, effective chemicals, and optimized doses. This information may be used to mitigate and reduce the fouling, scaling, and degradation of an RO membrane. Water data were obtained through daily sampling at different sampling points along the treatment train.

The turbidity of the raw water entering the Grand Forks water treatment plant (GFWTP) pilot fluctuated from 37.4 NTU to more than 670 NTU with an average of 105.29 NTU Figure 6.2.1. The noticeable spikes can be attributed to precipitation. As expected, the temperature of the raw water directly fluctuated with the seasons. The highest average water temperature was observed in the summer months, while the lowest was observed in winter (see the graph below). Tests on coagulation-sedimentation pretreatment effluent water quality confirmed that there is a direct relationship between temperature influent turbidity during this pilot study. Figure 6.2.1 also shows that the efficiency of removal decreases as influent turbidity decreases and efficiency of removal increases as influent turbidity increases.

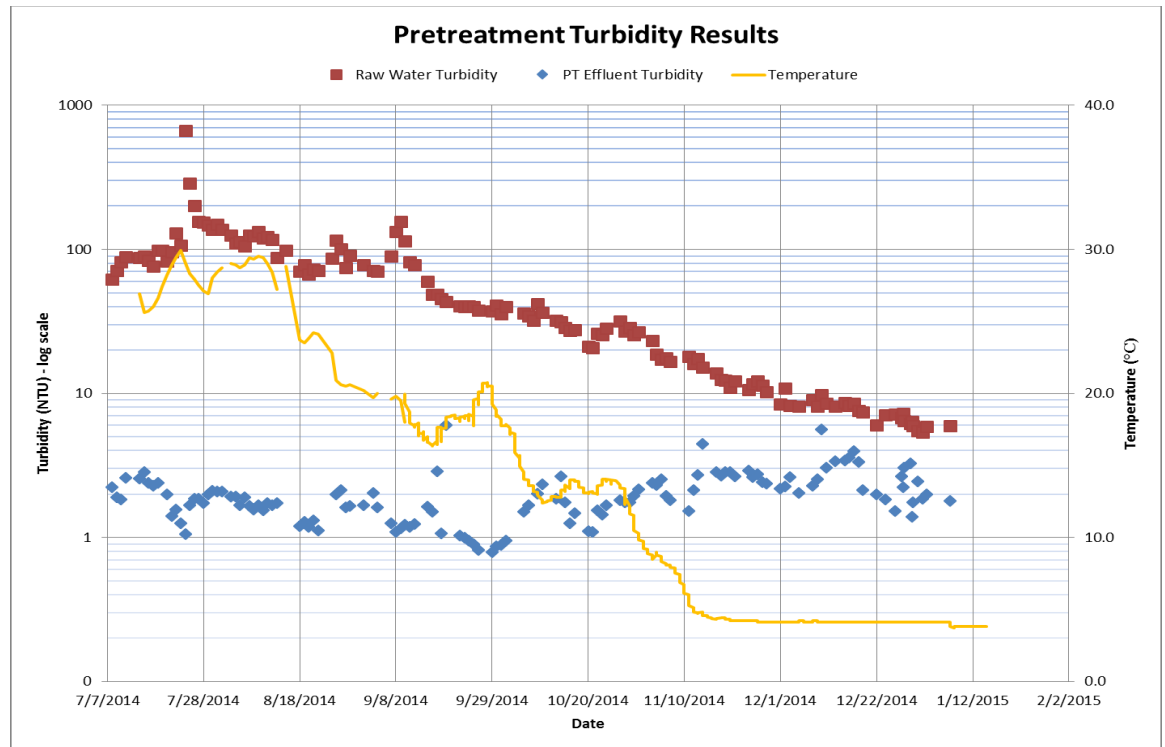


Figure 6.2.1. Effluent turbidity because of coagulation, flocculation, and sedimentation processes.

The trends for TOC and DOC, as observed in the graphs below, were closely related. Based on seasonal averages, the DOC and TOC values were higher during the summer months and lower during the winter months. Pretreatment effluent TOC refers to the post-sedimentation water quality or UF influent quality. The DOC values plotted in the graph show the overall TOC left in the filtrate water after passing through the Evoqua membrane, which has a pore size of 0.45 μm . From these two graphs, it is evident that a direct relationship exists between the TOC removal efficiency of the pretreatment train and the amount of TOC entering the plant.

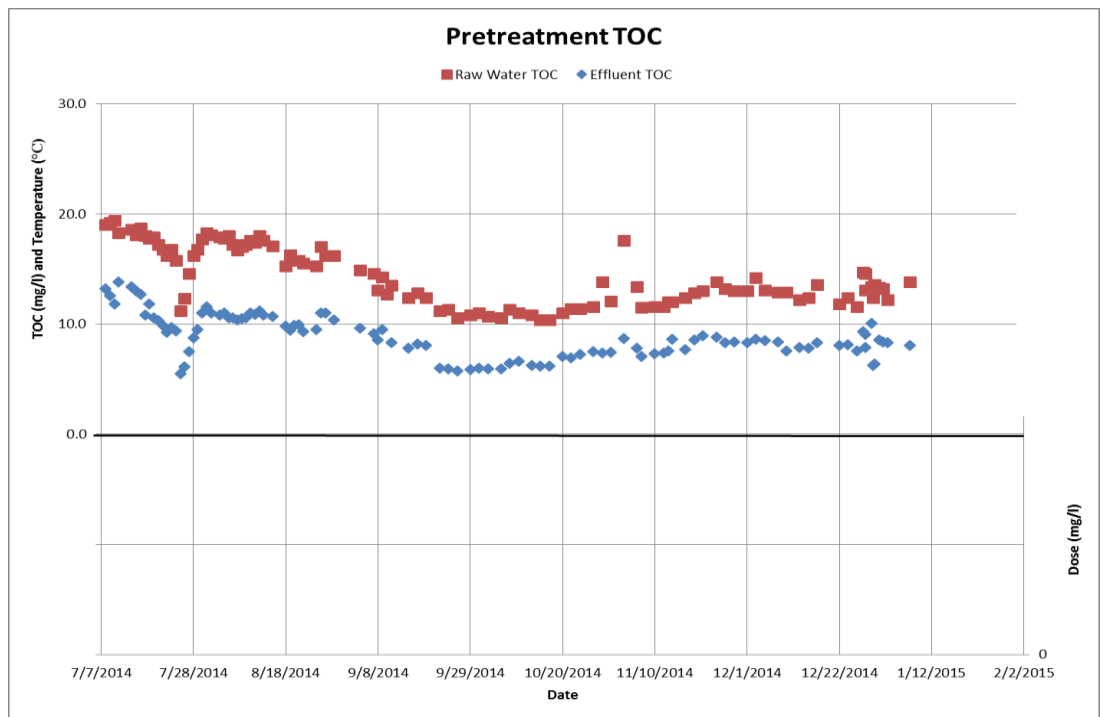


Figure 6.2.2. Effluent TOC because of coagulation, flocculation, and sedimentation processes.

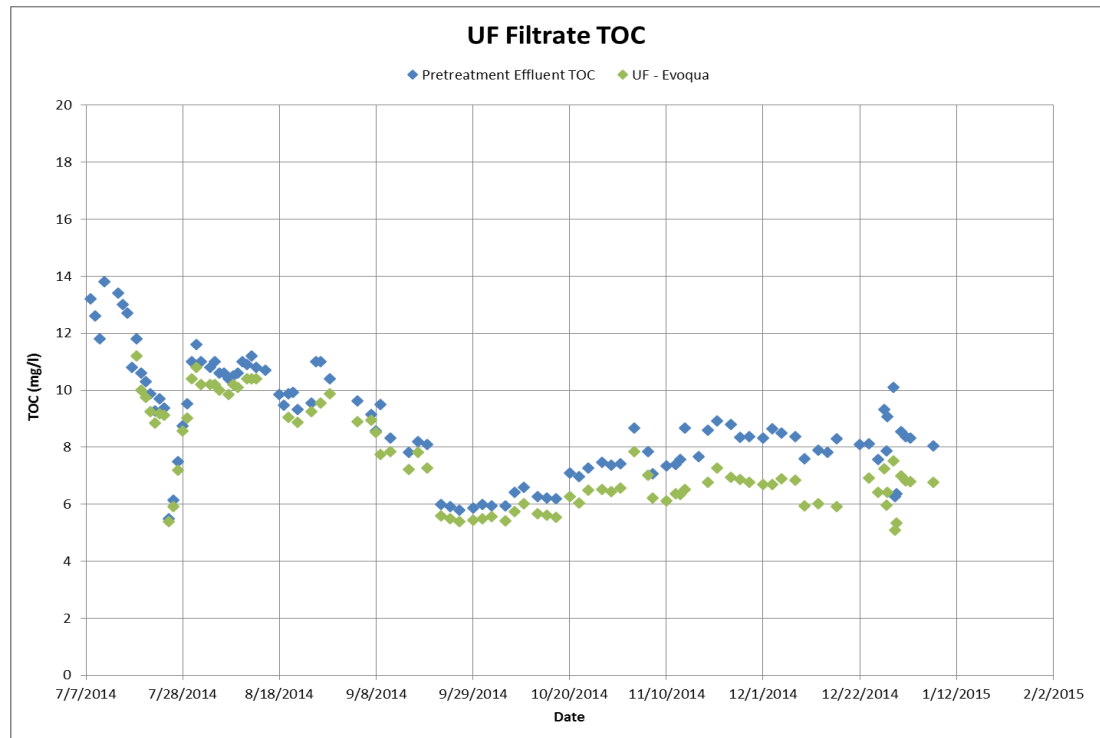


Figure 6.2.3. Effluent TOC content after the ultrafiltration process.

The constituents of water analyzed include ions, DOM, and silica (total and dissolved). The combination of these chemical species through different mechanisms such as chemical reactions, pH, temperature, and concentration polarization can lead to the formation sparingly soluble salts in water; which can precipitate, and result in scaling of the RO membrane. This is because once they start to accumulate on the membrane surface, they begin to exceed their solubility limits⁷⁸. In ROT, the most prevalent sparingly soluble salts of concern are CaSO₄, CaCO₃, and silica (unreactive). Scaling caused by sulfate compounds, such as BaSO₄ and SrSO₄, should also be monitored when these ions are present in water. The analysis of these chemical species for predicting fouling propensity of RO membranes will allow for the design of an effective method for preventing these ions from exceeding their solubility range.

6.3. Source water chemical analysis

During this RO system study, the complete characterization of water was carried out, as shown in Tables 6-1 and 6-2. These chemical analyses allow for the investigation of the balance of cation and anion concentrations in terms of equivalents. This ion balancing process is referred to as electroneutralization. For example, from Table 6-1, the sum of cation concentrations (7.36 meq/L) superseded that of anion concentrations (6.92 meq/L) in the GFWTP blended rivers being treated in this pilot study. The resulting treated source water analysis was not balanced and has a cation/anion difference of 3.077%. However, this cation/anion difference is acceptable ⁶⁸.

Table 6-2 shows the resulted chemical analysis of RO feed water. The sum of cation concentrations (6.16 meq/L) superseded that of anion concentrations (5.80 meq/L) in the RO feed water being treated by UF. The cation and anion difference of 2.999% is acceptable. The presence of any particular ion or compound in the bulk solution of the RO feed may lead to scaling of the RO membranes if solubility limits are exceeded ⁷⁸.

The Langelier Saturation Index (LSI) of raw water entering the pilot pretreatment unit was approximately 0.20 as shown in Table 6-1. The recommended LSI of RO feed water for preventing RO membrane scaling is between 1 and 1.5 ⁶⁸. Potential for scaling exists when LSI is positive, whereas it does not exist if LSI is 0. If the LSI is negative, the feed water demonstrates corrosive tendencies. Hence, reducing the alkalinity by the acidifying the source is one way by which the source water can be pretreated and the scaling propensity of the feed water can be reduced. After acidification of the raw water through the pretreatment unit, as seen in Table 6-2, the LSI value significantly reduced to -1.04, somewhat more corrosive than desirable. This research recommends maintaining

of the pH of the RO feed water 7.1 and 9, which will maintain the LSI value of the feed water between slightly negative and 1. This in turn will reduce the scaling and corrosive tendencies of the RO feed water.

Another benefit of pH adjustment is that it stops chemical species from exceeding their solubility range. As the water recovery rate of a system increases, so does the concentration of ions in the recycle water, which reduces the solubility of these ions. This reduction in solubility results in their precipitation near the surface of the membrane via adsorption onto the membrane surface.

Table 6-1. Chemical analysis work sheet for the GFWTP blend rivers ⁹¹.

Na ⁺	43.05	mg/L =	1.87	meq/L =	0.001870	m/kg water
K ⁺	7.18	mg/L =	0.18	meq/L =	0.000180	m/kg water
Ca ²⁺	55.94	mg/L =	2.80	meq/L =	0.002800	m/kg water
Mg ²⁺	29.90	mg/L =	2.49	meq/L =	0.002490	m/kg water
Ba ²⁺	0.05	mg/L =	0.001	meq/L =	0.000001	m/kg water
Mn ²⁺	0.07	mg/L =	0.001	meq/L =	0.000001	
Fe ²⁺	0.50	mg/L =	0.018	meq/L =	0.000180	
Sr ²⁺	0.16	mg/L =	0.004	meq/L =	0.000004	m/kg water
Sum of Cations			7.36	meq/L		
Cl ⁻	25.62	mg/L =	0.73	meq/L =	0.000730	m/kg water
F ⁻	0.20	mg/L =	0.01	meq/L =	0.000010	m/kg water
HCO ₃ ⁻	212.40	mg/L =	3.48	meq/L =	0.003480	m/kg water
SO ₄ ²⁻	128.97	mg/L =	2.69	meq/L =	0.002690	m/kg water
PO ₄ ³⁻	0.37	mg/L =	0.01			
NO ₃ ⁻	0.00	mg/L =	0.00	meq/L =	0.000000	m/kg water
Sum of Anions			6.92	meq/L		
Cation/Anion Difference		3.077%	Balance is	acceptable.		
Silica	12.50	mg/L				
Sum of Ions	503.63	mg/L				
TDS by calc.	516.13	mg/L				
TDS by evap.	400.40	mg/L				
pH	8.15					
Temp.	5.30	deg. C =	41.54	deg. F =		
Ionic Strength:	0.0111	m/kg water				
Ksp CaSO ₄ :	1.01E-04	IP CaSO ₄ :	1.88E-06	IP/Ksp:	0.02	
Ksp BaSO ₄ :	2.27E-10	IP BaSO ₄ :	4.71E-10	IP/Ksp:	2.07	
Ksp SrSO ₄ :	4.62E-07	IP SrSO ₄ :	2.69E-09	IP/Ksp:	0.01	
IP CaF ₂ max:	4.00E-11	IP CaF ₂ :	1.40E-13	IP/IP max	0.00	
		pCa			2.85	
		pAlk (= pHCO ₃ ⁻)			2.46	
		Stiff and Davis "K"			2.42	
		Langelier "C"			2.64	
Langelier Saturation Index						0.20
Ryznar Index						7.76
Stiff and Davis Index						0.42
Larson-Skold Index						0.98

Table 6-2. Chemical analysis work sheet for RO feed water ⁹¹.

Na ⁺	30.50	mg/L =	1.33	meq/L =	0.001330	m/kg water
K ⁺	5.38	mg/L =	0.14	meq/L =	0.000140	m/kg water
Ca ²⁺	51.90	mg/L =	2.60	meq/L =	0.002600	m/kg water
Mg ²⁺	25.00	mg/L =	2.08	meq/L =	0.002080	m/kg water
Ba ²⁺	0.05	mg/L =	0.001	meq/L =	0.000001	m/kg water
Mn ²⁺	0.02	mg/L =	0.001	meq/L =	0.000001	
Fe ²⁺	0.02	mg/L =	0.001	meq/L =	0.000001	
Sr ²⁺	0.14	mg/L =	0.004	meq/L =	0.000004	m/kg water
Sum of Cations			6.16	meq/L		
Cl ⁻	24.50	mg/L =	0.70	meq/L =	0.000700	m/kg water
F ⁻	0.20	mg/L =	0.01	meq/L =	0.000010	m/kg water
HCO ₃ ⁻	147.00	mg/L =	2.41	meq/L =	0.002410	m/kg water
SO ₄ ²⁻	128.00	mg/L =	2.67	meq/L =	0.002670	m/kg water
PO ₄ ³⁻	0.04	mg/L =	0.01			
NO ₃ ⁻	0.20	mg/L =	0.00	meq/L =	0.000000	m/kg water
Sum of Anions			5.80	meq/L		
Cation/Anion Difference		2.966%	Balance is	acceptable.		
Silica	10.20	mg/L				
Sum of Ions	412.72	mg/L				
TDS by calc.	422.92	mg/L				
TDS by evap.	328.00	mg/L				
pH	7.10					
Temp.	5.30	deg. C =	41.54	deg. F =		
Ionic Strength:	0.0096	m/kg water				
Ksp CaSO ₄ :	9.82E-05	IP CaSO ₄ :	1.74E-06		IP/Ksp:	0.02
Ksp BaSO ₄ :	2.14E-10	IP BaSO ₄ :	4.67E-10		IP/Ksp:	2.19
Ksp SrSO ₄ :	4.29E-07	IP SrSO ₄ :	2.67E-09		IP/Ksp:	0.01
IP CaF ₂ max:	4.00E-11	IP CaF ₂ :	1.30E-13		IP/IP max	0.00
		pCa			2.89	
		pAlk (= pHCO ₃ -)			2.62	
		Stiff and Davis "K"			2.40	
		Langelier "C"			2.63	
Langelier Saturation Index						-1.04
Ryznar Index						9.17
Stiff and Davis Index						-0.80
Larson-Skold Index						1.40

A goal of this pilot study is to obtain less than 3.0 and 2.0 SDI values 100% and at least 95% of the time, respectively. SDI measurements of the RO feed water were conducted during this pilot study. This test involves the measurement, over 15 min at 5 min intervals (from T(0) to T(15)), of the rate of decay of a water stream that flows through a 0.45 μm filter disc at a constant pressure of 30 psi. For example, in one of the SDI measurements at T (0), 500 mL of water passed through the filter in 36.82 s. However, the time required for 500 mL of water to pass through the filter continued to increase as the filter fouled. At T (15), 48.99 s were required to achieve 500 mL of flow through the filter. The filtrate water (RO feed water) during SDI measurement met the pretreatment water goal with an SDI of less than 1.65.

Another objective of this pilot study was to test various operating conditions that could be feasible in the future full-scale design of the GFWTP facility. Data were collected and evaluated for determining the optimal flux rate, chemical type and dose rates, and recovery rates. This will help ensure system reliability in terms of water quality consistency and maximized run time with reduced down time.

The RO performance was evaluated by the comparing two different flux rates—11 and 12 gfd at 13%/75% and 20%/82% element/system recovery rates, respectively. The cleaning protocols and different chemical types were assessed at various water temperatures. The selection of the optimized system will depend on the quality of the water produced.

6.4. RO operating parameters

For understanding the performance and effectiveness of RO, the following operational parameters need to be accurately measured: salt rejection (separation

efficiency), water flux, normalized permeate flux (performance), feed pressure, concentrate pressure, permeate pressure, permeate and concentrate conductivity, recovery, pH, feed flow, and temperature. These operational parameters can help predict fouling before it occurs and determine the effectiveness of RO in contaminant removal. For example, the ratio of the difference between feed water conductivity and permeate water conductivity to feed water conductivity is a function of the salt rejection rate. The higher the rejection rate, the better the performance of the RO. The highest RO rejection rate is between 95% and 99%. Any decrease in this RO rejection rate relative to the normalized baseline point can be an indication of membrane fouling or damage.

6.5. System or element recovery

The quantity of permeate water recovered during the RO process, called percent recovery, can be a measure of the membrane's condition (good or damaged). Percent recovery depends on the amount of concentrate that is sent either for refiltration or for disposal. A higher percent recovery indicates that less concentrate is sent for disposal and an increased quantity of permeate water is produced. A system with a high recovery rate can face problems such as diminished concentrate quality and scaling, eventually leading to membrane fouling. To minimize fouling, concentration polarization, precipitation, and scaling caused by high recovery systems, a proper method to control scaling must be established. The design of an effective system at a specific recovery rate depends on the feed water chemistry (especially, the solubility of sparingly soluble salts) and the preceding pretreatment stages. Properly designed pretreatment can remove materials and prevent soluble salts from exceeding their solubility limit when a high recovery RO system is used. This also implies that an RO unit should only be operated near its

designed recovery rate. Through simple calculations, plant operators can determine if an RO system is operating beyond its designed recovery rate range.

6.6. Concentration factor

The possibility of fouling of a membrane by its feed water depends on the dissolved salt concentration in the bulk solution of the feed and at the surface of the membrane. The increase in the concentration factor on the membrane surface is directly proportional to the recovery rate. At a high recovery rate, the concentration of ions in the concentrate-side flow starts increasing, thereby increasing the potential for fouling. For example, a concentration factor of 2 implies that the concentration of the concentrate stream is twice that of the feed water.

6.7. RO data normalization

If there are frequent changes in variables that affect the operation of an RO system, normalization of RO data is required before comparing with the baseline (the initial state of the membrane before the first run). Variables such as temperature and feed water chemistry are bound to change and influence the operational parameters of the RO system, such as feed pressure, system recovery, and permeate pressure. This in turn might affect the quality and quantity of the permeate water produced. RO data normalization allows comparison of data collected under different operating conditions. Normalized data aids in the determination of the absolute condition and performance of an RO system, allowing an operator to compare the collected data with a set standard for decision-making. Collecting and normalizing operational data, followed by trending the normalized data over time and comparing with the baseline will allow operators to predict fouling before it becomes irreversible. Three crucial values are to be calculated

and monitored for trend changes relative to baseline values: normalized permeate flow (NPF); normalized salt rejection (NSR); and normalized pressure differential (NPD) ⁷⁸.

6.7.1. Normalized permeate flow

NPF measures the effectiveness of an RO in producing permeate quantity corrected for temperature and net driving pressure conditions. This makes NPF a good indicator of membrane fouling. An NPF value decrease of 15% might indicate scaling or fouling, which would require the cleaning and permeate flush of the membrane surface. An increase in NPF can also indicate a damaged membrane. NPF can be expressed as follows:

$$NPF_t = \frac{NDP_i}{NDP_t} \times \frac{TCF_i}{TCF_t} \times Q_p \quad [6.7.1.1]$$

$$TCF = EXP \left(2640 \times \left(\left(\frac{1}{298} \right) - \left(\frac{1}{273 + FT} \right) \right) \right) \quad [6.7.1.2]$$

Here: NPF_t = normalized permeate flow at time t (gpm)

NDP_i = net driving pressure at the initial conditions of operation (psi)

NDP_t = net driving pressure calculated at time t (psi)

TCF_i = temperature correction factor based on temperature at the initial conditions of operation

TCF_t = temperature correction factor based on temperature at time t

Q_p = permeate flow (gpm)

TCF Explanation:

Water temperature is one of the key factors in the performance of reverse osmosis membranes. Membrane manufactures provide temperature correction factors for given operating temperatures and can vary by manufacturer and can also be calculated in different ways. The ASTM method as shown above with the Membrane Coefficient of 2640 is used for our purpose of finding variance in a RO. The Membrane Coefficient of 2640 is used, as the majority of our membranes will conform to this number and the effect on the calculations by using a specific coefficient for each membrane is negligible.

6.7.2. Normalized salt rejection

The salt rejection efficiency of an RO membrane has an impact on the quality of the permeate produced during filtration. If NSR decreases, the amount of contaminant on the permeate side of the membrane increases. Changes in NSR can be attributed to the fouling, scaling, or degradation of the RO membrane. Most ROTs have a rejection rate of 97%; if the rejection rate falls below 90%, the membrane may have deteriorated and may need to be checked and/or replaced immediately^{22, 26, and 78}. Studies have indicated that biofouling in membranes correlates to an increase in NSR^{5, 57, 67, 78, 89, 95, 102, and 103}. When biofouling occurs, patches of the membrane experience reduced porosity, thereby increasing salt rejection. It is normal to observe declines in NSR over time as membrane are exposed to chemical attack and continuous operations. An appropriate and optimized cleaning technique will help improve membrane performance and increase its life span. NSR can be expressed in terms of NSP as follows:

$$NSP_t = \frac{NDP_t}{NDP_i} \times \frac{C_{fb_i}}{C_{fb_t}} \times \frac{C_{f_i}}{C_{f_t}} \times SP \quad [6.7.2.1]$$

$$NSP = 100\% - NSR \quad [6.7.2.2]$$

$$NSR = \frac{C_f - C_p}{C_f} \times 100\% \quad [6.7.2.3]$$

$$C_{fb} = \frac{\left(\frac{Cb}{Cf}\right)}{1 - \left(\frac{Cf}{Cb}\right)} \quad [6.7.2.4]$$

Here: NSP_t = normalized salt passage at time t (%)

NSR = normalized salt rejection (%)

NDP_i = net driving pressure at the initial conditions of operation (psi)

NDP_t = net driving pressure calculated at time t (psi)

C_{fb_i} = salt concentration of the feed brine at the initial conditions of operation (mg/L)

C_{fb_t} = salt concentration of the feed brine at time t (mg/L)

C_{f_i} = feed salt concentration at the initial conditions of operation (mg/L)

C_{f_t} = feed salt concentration at time t (mg/L)

SP = salt passage – the amount of salt that passes through the membrane into the permeate stream (%)

C_{fb} = feed-brine salt concentration

C_b = brine (concentrate) salt concentration (mg/L)

C_f = feed salt concentration (mg/L)

6.7.3. Normalized Pressure Differential (NPD)

Pressure differential of an RO membrane system accounts for changes in flow and temperature. Changes in NPD can be attributed to the fouling, scaling, or degradation of the RO membrane and an increase in NPD can help identify if an RO membrane is dirty. However, it is normal to observe a rise in NPD over time as membranes are exposed to chemical attack and continuous operations. If NPD becomes 15% or greater than the baseline, an appropriate and optimized cleaning technique will help improve membrane performance and increase its life span^{22, 26, and 78}. NPD can be expressed in terms of PD as follows:

$$NPD = PD \times \frac{BAF}{AF} \quad [6.7.3.1]$$

$$PD = FP - CP \quad [6.7.3.2]$$

$$AF = \frac{PF + CF}{2} \quad [6.7.3.3]$$

Here: NPD = normalized pressure differential (psi)

PD = pressure drop (psi)

BAF = baseline average flow (gpm)

AF = average flow (gpm)

FP = feed pressure (psi)

CP = concentrate pressure (psi)

PF = permeate flow (gpm)

CF = concentrate flow (gpm)

6.8. Reverse osmosis

The performance and capability of a pilot plant can be evaluated based on the water quality. Table 6-3 summarizes the water quality during the RO process. TOC was reduced by approximately 94%. The RO permeate analyses showed that the RO membrane is efficient in the removal of ionic species. More than 90% of divalent ions and more than 80% of monovalent ions were removed. In addition, more than 98% of the TDS and conductivity were removed during the RO process. These data indicate that a treatment train consisting of a pretreatment unit, ultrafiltration, and RO is capable of treating surface water, to produce permeate that meets quality standards. In the future, post-treatment options will be considered to produce stable and noncorrosive water fit for distribution.

Table 6-3. Summary of finished water quality from the pilot RO study

Parameter	Units	Feed	Permeate	Rejection (%)
Ca ²⁺	mg/L	48.7	<1.00	99.4
Mg ²⁺	mg/L	19	<1.00	94.7
Na ⁺	mg/L	10.8	1.45	86.6
HCO ₃ as CaCO ₃	mg/L	125	3.4	97.3
Cl ⁻	mg/L	11.3	<2.00	82.3
SO ₄ ²⁻	mg/L	24.6	<2.00	91.9
SiO ₂	mg/L	15	<1.00	93.3
Dissolved SiO ₂	mg/L	14.8		100
pH	standard units	7.1	6.2	
Conductivity	μS/cm	448	8.9	98
TDS	mg/L	293	5.33	98.2
Total Alkalinity as CaCO ₃	mg/L	125	3.4	97.3
Total Hardness as CaCO ₃	mg/L	200	<2.00	99
TOC	mg/L	7.84	<0.50	93.6

6.8.1. RO operation

In accordance with the drafted protocol, four RO units (A, B, C, and D) ran simultaneously in parallel during phase I. However, RO units A and C were temporarily shut down for maintenance and cleaning after their membranes fouled, causing a 15% decrease in permeate recovery. The first objective of this phase was to compare the different operating conditions in order to determine a water recovery condition feasible for full-scale plant operation. During the phase 1 run, evaluations of two recovery rates, three types of antiscalants, and different flux rates were performed for determining impacts on the percent loss of permeability and the potential for irreversible fouling or damage. During this phase, normalized permeate flow, differential pressure, net driving

pressure (NDP), and NSP were monitored on a daily basis. Membrane A began operation at a permeate recovery of 82%, element recovery of 20%, and a flux of 11 gfd with an initial feed pressure of 150 psi and an average temperature of 18 °C. Membranes B, C, and D were operated at a permeate recovery of 75%, element recovery of 13%, and a flux of 11 gfd with an initial pressure of 140 psi and an average temperature of 18 °C. Element recovery was based on the manufacturer's recommendations.

As salts become more concentrated within the boundary layer of the membrane element because of the higher recovery rates, sparingly soluble chemical species will start precipitating, leading to membrane surface fouling. During this pilot study, an antiscalant was continuously introduced into the feed, and water was recycled to minimize the precipitation of these species. The objective of this task was to evaluate the effectiveness of different antiscalants in maximizing the solubility of chemical species and preventing membrane fouling. RO units A and B had the same antiscalant Vitec 4000 (Avista), but at different system and element recovery rates. PWT SpectraGuard with Organoguard was continuously fed into the feed water going into RO unit C, and AWC A-110 was fed into the feed water going into RO unit D. As previously mentioned RO B, C, and D have the same system and element recovery during this phase.

RO system performance (i.e., permeability) and separation efficiency (i.e., salt rejection) were examined for each RO unit as a function of time. For understanding any relationship, we need to investigate the underlying possible relationships among the principle features of RO systems or any physical phenomena that explain the observed variability. For this purpose, a statistical hypothesis was proposed, and its significance

was investigated before interpreting the results in the context of the explanations given by studies conducted in this field.

First, the uncertainty in the data set was quantified by modeling the likelihood of different possible outcomes. This helped explain the behavior of fundamental parameters, such as osmotic pressure, mass transfer, temperature and pressure dependence, and CP, by quantifying their relationships. This information helped predict operating characteristics like salt passage, permeability, scaling, and fouling. The stepwise regression method was applied for investigating linear or nonlinear relationships between these operating parameters. In this project, regardless of whether linear or nonlinear relationships are observed among the fundamental parameters, the quality of the numerical approach was checked by applying a numerical model. Notably, an earlier pilot study at the GFWTP on the relationships between the fundamental parameters of RO systems concluded that a cause–effect relationship exists between the parameters. However, the relationship between other operating parameters should be revisited in order to take unexplained variations and anomalies into account.

This study focused on the following research questions regarding permeability and salt rejection behavioral responses during the interaction of the RO system membrane with the RO system operating parameters during GFWTP blended river surface water treatment:

- Is there any relationship between these interacting RO system operating parameters? If so, is the relationship statistically significant?
- Are there outliers or influential observations in the data sets?

- Can a mechanistic model be constructed from the interaction between explanatory operating characteristics? If so, are the model assumptions met?

6.8.2. Methodology

The impetus for this research originates from the analyses of physicochemical processes that control separation in RO processes carried out during the pilot study at GFWTP. Daily variations in the permeability and salt passage rates were interpreted using the data analysis software JMP Pro. JMP (pronounced “jump”) is a computer program for exploring analytical statistics that enables users to investigate data ^{105, 106}.

In this study, JMP was employed for creating stepwise regression models. This approach involves the selection of a subset of effects for a regression model using an automated-fit model platform. Fit models are statistical models that identify any discrepancies in a distributed data set. This allows users to compare the predictive ability of different models with combinations of interaction effects among the operating parameters of the RO system. Regression reports provide a summary of the information regarding model fit, effect significance, and model parameters ^{105, 106}. The main approach is to build a model for a randomly selected set of observation points with the best prediction ability using a backward selection method. Different operating parameters are entered into the model, and the least significant parameters are removed until all the remaining parameters are significant for improving the model. This process is repeated until no statistical improvement in R^2 (coefficient of significance) is observed ¹⁰⁷.

Stepwise R^2 for the correlation relationship between the set of operating parameters would be characterized as follows: less than or equal to 0.20 as very weak; greater than 0.20 and less than or equal to 0.40 as weak; greater than 0.40 and less than or equal to 0.60 as moderate; greater than 0.60 and less than or equal to 0.80 as strong; and greater than 0.80 as very strong. For each step, the step history report records the effect (statistically) of removing a parameter from the model. The Std Error column in the output table, as shown in the result section, lists the estimate of the standard error of the coefficient, and the t-Ratio tests whether the true parameter is zero. The t-Ratio is the ratio of the estimate to its standard error and has a student's t-distribution under the hypothesis, given the usual assumptions for the model. Prob > |t| identifies the p-value for a two-tailed test ¹⁰⁷.

In the presentation of model results, the Nparm column shows the number of parameters (Nparm) associated with the effect. DF shows the degrees of freedom (DF) for the effect test. Ordinarily, Nparm and DF are the same (see tables in result section). They are different, however, if linear combinations are observed among the regressors, which implies that an effect cannot be tested fully. Sometimes, the DF is zero, indicating that no part of the effect is testable. Whenever DF is less than Nparm, notable lost DFs appear to the right of the line in the report.

In addition, the F ratio lists the F statistic for testing that the effect is zero. The F ratio is the ratio of the mean square for the effect divided by the mean square for error. The mean square for the effect is the sum of squares for the effect divided by its DF. Furthermore, Prob > F lists the p-value for the effect test ¹⁰⁷.

The recommended criterion for selecting a model is to choose the one corresponding to the smallest Bayesian information criterion (BIC) or corrected Akaike information criterion (CAIC) value (see Appendix II). Assuming that the model can be generalized, the accuracy of the selected model will be tested by applying it to data from RO systems that were not used in creating the model.

The interactions between the RO operating parameters from the constructed model will be observed using JMP's neural network profiler (NNP). The NNP displays prediction traces between the response and the effects. The vertical dotted line for each operating parameter shows its current value at a given day. This current value can be changed by the user to observe the changes occurring in the dependent variable. The horizontal dotted line shows the current predicted value of each targeted response (permeability or salt passage) for the current operating parameter value that might be responsible for the response behavior.

The black line within the plots on the graph shows how the predicted value of the targeted species changes with the individual operating parameter. The interaction profiler in the NNP is a way of changing the value of one RO parameter at a time while observing whether the predicted response of another parameter is affected. Some of the variables have profiles that show positive slopes, while others show interaction with negative slopes. An operating parameter with a positive slope indicates an increase in the dependent variable. A negative slope indicates that there is an inverse relationship between the operating and dependent variables¹⁰⁷.

6.9. Results and discussion

6.9.1. Reverse osmosis systems

Previous studies have shown that there is a linear relationship between membrane surface roughness, permeability, and salt passage^{85, 86}. As the surface roughness of the RO membranes increases, the permeate flux increases. Other investigations have also linked the rate of permeability fouling to membrane pore size^{68, 69, 71, 74, 76, 78, and 89}. Investigations into the use of RO systems for surface water treatment during a previous pilot study at the GFWTP have revealed a linear and a nonlinear correlation between the operating parameters and permeability and salt passage responses¹⁰⁸. These responses have been attributed to characteristics such as scaling and fouling of the membranes.

6.9.1.1. Reverse osmosis system A permeability

Figure 6.9.1.1.1 shows the distribution of normalized permeability rates for the duration for which RO system A ran during the pilot study (see equation 19, page 155). The patterns of the permeability rates vary during the pilot study. Figure 6.9.1.1.1 shows the normalized permeability of the RO membrane in unit A at two different flux rates with antiscalant A: at membrane recovery rate 20% and system recovery rate of 82%. At 11 gfd, the RO membrane in unit A experienced a 15% loss of permeate flow in the first seven days of operation. This loss can be explained by the concentration polarization (CP) phenomenon. The CP phenomenon results in the accumulation of an elevated concentration of solutes on the membrane surface and decrease in the permeation rate, because of increased osmotic pressure in the RO system.

The deposition of foulants on the RO membrane makes it necessary to immediately clean the RO membrane in unit A. The deposition of such a layer adversely

impacts the membrane permeability by affecting its hydraulic resistance and osmotic pressure⁸⁷. After the recovery cleaning conducted at low pH followed by high pH cleaning, the permeability of the RO membrane in unit A was restored to its initial permeate flow rate and operated at 11 gfd for 19 days, followed by a change in the flux to 12 gfd. At 12 gfd, the RO membrane in unit A experienced a steep decline in membrane permeability over six days before stabilization. It then took another 18 days after the operational change before another recovery cleaning was required. The lack of fouling following the operational change may have occurred because of the effectiveness of the antiscalant used for the RO membrane in unit A. On the contrary, fouling experienced by the RO membrane in unit A under the first operating conditions could have been caused by a lack of early optimization of the membrane operation (82% initial recovery operation rather than 75% recovery for initial membrane acclimation). Water permeation through the membrane also decreased as the temperature decreased (Figure 6.9.1.1.1 and 6.9.1.1.2). This can be explained by the fact that viscosity changes have an impact on

permeability and by using the solubility of some of the ions present in the RO feed water.

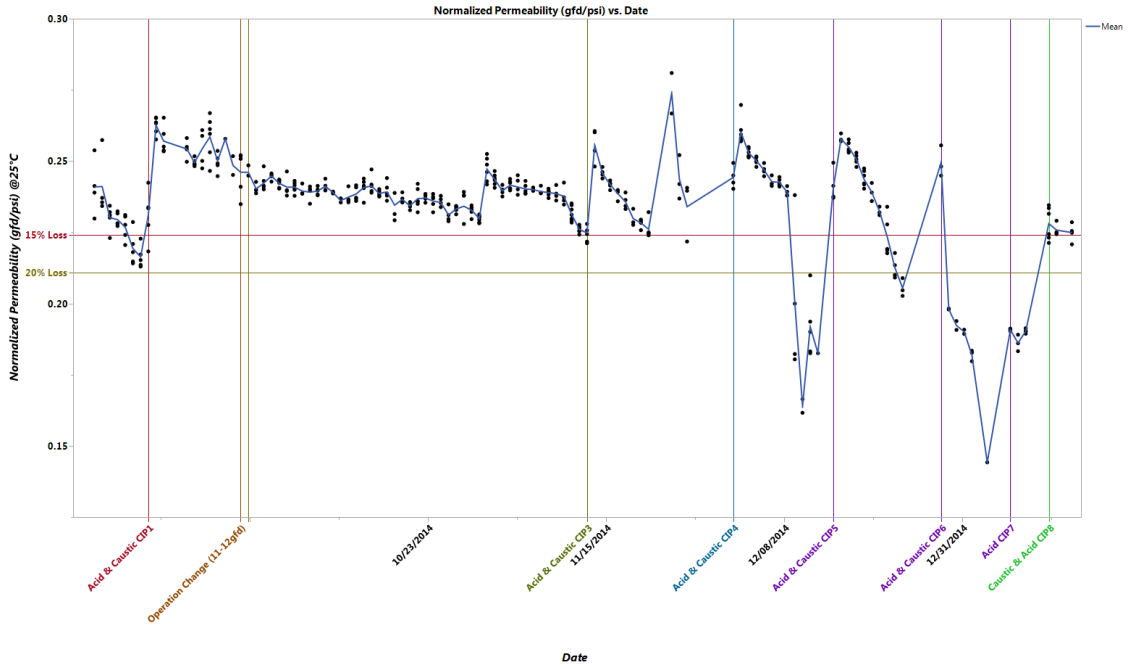


Figure 6.9.1.1.1. RO A normalized permeability observation by date.

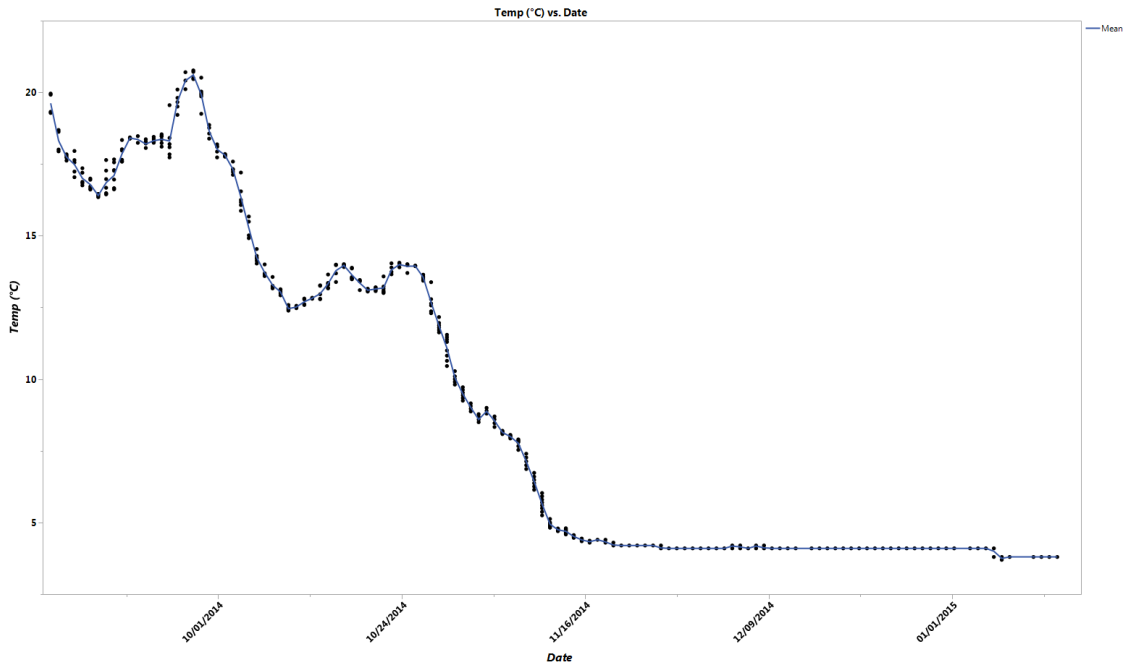


Figure 6.9.1.1.2. Temperature observed by date.

6.9.1.1.1. RO A permeability fitting stepwise regression mode

The stepwise regression model (see Section 5.5) constructed for the recorded permeability data shows that the proportion of variation in permeability, which is attributed to this model rather than to random error, was 98% ($R^2 = 0.975648$). All data collected during the pilot study were entered into the statistical regression, but not all were found to have a statistical correlation with permeability. The parameters that showed a statistical correlation were temperature, feed flow, net driving pressure (NDP), system recovery, and water flux. Stepwise R^2 for the relationship between permeability and operating parameters (temperature, feed flow, net driving pressure (NDP), system recovery, and water flux) was greater than 0.80. As a result, the interaction between these operating parameters would be characterized as very strong (see Section 5.5). Based on the interaction between permeability and the most significant operating parameters in the model, the prediction model expression can be expressed as follows:

$$\text{RO A-Permeability (gfd/psi)} = 0.125 + 0.0014T + 0.192FF - 0.004NDP + 0.002WF + 0.001SR \quad [6.9.1.1.1].$$

Here: T = temperature ($^{\circ}\text{C}$)

FF = feed flow (gpm)

NDP = net driving pressure (psi)

WF = water flux (gfd)

SR = system recovery (%)

The permeability rates predicted using this model exhibited random behavior, suggesting that the model fits the data well. Therefore, the model accurately predicted the quantitative dependence of permeability on temperature, system recovery, feed flow, NDP, and flux, and its strong interaction with these operating parameters.

Complex behavioral patterns of the permeability rate were recorded during the pilot study.

Figure 6.9.1.1.1.1 shows that the pattern of permeability rates created by the prediction model were well-fitted with the observed permeability rates. Notably, there was a missing point in the predicted model (date of missing date); hence, the data spreadsheet was checked again to determine the missing data in the values produced by the model. Indeed, there was a missing point, which may be attributed to system shutdown during membrane cleaning, equipment malfunction, or human error during data collection.

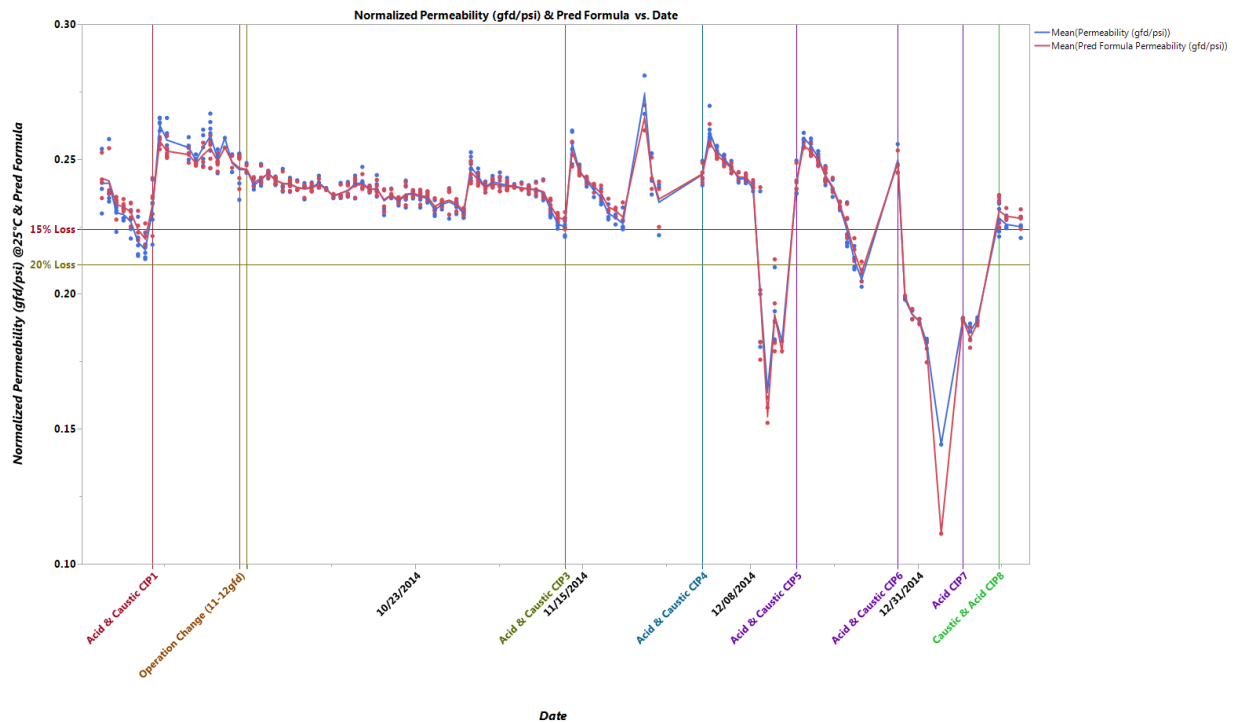


Figure 6.9.1.1.1.1. Permeability model predictions by date. Blue points represent the measured permeability rate data by date. Red points represent the predicted permeability rate range using the most significant operating parameter by date (RO A).

In Table 6-4, the estimate column lists the parameter estimates for RO A system operating conditions. These estimates are the coefficients of the model used to predict the

permeability response. The table shows that values of $\text{prob}>|t|$ for independent variables were <0.001 , which is less than or equal to the 0.05 significance level. Because there was a statistically significance relationship between permeability and variables such as the temperature, feed flow, system recovery, NDP, and water flux, the null hypothesis was rejected.

The estimate coefficient associated with NDP (-0.003965) was negative, indicating an inverse relationship in which higher numeric values for NDP are associated with lower numeric values for permeability (Table 6-4). The estimate coefficient associated with temperature, feed flow, system recovery, and water flux was positive. This indicates a direct relationship in which higher numeric values for temperature, feed flow, system recovery, and water flux are associated with higher numeric values for permeability. This result implies that the five operating parameters listed in Table 6-4 are the only significant fundamental parameters that predicted the permeability response. All other insignificant parameters were removed from the model, as described in Section 5.5.

Table 6-4. RO unit A parameter estimates

Parameters	Estimate	Std Error	t Ratio	Prob> t
Temp (°C)	0.0013811	0.000265	5.22	<.0001*
Feed Flow (gpm)	0.1933087	0.005554	34.84	<.0001*
System Recovery (%)	0.0010979	0.000324	3.39	0.0008*
NDP (psi)	-0.003965	3.029e-5	-130.9	<.0001*
Water Flux (gfd)	0.0014517	0.000268	5.42	<.0001*

Temperature, feed flow, system recovery, NDP, and flux are also significant in predicting the permeability response based on the F statistics. The probability of F statistic for the overall regression relationship is <0.0001 , which is less than or equal to the 0.05 significance level. We have rejected the null hypothesis, which states that there

is no relationship between the set of independent variables and the dependent variable ($R^2 = 0$). A statistically significant relationship existed between the set of independent variables and the dependent variable (see Table 6-5).

Table 6-5. RO A data effect tests

Parameters	Nparm	DF	Sum of Squares	F Ratio	Prob > F
Temp (°C)	1	1	0.00019419	27.203	<.0001*
Feed Flow (gpm)	1	1	0.00864321	1211.573	<.0001*
System Recovery (%)	1	1	0.00008188	11.4775	0.0008*
NDP (psi)	1	1	0.12223042	17133.80	<.0001*
Water Flux (gfd)	1	1	0.00020926	29.3327	<.0001*

6.9.1.1.2. Permeability neural networks using the neural platform

Figures 6.9.1.1.2 shows the interactions between the permeability rate and the most significant operating parameters (temperature, feed flow, system recovery, NDP, and water flux) used in creating the model. The prediction profiler shows prediction traces for each independent parameter. The vertical dotted line for each parameter correlated with its current setting and can be changed at a time to examine its effect on the dependent variable. A positive (direct) relationship was observed between the permeability and temperature, feed flow, system recovery, and water flux. In contrast, the graph indicated a negative (inverse) relationship when permeability interacts with NDP.

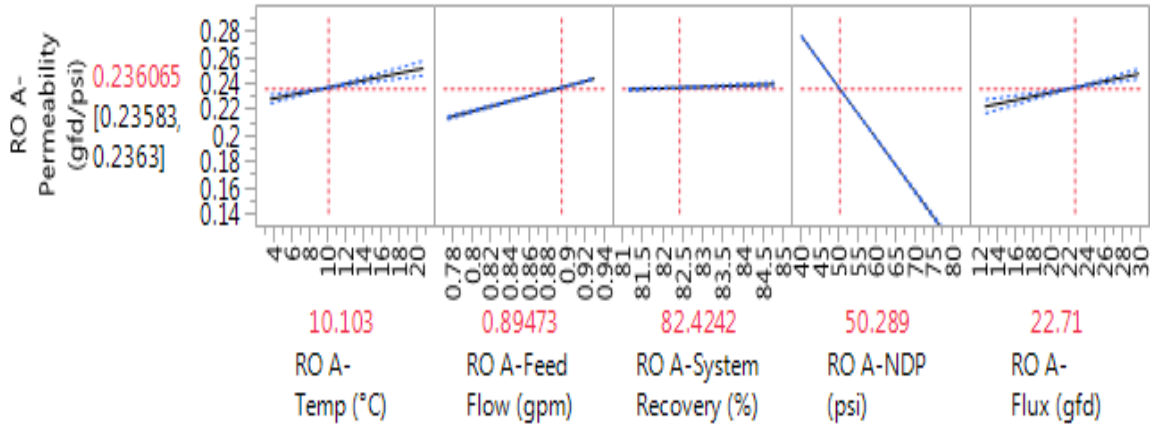


Figure 6.9.1.1.1.2. Behavior of permeability and their relation with temperature, feed flow, system recovery, NDP, and flux.

6.9.1.2. Reverse osmosis system B permeability

Figure 6.9.1.2.1 shows variations in the rates of permeability in RO system B. The figure shows the normalized permeability of the RO membrane in unit B at a constant flux rate (11 gfd) and a constant recovery rate (75%) using antiscalant B, which is the same as the chemical used in RO unit A. During the first 20 days of operation, the permeability of the RO membrane in unit B increased by 20% before stabilization. It is believed that the low (75%) recovery on startup provided an beneficial acclimation of the membrane. The first recovery clean was carried out approximately 90 days after the initial startup, which correlates with the decrease in the feed water temperature. This suggests that loss of permeability may be explained by changes in viscosity and solubility of the chemical species. At higher temperatures, chemical bonds between molecules and atoms are easily broken (solubility is high). At lower temperatures, in contrast, more energy is required to break the bonds between species (solubility decreased).

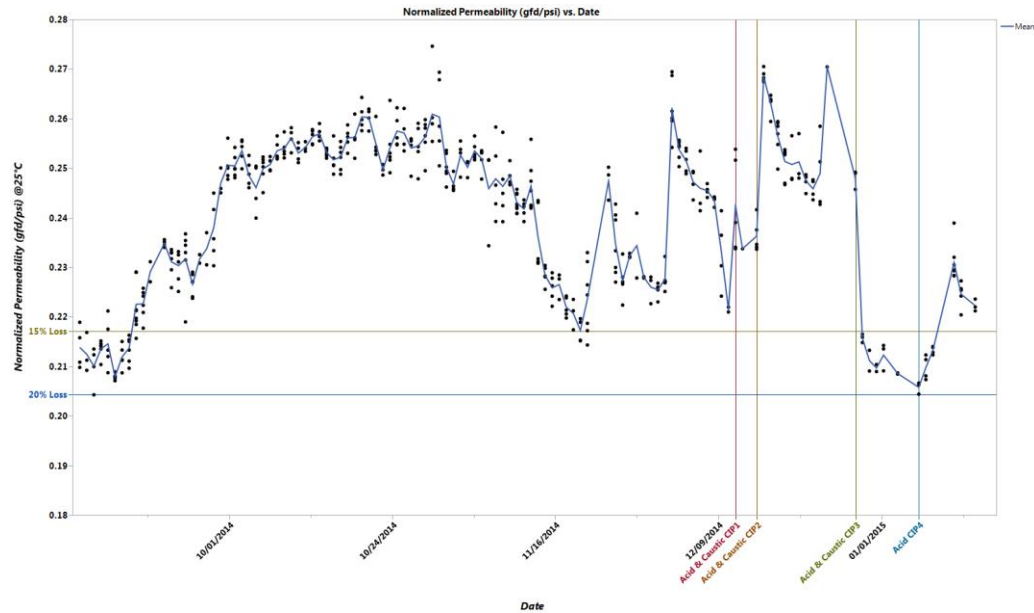


Figure 6.9.1.2.1. RO B normalized permeability observation by date.

In Figure 6.9.1.2.2, the pattern of permeabilities created by the model somewhat fit the behavioral pattern of the actual RO B measurements of permeability. This suggests that the model created using estimate coefficients from the RO A system and applied to the operating parameters of the RO B system demonstrated the completeness of the model's predictive reliability. It also shows accurate characterization of the complex permeability phenomenon. Because of the differences (system recovery and water flux) in the two systems, there is only a low expectation that the plot of the model would match the observed data plot. Model-predicted permeabilities agreed within 10% of actual RO B permeabilities and generally were higher than observed permeabilities. Despite this, we did observe that some model-predicted permeabilities closely matched the observed RO B permeability pattern and values.

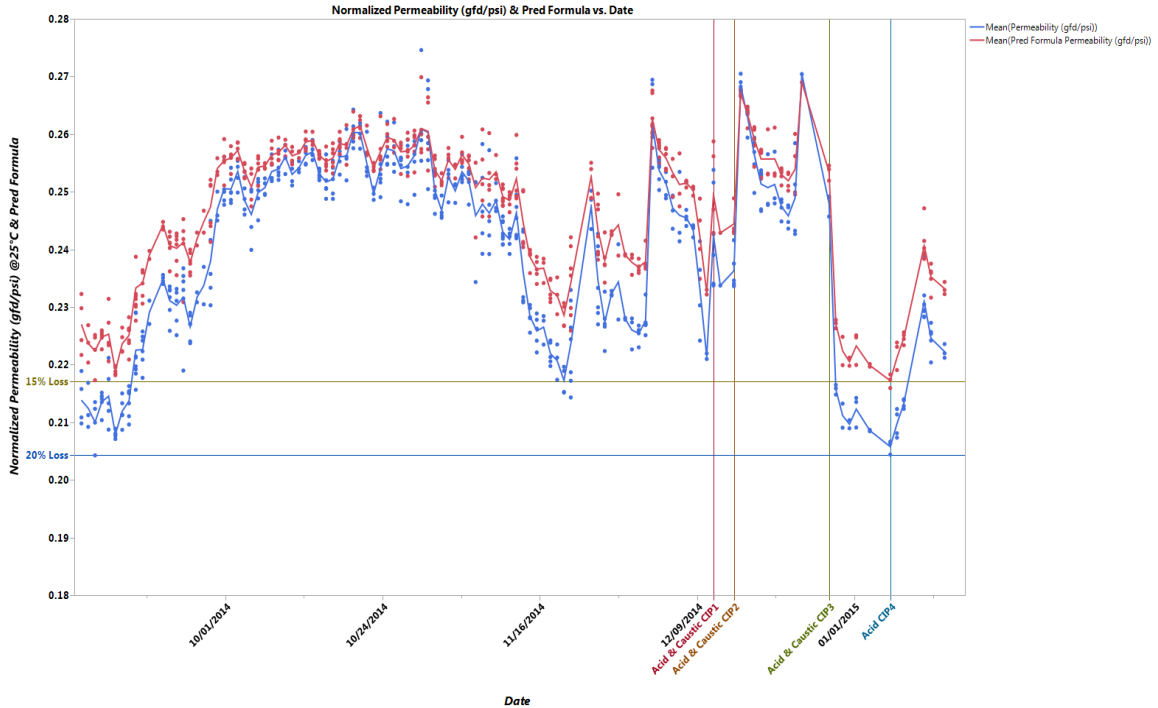


Figure 6.9.1.2.2. Permeability model predictions by date. Blue points represent the measured permeability data by date. Red points represent the predicted permeability range using the most significant operating parameters by date (RO B).

6.9.1.3. Reverse osmosis system C permeability

The observed permeability in RO system C rapidly increased in the first few days before stabilization and slowly decreased due to fouling (Figure 6.9.1.3.1). The figure also shows the normalized permeability of the RO membrane in unit C at different flux rates (11 gfd and 12 gfd) and different recovery rates (75% and 82%) using antiscalant C. At 11 gfd, the RO membrane in unit C experienced a slight increase in the permeate flow during the first 15 days of operations before stabilization. However, once an operational condition was changed from 11 gfd to 12 gfd and from 75%/13% to 82%/20% system/element water recovery, the RO membrane in unit C experienced fouling. This triggered the necessity of immediately cleaning the membrane after 12 days' operation. The sudden decline in the permeate flow can be attributed to the lack of effectiveness of

the antiscalant supplied by the manufacturer and the impact of temperature on the solubility of the chemical species in the RO feed water. This led to precipitation of ion species and scaling of the membrane surface, thereby reducing permeability.

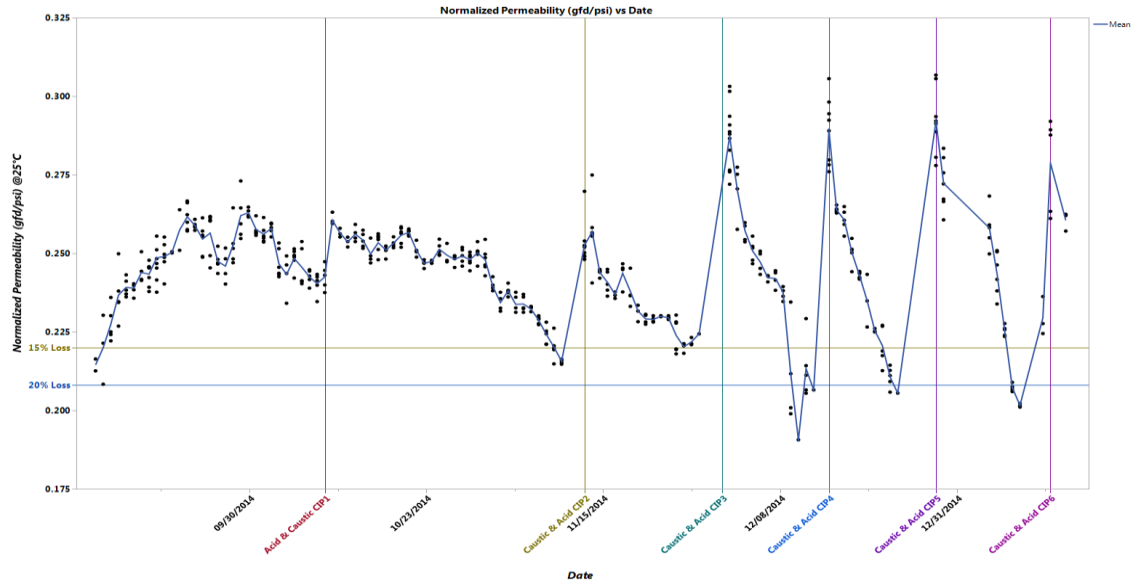


Figure 6.9.1.3.1. Change in permeability rates by date in RO C.

Figure 6.9.1.3.2 shows that the pattern of permeabilities created by the model fits the behavioral pattern of the actual measurements of permeability quite well. The figure also suggests that the model created using estimated coefficients from the RO system A and applied to the RO system C operating parameters demonstrates the completeness of the model's predictive reliability. The figure also shows accurate characterization of the complex permeability phenomenon. We observed that the model-predicted permeabilities

generally matched the observed RO C permeability patterns and values well.

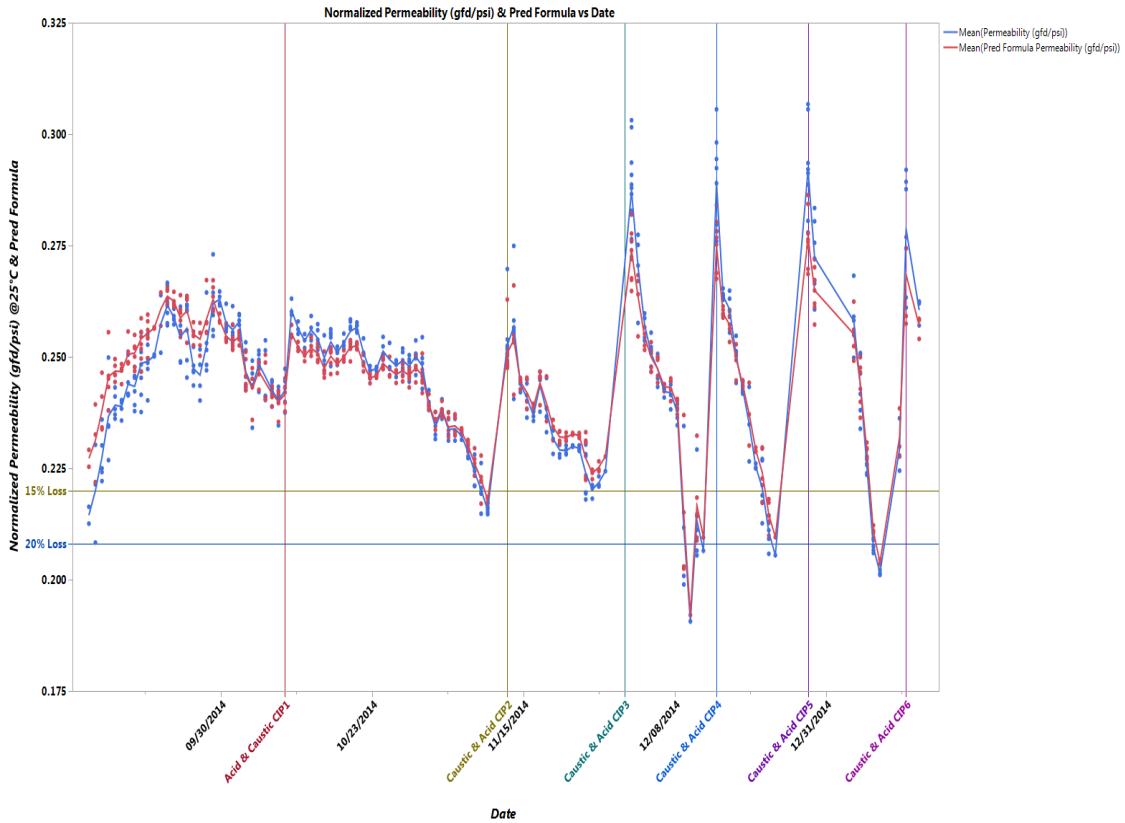


Figure 6.9.1.3.2. Permeability model predictions by date. Blue points represent the measured permeability rate data by date. Red points represent the predicted permeability range using the most significant operation parameters by date (RO C).

6.9.1.4. Reverse osmosis system D permeability

As shown in Figure 6.9.1.4.1, the permeability rapidly increased in RO D several days before stabilization. The figure also shows the normalized permeability of the RO membrane in unit D at different flux rates and different recovery rates using antiscalant D. At 11 gfd and 75%/13% system recovery, the RO membrane in unit D experienced a slight increase in permeate flow during the first six days of operation before stabilization. Once the operational flux condition was changed from 11 gfd to 12 gfd and from

75%/13% to 82%/20% water recovery, the RO membrane in unit D experienced fouling before eventually stabilizing without requiring any cleaning. The permeability eventually decreased in the second week of November, but not quite reaching the 15% permeability loss mark that would have required chemical cleaning. The relatively good performance is attributed to the effectiveness of the antiscalant chemical in preventing membrane fouling. The late-October and early-November decrease in temperature, however, caused the chemical ion species in the RO feed water to exceed their solubility limits. As a result, they began to precipitate, scale, and eventually foul the membrane.

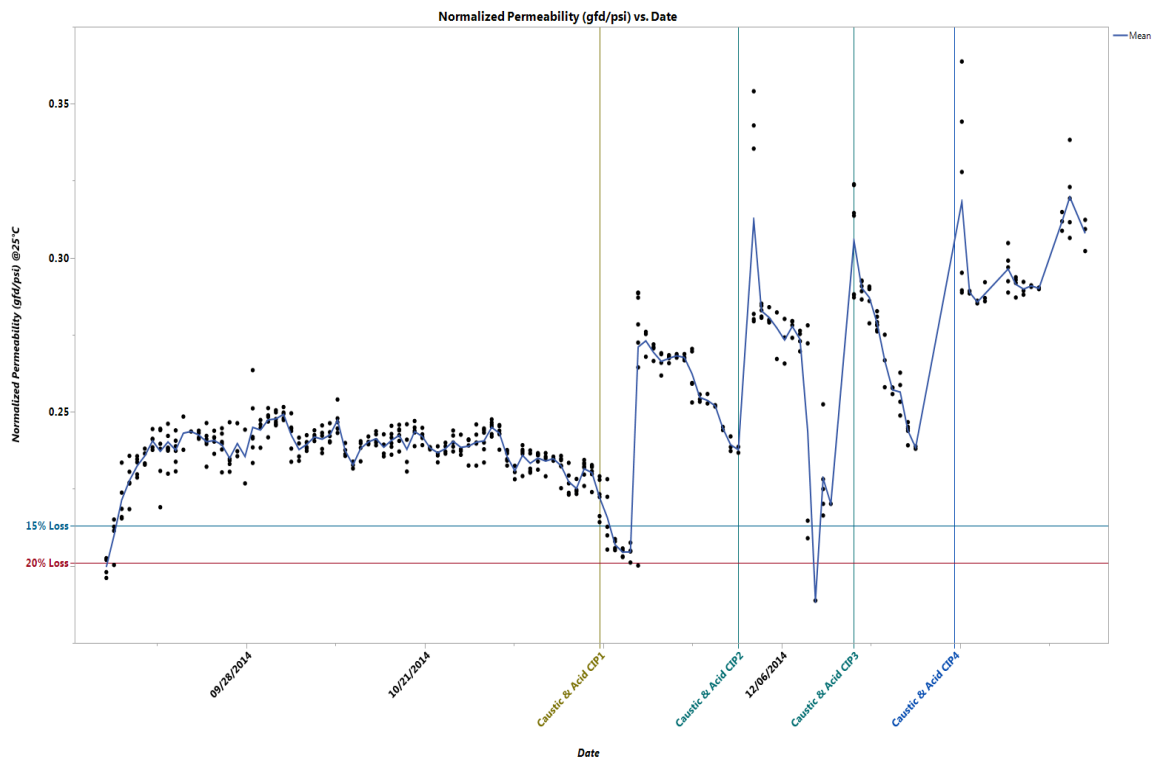


Figure 6.9.1.4.1. Change in permeability rates by date in RO D.

Figure 6.9.1.4.2 shows that the pattern of permeabilities created by the model generally fit the behavioral pattern of the actual RO D measurements of permeability.

The figure, suggests that the model created using estimate coefficients from RO system A and applied to the operating parameters of RO system D demonstrates the completeness

of the model's predictive reliability. The figure also demonstrates accurate characterization of the complex permeability phenomenon. The model-predicted permeabilities were generally found to match the observed RO D permeability patterns, and model-predicted values were within 10% of observed values.

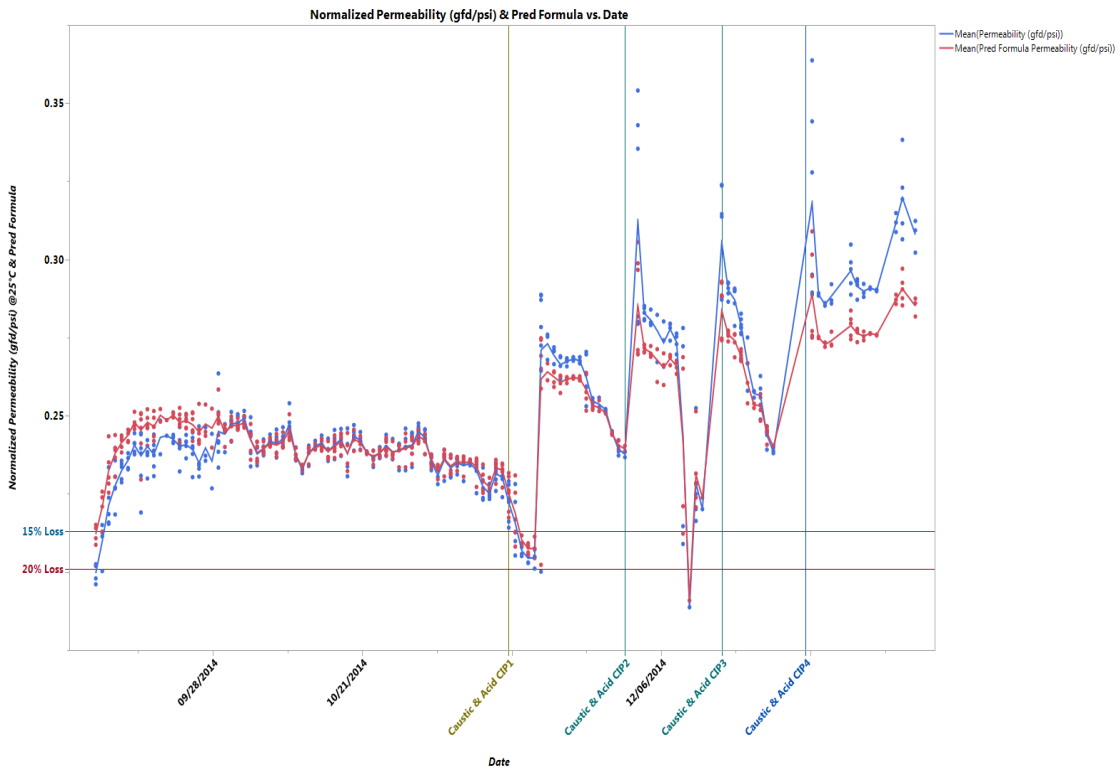


Figure 6.9.1.4.2. Permeability model predictions by date. Blue points represent the measured permeability data by date. Red points represent the predicted permeability range using the most significant operating parameter by date (RO D).

6.9.1.5. Reverse osmosis system D salt passage

NSP helps in the evaluation of changes in the membrane salt rejection rate, caused by membrane fouling and scaling, or changes in membrane permeability, caused by exposure to feed water constituents. The overall concentration of salt transport (%) through the RO D membrane barrier exhibited clear variation by day, with most of the

salt passage through the membrane being greater than 1% (Fig. 6.9.1.5.1). The changes in the measured concentration of solutes in the permeate stream can be attributed to clean in place protocols and concentration polarization (CP). CP causes the accumulation of elevated concentrations of ions on the membrane surface, possibly increasing the chances that ions will pass through the membrane.

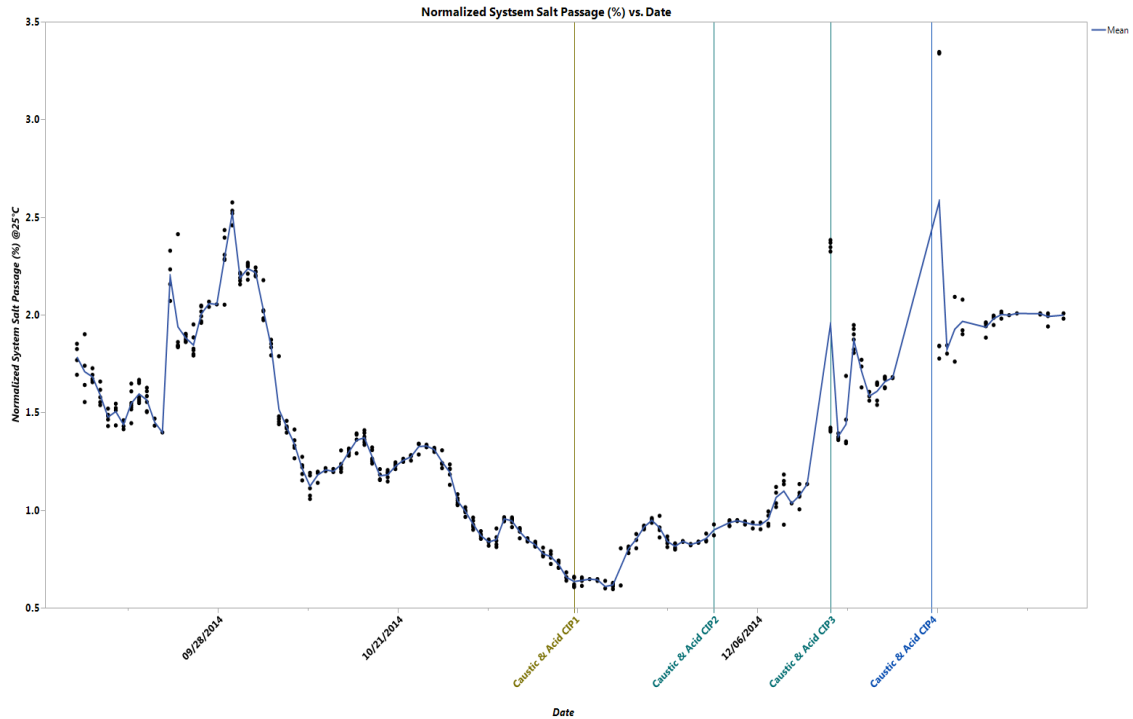


Figure 6.9.1.5.1. Change in percentage of salt passage concentrations by date in RO system D.

6.9.1.5.1. Salt passage fitting stepwise regression model

The salt passage model shows that salt passage variation, which can be attributed to this model rather than to random error, is 99% ($R^2 = 0.994439$). All data collected during the pilot study were entered into the statistical regression, but not all were found to have a statistical correlation with salt passage. The parameters that showed a statistical correlation were temperature, feed flow, post-recycle feed conductivity, system recovery,

permeate TDS, manufacturer's rated salt passage, and water flux. Stepwise R^2 for the relationship between salt passage and the set of operating parameters was greater than 0.80. This implies that interaction between these operating parameters would be very strong (Section 5.5). The prediction model expression, based on the interaction between salt passage and the most significant fundamentals in the model, is given below:

$$\text{RO D-Salt passage System (\%)} = -9.145 + 0.0944T + -1.991FF + 0.0437P\text{-TDS} + 0.121SR + 0.0004PFC + 2.7712MSP + 0.0667WF \quad [6.9.1.5.1.1]$$

Here: T = temperature ($^{\circ}\text{C}$)

FF = feed flow (gpm)

PFC = post-recycle feed conductivity ($\mu\text{S}/\text{cm}$)

WF = water flux (gfd)

SR = system recovery (%)

TDS = permeate total dissolved solids (mg/L)

MSP = manufacturer's rated salt passage (%)

The salt passage values predicted using this model exhibited random behavior, suggesting that the model fits the data well (Figure 6.9.1.5.1.1). The model, thus, correctly predicts the quantitative dependence of system salt passage on independent parameters and its strong interaction with these parameters.

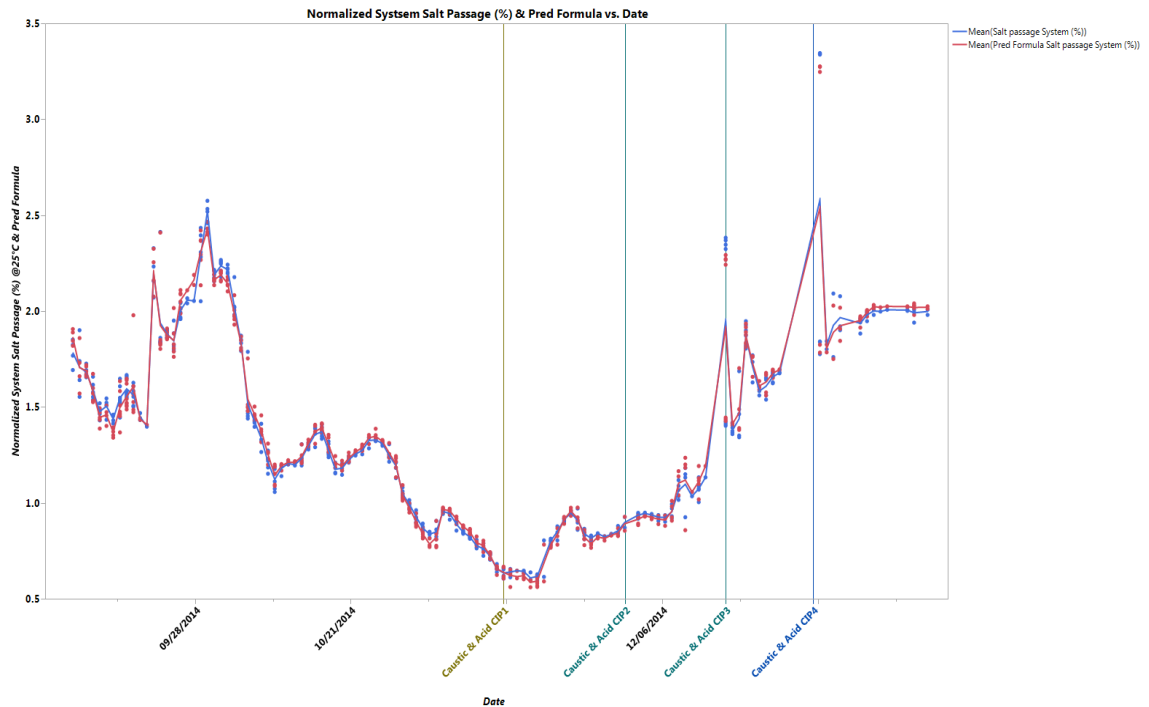


Figure 6.9.1.5.1.1. Percent of salt passage model predictions by date. Blue points represent the measured percentage of salt passage concentration data by date. Red points represent the predicted percentage of salt passage concentration range using the most significant fundamental characteristics by each day (RO D).

In Table 6-6, the estimate column lists the parameter estimates for the operating parameters of the RO D system. These estimates include the coefficients of the model used to predict the system salt passage response. For independent variables, the probabilities of t statistic (i.e., $\text{prob}>|t|$) were <0.001 , which is less than or equal to the 0.05 significance level. Because there was a statistically significance relationship between permeability and variables such as the temperature, feed flow, post-recycle feed conductivity, system recovery, permeate TDS, manufacturer’s rated salt passage, and water flux, the null hypothesis was rejected. In conclusion, there is a statistically significant relationship between the system salt passage and the independent variables.

The estimate coefficient associated with feed flow and permeate TDS was negative, indicating inverse relationships. That is, higher numeric values for feed flow

and permeate TDS are associated with lower numeric values for the system salt passage (Table 6-6). The estimate coefficient associated with temperature, postrecycle feed conductivity, system recovery, manufacturer’s rated salt passage, and water flux was positive, indicating a direct relationship. This implies that higher numeric values for the above-mentioned parameters are associated with higher numeric values for system salt passage. Hence, the listed seven operating parameters used in this model expression are the significant fundamental parameters that predicted the response in system salt passage. All other insignificant parameters were removed from the model (see Section 5.5).

Table 6-6: RO D parameter estimates

Parameters	Estimate	Std Error	t Ratio	Prob> t
Temp (°C)	0.0944486	0.005421	17.42	<.0001*
Feed Flow (gpm)	-1.990626	0.173786	-11.45	<.0001*
Permeate TDS	-0.000433	1.44e ⁻⁵	-30.06	<.0001*
Postrecycle Feed Conductivity (µS/cm)	0.1207933	0.002171	55.63	<.0001*
System Recovery (%)	0.0437187	0.00198	22.088	<.0001*
Manufacturer’s Rated Salt Passage (%)	2.7711561	0.084642	32.74	<.0001*
Water Flux (gfd)	0.0667333	0.004761	14.02	<.0001*

Temperature, feed flow, permeate TDS, postrecycle feed conductivity, system recovery, membrane salt passage, and flux are significant for predicting the response in system salt passage based on the F statistics. The probability of the F statistic for the overall regression relationship was <0.0001, which is less than or equal to the 0.05 significance level. The null hypothesis that there is no relationship between the set of independent variables and the dependent variable ($R^2 = 0$) was rejected. The research

hypothesis that there is a statistically significant relationship between the set of independent variables and the dependent variable was supported (Table 6-7).

Table 6-7: RO D effect tests

Parameters	Nparm	DF	Sum of Squares	F Ratio	Prob > F
Temperature (°C)	1	1	0.4407635	303.5768	<.0001*
Feed Flow (gpm)	1	1	0.1904975	131.2055	<.0001*
Permeate TDS	1	1	0.7080109	487.6440	<.0001*
Postrecycle Feed Conductivity (µS/cm)	1	1	1.3117814	903.4923	<.0001*
System Recovery (%)	1	1	4.4930086	3094.569	<.0001*
Salt passage Membrane (%)	1	1	1.5562821	1071.893	<.0001*
Water Flux (gfd)	1	1	0.2852986	196.5001	<.0001*

6.9.1.6.Reverse osmosis system C salt passage

The overall concentration of salt transport (%) through the RO C membrane barrier exhibited clear variations by day (Fig. 6.9.1.6.1). Most of the system salt passage data were below 1%–1.5%.

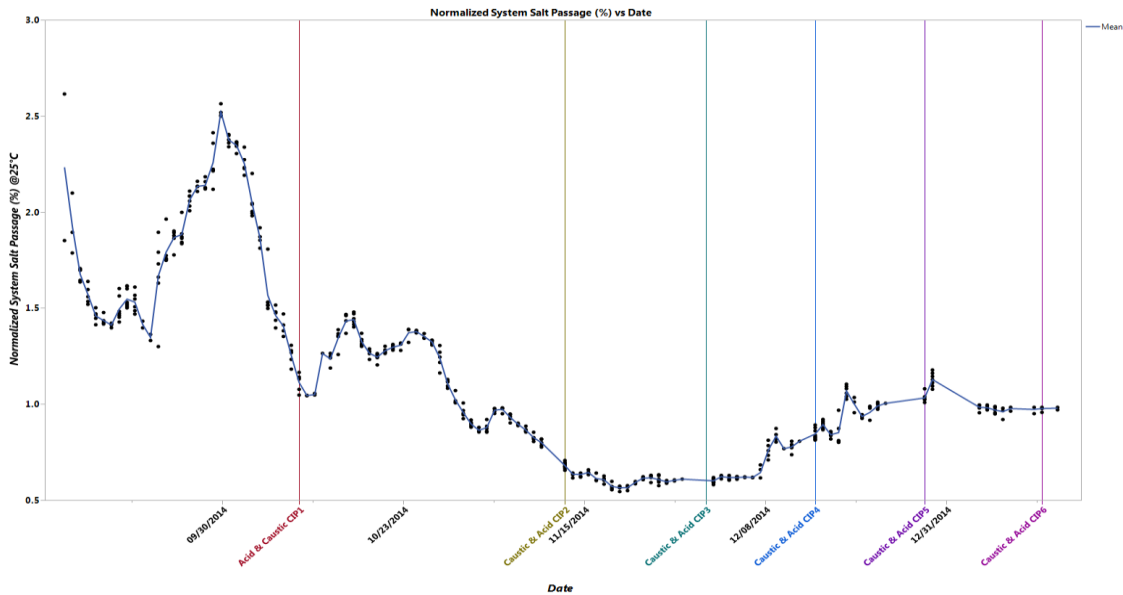


Figure 6.9.1.6.1. Change in the percent of salt passage concentrations by date in RO C

Figure 6.9.1.6.2 shows that the pattern of system salt passage created by the model (based on RO D system estimate coefficients) fit the behavioral pattern of the actual measurements of the system salt passage in RO system C. Figure 6.9.1.6.1.2 suggests that the model created using the estimated coefficients from RO system D and applied to RO system C operating parameters demonstrates the completeness of the model's reliability. It shows accurate characterization of the complex system salt passage phenomenon.

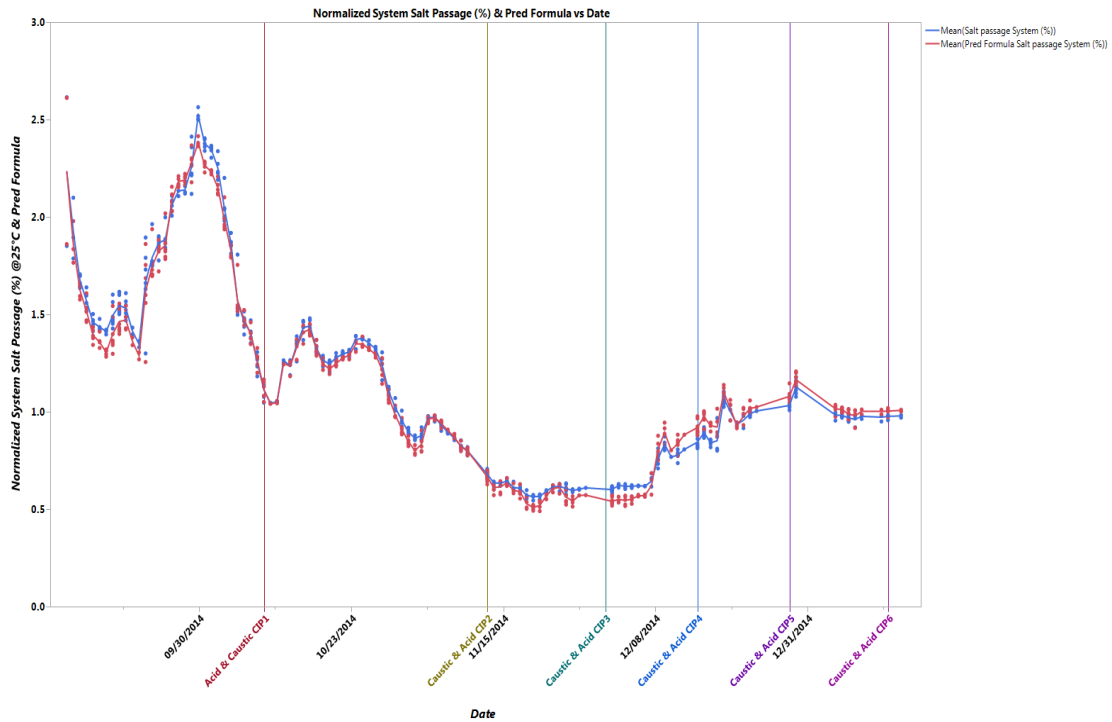


Figure 6.9.1.6.2. System salt passage model predictions by date. Blue points represent the measured percent of system salt passage data by date. Red points represent the predicted percent system salt passage using the most significant operation parameters by date (RO C).

6.9.1.7. Reverse osmosis system B salt passage

The overall concentration of salt transport (%) through the RO B membrane barrier exhibited clear variations by day (Fig. 6.9.1.7.1). Most of the system salt passage

was below 1%–1.5%.

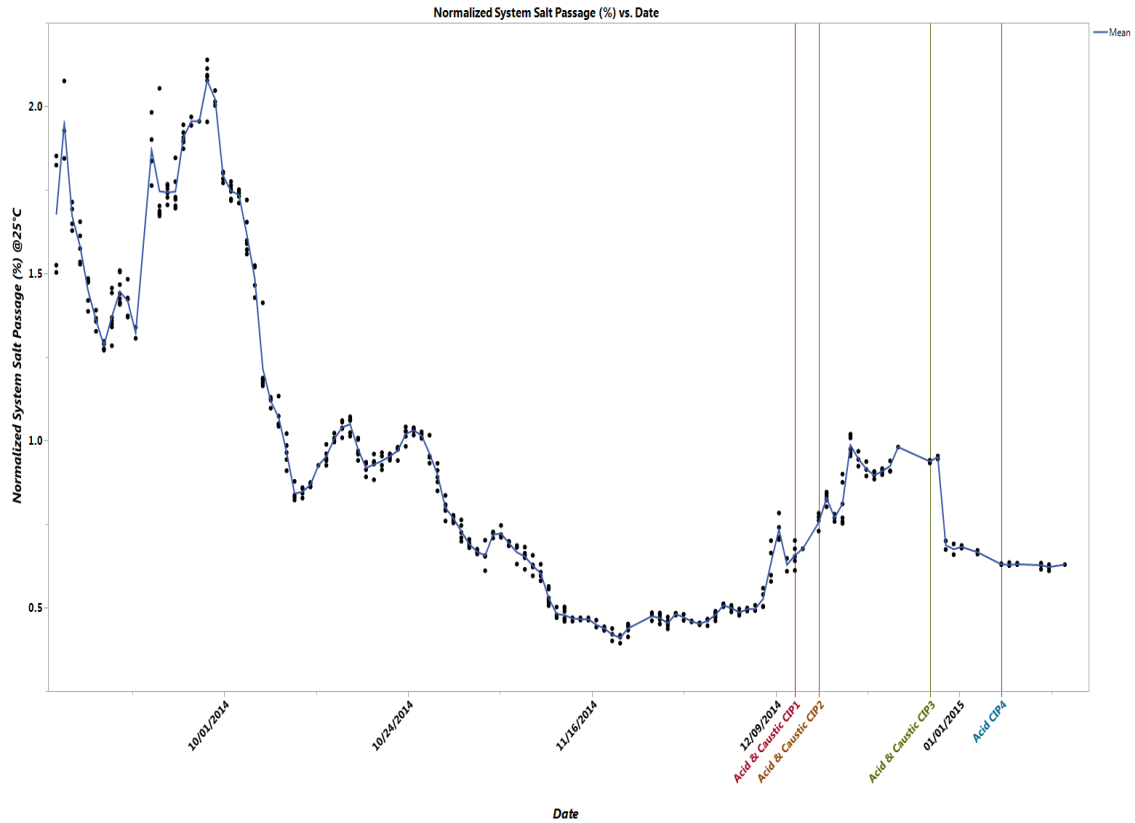


Figure 6.9.1.7.1. RO B normalized system salt passage observation by date.

In Figure 6.9.1.7.2, the pattern of system salt passage created by the model (based on RO D system estimated coefficients) somewhat fit the behavioral pattern of the actual measurements of system salt passage rate in RO system B. The model created using estimate coefficient from RO system D and applied to the operating parameters of RO system B demonstrates only fair model reliability, completeness of the predicting ability, and characterization accuracy of the complex system salt passage phenomenon. This may reflect the differences in the recovery rate between the RO D and RO B systems (82% for RO D and 75% for RO B) and the change in flux in RO D from 11 gfd to 12 gfd while RO B remained at 11 gfd throughout the duration of the pilot study. In addition, the

inconsistencies between the model and the actual measurements of salt passage in RO B system can also be attributed to the cleaning chemicals, techniques and the different type of antiscalant that was used. The modeling of the salt passage should be explored in the future.

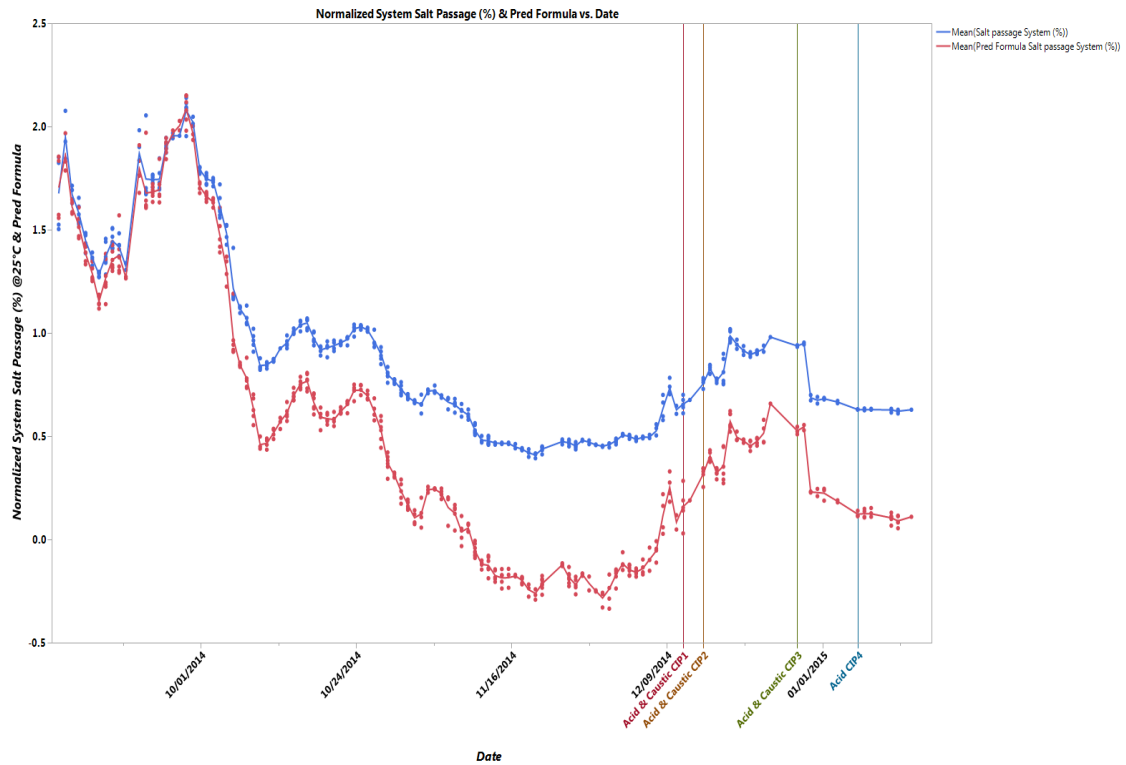


Figure 6.9.1.7.2. System salt passage model predictions by date. Blue points represent the measured percent of system salt passage data by date. Red points represent the predicted percent system salt passage using the most significant operation parameters by date (RO B).

6.9.1.8. Reverse osmosis system A salt passage

The overall concentration of salt transport (%) through the RO A membrane barrier exhibited clear variations by day (Fig. 6.9.1.8.1). RO A operations used the same antiscalant as RO B. RO A, C, and D used similar patterns of water flux (11 gfd acclimation period transition to 12 gfd after approximately 19 days). In addition, RO A

system ran at 82% system recovery throughout the duration of the pilot study. RO C and D systems initially ran at 75% system recovery and were changed to 82% while RO B system ran at 75% recovery during the pilot study. Most of the system salt passage data were below 1%–1.5%.

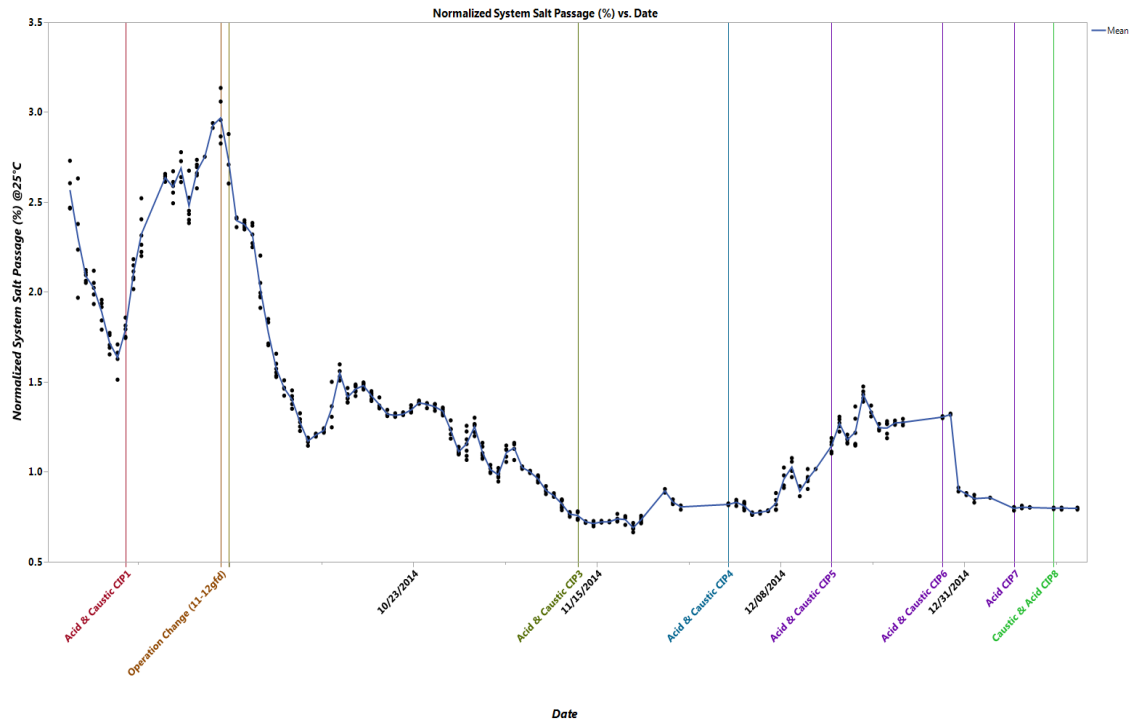


Figure 6.9.1.8.1. Change in the normalized system salt passage concentration by date in RO A.

In Figure 6.9.1.8.2, the pattern of system salt passage created by the model (based on RO D system estimated coefficients), fit with the behavioral pattern of the actual measurements of system salt passage in RO system A. Figure 6.9.1.8.2 suggests that the model created using the estimate coefficients from RO system D and applied to RO system A operating parameters demonstrates the model’s reasonable reliability, completeness, and accurate characterization of the complex system salt passage

phenomenon.

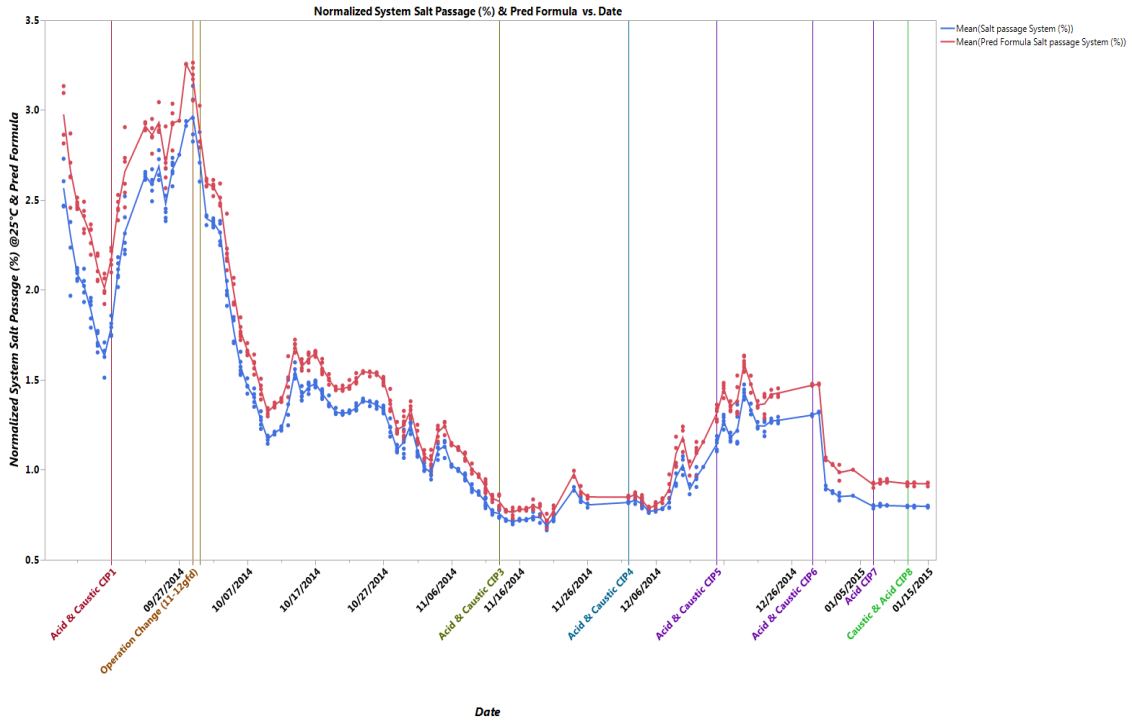


Figure 6.9.1.8.2. System salt passage model predictions by date. Blue points represent the measured percent of system salt passage data by date. Red points represent the predicted percent system salt passage using the most significant operation parameters by date (RO A).

6.10. Conclusion

A pilot-scale study was conducted for investigating the roles of antiscalant, temperature, feed flow, net driving pressure (NDP), system water recovery, permeate TDS, postrecycle feed conductivity, manufacturer’s rated salt passage, and water flux on the rate of RO membrane fouling when exposed to surface water containing DOM and CM. Three different antiscalants from three separate suppliers were used. The same antiscalant was used in RO A and B (called Anti-A), while Anti-C was used for operating RO unit C. Anti-D was used for operating RO D operations. RO membranes A, C, and D

started at 11 gfd for first 19 days before the operation changed to 12 gfd. RO B, in contrast, ran at 11 gfd throughout the pilot study. Membrane operations were characterized for recovery rate, flux rate, and other operating conditions, These mechanisms correlated with the decline in the permeability and rate of salt passage caused by membrane fouling⁸⁵. Permeability decline and increase in solute concentration in the permeate stream can be explained by the adsorption of organic compounds onto the membrane surface, which blocks the membrane pores and causes permeability decline. A statistically significant (98%) relationship exists between the permeability and variables of temperature, feed flow, system water recovery, NDP, and water flux. In addition, there is a statistically significant (99%) relationship between the system salt passage and variables of temperature, feed flow, permeate TDS, postrecycle feed conductivity, system recovery, manufacturer's rated salt passage, and water flux.

The overall relationship and interaction between the RO system performance and its operating conditions were statistically significant, and its strength was accurately characterized using data-mining techniques. The estimate coefficient of all variables was also statistically significant, and the directions of the relationships were accurately characterized by these techniques. The methodology developed in this study for RO A permeability and RO D salt passage model was somewhat generalizable. This generalizability of RO A permeability and RO D salt passage model was reasonably good for RO A, RO B, RO C, and RO D system permeability prediction.

The salt passage model created using estimated coefficients from RO system D and applied to RO system B operating parameters demonstrates only fair model reliability, completeness, and characterization accuracy of the complex system salt

passage phenomenon. There is a low expectation that the plot of the salt passage model (based on RO D system estimated coefficients) would match the observed data plot in the RO B system because of differences between the two systems. Some model-predicted salt passages were observed to closely match the observed RO B pattern and values. But in many cases, the salt passage observed in RO B had significant discrepancies with model predicted values. This may reflect the differences in the recovery rate and water flux rate between the RO D and RO B systems. The modeling of salt passage should be explored in the future.

This research demonstrated that a significant impact of antiscalant and recovery rate was observed for the prevention of irreversible fouling. Depending on the system design and pretreatment train, scale inhibitors should be used to alter the water chemistry of the dissolved salts concentrated in brine and scale the membranes. In conclusion, of the three antiscalants used in this pilot study, the one used in RO unit D was highly effective in slowing down the precipitation of scale-forming salts. This was done by preventing nucleation and by modifying the crystals forming on the membrane surface, thereby reducing the need for frequent clean-in-place (CIP) to restore membrane performance.

The model building approach of this study can be applied to pilot studies of other RO systems, regardless of their operating conditions and changing water chemistry. A consideration of this model is the representativeness of the variable construct using stepwise regression. Stepwise regression is designed to find the most effective predictors for predicting the dependent variables to form a model. The profiler, however, indicates only a linear relationship between the interacting variables. In comparison, neural

networks can detect nonlinear relationships and all possible interactions between these variables. The prediction model developed in this study employed independent variables (temperature, feed flow, NDP, system water recovery, permeate TDS, postrecycle feed conductivity, manufacturer's rated salt passage and water flux), which were measured on the same day as the dependent variable (performance and system salt passage).

CHAPTER VII

RO MEMBRANE FOULING MITIGATION

7.1. Abstract

A major hindrance to the application of reverse osmosis (RO) for reuse or reclamation of water is organic fouling. Despite continuous research for the enhancement of membrane performance recovery, there is need for further research on processes that can mitigate or prevent organic fouling and their mechanisms. This study described an effective cleaning sequence and recommended a cleaner to restore RO membrane performance. The RO performance was influenced by concentration polarization (CP), caused by retention of dissolved organic matter (DOM) and colloidal material (CM) complexes on the membrane surface. The effects of fouling on RO permeability and salt rejection were determined by comparing the permeability of a clean membrane with that of a fouled membrane, and by relating RO permeability and salt rejection to the cleaning sequence used for the recovery process.

The reported results indicate that the performance recovery of RO membranes is dependent on the physicochemical properties of the membrane foulant, the cleaners, and cleaning sequence. Caustic cleaning followed by acid cleaning afforded high cleaning power during membrane cleaning and effectively restored the permeability to greater than 100%. On the other hand, acid cleaning followed by caustic cleaning led to only partial

restoration of the ion retention (salt rejection) property of the membrane. The use of either acid cleaning or caustic cleaning alone or individually resulted in partial recovery of water flux, while a specific manufacturer-recommended sequence of caustic cleaning followed by acid cleaning or acid cleaning followed by caustic cleaning generally led to complete water flux recovery.

7.2. Introduction

Multiple cleaning procedures were put in place for phase 1, in case any one of the membranes experience fouling issues. One of the recommendations in the draft protocol of the pilot study requires that chemical cleaning of the membrane elements should be performed when the feed-to-concentrate pressure drop exceeds 15% of baseline. The objective of this task is to evaluate the effectiveness of the chemical cleaning regimes for restoring the permeate rate of the membrane system after fouling (when the solute rejection exceeds 10%). Two categories of cleaning (high- and low-pH cleaning) and four chemicals (from Avista, GE, PWT, and AWC) recommended by different manufacturers were evaluated during this task. The same chemicals (under high- and low-pH cleaning conditions) were assigned to a particular RO unit. For example, RO A and RO B were assigned Avista P303 (a low-pH cleaner) and Avista P312 (a high-pH cleaner), while RO C was assigned PWT Lavasol I (a low-pH cleaner) and PWT Lavasol II (a high-pH cleaner). On the other hand, RO D was assigned AWC C-236 (a low-pH cleaner) and AWC C-209 (a high-pH cleaner).

7.3. Results and Discussion

The RO membrane A was cleaned after the membrane experienced 15–20% loss in permeate flow according to the draft protocol. Figure 7.3.1 shows that the initial permeability rate through the membrane was 100% (blue bar graph). The bars to the right of the blue bar represent the new permeability after fouling (red), the recovered permeability after low-pH cleaning (green), and the recovered after high-pH cleaning

(purple). Six membrane cleans were performed during the operations of RO system A. Overall, flux declined with the sequence of acid cleaning followed by caustic cleaning when Avista was used as the cleaning chemical. However, when the cleaning chemical was switched to AWC under the same cleaning sequence, the flux of the RO system increased.

The combined process of acid cleaning followed by caustic cleaning demonstrated a lower cleaning efficiency. In addition, a single acidic cleaning conducted on 7th January exhibited an even lower permeate recovery than for the acid–caustic sequence. Thus in terms of high recovery, the sequential use of acid and caustic cleaning is more effective than acid or caustic cleaning alone in removing both acidic and basic fractions of natural organic matter (NOM). The sequence of the cleaner–membrane interaction appeared to be a major factor governing the recovery of the performance of the RO membranes. Such a cleaner–membrane interaction sequence was also a dominating factor that might have affected the observed post-cleaning salt passage for RO A, RO B, RO C, and RO D.

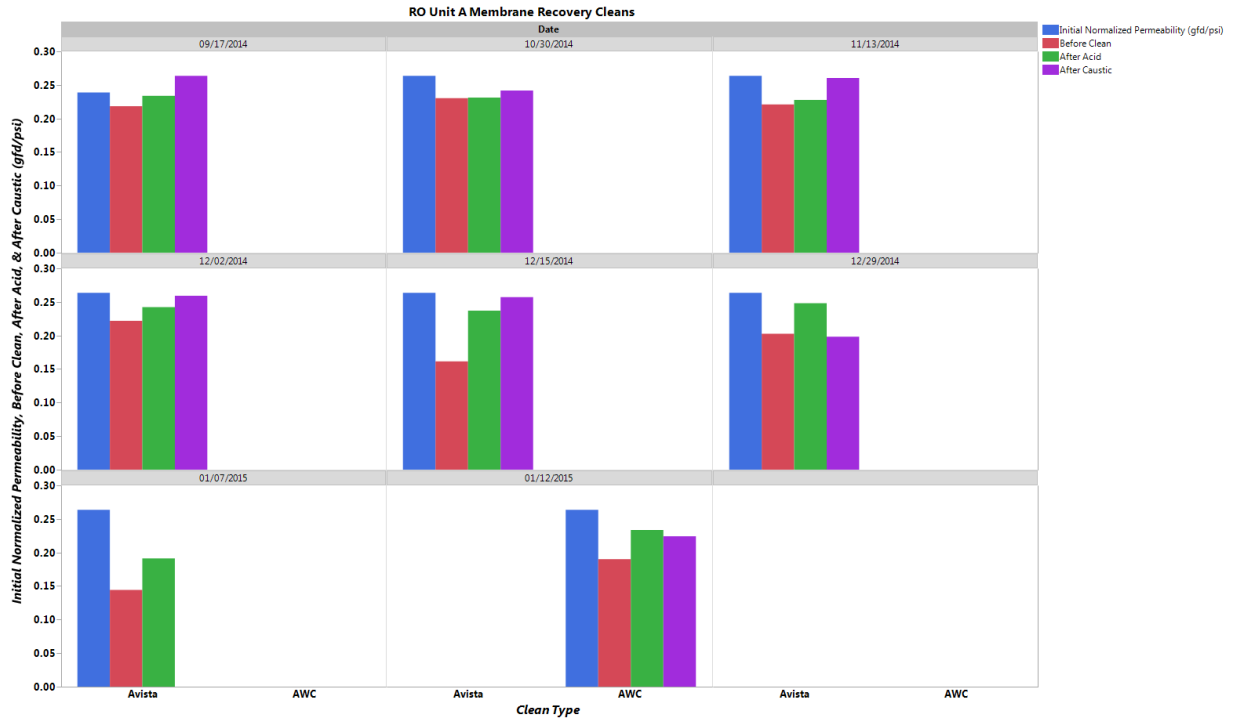


Figure 7.3.1. Unit A RO membrane recovery cleans.

The RO membrane B was cleaned after the membrane experienced 15–20% loss in permeate flow, according to the draft protocol. Figure 7.3.2 shows that the initial permeability rate through the membrane was 100% (blue bar graph). The bars to the right of the blue bar represent the new permeability after fouling (red), the recovered permeability after low-pH cleaning (green), and recovered permeability after high-pH cleaning (purple). Four membrane cleans were carried out during the operations of RO system B. Overall, the flux declined with the sequence of acid cleaning followed by caustic cleaning when Avista was used as the cleaning chemical. Therefore, the combined process of acid cleaning followed by caustic cleaning demonstrated a lower cleaning power. In addition, an even lower permeate recovery was observed with a single acidic clean carried out on 7th January, as compared to that observed using an acid–caustic sequence. Hence, in terms of high recovery, the sequential use of acidic and caustic

cleaning is more effective than acidic or caustic cleaning alone in removing both acidic and basic fractions of NOM.

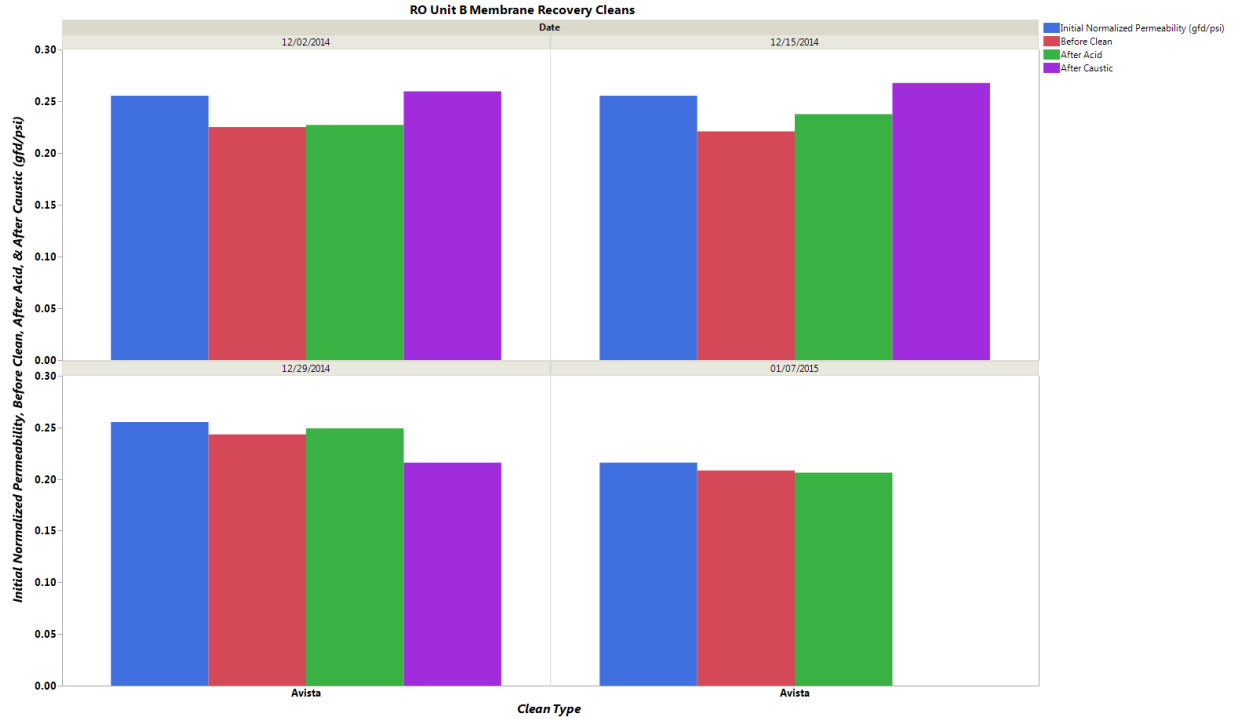


Figure 7.3.2. Unit B RO membrane recovery cleans.

The RO membrane C was cleaned after the membrane experienced 15%–20% loss in permeate flow, according to the draft protocol. Figure 7.3.4 shows that the initial permeability rate through the membrane was 100% (blue bar graph). The bars to the right of the blue bar show the new permeability after fouling (red), the recovered permeability after low-pH cleaning (green), and recovered permeability after high-pH cleaning (purple). Four membrane cleans were performed during the operations of the RO system C. Overall, the flux decreased with the sequence of acidic cleaning followed by caustic cleaning when Avista was used as the cleaning chemical. Therefore, the combined process of acidic cleaning followed by caustic cleaning demonstrated a lower cleaning

efficiency. In addition, an even lower permeate recovery was observed when a single acidic clean was performed on 7th January, as compared to that observed on using the acid–caustic sequence. Hence, in terms of high recovery, the sequential use of acidic and caustic cleaning was more effective than acid or caustic cleaning alone in removing both acidic and basic fractions of NOM.

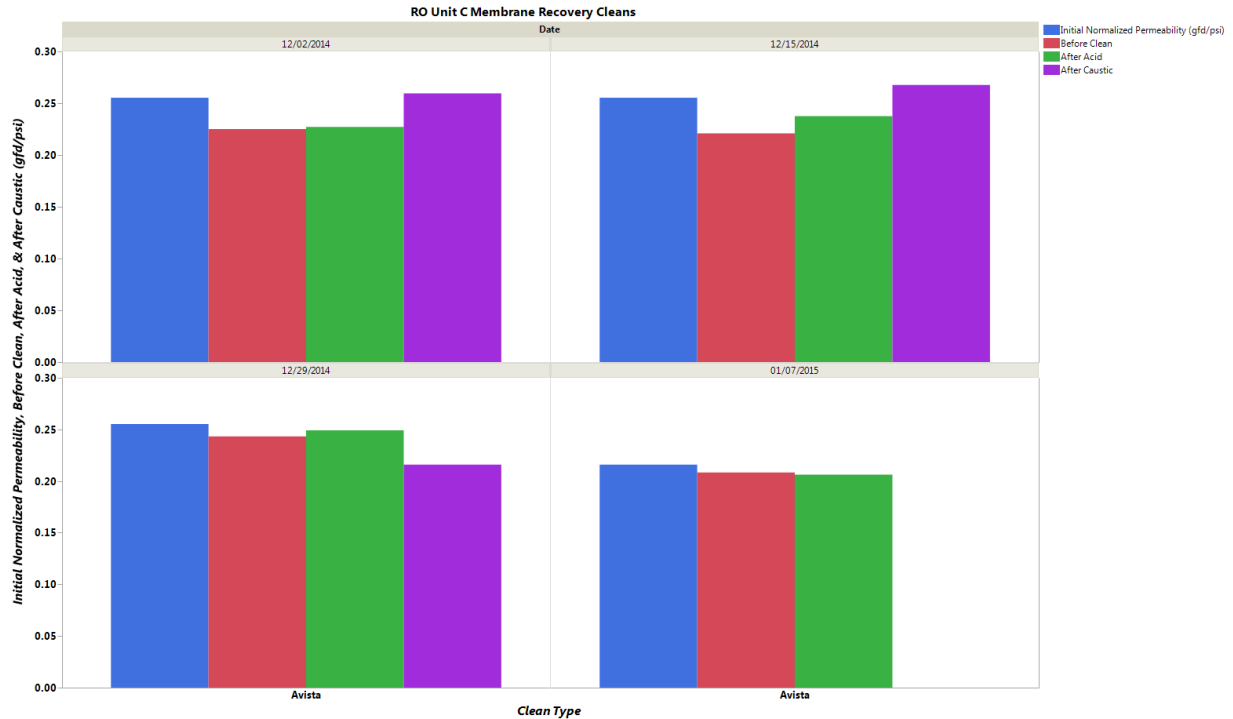


Figure 7.3.3. Unit C RO membrane recovery cleans.

The RO membrane D was cleaned after the membrane experienced 15–20% loss in permeate flow, according to the draft protocol. Figure 7.3.5 shows that the initial permeability rate through the membrane was 100% (blue bar graph). The bars to the right of the blue bar represent the new permeability after fouling (red), recovered permeability after high-pH cleaning (green), and recovered permeability after low-pH cleaning (purple). Four membrane cleans were performed during the operations of the RO system

D. Overall, the flux increased with the sequence of caustic cleaning followed by acidic cleaning when AWC was used as the cleaning chemical. Thus, the combined process of caustic cleaning followed by acid cleaning demonstrated a greater cleaning power. Studies have demonstrated that the presence of OH^- ions in caustic chemicals promotes the disruption of the foulant layer^{100, 101}. The use of caustic cleaners lead to increased ionic strength, pH, and solubility of NOM particles and the flux recovery observed in RO system D. Song has stated increased pH increases the negative charge on NOM due to the deprotonation of the carboxyl $-\text{COOH}$ and phenolic $-\text{OH}$ groups in their structure^{100, 101}. Conversely, studies have also shown that the presence of Na^+ ions in caustic chemicals lowers the negative charge of NOM by binding with the negatively charged groups during cleaning^{103, 104}. Acidic cleaning effectively removes inorganic precipitates from the membrane surface and membrane pores. Hence, the use of a caustic–acidic sequence was more effective, in terms of high permeability recovery, than an acid–caustic sequence when removing NOM foulants for restoring RO membrane permeability.

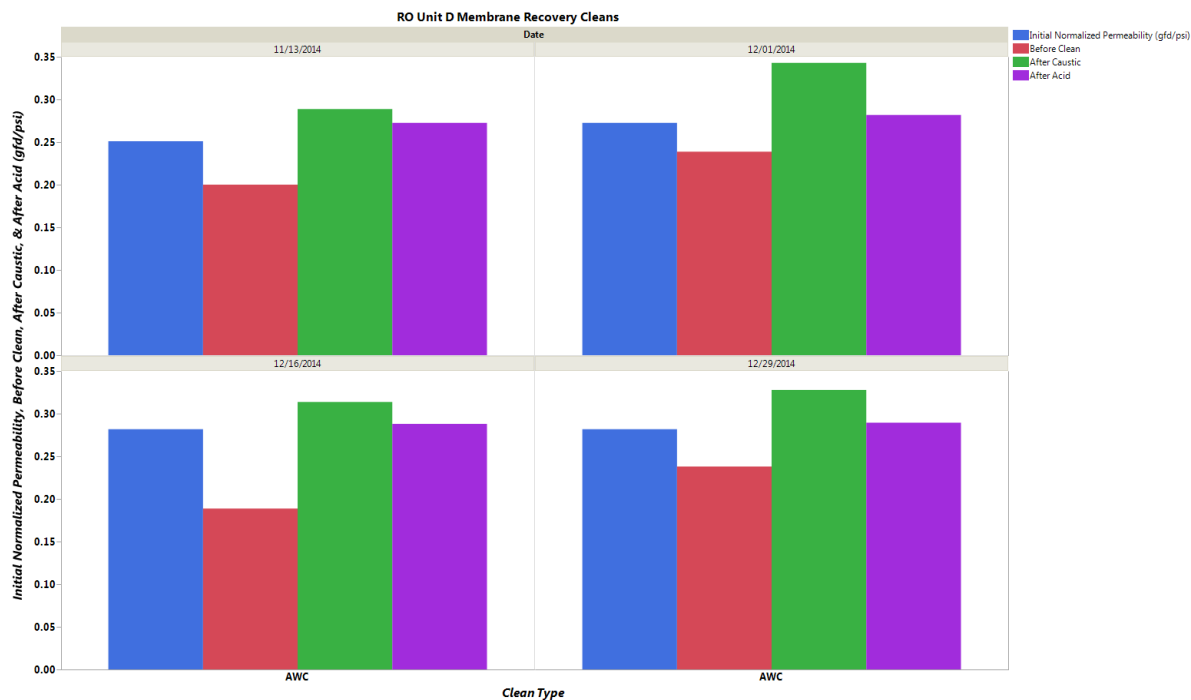


Figure 7.3.4. Unit D RO membrane recovery cleans.

7.4. Conclusion

The RO systems A, C, and D ran at the same water flux recovery (82%), and RO system B ran at a permeate recovery (75%) lower than those of the other three RO systems. RO systems A and B used the same antiscalant, while RO systems C and D used different antiscalants. Fewer chemical cleans were performed for RO systems B, C, and D than for RO system A, which was subjected to six cleans during the pilot study. The difference in the need for cleans between RO systems A and B is due to the lower flux recovery for RO B (75%) than RO A (82%). The lower number of cleans for RO systems C and D might be attributed to the effectiveness of the antiscalant used in these RO systems as they were run at the same water flux recovery as RO A.

The results indicate that the permeability performance recovery of RO membranes depends on the physicochemical properties of the membrane foulant and the cleaners, and

the sequence in which the cleaner was applied. The sequence of the cleaner–membrane interaction is a major factor governing the recovery of the RO membrane performance. Such a cleaner–membrane interaction sequence also indicates organics as the major foulant in the RO feed water. The use of caustic cleaning followed by acidic cleaning demonstrated greater cleaning power and effectively restored permeability to >100%. On the other hand, acidic cleaning followed by caustic cleaning only partially restored the ion retention (salt rejection) property of the membrane. This study also showed that the use of acidic or caustic cleaning alone was not effective in water flux recovery when compared to the combination of the two, and only caused partial permeability restoration.

REFERENCE

- ¹ Voros N. G., Maroulis Z. B., Marinos-Kouris D., Salt and water permeability in reverse osmosis membranes. *Desalination* 104 (1996) 141-154
- ² Sablani, S. S., Goosen, M. F.A., Al-Belushi, R. and Gerardos, V. Influence of spacer thickness on permeate flux in spiral-wound seawater reverse osmosis systems. *Desalination* 146 (2002) 225-230
- ³ Karime, Mohamed, S. Bouguecha, and B. Hamrouni. "RO membrane autopsy of Zarzis brackish water desalination plant." *Desalination* 220.1 (2008): 258-266.
- ⁴ Sablani, S. S., Goosen, M. F. A., Al-Belushi, R., and Wilf, M., Concentration Polarization in Ultrafiltration and Reverse Osmosis: A Critical Review. *Desalination* 141 (2001) 269-289
- ⁵ Ridgway H. F., Bacteria and Membranes: Ending a Bad Relationship. *Desalination*, 83 (1991) 53
- ⁶ Cherkasov A. N., Tsareva S. V., and Polotsky A. E., *Journal Membrane Science* 104 (1995) 157-165.
- ⁷ Nystrom M., Ruohomaki K., and Kaipa L., Humic acid as a fouling agent in filtration. *Desalination*. 106 (1996) 78-86.
- ⁸ Domany Z., Galambos I., Vatai G., Bekassy-Molnar E., Humic substances removal from drinking water by membrane filtration. *Desalination* 145 (2002) 333-337
- ⁹ Kabsch-Korbutowicz M., Majewska-Nowak K., and Winnicki T., Analysis of membrane fouling in the treatment of water solutions containing humic acids and mineral salts. *Desalination* 126 (1999) 179-185.
- ¹⁰ Tu S-C., Ravindran V., Den W., and Pirbazari M., Predictive membrane transport model for nanofiltration processes in water treatment, *AIChE Journal* 47(6) (2001) 1346-1362.

- ¹¹ Yiantsios, S. G., D. Sioutopoulos, and A. J. Karabelas. "Colloidal fouling of RO membranes: an overview of key issues and efforts to develop improved prediction techniques." *Desalination* 183.1 (2005): 257-272.
- ¹² Park, Chanhyuk, et al. "Variation and prediction of membrane fouling index under various feed water characteristics." *Journal of Membrane Science* 284.1 (2006): 248-254.
- ¹³ Al-Amoudi, Ahmed Saleh. "Factors affecting natural organic matter (NOM) and scaling fouling in NF membranes: a review." *Desalination* 259.1 (2010): 1-10.
- ¹⁴ Bieroza, Magdalena, Andy Baker, and John Bridgeman. "Relating freshwater organic matter fluorescence to organic carbon removal efficiency in drinking water treatment." *Science of the Total Environment* 407.5 (2009): 1765-1774.
- ¹⁵ Cho, Jaeweon, Gary Amy, and John Pellegrino. "Membrane filtration of natural organic matter: initial comparison of rejection and flux decline characteristics with ultrafiltration and nanofiltration membranes." *Water Research* 33.11 (1999): 2517-2526.
- ¹⁶ Volk, Christian, et al. "Impact of enhanced and optimized coagulation on removal of organic matter and its biodegradable fraction in drinking water." *Water Research* 34.12 (2000): 3247-3257.
- ¹⁷ Hong, Seungkwan, and Menachem Elimelech. "Chemical and physical aspects of natural organic matter (NOM) fouling of nanofiltration membranes." *Journal of membrane science* 132.2 (1997): 159-181.
- ¹⁸ Wilf M., and Klinko K., Effective new pretreatment for seawater reverse osmosis systems. *Desalination* 117 (1998) 323-331.
- ¹⁹ Glueckstern P., Priel M., Wilf M., Field evaluation of capillary UF technology as a pretreatment for large seawater RO systems. *Desalination* 147 (2002) 55-62
- ²⁰ Glueckstern P. and Priel M., Advanced concept of large seawater desalination systems for Israel. *Desalination* 119 (1998) 33-45
- ²¹ Karakulski K., Gryta M., Morawski A., membrane processes used for potable water quality improvement. *Desalination* 145 (2002) 315-319.
- ²² Chapman H., Vigneswaran S., Ngo H.H., Dyer S., Ben Aim R., Pre-flocculation of secondary treated wastewater in enhancing the performance of microfiltration. *Desalination* 146 (2002) 367-372
- ²³ Nguyen M.T., Ripperger S., Investigation on the effect of flocculants on the filtration behavior in microfiltration of fine particles. *Desalination* 147 (2002) 37-42.

- ²⁴ Han B., Runnels T., Zimbron J., Wickramasinghe R., Arsenic removal from drinking water by flocculation and microfiltration. *Desalination* 145 (2002) 293-298
- ²⁵ Choksuchart P., Heran M., Grasmick A., Ultrafiltration enhanced by coagulation in an immersed membrane system. *Desalination* 145 (2002) 265-272
- ²⁶ Park P.K., Lee C.H., Choi S.J., Choo K.H., Kim S.H., Yoon C.H., Effect of the removal of DOMs on the performance of a coagulation –UF membrane system for drinking water production. *Desalination* 145 (2002) 237-245.
- ²⁷ Guigui C., Rouch J.C., Durand-Bourlier L., Bonnelye V., Aptel P., Impact of coagulation conditions on the in-line coagulation/UF process for drinking water production. *Desalination* 147 (2002) 95-100
- ²⁸ Lopez-Ramirez J.A., Marquez D.S., Alonso J.M.Q., Comparison studies of feedwater pre-treatment in reverse osmosis pilot plant. *Desalination* 144 (2002) 347-352
- ²⁹ Shaalan H.F., Development of fouling control strategies pertinent to nanofiltration membranes. *Euromed* May 2002.
- ³⁰ Goosen M.F.A., Sablani S.S., Al-Maskari S.S., Al-Belushi R.H., Wilf M., Effect of feed temperature on permeate flux and mass transfer coefficient in spiral-wound reverse osmosis systems. *Desalination* 144 (2002) 367-372
- ³¹ Koltuniewicz A. and Noworyta A., Dynamic properties of ultrafiltration systems in light of the surface renewal theory. *Industrial Engineering and Chemical Research* 33 (1994) 1771-1779
- ³² Chen V., Fane A. G., Madaeni S., Wenten I. G., Particle deposition during membrane filtration of colloids: transition between concentration polarization and cake formation. *Journal of Membrane Science* 125 (1997) 109-122
- ³³ Jackson D., Sablani S., Goosen M. F. A., Dal-Cin M., Wilf M., Al-Belushi R., and Al-Maskri R., Effect of cyclic feed water temperature changes on permeate flux in spiral wound RO systems. *J. Membrane Science*, (Submitted 2004).
- ³⁴ Song, L., A new model for the calculation of the limiting flux in ultrafiltration, *Journal of Membrane Science* 144 (1998) 173-185
- ³⁵ Tran-Ha M. H. and Wiley D. E., The relationship between membrane cleaning efficiency and water quality, *Journal of Membrane Science* 145 (1998) 99-110.
- ³⁷ Mores W.D., Davis R.H., Direct observation of membrane cleaning via rapid backpulsing. *Desalination* 146 (2002) 135-140

- ³⁶ Mohammadi T., Madaeni S. S., and Moghadam M. K., Investigation of membrane fouling. Euromed 2002 Conf. Proc. Vol. 1 No. 1, pg 1 4-6 May 2002 Sharm El-Sheikh, Egypt.
- ³⁷ Greenlee, Lauren F., et al. "Reverse osmosis desalination: water sources, technology, and today's challenges." *Water research* 43.9 (2009): 2317-2348.
- ³⁸ Wilf, M., and C. Bartels. "Integrated membrane desalination systems current status and projected development." *Desalination and Water Reuse International Forum & Exhibition, Tianjin, China*. 2006.
- ³⁹ Wilf, Mark, and Kenneth Klinko. "Optimization of seawater RO systems design." *Desalination* 138.1 (2001): 299-306.
- ⁴⁰ Wilf, Mark, and Craig Bartels. "Optimization of seawater RO systems design." *Desalination* 173.1 (2005): 1-12.
- ⁴¹ Xu, Jia, et al. "A pilot study of UF pretreatment without any chemicals for SWRO desalination in China." *Desalination* 207.1 (2007): 216-226.
- ⁴² Semiat, Raphael, Iris Sutzkover, and David Hasson. "Characterization of the effectiveness of silica anti-scalants." *Desalination* 159.1 (2003): 11-19.
- ⁴³ Shih, Wen-Yi, et al. "A dual-probe approach for evaluation of gypsum crystallization in response to antiscalant treatment." *Desalination* 169.3 (2004): 213-221.
- ⁴⁴ Song, Lianfa, and Menachem Elimelech. "Theory of concentration polarization in crossflow filtration." *J. Chem. Soc., Faraday Trans.* 91.19 (1995): 3389-3398.
- ⁴⁵ Teuler, A., K. Glucina, and J. M. Laine. "Assessment of UF pretreatment prior RO membranes for seawater desalination." *Desalination* 125.1 (1999): 89-96.
- ⁴⁶ Rahardianto, Anditya, et al. "Diagnostic characterization of gypsum scale formation and control in RO membrane desalination of brackish water." *Journal of Membrane Science* 279.1 (2006): 655-668.
- ⁴⁷ Rahardianto, Anditya, et al. "High recovery membrane desalting of low-salinity brackish water: Integration of accelerated precipitation softening with membrane RO." *Journal of Membrane Science* 289.1 (2007): 123-137.
- ⁴⁸ Plottu-Pecheux, Anne, et al. "Comparison of three antiscalants, as applied to the treatment of water from the River Oise." *Desalination* 145.1 (2002): 273-280.
- ⁴⁹ Allam, J., G. K. Pearce, and K. Chida. "Ultrafiltration Pre-treatment to RO: Trials at Kindasa Water Services, Jeddah, Saudi Arabia." *IDA Conference in Bahamas*. 2003.

- ⁵⁰ Pearce, G. K. "The case for UF/MF pretreatment to RO in seawater applications." *Desalination* 203.1 (2007): 286-295.
- ⁵¹ Kim, Suhan, and Eric Hoek. "Modeling concentration polarization in reverse osmosis processes." *Desalination* 186.1 (2005): 111-128.
- ⁵² Ghafour, Essam EA. "Enhancing RO system performance utilizing antiscalants." *Desalination* 153.1 (2003): 149-153.
- ⁵³ Brehant, A., V. Bonnelye, and M. Perez. "Assessment of ultrafiltration as a pretreatment of reverse osmosis membranes for surface seawater desalination." *Water Supply* 3.5 (2003): 437-445.
- ⁵⁴ Bu-Rashid, Khalid Ahmed, and Wolfgang Czolkoss. "Pilot tests of multibore UF membrane at Addur SWRO desalination plant, Bahrain." *Desalination* 203.1 (2007): 229-242.
- ⁵⁵ Tiwari, S. A., et al. "Assessment of an ultrafiltration pre-treatment system for a seawater reverse osmosis plant." *International journal of nuclear desalination* 2.2 (2006): 132-138.
- ⁵⁶ Wijmans, J. G., and R. W. Baker. "The solution-diffusion model: a review." *Journal of membrane science* 107.1 (1995): 1-21.
- ⁵⁷ Vrouwenvelder, J. S., et al. "Biofouling potential of chemicals used for scale control in RO and NF membranes." *Desalination* 132.1 (2000): 1-10.
- ⁵⁸ Vedavyasan, C. V. "Pretreatment trends—an overview." *Desalination* 203.1 (2007): 296-299.
- ⁵⁹ Morenski, F. "Current pretreatment requirements for reverse osmosis membrane applications." *PROCEEDINGS OF THE INTERNATIONAL WATER CONFERENCE. VOL. 53. ENGINEERS SOCIETY OF WESTERN PENNSYLVANIA, 1992.*
- ⁶⁰ Kremen, Seymour S., and Matt Tanner. "Silt density indices (SDI), percent plugging factor (% PF): their relation to actual foulant deposition." *Desalination* 119.1 (1998): 259-262.
- ⁶¹ Hassan, A. M., et al. "A new approach to membrane and thermal seawater desalination processes using nanofiltration membranes (Part 1)." *Desalination* 118.1 (1998): 35-51.
- ⁶² Boffardi, B. P. "Scale Deposit Control for Reverse Osmosis Systems." *Technical Bulletin* 4-165 (1996): 307-319.
- ⁶³ Iler, Ralph K. *The chemistry of silica: solubility, polymerization, colloid and surface properties, and biochemistry.* Wiley, 1979.

- ⁶⁴ K. Momozaki, M. Kira, Y. Murano, M. Okamoto, and F. Kawamura, "Polyacrylamide Based Treatment Program for Open Recirculating Cooling Water System with High Silica Content," Paper No. 92-11, International Water Conference (Pittsburgh, PA, Oct-1992).
- ⁶⁵ Amjad, Zahid, John F. Zibrida, and Robert W. Zuhl. "A new antifoulant for controlling silica fouling in reverse osmosis systems." IDA World Congress on Desalination and Water Reuse, Madrid. 1997.
- ⁶⁶ Kamp, Peer C., Joop C. Kruithof, and Henk C. Folmer. "UF/RO treatment plant Heemskerk: from challenge to full scale application." *Desalination* 131.1 (2000): 27-35.
- ⁶⁷ Vrouwenvelder, H. S., et al. "Biofouling of membranes for drinking water production." *Desalination* 118.1 (1998): 157-166.
- ⁶⁸ Water, Dow, and Process Solutions. "FILMTEC™ Reverse Osmosis Membranes Technical Manual." (2009): 609-00071.
- ⁶⁹ Guo, Wenshan, Huu-Hao Ngo, and Jianxin Li. "A mini-review on membrane fouling." *Bioresource technology* 122 (2012): 27-34.
- ⁷⁰ Li, Qilin, and Menachem Elimelech. "Organic fouling and chemical cleaning of nanofiltration membranes: measurements and mechanisms." *Environmental Science & Technology* 38.17 (2004): 4683-4693.
- ⁷¹ Zhang, Miaomiao, et al. "Fouling and natural organic matter removal in adsorbent/membrane systems for drinking water treatment." *Environmental science & technology* 37.8 (2003): 1663-1669.
- ⁷² Tang, Chuyang Y., T. H. Chong, and Anthony G. Fane. "Colloidal interactions and fouling of NF and RO membranes: a review." *Advances in colloid and interface science* 164.1 (2011): 126-143.
- ⁷³ Jin, Xue, et al. "Effects of feed water temperature on separation performance and organic fouling of brackish water RO membranes." *Desalination* 239.1 (2009): 346-359.
- ⁷⁴ Ng, How Y., and Menachem Elimelech. "Influence of colloidal fouling on rejection of trace organic contaminants by reverse osmosis." *Journal of Membrane Science* 244.1 (2004): 215-226.
- ⁷⁵ Lee, Sangyoup, Jaeweon Cho, and Menachem Elimelech. "A novel method for investigating the influence of feed water recovery on colloidal and NOM fouling of RO and NF membranes." *Environmental engineering science* 22.4 (2005): 496-509.

- ⁷⁶ Shi, Xiafu, et al. "Fouling and cleaning of ultrafiltration membranes: A review." *Journal of Water Process Engineering* 1 (2014): 121-138.
- ⁷⁷ U.S. Geological Survey, 2001, National Water Information System data available on the World Wide Web (Water Data for the Nation), accessed [June 23, 2015], at <http://water.usgs.gov/edu/earthhowmuch.html>
- ⁷⁸ American Water Works Association, American Society of Civil Engineers. *Water Treatment Plant Design*. New York: McGraw Hill, 2012. Print
- ⁷⁹ Neofotistou, Eleftheria, and Konstantinos D. Demadis. "Use of antiscalants for mitigation of silica (SiO₂) fouling and deposition: fundamentals and applications in desalination systems." *Desalination* 167 (2004): 257-272.
- ⁸⁰ Gabelich, Christopher J., et al. "Control of residual aluminum from conventional treatment to improve reverse osmosis performance." *Desalination* 190.1 (2006): 147-160.
- ⁸¹ Freeman, Scott DN, and Randall J. Majerle. "Silica fouling revisited." *Desalination* 103.1 (1995): 113-115.
- ⁸² Sheikholeslami, Roya, et al. "Pretreatment and the effect of cations and anions on prevention of silica fouling." *Desalination* 139.1 (2001): 83-95.
- ⁸³ Kerry J. Howe and Mark M. Clark. *Coagulation Pretreatment for Membrane Filtration*. American Water Works Association, 2002. Print.
- ⁸⁴ Wang, Yan, et al. "The effect of total hardness on the coagulation performance of aluminum salts with different Al species." *Separation and Purification Technology* 66.3 (2009): 457-462.
- ⁸⁵ Nghiem, Long Duc, Poppy Jane Coleman, and Christiane Esendiller. "Mechanisms underlying the effects of membrane fouling on the nanofiltration of trace organic contaminants." *Desalination* 250.2 (2010): 682-687.
- ⁸⁶ Al-Amoudi, Ahmed Saleh. "Factors affecting natural organic matter (NOM) and scaling fouling in NF membranes: a review." *Desalination* 259.1 (2010): 1-10.
- ⁸⁷ Tang, Chuyang Y., T. H. Chong, and Anthony G. Fane. "Colloidal interactions and fouling of NF and RO membranes: a review." *Advances in colloid and interface science* 164.1 (2011): 126-143.
- ⁸⁸ Al-Amoudi, Ahmed, and Robert W. Lovitt. "Fouling strategies and the cleaning system of NF membranes and factors affecting cleaning efficiency." *Journal of Membrane Science* 303.1 (2007): 4-28.
- ⁸⁹ Howe, Kerry J., et al. *Principles of water treatment*. John Wiley & Sons, 2012.

- ⁹⁰ Gabelich, Christopher J., et al. "Control of residual aluminum from conventional treatment to improve reverse osmosis performance." *Desalination* 190.1 (2006): 147-160.
- ⁹¹ ASTM (1998). *Standard Practice for Calculation and Adjustment of the Langelier Saturation Index for Reverse Osmosis*. D 3739-94.
- ⁹² Nyer, Evan K., ed. *In situ treatment technology*. CRC Press, 2010.
- ⁹³ Reynolds, Tom D. *Unit operations and processes in environmental engineering*. Brooks, 1977.
- ⁹⁴ Mänttari, Mika, et al. "Fouling effects of polysaccharides and humic acid in nanofiltration." *Journal of Membrane Science* 165.1 (2000): 1-17.
- ⁹⁵ Elimelech, Menachem, et al. "Role of membrane surface morphology in colloidal fouling of cellulose acetate and composite aromatic polyamide reverse osmosis membranes." *Journal of membrane science* 127.1 (1997): 101-109.
- ⁹⁶ Ghosh, Kunal, and M. Schnitzer. "Macromolecular structures of humic substances." *Soil Science* 129.5 (1980): 266-276.
- ⁹⁷ Suess, Erwin. "Interaction of organic compounds with calcium carbonate-II. Organo-carbonate association in recent sediments." *Geochimica et Cosmochimica Acta* 37.11 (1973): 2435-2447.
- ⁹⁸ Song, Lianfa, and Menachem Elimelech. "Particle deposition onto a permeable surface in laminar flow." *Journal of colloid and interface science* 173.1 (1995): 165-180.
- ⁹⁹ Graham, S. I., R. L. Reitz, and C. E. Hickman. "Improving reverse osmosis performance through periodic cleaning." *Desalination* 74 (1989): 113-124.
- ¹⁰⁰ Elimelech, Menachem, et al. "Role of membrane surface morphology in colloidal fouling of cellulose acetate and composite aromatic polyamide reverse osmosis membranes." *Journal of membrane science* 127.1 (1997): 101-109.
- ¹⁰¹ Van Houtte, Emmanuel, et al. "Treating different types of raw water with micro-and ultrafiltration for further desalination using reverse osmosis." *Desalination* 117.1 (1998): 49-60.
- ¹⁰² Chemical cleaning of PS ultrafilters fouled by the fermentation broth of glutamic acid, *Sep. Purif. Technol.* 42 (2005) 181–187.
- ¹⁰³ Tran-Ha, Minh H., and Dianne E. Wiley. "The relationship between membrane cleaning efficiency and water quality." *Journal of membrane science* 145.1 (1998): 99-110.

¹⁰⁴ Song, Wonho, et al. "Nanofiltration of natural organic matter with H₂O₂/UV pretreatment: fouling mitigation and membrane surface characterization." *Journal of Membrane Science* 241.1 (2004): 143-160.

¹⁰⁵ Attewell, P., and Monaghan, D., 2013. *Data Mining: An Introduction for Social Scientists*. City University of New York, Graduate Center.

¹⁰⁶ Ramirez, J. G., Ramirez, B. S., 2009. *Analysing and Interpreting Continuous Data Using JMP: A Step-by-Step Guide*. Cary, NC: SAS Institute Inc.

¹⁰⁷ SAS Institute Inc. 2012. *JMP 10 Modeling and Multivariate Methods*. Cary, NC: SAS Institute Inc.

¹⁰⁸ Erickson M. G. (2015). *Grand Forks Water Treatment Plant Pretreatment, Ultrafiltration, and Reverse Osmosis Membrane Pilot Study* (Unpublished master's thesis). University of North Dakota, Grand Forks, North Dakota.

APPENDIX I


Table API-0-1: GFWTP pilot study procedures of testing and the parameters that were tested.

Analyst		Test	Analytical Method	Lab (L) / Online (OL)
GFWTP Lab		pH	Standard Method (SM) 4500H+B	L
		Turbidity	SM2130B	L
		TOC	SM5310C	L
		Alkalinity	SM2320B	L
		Hardness	SM2340C	L
		Aluminum	Eriochrome Cyanine R Method 3641-SC	L
		SDI	ASTM procedure D4189-95	L
		HPC	SM9215B	L
	Chlorine	SM4500C1-G	L	
Online Measurement (GFWTP)	Pretreatment	Flow	Endress+Hauser Promag	OL
		Influent pH	GLI Model 53	OL
		Effluent pH	HACH sc200	OL
		Influent Turbidity	HACH Surface Scatter 6	OL
		Effluent Turbidity	GLI Model 53	OL
	UF	Flow	All UF online instrumentation was provided by GE	OL
		Turbidity		OL
		pH		OL
		Temperature		OL
		TMP		OL
	RO	Tank Level	OL	
		Flow	GF Signet	OL
		pH	Provided by Wiggins	OL
		Temperature	Provided by Wiggins	OL
		Pressure	WKA pressure transmitters	OL
Conductivity		GF Signet	OL	
ORP	GF Signet	OL		
Tank Level	Erecta Switches	OL		
Outside Lab (Fargo WTP Lab)	Cation/Anion Analysis	Silica	EPA 200.7	L
		Barium	EPA 200.7	L
		Total Phosphorus as PO4	Hach	L
		Strontium	EPA 200.7	L
		Orthophosphate	Hach	L
		Nitrate-Nitrite as N	EPA 300.0	L
		Copper	EPA 200.9	L
		Conductivity	SM 2510B	L
		pH	SM 4500-H B	L
		Total Dissolved Solids (TDS)	SM 2540 C	L
		Chlorine	EPA 300.0	L
		Fluoride	EPA 300.0	L
		Sulfate	EPA 300.0	L
		Calcium	EPA 200.7	L
		Iron	EPA 200.7	L
		Magnesium	EPA 200.7	L
		Manganese	EPA 200.7	L
		Potassium	EPA 200.7	L
		Sodium	EPA 200.7	L
		Bicarbonate as CaCO3	SM 2320B	L
Carbonate as CaCO3	SM 2320B	L		
Hydroxide as CaCO3	SM 2320B	L		
Phenolphthalein as CaCO3	SM 2320B	L		
Total Alkalinity as CaCO3	SM 2320B	L		
Total Suspended Solids (TSS)	SM 2540D	L		
Outside Lab (MWH)		HAA5	SM 6251B	L
		THM	EPA 524.2	L
		NDMA	EPA 521	L
		MIB/Geosmin	SM 6040D	L
		Emerging Contaminant	LC-MS-MS	L
Outside Lab (University of Colorado, Boulder)		TOC	TOC-V _{CSH} analyzer (Shimadzu Corp.)	L
		Size Exclusion Chromatography	Agilent 1200 LC system w. Protein-Pak 125 column	L
		Fluorescence	John Yvon Horiba FluoroMax-4 spectrofluorometer	L
		Polarity Rapid Assessment Method	Extract Clean SPE kit catalog #210100 (Alltech Associates)	L

Table API-0-2. Daily data analysis recording sheet

Membrane Phase II Pilot Study _____		Date: _____	S M T W TH F S	
City of Grand Forks _____				
On-site Personnel: _____				
Membrane Pilot Study Status:				
<input type="checkbox"/> Cation/Anion Sampling <input type="checkbox"/> RO #1 CIP <input type="checkbox"/> RO #4 CIP <input type="checkbox"/> SDS Sampling <input type="checkbox"/> RO #2 CIP <input type="checkbox"/> Other <input type="checkbox"/> UF CIP <input type="checkbox"/> RO #3 CIP				
Log				
(List of daily work, upstream water quality, anything that may cause discrepancies in test results)				
Sample Time: _____ am / pm				
Raw Blend				
pH	_____		Temp	_____ Deg C
Turbidity	_____	NTU	TOC	_____ Yes/No
Total Hardness	_____	mg/l as CaCO ₃		
Ca Hardness	_____	mg/l as CaCO ₃	Mg Hardness	_____ mg/l as CaCO ₃
P Alkalinity	_____	mg/l as CaCO ₃	M Alkalinity	_____ mg/l as CaCO ₃
Pretreatment Effluent				
pH	_____		Temp	_____ Deg C
Turbidity	_____	NTU	TOC	_____ Yes/No
Total Hardness	_____	mg/l as CaCO ₃		
Ca Hardness	_____	mg/l as CaCO ₃	Mg Hardness	_____ mg/l as CaCO ₃
P Alkalinity	_____	mg/l as CaCO ₃	M Alkalinity	_____ mg/l as CaCO ₃
UF Filtrate				
pH	_____		Temp	_____ Deg C
Conductivity	_____	µS/cm	TOC	_____ Yes/No
Total Hardness	_____	mg/l as CaCO ₃		
Ca Hardness	_____	mg/l as CaCO ₃	Mg Hardness	_____ mg/l as CaCO ₃
P Alkalinity	_____	mg/l as CaCO ₃	M Alkalinity	_____ mg/l as CaCO ₃
RO Feed				
Aluminum	_____	ppm		
RO Pemeate - #1				
pH	_____		Temp	_____ Deg C
Conductivity	_____	µS/cm	TOC	_____ Yes/No
RO Pemeate - #2				
pH	_____		Temp	_____ Deg C
Conductivity	_____	µS/cm	TOC	_____ Yes/No
RO Pemeate - #3				
pH	_____		Temp	_____ Deg C
Conductivity	_____	µS/cm	TOC	_____ Yes/No
RO Pemeate - #4				
pH	_____		Temp	_____ Deg C
Conductivity	_____	µS/cm	TOC	_____ Yes/No

Table API-0-3. Daily data instrument recording sheet

Date		Time		Operator									
Pretreatment													
Influent Flowrate (gpm)	Coagulation Settings		Acid Settings		Influent Water Quality								
	Coagulant (type)	mL/min	Acid (yes / no)	mL/min	pH	Turbidity (NTU)	pH	Turbidity (NTU)	Floc Speed (rpm)	Feed Tank (% full)			
Chemical Tank Level less than 25% full (yes / no): Notes / Comments:													
MF/UF													
Operations							Pressure			Maintenance Wash		Turbidity	
Time Since BW (min)	TMP (psi)	Resistance	Flux (gfd)	Permeability (gfd/psi)	Filtrate Flow (gpm)	Pump Speed (%)	Feed Pressure (psi)	Filtrate Pressure (psi)	Last Air Test Result (psi/min)	Time Since Cl MW (filt. hrs)	Time Since Acid MW (filt. hrs)	Feed (NTU)	Filtrate (mNTU)
Chemical Tank Level less than 25% full (yes / no): Alarms / Notes / Comments:													
RO Feed													
Tank Levels		SDI Measurements											
(% full)	0 minutes	5 minutes	10 minutes	15 minutes									
Notes / Comments:													
RO #1 Skid													
Chemical	Pressure (psi)					Flow (gpm)							
Antiscalant (gal)	Cartridge Filter In	Cartridge Filter Out	Primary Pressure	Permeate Pressure	Concentrate Pressure	Influent	Permeate	Concentrate	Recycle				
Notes / Comments:													
RO #2 Skid													
Chemical	Pressure (psi)					Flow (gpm)							
Antiscalant (gal)	Cartridge Filter In	Cartridge Filter Out	Primary Pressure	Permeate Pressure	Concentrate Pressure	Influent	Permeate	Concentrate	Recycle				
Notes / Comments:													
RO #3 Skid													
Chemical	Pressure (psi)					Flow (gpm)							
Antiscalant (gal)	Cartridge Filter In	Cartridge Filter Out	Primary Pressure	Permeate Pressure	Concentrate Pressure	Influent	Permeate	Concentrate	Recycle				
Notes / Comments:													
RO #4 Skid													
Chemical	Pressure (psi)					Flow (gpm)							
Antiscalant (gal)	Cartridge Filter In	Cartridge Filter Out	Primary Pressure	Permeate Pressure	Concentrate Pressure	Influent	Permeate	Concentrate	Recycle				
Notes / Comments:													

Appendix II

System Design and Control of Operating Parameters

A. Design Criteria

Design criteria for a full-scale flocculation system are provided in the tables below. The table presents key design parameters for lamella plate settlers ¹⁰⁸.

Key Flocculation Design Criteria

Design Criterion	Description
Flocculation or Detention Time	<p>Flocculation time depends on basin volume, baffling, staging and the flow rate through the process. The flocculation time must be long enough to allow for particles to interact and aggregate to create the floc, but not too long because flocs can begin to shear. The theoretical detention time (without considering the effects of baffling) is the typical parameter used to describe flocculation time. It is calculated by the following equation:</p> $T = V/Q$ <p>Where:</p> <p style="padding-left: 40px;">T = Detention Time (min)</p> <p style="padding-left: 40px;">V = Volume of Flocculation Basin (gal)</p> <p style="padding-left: 40px;">Q = Flow (gpm)</p> <p>Typical flocculation times range from 15 to 30 min.</p>
Flocculation Velocity Gradient	<p>The mixing intensity or energy input, also known as the G value, is a measurement of the energy imparted to the water. This parameter varies significantly with water temperature and is calculated using the energy dissipation rate in the fluid. The G value in full-scale basins is:</p> $G = 388P^{0.5}$

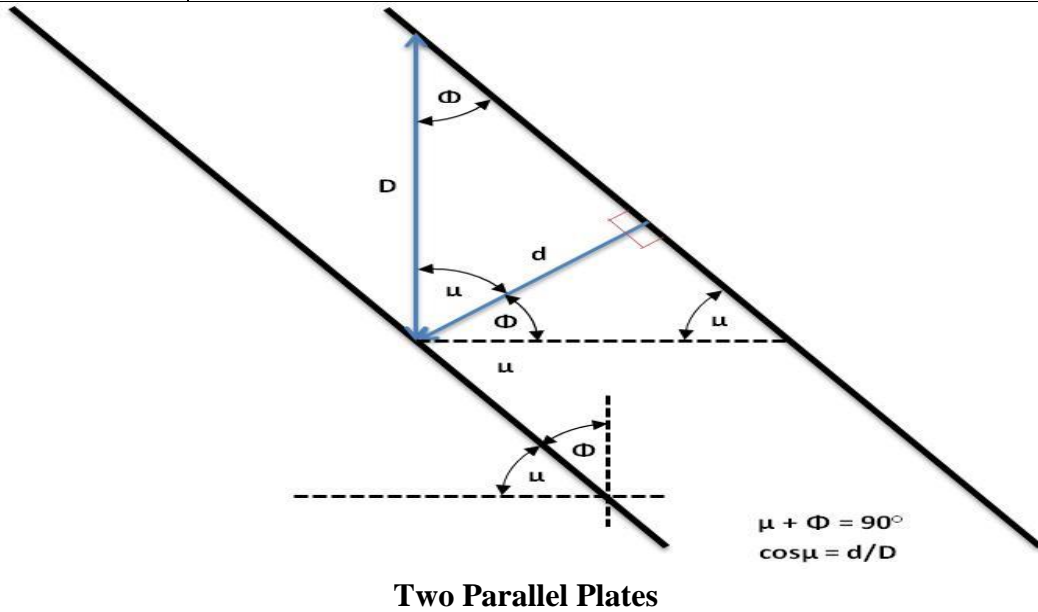
Design Criterion	Description
	<p>Where:</p> <p style="text-align: center;">$G = \text{Velocity Gradient (sec}^{-1}\text{)}$</p> <p style="text-align: center;">$P = \text{power (kW or hp) applied to the mix motor (may be read directly from variable frequency drive (VFD) display)}$</p> <p>G values can range from 10 to 150 sec⁻¹ depending on the type of flocculation process.</p>
Number of Flocculation Stages	In order to avoid floc shearing, multiple (3 is typical) flocculation stages are employed, with gradually reduced mixing intensity in each stage. This is often described as “tapered flocculation.”
Operational Flexibility (to facilitate treatment of varying water quality)	The flocculation basin and associated processes (mixing, chemical feed, etc.) should be designed to facilitate effective and consistent treatment of feeds with varying source water quality by providing operational flexibility to adjust mixing intensity within each flocculation stage, apart from adjusting chemical dosages and adding a flocculation aid.

Key Plate Settler Design Criteria

Design Criterion	Description
Surface Loading Rate	<p>The surface loading rate for each plate is the primary design criterion for plate settlers. The surface loading rate is calculated as:</p> $\text{Surface Loading Rate } \left(\frac{\text{gpm}}{\text{sf}} \right) = \frac{Q}{A}$ <p>Where:</p> <p style="text-align: center;">$Q = \text{flow into the system (gpm)}$</p> <p style="text-align: center;">$A = \text{projected plate settler surface area (ft}^2\text{) which is the sum of the horizontally projected area of all of the plate surface areas}$</p>

Design Criterion	Description
Basin Dimensions and Flow Velocity	<p>The basin dimensions, particularly the length, affect the detention time required to settle out floc particles. The following equation depicts the relationship between basin dimensions and settling velocity:</p> $V_{f\max} = \frac{V_s L}{d}$ <p>Where:</p> <p>V_f = velocity of the fluid</p> <p>V_s = velocity of the settling particle</p> <p>L = length of the basin</p> <p>d = depth of the basin</p> <p>V_s must always be greater than V_f for floc to settle.</p>
Inclined Plate Angle	<p>The angle of the inclined plate (measured from horizontal as zero) will alter the distances that the settling particle travels vertically, as well as the projected surface area that affects the surface loading rate. The vertical distance a particle travels as it settles can be calculated as follows:</p> $D = d / \cos \mu$ <p>Where:</p> <p>D = vertical distance the particle travels</p> <p>d = distance between the plates (perpendicular to plates)</p> <p>μ = plate positioning angle</p> <p>The industry standard positioning for inclined plates is 55-60° for self-cleaning purposes.</p>
Distance between Plates	<p>The distance between settler plates also affects particle settling. This relationship is depicted in the equation above for the Inclined Plate Angle.</p>

Design Criterion	Description
Launder Weir Loading	Launder weir loading is a measure of the water flow per unit distance of clarified effluent that travels from the plate settler and into the effluent weir. This criterion is typically given in units of gpm/ft.



B. Operational Considerations

The operational mechanisms that impact the effectiveness of flocculation/high-rate clarification, are summarized in the table below ¹⁰⁸.

Flocculation/High Rate Clarification Operational Considerations

Process	Operational Consideration	Description
Flocculation	Mixing Speed	Optimize the mixing intensity (or energy) to yield the desired floc size and density and provide operational flexibility to change the mixing speed to account for varying water quality.
	Flocculation Time	Provide adequate and adjustable flocculation time to optimize floc formation.
	Short Circuiting	Confirm that mixing within the flocculation basin is efficient and minimizes short circuiting that results in less efficient flocculation for portions of the flow through the basin.
	Coagulant Dose	Optimize the coagulant dose for variations in water quality and allow for application of a range of doses.
	Polymer Dose/Location	Design for multiple polymer dosing locations and a range of polymer doses.
High-Rate Clarification	Surface Overflow Rate	Weirs, submerged orifices, and other proprietary designs are employed to collect clarified water. These should be designed to ensure even flow distribution.

Process	Operational Consideration	Description
	Short Circuiting	The design should accommodate uniform flow through the process to avoid short circuiting, which could impact the performance of the system and the quality of the clarified water.

C. Advantages and Disadvantages

The advantages and disadvantages of flocculation and high-rate clarification with plate settlers are summarized in the table below ¹⁰⁸.

Advantages and Disadvantages for Flocculation and High-rate Clarification

Process	Advantages	Disadvantages
Flocculation	<ul style="list-style-type: none"> • Mechanical mixing <ul style="list-style-type: none"> ○ More operational control (i.e. intensity of mixing) ○ Ability to operate using tapered flocculation encourages the rapid growth of larger floc particles • Hydraulic mixing <ul style="list-style-type: none"> ○ No mechanical parts ○ Less maintenance required 	<ul style="list-style-type: none"> • Mechanical mixing <ul style="list-style-type: none"> ○ Dependent on seasonal changes such as water quality and temperature ○ Requires more maintenance and hands on operation • Hydraulic mixing <ul style="list-style-type: none"> ○ Less uniform mixing ○ Less operational control ○ Variable performance based on different flow rates through the process
High Rate Clarification through Lamella Plate	<ul style="list-style-type: none"> • Higher surface loading rate resulting in a smaller process footprint than conventional sedimentation. • Modular design allows for future 	<ul style="list-style-type: none"> • No buffer volume for flow fluctuations • Many surfaces for particle accumulation

Settlers	expansion <ul style="list-style-type: none"> • Improved performance/consistency • Cost effective • Plates can be capped to allow variable surface overflow rates 	<ul style="list-style-type: none"> • Limited storage capacity for settled sludge (under plates) • Shorter detention time, compared to conventional sedimentation, which may lead to particle loading onto downstream technologies
----------	---	---

D. Design Criteria

The design parameter for MF/UF systems that impacts the operations of these units includes flux, recovery, and transmembrane pressure (TMP). Descriptions of these parameters, as well as several other key terms applicable to MF/UF systems, are presented in the table below ¹⁰⁸.

MF/UF Design Criteria

Term	Definition
Flux	<p>The permeate or filtrate flux through MF/MF membranes depends largely on transmembrane pressure and water temperature. Design flux rates depend on feed water quality and the frequency of backwashing and cleaning (described in more detail below). Flux is defined as:</p> $J = \frac{Q}{A}$ <p>Where:</p> <p style="margin-left: 40px;">J = Flux (g/d/ft²)</p> <p style="margin-left: 40px;">Q = filtrate flow (gpd)</p> <p style="margin-left: 40px;">A = membrane surface area (ft²)</p>
Recovery	<p>Recovery, or feed water recovery, is the product volume over a given period divided by the feed water flow volume, as</p>

Term	Definition
	<p>depicted by the equation below:</p> $R = \frac{Q_p}{Q_f}$ <p>Where:</p> <p>R = recovery of the membrane unit</p> <p>Q_p = filtrate flow produced by the membrane unit (gpd)</p> <p>Q_f = feed flow to the membrane unit (gpd)</p> <p>Typical MF/Uf recoveries range from 85% to over 95%.</p>
Transmembrane Pressure	<p>The driving force for the transport of water across a micro porous membrane (i.e. a pressure gradient across the membrane) or:</p> $TMP = P_f - P_p$ <p>Where:</p> <p>TMP = transmembrane pressure (pounds per square inch (psi))</p> <p>P_f = feed pressure (psi)</p> <p>P_p = filtrate pressure (i.e., backpressure) (psi)</p>
Backwash	<p>A cleaning operation that typically involves periodic reverse flow through the membrane to remove foulants accumulated at the membrane surface. Backwashes can be performed with chlorinated or unchlorinated water.</p>
Enhanced Flux Maintenance	<p>EFM is a cleaning procedure that involves cleaning the membranes with a chemical solution. EFM is typically carried</p>

Term	Definition
(EFM)	out multiple times per week. The frequency and chemicals used should be evaluated during pilot testing.
Clean-In Place (CIP)	A CIP is the periodic application of a chemical solution or (series of solutions) to a membrane to remove accumulated foulants and thus restore permeability and recovery to baseline levels.
Membrane Fouling	Reversible fouling is the reduction in filtrate flux that can be restored by mechanical or chemical means. Irreversible fouling is permanent loss in filtrate flux capacity.

E. Operational Considerations

There are several operation and maintenance practices related to **MF/UF** systems that have a significant impact on the performance of the system. These operational practices should be continuously monitored and improved to enhance system performance and reduce treatment costs. Descriptions of these practices are described in the table below

108

Table: MF/UF Operational Considerations

Operational Consideration	Description
Backwash frequency and duration	Backwashes are implemented relatively frequently – every 5 men to several hours - and have a relatively short duration of 3 to 180 s. Backwash frequency and duration should be optimized to enhance system performance while maximizing recovery.

EFM frequency and chemical usage	EFM processes should be optimized (frequency, chemical selection and dose, duration, etc.) to maximize membrane treatment efficiency and reduce treatment costs.
Pretreatment	Pretreatment of MF/UF membranes may be required, depending on the water quality. Pretreatment can mitigate feed water quality fluctuations, which will improve the performance of the MF/UF system and decrease treatment costs and maintenance (e.g., backwashing).

F. Advantages and Disadvantages

The primary benefit of MF/UF membrane systems is the provision of reliable and consistent filtrate water quality, regardless of source water variability. Advantages and disadvantages of MF/UF systems are presented in the table below. These advantages and disadvantages should be evaluated through pilot testing to better define and understand the impact on utility and water quality¹⁰⁸.

Table: Advantages and Disadvantages to MF/UF

Process	Advantages	Disadvantages
MF/UF	<ul style="list-style-type: none"> • Provides consistent water quality • Automated operation (backwashes, etc) and reduced operator time • Smaller footprint and higher filtration rates compared to conventional filtration • High water recovery (>95% for some systems) 	<ul style="list-style-type: none"> • High capital investment • Liquid residuals streams require management

G. Design Criteria

The primary RO design parameters are outlined in the table below¹⁰⁸.

Table: RO Design Criteria

Term	Definition
Flux	<p>The rate at which the permeate water passes through the membrane is defined by the equation below:</p> $J = \frac{Q}{A}$ <p>Where:</p> <p>J = Flux (g/d/ft²) Q = filtrate flow (gpd) A = membrane surface area (ft²)</p> <p>However, for RO membranes, pressure must be applied in excess of the osmotic pressure to force the water through the membrane, as shown in the equation below:</p> $J = K(\Delta P - \Delta \pi)$ <p>Where:</p> <p>J = Flux (g/d/ft²) K = mass transfer coefficient (g/d/ft²) ΔP = pressure difference between feed and product water (psi) Δπ = osmotic pressure difference between feed and product water (psi)</p>
Recovery	<p>Recovery is the quotient of the feed water flow rate and the permeate as follows:</p> $R = \frac{Q_p}{Q_f}$ <p>Where:</p> <p>R = recovery of the membrane unit Q_p = filtrate flow produced by the membrane unit (gpd) Q_f = feed flow to the membrane unit (gpd)</p> <p>Recoveries for RO systems treating water with low salinity; recovery ranges from 75 to 85 percent. As recovery rates increase, the rate of membrane scaling and permeate salinity also increase.</p>
System Staging	<p>RO systems may be single-stage, two-stage, or three-stage systems for increasing recovery and water quality. An example of a two-stage RO system is shown in the figure above.</p>
Transmembrane Pressure	<p>The driving force for the transport of water across a semipermeable membrane (i.e. a pressure gradient across the membrane) or:</p> $TMP = P_f - P_p$

Term	Definition
	Where: TMP = transmembrane pressure (psi) P_f = feed pressure (psi) P_p = filtrate pressure (i.e., backpressure) (psi)
Cleaning Procedures	See description in Error! Reference source not found. for backwash, EFM, and CIP.

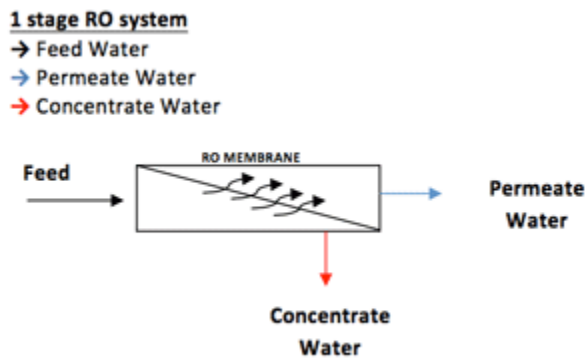


Figure: Illustration of a One-stage RO Treatment System

(Source: [http:// puretecwater.com/](http://puretecwater.com/))

H. Operational Considerations

Operational considerations that should be considered for an RO system are summarized in the table below¹⁰⁸.

Table: RO Operational Considerations

Operational Consideration	Description
Water Temperature	Water temperature significantly affects membrane life, hydraulic performance/required membrane surface area, and the solubility of salts and silica, which affects the membrane recovery and contaminant removal. Operations will need to be adjusted to maintain the performance at different temperatures.
Membrane Cleaning	Membrane cleaning and frequency, including the selection and use of chemicals, directly impacts membrane performance and membrane life. Manufacturer's recommend cleaning conditions such as temperature, pH range, frequency, duration, and chemicals.
Fouling Indices	Fouling affects membrane pretreatment requirements, performance, operating costs, and cleaning

	<p>frequencies. The silt density index (SDI) and mini plugging factor index (MPFI) are the most common fouling indices and are determined from simple membranes tests to monitor the effects of fouling on the membranes over time.</p>
Scale Formation	<p>As constituents (calcium carbonate, barium, sulfate, and silica) are concentrated in the concentrate stream, the solubility limits of certain constituents may be reached. When these saturation levels are exceeded, precipitates form and scale the surface of the membrane. As scale accumulates on the membrane, more pressure, as well as energy, is required to achieve the same recovery.</p> <p>Depending on the nature and severity of the scaling, it may or may not be possible to removal the scale with conventional membrane cleaners. Physical damage, or irreversible fouling, may occur when the scale deposits scratch or penetrate the membrane layer, which may require membrane replacement.</p>

I. Advantages and Disadvantages

Advantages and disadvantages of RO membrane systems are summarized in Table below

108

Table: Advantages and Disadvantages of RO

Advantages	Disadvantages
<ul style="list-style-type: none"> • Provides consistent water quality • Modular construction for ease of installation • Widely used in industry • Automated operation • Expected membrane life is at least 5 years with proper maintenance 	<ul style="list-style-type: none"> • High capital cost • Energy intensive • Produces concentrated (high TDS) waste stream that requires management and/or disposal

